Mémoires de Géologie (Lausanne) N° 18, 1994

Jurassic and Cretaceous radiolarian biostratigraphy and sedimentary evolution of the Budva Zone (Dinarides, Montenegro)

by **Špela Goričan**

IMPRIMERIE CHABLOZ S.A., TOLOCHENAZ ISSN 1015-3578

Cover illustration: *Panoramic view of the area around Kotor Bay showing the two superposed tectonic units of the Budva Zone and the overthrusting High Karst Zone (massive light limestone in the background). The town of Tivat (on the left) lies on the Dalmatian Zone (for tectonic map see Fig. 1.2).*

Université de Lausanne
Faculté des Sciences

Institut de Géologie
et Paléontologie

Jurassic and Cretaceous radiolarian biostratigraphy and sedimentary evolution of the Budva Zone (Dinarides, Montenegro)

Špela Goričan

Mémoires de Géologie (Lausanne) No. 18, 1994

thèse de doctorat
présentée à la Faculté des Sciences
de l'Université de Lausanne

Jury de thèse:

Peter O. Baumgartner (directeur, Université de Lausanne)
Claude Joseph (président, Université de Lausanne)
Patrick De Wever (expert, Centre de la Recherche Scientifique, Paris)
Jean Guex (expert, Université de Lausanne)
Gérard M. Stampfli (expert, Univeristé de Lausanne)

Author's present address:
Paleontološki inštitut Ivana Rakovca ZRC SAZU, Gosposka 13, 61 000 Ljubljana , SLOVENIA

CONTENTS

Abstract

The Budva Zone is the northernmost part of a long belt of Mesozoic basinal deposits, which extend southward to the Krasta–Cukali Zone in Albania and Pindos–Olonos Zone in Greece.

Lowermost Jurassic to middle Cretaceous formations are defined and described. Radiolarians from 105 samples collected in ten sections allowed us to date pelagic sequences and to constrain ages of intervening carbonate gravity-flow deposits.

Systematics of about 200 recorded radiolarian species is discussed and supported by illustrations. For the Middle Jurassic to Turonian time interval, a local radiolarian zonation is constructed by means of the Unitary Association Method (Guex, 1977, 1991). One hundred and thirty-nine taxa were used in the database. Fourty-eight Unitary Associations are established and grouped into 15 distinct "zones". The calibration is based on the existing zonations.

The Budva Zone formations are correlated to time-equivalent lithologies in the tectonically overthrusting High Karst Platform. The correlation reveals a close relationship between the sedimentary and tectonic activity of the High Karst Platform margin, and facies evolution in the adjacent Budva Basin.

The Hettangian to Sinemurian lime-poor "Passée Jaspeuse" Formation coincides with a subsidence of the High Karst Platform margin. In the Pliensbachian to lower Toarcian the entire basin was characterized by resedimented carbonates (Lower Bar Limestone Member). The margin-ward propagation of radiolarite sedimentation (Lastva Radiolarite) and retreat of resedimented carbonates (Upper Bar Limestone Member) in the Middle Jurassic are related to a development of continuous oolitic bars on the platform. The maximum expansion of radiolarites was attained in the Oxfordian and Kimmeridgian, when the platform margin was fringed by a large reef complex. Most of the carbonate mud in the Jurassic basinal succession was probably of platform origin. Periods of reduced periplatform-ooze supply were characterized by lime-poor to lime-free basinal sedimentation.

In the late Tithonian, distal sequences show a transition from siliceous to carbonate deposition (Praevalis Limestone). In the Hauterivian-Barremian, again, radiolarite sedimentation (Bijela Radiolarite) progressively replaced pelagic carbonates and persisted to the Turonian. These facies changes are correlative with synchronous shifts in the Southern Alps and Apennines. The Budva Basin, however, differs from other Tethyan basins by a lower proportion of carbonate in the Upper Jurassic and Cretaceous sequences.

The composition and distributional pattern of resedimented carbonates changed significantly by Late Jurassic time. Prior to that time, in the Early and Middle Jurassic, carbonate gravity-flow deposits were composed of remobilized pelagic sediments and penecontemporaneous platform debris. Contrary to this, since the Tithonian the bulk of the resedimented carbonates was derived from the erosion of lithified shallow water limestones. Coarse grained calcareous turbidites became restricted to the northwestern depositional area. This facies change is believed to reflect the evolution from an extensional to a compressive regime in the internal domains of the Dinaric Tethys, which induced a differential uplift of the High Karst Platform.

Résumé

La Zone de Budva appartient à la partie la plus septentrionale d'une longue chaine de bassins sédimentaires mésozoïques qui s'étend du sud de la Zone de Krasta-Cukali en Albanie à la Zone du Pinde-Olonos en Grèce.

Les formations du Jurassique basal au Crétacé moyen que nous avons étudiées sont définies et décrites. Ces dépôts sédimentaires nous ont livré environ 200 espèces de radiolaires qui sont décrits et illustrés dans la partie systématique de notre travail.

Une zonation locale basée sur ces radiolaires a été établie à l'aide de la méthode des Associations Unitaires (Guex 1977, 1991) pour l'intervalle Jurassique moyen à Turonien. Cette zonation est basée sur la distribution stratigraphique de 139 espèces distinctes. Le traitement de nos données nous a permis de construire 48 Associations Unitaires qui ont été groupées en 15 "zones". Notre zonation est calibrée avec les échelles biochronologiques préexistantes.

Les formations marines relativement profondes de la zone de Budva ont été corrélées avec les dépôts sédimentaires peu profonds de la Plateforme du Haut Karst qui lui sont sus-jacents par charriage tectonique. Ces corrélations mettent en évidence un parallèlisme clair entre l'activité tectonique et sédimentaire qui affecte la Plateforme du Haut Karst et l'évolution du Bassin de Budva qui lui est adjacent.

La "Passée Jaspeuse" de l'Hettangien-Sinémurien, pauvre en carbonate, coïncide avec une subsidence du bord de la Plateforme du Haut Karst. Au Pliensbachien-Toarcien inférieur, la totalité du bassin était caractérisée par des calcaires resédimentés (membre calcaire inférieur de Bar). La propagation progressive de la sédimentation radiolaritique vers la

marge de la plateforme (Radiolarite de Lastva) et le retrait des dépôts resédimentés (membre calcaire supérieur de Bar) au Jurassique moyen sont liés au développement de barres oolitiques continues sur cette plateforme. L'expension maximale des dépôts radiolaritiques est atteinte à l'Oxfordien-Kimmeridgien, lorsque la marge de la plateforme est bordée d'un vaste complexe récifal. L'essentiel des vases carbonatées que l'on trouve dans la séquence bassinale provenait probablement de la plateforme. Les épisodes de faible production de vases calcaires "périplateforme" correspondaient, dans le bassin, à une sédimentation pauvre en carbonates.

Au Tithonique supérieur, les séquences distales montrent un passage de dépôts siliceux à des dépôts carbonatés (Calcaires de Praevalis). A l'Hauterivien-Barrémien, la sédimentation radiolaritique (Radiolarite de Bijela) remplace progressivement les carbonates pélagiques et persiste jusqu'au Turonien. Ces variations de la proportion de carbonate sont synchrones avec celles qui ont été reconnues dans les Alpes Méridionales et les Appenins. Le bassin de Budva diffère néanmoins des autres bassins téthysiens par une proportion plus faible de carbonates dans les séquences du Jurassique supérieur et du Crétacé.

La composition et la nature de la répartition des carbonates resédimentés change de façon drastique au Jurassique terminal. Au Jurassique inférieur et moyen, les carbonates resédimentés étaient composés de matériaux pélagiques remobilisés et de débris de la plateforme pénécontemporaine. A partir du Tithonique au contraire, l'essentiel de ces resédiments provient de l'érosion de dépôts calcaires lithifiés et peu profonds. Les turbidites à forte granulométrie sont alors restreintes à la partie nordouest du domaine sédimentaire. Ce changement de faciès résulte de l'évolution d'un régime d'extension tectonique vers un régime compressif dans le domaine des Dinarides, induisant un soulèvement de la Plateforme du Haut Karst.

Povzetek

Cona Budva je najsevernejši del dolgega pasu mezozojskih globljemorskih sedimentnih kamnin na jugozahodnem delu Balkanskega polotoka, ki se iz Črne gore nadaljujejo proti jugu v cono Krasta–Cukali v Albaniji in Pindos–Olonos v Grčiji.

V delu so definirane in opisane jurske ter spodnje in srednjekredne formacije. Njihova starost je določena z radiolariji.

Predstavljenih je 200 vrst radiolarijev z desetih profilov. S pomočjo metode unitarnih asociacij (Guex, 1977, 1991) smo za obdobje od srednje jure do turonija izdelali lokalno conacijo, ki temelji na 139 izbranih vrstah radiolarijev. Ugotovili smo 48 unitarnih asociacij, ki smo jih združili v 15 con. Po primerjavi z obstoječimi conacijami smo cone uvrstili v standardne kronostratigrafske enote.

Formacije cone Budva smo primerjali z enako starimi litološkimi členi cone Visokega Krasa, ki je na cono Budva narinjena. Primerjava kaže tesno odvisnost facialnih razvojev v bazenu Budva od produkcije in tektonskih premikov na robu sosednje platforme Visokega Krasa.

Začetek formacije "Passée Jaspeuse" bogate s kremenico se ujema s tonjenjem roba platforme na meji trias-jura. V pliensbachiju in spodnjem toarciju so se v celotnem bazenu odlagali karbonatni turbiditi (spodnji člen Barskega apnenca). Umik karbonatnih turbiditov proti robu bazena (zgornji člen Barskega apnenca) in sočasna sedimentacija radiolaritov distalno (radiolariti Lastve) sta bila pogojena z nastankom zveznih oolitnih barier na robu platforme v srednji juri. Radiolariti so dosegli največji obseg v oxfordiju in kimmeridgiju, ko so na robu platforme uspevali koralni in stromatoporoidni grebeni. Večina karbonatnega mulja v jurskih bazenskih sedimentih je verjetno prihajala s platforme. Za obdobja z zmanjšanim dotokom karbonatnega mulja so bili značilni bazenski sedimenti bogati s kremenico.

V zgornjem tithoniju so v distalnih delih bazena radiolarite zamenjali kremenasti apnenci (apnenec Praevalis). Nad njimi ležijo zopet radiolariti (radiolariti Bijele), ki so se odlagali od hauterivija ali barremija do turonija. Te facialne spremembe so istočasne z nihanjem vsebnosti karbonata na profilih v Južnih Alpah in Apeninih. Bazen Budva se razlikuje od drugih bazenov Tetide po manjši vsebnosti karbonata predvsem v zgornjejurskih in krednih kamninah.

Presedimentirani karbonati so se v zgornji juri izrazito spremenili po sestavi in lateralni razširjenosti. V spodnji in srednji juri so bili karbonatni turbiditi sestavljeni iz prenešenih pelaških sedimentov in enako starih elementov s platforme. V tithoniju in kredi je večina klastov nastala z erozijo litificiranih plitvovodnih apnencev. Grobozrnate breče so se v tem času odlagale samo v severozahodnem delu bazena. Ta facialni obrat je verjetno povezan z začetkom kompresivne tektonike v oceanskih predelih notranjih Dinaridov, ki je povzročila dvig platforme Visokega Krasa.

1. INTRODUCTION

1.1 Geological outline

Geographically, the area studied comprises a narrow, less than 10 km wide and about 100 km long NW to SE oriented belt, situated in coastal Montenegro between the Albanian border in the south and Hercegnovi in the north (Figs. 1.1, 1.2).

Geologically, the Budva Zone (Petković, 1956) is a part of External Dinarides (Fig. 1.1). Tectonically, the Budva Zone is represented by several thrust units, underlain by the Dalmatian Zone (Aubouin, 1960) in the southwest and overlain by the High Karst Zone (Kossmat, 1924) in the northeast. The nappes were emplaced to the southwest. The name "Dalmatian Zone" as used in this paper is a synonym of the Parautochthon (Antonijević et al., 1969a,b; Mirković et al., 1968a,b; Marković, 1966a,b; Kalezić et al., 1976) and South Adriatic Zone (Grubić, 1980), and partly of the Adriatic--Ionian Zone (Kossmat, 1924; Dimitrijević, 1982).

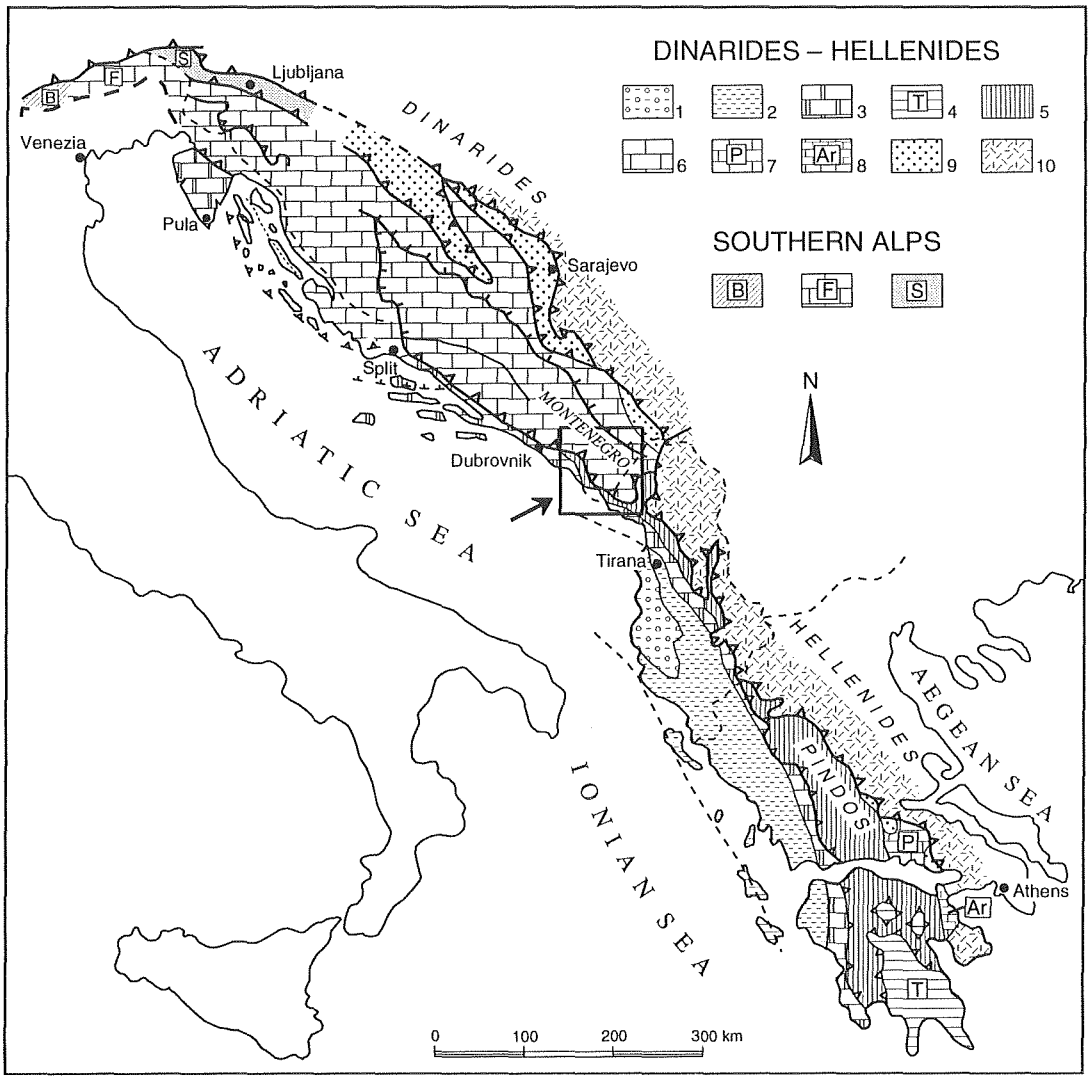

Fig. 1.1: Schematic tectonic map of the Dinarides, Hellenides and Southern Alps showing the position of the Budva Zone (5) and its relationship with the neighbouring tectonic units. The position of the Internal Dinarides (10) comprising the Ophiolitic Complex is indicated (after Celet, 1977).

1. Dalmatian–Albanian Foredeep, 2. Ionian Zone, 3. Dalmatian and Gavrovo Zones, 4. Tripolitza Zone, 5. Budva–Cukali–Pindos Zone, 6. High Karst Zone, 7. Parnassos Zone, 8. Argolid, 9. Bosnian and Beotian Zones, 10. Internal Dinarides and Hellenides, B. Belluno, F. Friuli, S. Slovenian Zone. The framed area is enlarged in Fig. 1.2.

The front of the Budva Zone overthrust can be traced from Bar to Sutomore and from Budva to Hercegnovi (Fig. 1.2). South of Bar the High Karst Zone was emplaced over the Budva Zone and brought in contact with the Dalmatian Zone. The outcrop of the Budva Zone wedges out near Konavlje north of Kotor Bay (Marković, 1966a,b). This area marks the northwest termination of an about 800 km long belt of basinal deposits represented by the Pindos-Olonos Zone in Greece and Krasta-Cukali Zone in Albania.

The Budva Zone itself comprises several thrust sheets (Figs. 1.2, 1.3). In the Kotor area two tectonic units are distinguished, the Devesilje Tectonic Unit overthrusted by the Vrmac Tectonic Unit. The central part between Kotor and Petrovac is more complex, composed of several smaller discontinuous recumbent folds. In general, a subdivision between a lower and an upper tectonic unit is possible.

The present disposition of the tectonic units corresponds approximately to the Mesozoic paleogeography. The Budva Zone was a narrow basin between two carbonate platforms, the "Adriatic Platform" in the west and the "Dinaric Platform" in the east (D'Argenio et al., 1971).

In this paper the terms Dalmatian, Budva and High Karst Zone refer to the tectonic units corresponding to the paleogeographic units: Dalmatian Platform, Budva Basin, and High Karst Platform.

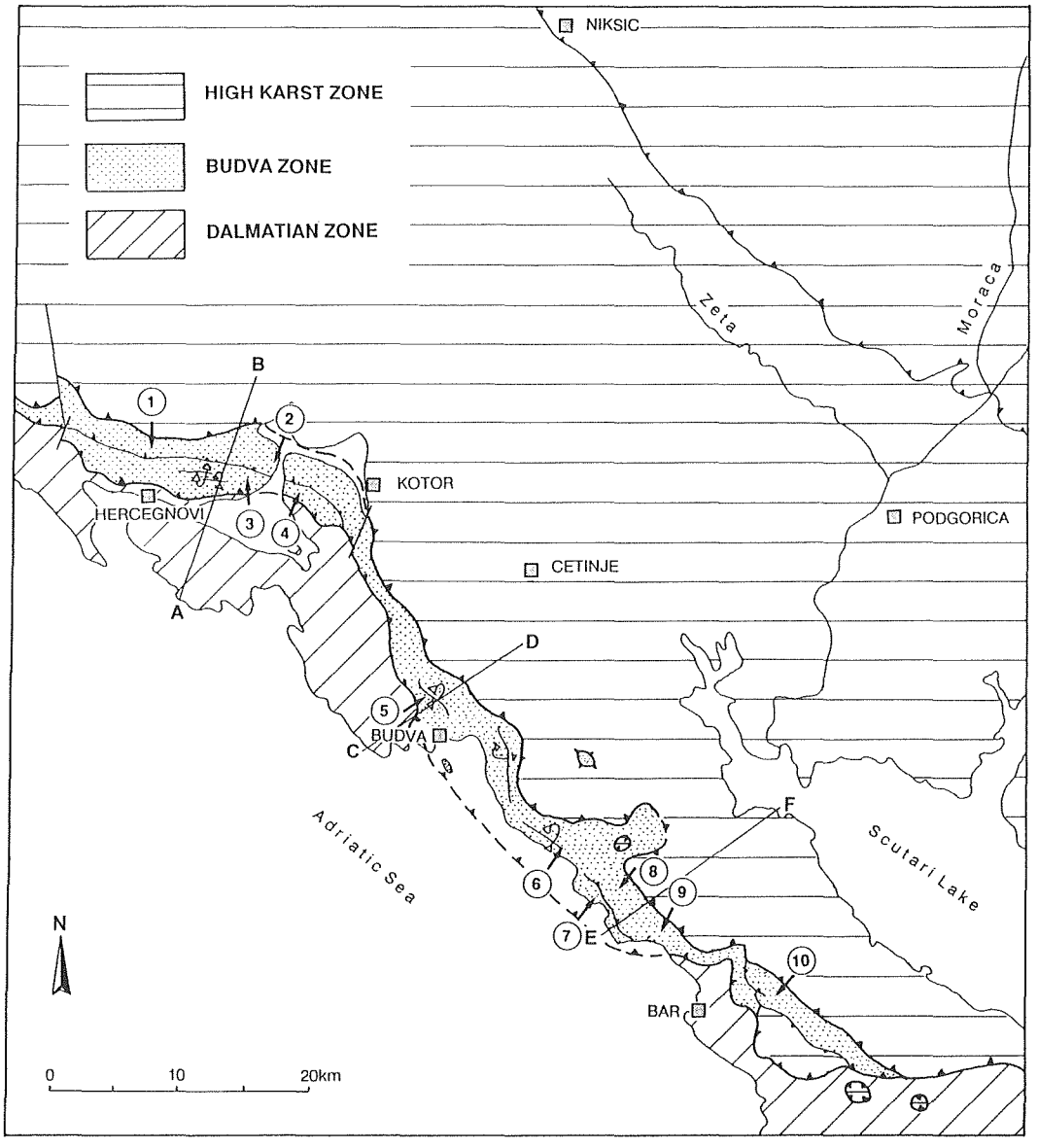

Fig. 1.2: Simplified tectonic map of the Montenegrin littoral (after Mirković, in press) and location of the sections studied: 1. Česma, 2. Verige, 3. Bijela, 4. Gornja Lastva, 5. Grbaljska Lastva, 6. Petrovac, 7. Čanj, 8. Din Vrh, 9. Sutomore, 10. Bar. Location of cross-sections (see Fig. 1.3) is also indicated.

The oldest outcropping formation in the Budva Zone is composed of Lower Triassic red marine sandstones, dolomites, and marly limestones. The Middle Triassic is characterized by the "Anisian Flysch" or limestone--dolomite sequence, overlain by a volcano-sedimentary sequence, which consists of volcanic and volcanoclastic rocks alternating with cherts or limestones. The Upper Triassic to Maastrichtian succession displays an alternation of pelagic limestones, radiolarites, and resedimented carbonates which is overlain by flysch deposits of Paleocene to lower Eocene age.

This study encompasses the Triassic-Jurassic to middle Cretaceous formations. The following lithostratigraphic units are recognized (Figs. 1.4, 1.5):

– *Halobia* limestone: bedded cherty limestone; Upper Triassic.

– "Passée Jaspeuse": alternation of calcareous chert and shale beds; Triassic-Jurassic boundary to the Sinemurian-? lower Pliensbachian.

– Bar Limestone: carbonate gravity-flow deposits; ? upper Sinemurian-lower Pliensbachian to lower Toarcian (Lower Member), upper Toarcian?-Aalenian to lower Oxfordian (Upper Member).

– Lastva Radiolarite: alternation of chert and shale layers; Toarcian? to Tithonian.

– Praevalis Limestone: reddish cherty limestone with marls; upper Tithonian to upper Aptian-lower Albian.

– Bijela Radiolarite: alternation of shales and cherts; Hauterivian-lower Barremian to Turonian.

– *Globotruncana* limestone: Coniancian? to Maastrichtian.

Locally, pelagic deposits are displaced by platform-derived resedimented carbonates of the Tithonian to Neocomian and Albian to Late Cretaceous age.

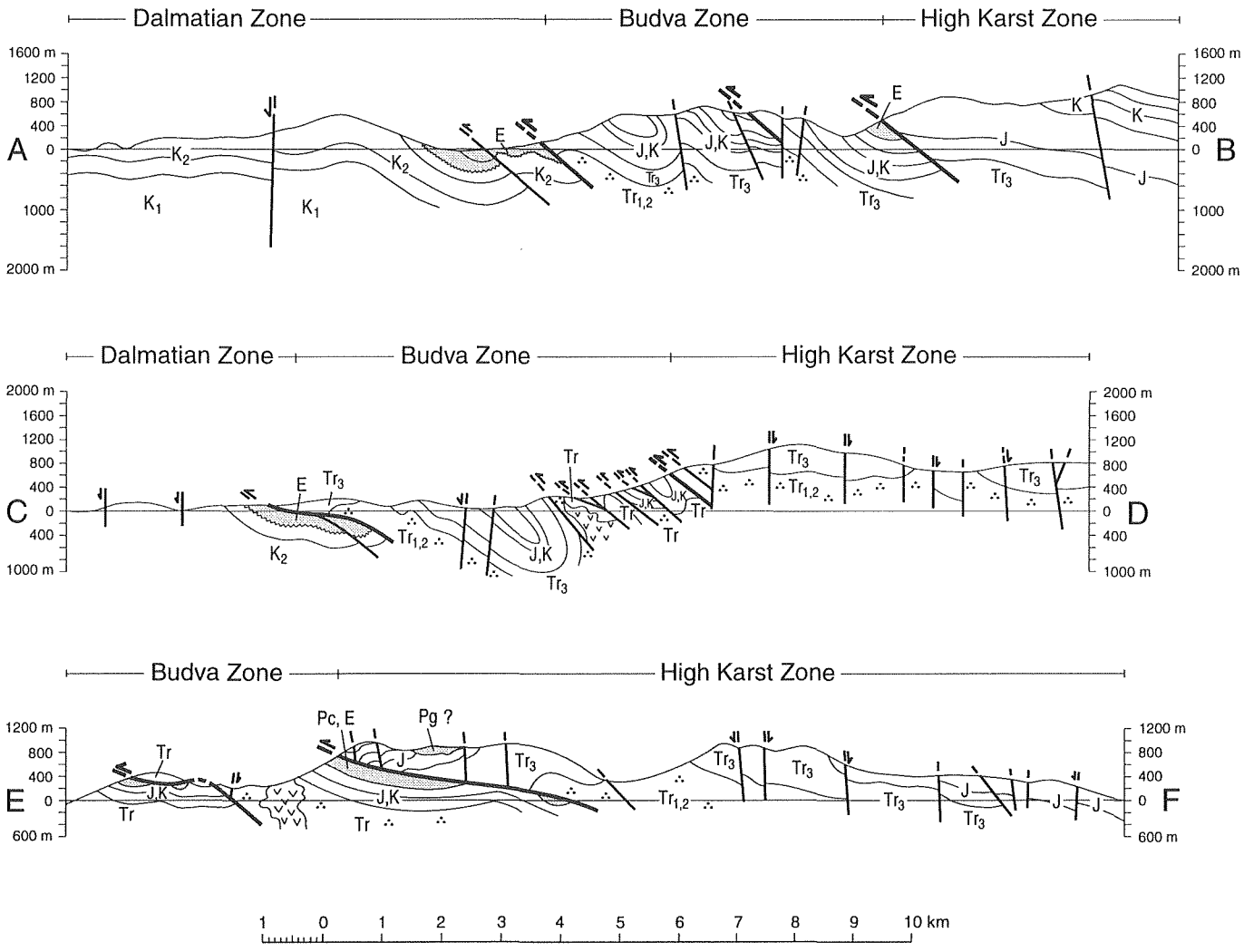

Fig. 1.3: Cross-sections through the Dalmatian, Budva and High Karst Zones (simplified after Antonijević et al., 1969a; Mirković et al., 1968a). See Fig. 1.2 for the location of cross-sections.

1.2 Aim of study and organization of chapters

The objectives of this study were:

1. – To date the Jurassic to mid-Cretaceous formations by means of radiolarians, since they are generally the only stratigraphically important fossils present.

2. – To reconstruct the Budva Basin evolution through this time interval.

3. – To contribute to the establishing of a Tethyan radiolarian zonation with a special emphasis on the Middle and Upper Jurassic.

The first part of this paper (Chapters 1 to 5) deals with the stratigraphy of the Jurassic and Cretaceous succession.

Individual lithostratigraphic units are presented in Chapter 2. The description includes lithology, age assignment and lateral distribution of each formation. Fossil content other than radiolarians is indicated. Each formation is further correlated to coeval lithologies of the High Karst Zone. Time-equivalent basinal deposits of other Tethyan regions are briefly mentioned. Paleogeographic relationships are discussed in order to distinguish between local and regional (Tethyan) factors determining the type of sediment accumulation in the Budva Basin.

Sedimentation rates of pelagic deposits are examined separately in Chapter 3.

A recapitulation of sedimentary events and probable causes for temporal and spatial facies variations in the Budva Basin are synthesized in Chapter 4.

The lithostratigraphic units of the Budva Zone, Pindos Zone and Krasta-Cukali Zone are correlated in Chapter 5. A possible paleogeographic termination of the Budva Basin toward the northwest is discussed.

The second part of this paper provides details about radiolarian dating (Chapter 6), systematic description of taxa (Chapter 7) and species content of the samples studied (Appendix).

1.3 Historical review

The Montenegrin littoral was first mapped by Bukowski (1903, 1904, 1909a, 1909b, 1912, 1927). He recognized several Triassic formations, but believed that all the younger Mesozoic units were either of Tithonian or Late Cretaceous age.

A systematic mapping was carried out in the frame of the "Basic Geological Map", a national Yugoslav project, in the 1960's (Antonijević et al., 1969a,b; Mirković et al., 1968a,b). In the Budva Zone, the presence of Lower, Middle and Upper Jurassic could be documented by age-diagnostic platform-derived biodetritus in redeposited limestones. Early and Late Cretaceous ages were determined by calpionellids and planktic foraminifera. Nevertheless, the Jurassic series remained undifferentiated in the map.

On the basis of lithological and faunal characteristics, the Budva Zone in the Kotor-Budva sheet was subdivided in three units (Antonijević et al., 1969b): a northeastern and northwestern zone extending from Hercegnovi to Čanj, with an intermediate central zone in the area between Budva and Petrovac. The authors concluded that the Budva Basin was shallower toward the northwest.

Since then, a synthesis of previous mapping was published by Kalezić et al. (1976) on a 1:200 000 map, which included the coastal part, and by Mirković (in press) for the entire area of Montenegro. Cadet (1970, 1978) reviewed the regional geology of the area around Kotor Bay. Bešić (1975, 1980, 1983) summarized the previous knowledge on the biostratigraphy, tectonics and paleogeography of Montenegro, essentially based on his own investigations, which he started in the early 1930's.

Several researchers focussed on individual formations of the Budva Zone. Dimitrijević (1967) published a comprehensive study on the Middle Triassic "Flysch". Facies associations are characteristic of both the Budva Zone and the southwestern part of the High Karst Zone. The clastic component includes reworked Paleozoic rocks. The maximum thickness reaches 500 m. The general paleotransport direction was from the northeast to the southwest. The Middle Triassic volcanism of the Montenegrin littoral was investigated by Djordjević and Knežević (Djordjević & Knežević, 1969; Knežević, 1975, 1976). The volcanoclastics were studied by Obradović (1979). Cafiero and De Capoa Bonardi (1980, 1981) examined the upper Triassic halobiids and conodonts.

Little attention was paid to the Jurassic and Lower Cretaceous succession. Radoičić has worked extensively but published a relatively small part of her results, mostly in general papers dealing with the paleogeography of the External Dinarides (Radoičić in D'Argenio et al., 1971; Radoičić, 1982, 1987a, 1987b; Radoičić & D'Argenio, 1988) or particular fossil content (Radoičić, 1967, 1987c). Vidović et al. (1958) presented the regional distribution of the Upper Cretaceous beds with globotruncanids. Obradović et al. (1988, 1989) described carbonate turbidites of Cretaceous age. Maastrichtian and Paleogene deposits were studied by Pavić (1970).

Radiolarian work in the Budva Zone was initiated in the late 1980's (Obradović et al., 1986; Goričan, 1987; Obradović & Goričan, 1989). Lower Jurassic, Middle Jurassic and middle Cretaceous radiolarian assemblages were obtained from the Gornja Lastva section near Tivat.

A complete bibliography between 1838 and 1983 on the geology of Montenegro was compiled by Živaljević (1989).

1.4 Summary description of localities

The location of the sections studied is indicated in Fig. 1.2. Lithological columns are presented in Fig. 1.4. They are arranged in axial northwest to southeast direction. The ages of the exposed lithostratigraphic units are summarized in Fig. 1.5. Different formations are discussed in detail in Chapter 2.

For each locality, its tectonic position within the Budva Zone is indicated. The thrust sheet directly underlying the High Karst Zone is considered the upper tectonic unit.

1. Locality name: **Česma**

Upper tectonic unit

Location and access: along a path between the villages Sasovići and Žlijebi, north of Hercegnovi.

Stratigraphy: The section consists of 250 m of calcarenites and carbonate breccia megabeds. A 30 m thick sequence of bedded dolomite and dolomitic limestone containing about 50 % of replacement chert is intercalated in the lower half. Globotruncanids were found in the dolomitic siliceous limestones near the top.

Previous work: Lower part of the section illustrated by Pavić (1970) and Cadet (1978).

Remarks: Cadet (1978) suggested a tectonic contact between the Cretaceous succession and the overlying Paleogene breccias, which implied the existence of an intermediate Izvor Česma Thrust Sheet between the Budva Zone and the High Karst Zone. According to Pavić (1970) and Mirković (personal communication, 1990) the contact is sedimentary, the whole sequence thus belongs to the Budva Zone.

Fig. 1.4 (p. 14): Lithological columns of the sections studied. Names of the formations are indicated. For detailed sections with sample numbers see Figs. 2.1, 2.2, 2.3, 2.5.

LEGEND:

Lithology:

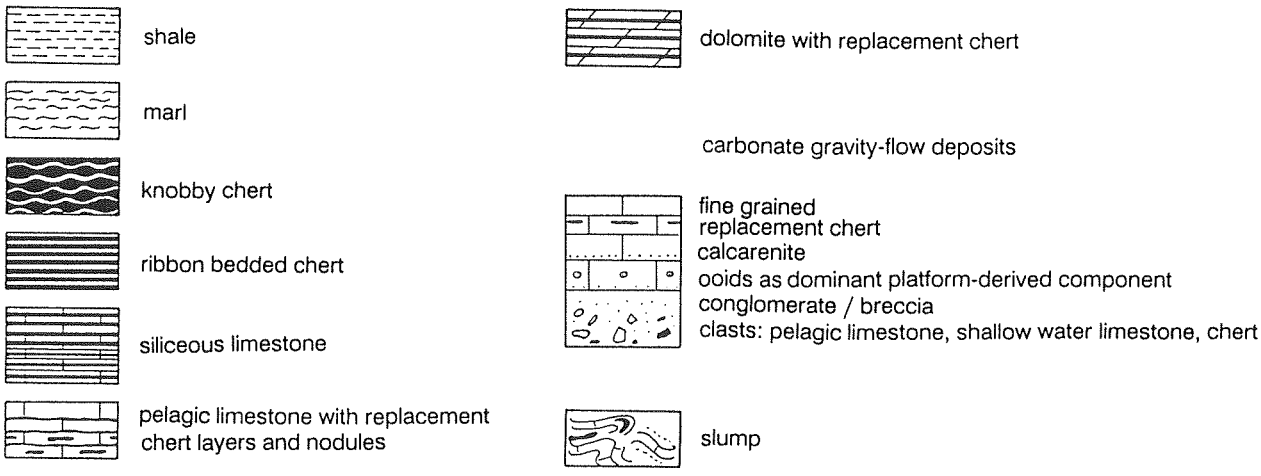

Abbreviations of the lithostratigraphic units:

BLL	Bar Limestone – Lower Member
BLU	Bar Limestone – Upper Member
BR	Bijela Radiolarite
GL	*Globotruncana* limestone
HL	*Halobia* limestone
LR	Lastva Radiolarite
PJ	"Passée Jaspeuse"
PL	Praevalis Limestone
RC	resedimented carbonates

Fig. 1.5 (p. 15): Stratigraphic range of the formations for the sections shown in Fig. 1.4.

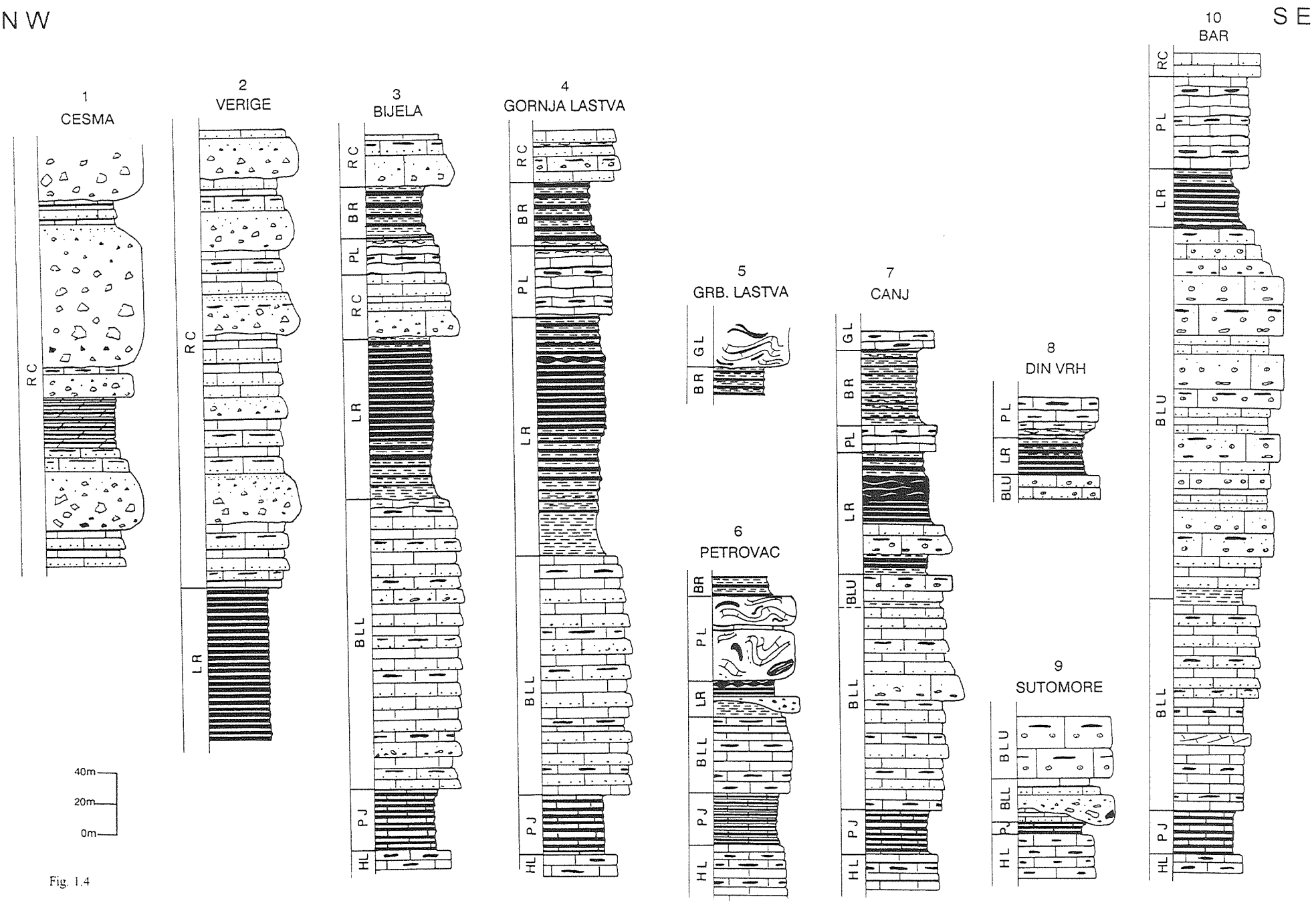
NW
SE
1
CESMA
2
VERIGE
3
BIJELA
4
GORNJA LASTVA
5
GRB. LASTVA
6
PETROVAC
7
CANJ
8
DIN VRH
9
SUTOMORE
10
BAR
RC
LR
BR
PL
BLL
PJ
HL
GL
BLU
40m
20m
0m

Fig. 1.4

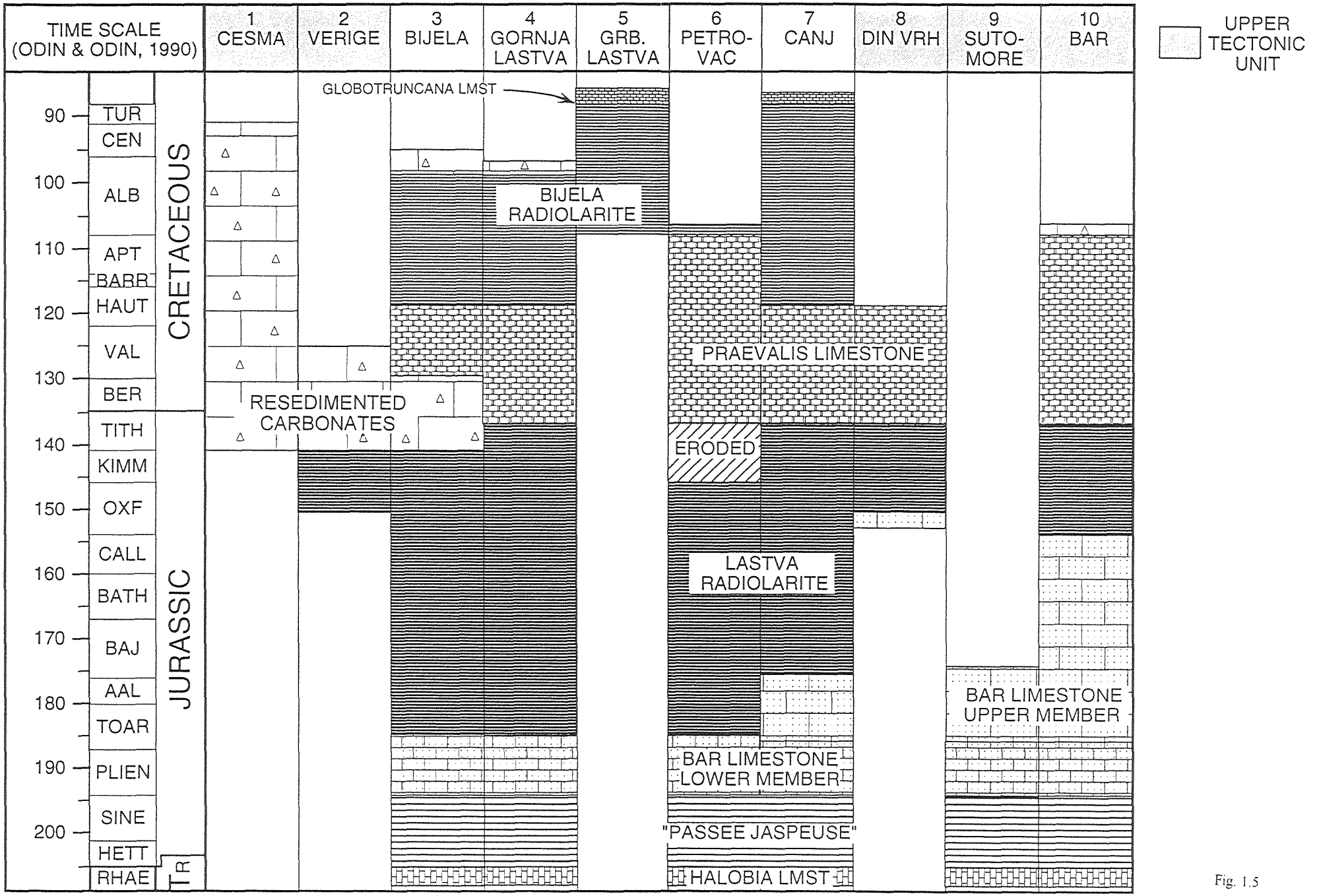
TIME SCALE (ODIN & ODIN, 1990)
1 CESMA
2 VERIGE
3 BIJELA
4 GORNJA LASTVA
5 GRB. LASTVA
6 PETRO-VAC
7 CANJ
8 DIN VRH
9 SUTO-MORE
10 BAR
UPPER TECTONIC UNIT
90
100
110
120
130
140
150
160
170
180
190
200
TUR
CEN
ALB
APT
BARR
HAUT
VAL
BER
TITH
KIMM
OXF
CALL
BATH
BAJ
AAL
TOAR
PLIEN
SINE
HETT
RHAE
CRETACEOUS
JURASSIC
TR
GLOBOTRUNCANA LMST
BIJELA RADIOLARITE
PRAEVALIS LIMESTONE
RESEDIMENTED CARBONATES
ERODED
LASTVA RADIOLARITE
BAR LIMESTONE UPPER MEMBER
BAR LIMESTONE LOWER MEMBER
"PASSEE JASPEUSE"
HALOBIA LMST

Fig. 1.5

2. Locality name: **Verige**

Upper tectonic unit

Location and access: At the Verige isthmus in the Bay of Kotor, along the littoral road, NE of Kamenari.

Stratigraphy: About 70 m of the Lastva Radiolarite overlain by 300 m of reef-derived breccias and turbidites were studied.

Previous work: Čadjenović et al. (1988), Radoičić & D'Argenio (1988) under the name Vrmac sequence.

3. Locality name: **Bijela**

Lower tectonic unit

Location and access: A small church about 1 km NE from Bijela is built on the base of the Bar Limestone Formation. The Jurassic part of the section was sampled on the slope northward. The Cretaceous formations and the contact with the underlying Lastva Radiolarite are exposed along the road from Kamenari to Kruševice.

Stratigraphy: The "Passée Jaspeuse" is overlain by the Bar Limestone, Lastva Radiolarite, resedimented limestones, Praevalis Limestone and Bijela Radiolarite.

4. Locality name: **Gornja Lastva**

Lower tectonic unit

Location and access: near Tivat, along the road from Donja Lastva to Gornja Lastva.

Stratigraphy: A continuous 430 m thick succession ranging from the base of the Jurassic to the end of the Albian was investigated. It consists of 40 m of the "Passée Jaspeuse", 150 m of Bar Limestone, 150 m of Lastva Radiolarite, 50 m of Praevalis Limestone and 35 m of Bijela Radiolarite in contact with resedimented limestone.

Previous work: Cadet (1978), Obradović et al. (1986), Goričan (1987), Radoičić & D'Argenio (1988), Obradović & Goričan (1989). The samples of Goričan (1987) were reexamined.

5. Locality name: **Grbaljska Lastva**

Lower tectonic unit

Location and access: The section is exposed in a gorge east of the village Grbaljska Lastva located 6 km from Budva in the direction of Tivat.

Stratigraphy: An 11 m thick sequence of the Bijela Radiolarite is overlain by *Globotruncana* limestone that exhibits slump folding.

6. Locality name: **Petrovac**

Lower tectonic unit

Location and access: Along the road Petrovac – Podgorica. The section starts at the junction with the main littoral road Budva – Bar.

Stratigraphy: Lower Jurassic to mid-Cretaceous sequence comprises the "Passée Jaspeuse", Bar Limestone, Lastva Radiolarite, and Praevalis Limestone in contact with the Bijela Radiolarite. Structurally, the succession exposed belongs to the reversed limb of a syncline which, in addition, is intensely folded internally. A breccia, consisting of large blocks of limestone, radiolarite and shales was observed within the Lastva Radiolarite. It wedges out in a distance of a few meters. At present we are not sure if it is of synsedimentary or tectonic origin.

7. Locality name: **Čanj**

Lower tectonic unit

Location and access: The section starts on the beach of the small bay of Pečin, 1 km NW from Čanj south of Petrovac. It is exposed on the slope toward NNE.

Stratigraphy: The Upper Triassic to Turonian succession is 350 m thick. The *Halobia* limestone is overlain successively by the "Passée Jaspeuse", Bar Limestone, Lastva Radiolarite, Praevalis Limestone and Bijela Radiolarite in contact with the *Globotruncana* limestone.

8. Locality name: **Din Vrh**

Upper tectonic unit

Location and access: 3.5 km in direct line north from Čanj between Velja Glava (603 m) and Ilijino Brdo hills. A path goes to the north from the main road about 2 km from Mišići.

Stratigraphy: The section studied comprises 25 m of the Lastva Radiolarite and 15 m of Praevalis Limestone. The contact with the underlying Bar Limestone is exposed.

9. Locality name: **Sutomore**

Upper tectonic unit

Location and access: The section is exposed in a ravine 1 km in a direct line north of Sutomore near Zankovići.

Stratigraphy: The "Passée Jaspeuse" and both members of the Bar Limestone were examined.

10. Locality name: **Bar**

Upper tectonic unit

Location and access: Along a mule track from the ruins of the medieval city of Stari Bar toward the NE to the village Mali Mikulići. The Upper Jurassic to Cretaceous part is exposed by a waterfall in a gorge near the path.

Stratigraphy: A complete lowermost Jurassic to Aptian-Albian succession was studied. It comprises 30 m of the "Passée Jaspeuse", a magnificent 360 m thick sequence of the Bar Limestone, about 40 m of the Lastva Radiolarite and 50 m of the Praevalis Limestone overlain by calcarenites.

2. DESCRIPTION OF FORMATIONS

2.1 *Halobia* limestone

The upper part of the *Halobia* limestone is exposed at the base of the sections studied (Fig. 2.1). This limestone is comprised of stratified pelagic lime mudstone with replacement chert as nodules or layers and sometimes marl intercalations. Bed thickness as well as chert and marl frequency are highly variable among different sections.

Cafiero and De Capoa Bonardi (1980, 1981) studied halobiids and conodonts from this formation. The highest part of their sections is assigned to the Norian. Lastva, Bijela and Rebro (Petrovac in our work) localities represent the downward continuation of the sections we studied. The estimated position of the Alaunian conodont assemblage in the Lastva section is about 40 m below the contact with the "Passée Jaspeuse."

In the Petrovac section a sample situated 25 m below the contact with the "Passée Jaspeuse" contained the following conodonts (determination by F. Hirsch): atavistic forms of *Epigondolella bidentata* MOSHER lineage and an advanced stage of *Misikella hernsteini* (MOSTLER). At Čanj sample at 0.30 m yielded a "neospathic" form, transitional between *Misikella hernsteini* and *M. posthernsteini* KOZUR. Both samples are assigned to the Rhaetian. The carbonate pelagic sedimentation continued to the uppermost Triassic at least in some areas of the Budva Basin.

2.2 "Passée Jaspeuse"

2.2.1 Definition

The "Passée Jaspeuse" (Fig. 2.1) is a unit of bedded calcareous chert alternating with shale or marl. The sequence is generally 30–40 m thick. It contains higher proportions of silica and clay constituents than the underlying *Halobia* limestone and can easily be distinguished by its characteristic dark brownish red and green colours.

Radiolarian dating combined with conodont data from the *Halobia* limestone places the base of the "Passée Jaspeuse" near the Triassic-Jurassic boundary; the upper part is Sinemurian- ?lower Pliensbachian (Chapter 6.1).

This lithostratigraphic unit bears a close resemblance to the time-equivalent beds of the Pindos Zone, therefore we retained the same name "Passée Jaspeuse", proposed by Fleury (1980) for the middle part of the "Calcaire de Drimos" Formation (Dercourt et al., 1973).

2.2.2 Facies description and lateral distribution

The "Passée Jaspeuse" facies can be classified as radiolarite in the broad sense of the term. Beds of 3–5 cm (rarely up to 10 cm) of calcareous clayey chert of variegated dark colour prevail. The average amount of dispersed silica is estimated to 60 %. The internal part of beds usually contains replacement chert. Light grey siliceous micrite beds are intercalated. Shale to marl interlayers represent up to 60 percents of the sequence.

Some chert beds are laminated; these laminations consist of densely packed sponge spicules and radiolarians. The spicules are oriented parallel. The enrichment of siliceous organisms indicates sorting by currents.

Especially in the lower part of the sequence up to 20 cm thick beds of breccias are interstratified. These contain mm-sized clasts of replacement chert or lenticular, compacted clasts of grey micrite in a mud matrix. The clast to matrix ratio does not exceed 30 %. Graded mud-supported resedimented carbonates (bed thickness 10–20 cm) are present. They include peloids, rare crinoids, thick-shelled ostracods, nodosariids, and filaments, the latter being oriented parallel to the lamination. The top of such beds consists of phantoms of radiolarians in a lime-mud matrix. Flute casts and slump folding were rarely observed. The sedimentary structures indicate that the "Passée Jaspeuse" succession is at least partly of turbiditic origin.

Siliceous fossil remains are present in all chert and limestone beds. Sponge spicules prevail over radiolarians. Only rare poorly preserved radiolarians were obtained by HF etching, because radiolarians were probably first calcified and later replaced by silica, which makes the extraction difficult. The position of samples is shown in Fig. 2.1; species content is listed in Chapter 6.1.

The base of the sequence in the Bar and Gornja Lastva sections contains radiolarians of presumably Hettangian age. An aberant conodont element was found with radiolarians at the Bar section. Whether it is reworked or the radiolarian fauna belongs to the topmost Triassic cannot be stated at present. The top of the "Passée Jaspeuse" unit is assigned to the Sinemurian-?lower Pliensbachian in the Petrovac, Lastva and Bar sections. No determinable radiolarians have been found at Bijela and Sutomore. The radiolarian data are too scarce to demonstrate either a synchronism or diachronism of formational limits.

The "Passée Jaspeuse" is present in all sections studied, in the upper as well as in the lower tectonic unit.

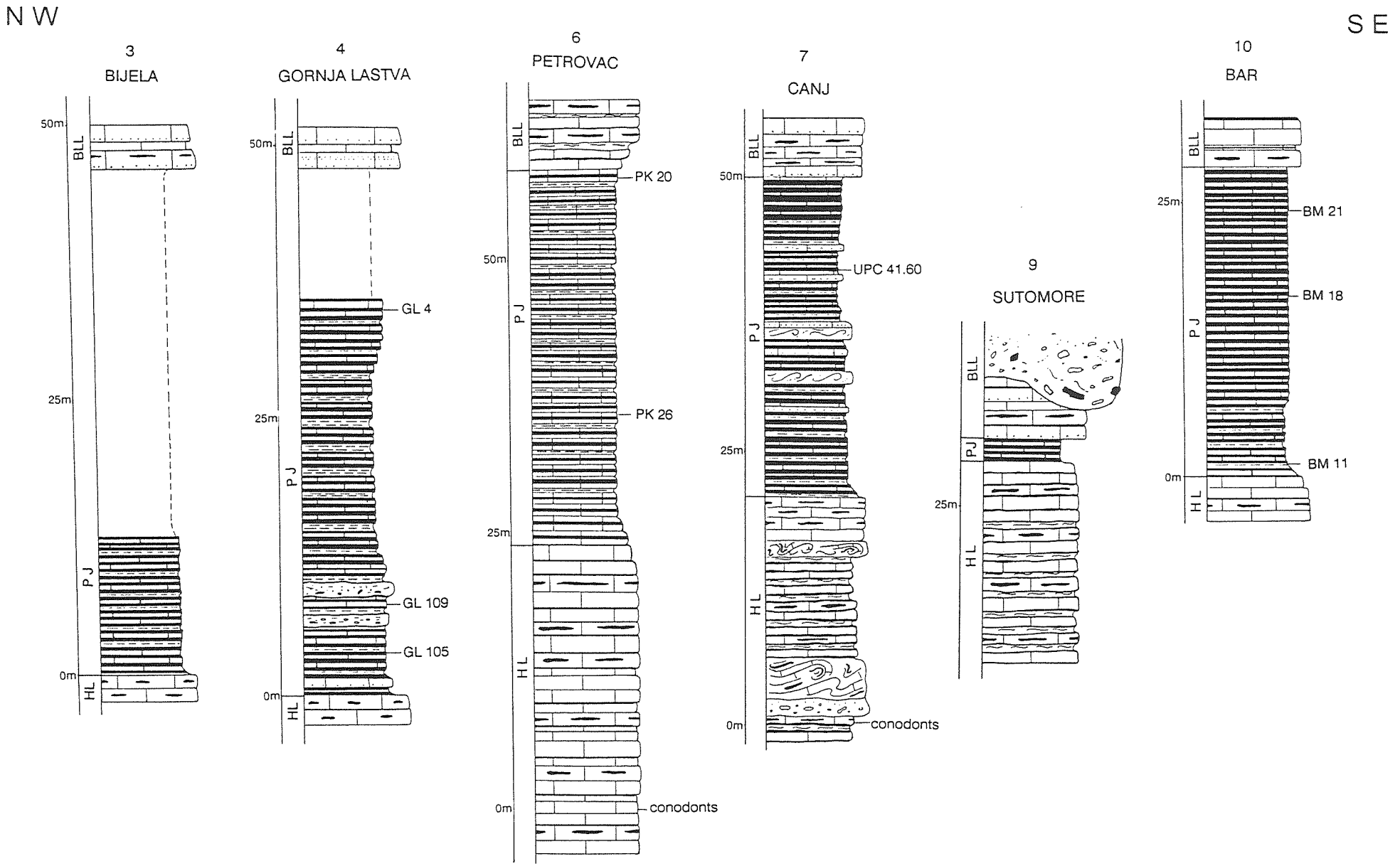

Fig. 2.1: Lithological columns of the *Halobia* limestone and "Passée Jaspeuse" showing the position of samples. Legend : same as Fig. 1.4.

2.2.3 Paleogeographic relationship with the High Karst Platform

Radoičić (1987a) gave a synthesis of the Liassic facies distribution on the adjacent High Karst Carbonate Platform. The Rhaetian-Liassic tectonic events caused a disintegration of the platform and differential subsidence of newly formed blocks. In the interior of the platform shallow marine sedimentation continued, whereas the southwestern margin (Lovčen-Rumija depression) facing the Budva Basin was characterized by pelagic deposition. The pelagic succession consists of marly nodular limestone containing brachiopods, crinoidal detritus, rare foraminifera (*Involutina liassica* (JONES)), radiolarians, and occasional juvenile ammonites. It is overlain by oolitic limestones.

The retreat of the carbonate production into the interior of the High Karst Platform diminished the shallow-water fine-carbonate supply to the Budva Basin. A reduced periplatform-ooze input could be responsible for the lime-poor sedimentation in the basin (see Baumgartner, 1987). In addition, the Budva Basin probably subsided to greater depth.

2.3 Bar Limestone

2.3.1 Definition

Type section: Bar (location Fig. 1.2, p. 16; Figs. 1.4, 2.2). The formation is named after the type locality.

The Bar Limestone Formation is a succession of carbonate gravity-flow deposits. It conformably overlies the "Passée Jaspeuse". The lithological contact is marked by a sharp change in colour and silica content. The "Passée Jaspeuse" is dark reddish and greenish calcareous chert containing about 60% of dispersed silica. The Bar Limestone is light grey and contains only a minor (10–20 %) amount of silica in form of replacement chert.

The thickness of the Bar Limestone varies from 50 m (Petrovac section, distal facies) to nearly 400 m (Bar section, proximal facies).

The age of this formation is constrained by radiolarians from underlying and overlying strata (Chapter 6) and confirmed by rare benthic foraminifera in the turbidite beds. The lower limit is dated as upper Sinemurian-?lower Pliensbachian. The top is diachronous. It ranges from probably Toarcian (Bijela, Gornja Lastva sections) to the Oxfordian (Din Vrh, Bar).

Previous work: The turbiditic character of the Jurassic carbonate succession was recognized by several authors: Cadet (1978), Obradović et al. (1986), Radoičić (1987a, 1987b), Radoičić & D'Argenio (1988). No stratigraphic or sedimentologic study has been devoted to this particular lithostratigraphic unit, therefore no name has previously been introduced.

On the basis of vertical facies changes and different lateral distribution we subdivided the Bar Limestone in two members.

2.3.2 Lower Bar Limestone Member

2.3.2.1 General description

The Lower Bar Limestone Member (Fig. 2.2) was deposited on both tectonic units of the Budva Zone. It is 50 m (Petrovac) to 170 m (Bijela) thick. It consists of generally well graded and stratified resedimented limestone. Replacement chert nodules and beds are present throughout the sequence and constitute 10–20 % .

Predominant lithologies are calcarenite to calcilutite incomplete Bouma sequences. These are composed of graded calcarenite beds (20–60 cm) (Ta), calcarenite with coarse horizontal lamination (Tb), fine parallel lamination unit (Td), and structureless calcilutite beds (Te). Ripple-cross lamination (Tc) was rarely observed. The sequences are usually amalgamated with the top- or more often the base-cut-out. The similar composition (radiolarian/spicule mudstone to wackestone) and local absence of lamination make the distinction between Bouma divisions Td and Te difficult.

Some conglomerate beds are intercalated. Coarser resediments are generally represented by 0.5 m to 1.5 m thick composite beds of conglomerates grading upward to calcarenite. Well individualized thick units of conglomerate and debris breccia occur locally.

2.3.2.2 Composition and probable sources

Finer-grained conglomerates (Pl. 27, fig. 4) and calcarenites show a bimodal grain size distribution. Granule to pebble size limestone fragments are embedded in a calcarenite matrix. The limestone clasts to matrix ratio depends on the size of clasts. Centimeter-sized pebbles are densely packed in only 5–10 % of matrix. Sutured pressure-dissolution contacts are common. A part of the initial matrix was probably removed by pressure-dissolution. Granule size limestone clasts represent only about 30–40 % of sediment. In calcarenite beds they occur sporadically.

Calcarenite microfacies (Pl. 27, fig. 5) are characterized by 50–60 % clasts in mudstone matrix, mostly recrystallized to microsparite and partly to pseudosparite. Sorting is poor to moderate. Grains comprise skeletal debris, ooids, aggregates and peloids. Most of biodetritus has micrite envelopes. Biodetritus was transported as individual grains. Larger gastropods are usually filled by foraminifera and other debris.

In the calcisiltite fraction (Pl. 27, fig. 2) pellets prevail over other allochems. The fine carbonate beds are mudstones to wackestones containing calcified radiolarians and sponge spicules. Nodosariids occur sporadically. The lime-mud component is probably platform-derived.

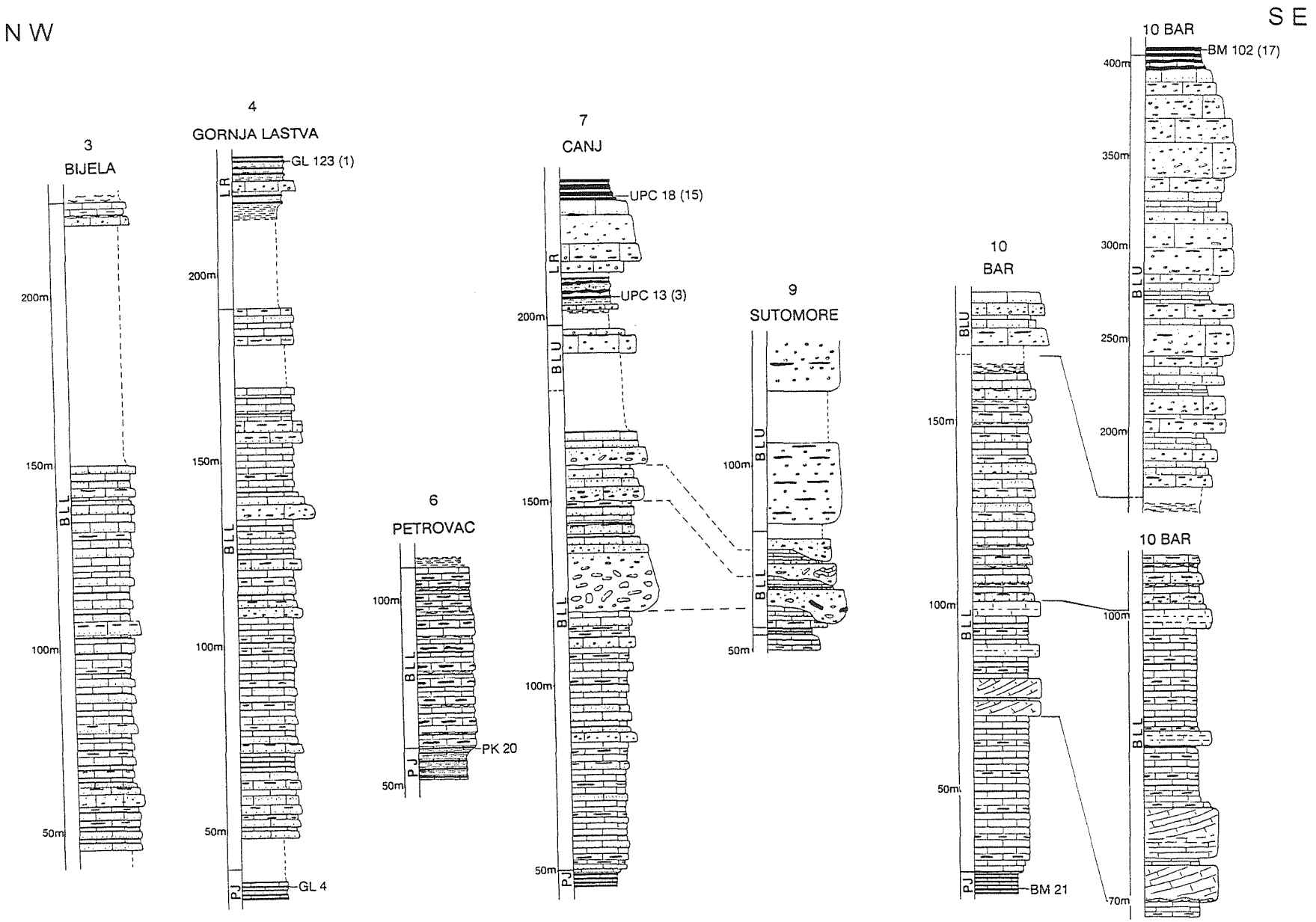

Fig. 2.2: Lithological columns of the Bar Limestone Formation; position of samples from underlying "Passée Jaspeuse" and overlying Lastva Radiolarite is also shown (number within brackets refers to corresponding unitary association). Dashed lines between the Čanj and Sutomore sections show a probable correlation of mass-flow deposits.
Legend: same as Fig. 1.4. Note the different scale for the two columns on the right.

Partial dolomitization of matrix and clasts occasionally occurs.

Limestone clasts: Most lime-clasts found in conglomerates and coarse-grained calcarenites have mudstone to wackestone texture. They contain calcified radiolarians and sponge spicules. Filaments, thin shelled gastropods and nodosariids (*Frondicularia*, *Lenticulina*) rarely occur. Clasts are rounded to subrounded with low sphericity. Clast boundaries are often deformed when in contact with bioclasts and ooids. These clasts can be considered as intraclasts of coeval pelagic sediment, reworked in a semilithified state.

Minor amounts of pelletal calcisiltite and fine-grained calcarenite clasts showing heterogenous origin of debris and sometimes internal grading were found. They indicate that at least a part of the preceding turbidite sequence was eroded and redeposited downslope. Rare unfossiliferous pure micrite clasts are present. They could possibly originate from the platform.

Ooids: The frequency of ooids increases rapidly upsection in the Bar Limestone. At the base they are rare, relatively small, mostly superficial. From the middle part of the Lower Member upward they constitute 30–40 % of the extraclast component in calcarenites. Most of them are large (up to 1 mm in diameter), spherical, with only a small nucleus. They show concentric and, more seldom, radial structures.

Peloids: Large rounded micrite grains commonly occur in calcarenite. Small spherical pellets are especially abundant in siltsized intervals.

Foraminifera: The following genera and species were found in the lower member of the Bar Limestone (determination by M. Septfontaine, for the diagnostic species the position in the sections is indicated in brackets):

Amijiella amiji (HENSON) (Gornja Lastva 135.20 m)
Everticyclammina sp.
Frondicularia sp.
Involutina liassica (JONES) (Bijela 59.30 m)
Involutina sp.
Lenticulina sp.
Mesoendothyra sp.
Ophtalmidium martanum (FARINACCI)
Planiinvoluta sp.
Protopeneroplis sp. (Gornja Lastva 108.60 m)
Pseudocyclammina liasica HOTTINGER emend. SEPTFONTAINE (Bijela 81.80 m)
Siphovalvulina sp.
Valvulina sp.

Pseudocyclammina liasica ranges from the middle Domerian to the lower Toarcian (Septfontaine et al., 1991).

Foraminifera originated from open marine (nodosariids, *Involutina*) to shallow platform environment. Most of Lituolidae are ubiquitous. In the Domerian they inhabited either inner shelf protected lagoons or platform margin, except *Pseudocyclammina liasica*, which seems to have been restricted to the lagoonal facies (Septfontaine, 1985). An occasional sediment supply from the inner shelf is thus possible.

Other biodetritus: The most abundant biodetrital component are crinoid and echinoid fragments which can constitute up to 15 % of grains. Their frequency varies irregularly through the formation. Thick-shelled bivalves and gastropods are abundant. Most echinoderm and mollusc fragments are coated with a micrite envelope. Oncoids and complex aggregates are common. Occasionaly they form up to 30 % of grains. Fragments of algae are present, among them *Cayeuxia* sp. and *Thaumatoporella parvovesiculifera* (RAINERI) are the most frequent. Rare bryozoans occur.

Individual grains originated from platform and platform-basin transitional environments. Platform-margin derived debris prevails. There is no evidence of platform limestone clasts, transported in a well lithified state. In addition, no fossils restricted to an age older than Domerian have been found. It is thus concluded that platform-derived elements were penecontemporaneously resedimented by turbidites in the basin.

2.3.2.3 Facies association, lateral distribution and depositional environment

Facies associations recognized in the Lower Member of the Bar Limestone Formation are briefly described for each locality. For each section its present position on the lower or upper tectonic unit is indicated.

Bijela and **Gornja Lastva** sections (lower tectonic unit): Both sections are characterized by similar facies associations with volumetrically important classical turbidite facies. These turbidite sequences show a graded calcarenite layer, and rarely a clast-supported conglomerate to pebbly calcarenite unit at the base. Several tens of meters thick levels, however, entirely consist of base-absent Bouma sequences. Partial dolomitization was observed only in these two sections.

Petrovac section (lower tectonic unit): The sequence is characterized by a uniform basin-plain facies association. It is only 50 m thick and consists of fine, often faintly laminated limestone with thin interbeds of marl. In the slightly reddish upper part, bioturbation is frequent.

Sutomore section (upper tectonic unit): Three superposed sequences of debris-flow breccia were deposited which show typical inverse to normal grading. The biggest clasts reach 60 cm in diameter. Blocks of bedded internally folded slope dposits are caught up in breccias. The first debris-flow breccia contains big clasts of red vitreous chert probably derived from the underlying Upper Triassic strata. Disorganized debris-flow breccias are overlain by a graded pebble-sized conglomerate to calcarenite unit.

These two-layer deposits alternate with fine-grained carbonates. The thickness of the same breccia bed varies from 2 to 8 meters in a distance of a few meters. This facies association laterally interfingers with classical carbonate turbidites. The composition of debris-flow breccias and small scale facies distribution fit well with the depositional model proposed by Krause and Oldershaw (1979). Such carbonate gravity flows initiated on the slope and moving downslope build their own channels, which explains the moderate thickness of the Lower Bar Limestone Member (25 m in comparison with 150 m in other sections) and the underlying "Passée Jaspeuse" (2 m vs. 30–40 m). The moderate thickness can be, in addition, related to the paleogeographic position of this section on the upper part of the slope (see Fig. 4.3a, Chapter 4).

Čanj section (lower tectonic unit): This Lower Bar Limestone Member is 120 m thick. The lower half is dominated by fine-grained turbidites organized in base-cut-out Bouma sequences. Medium-grained turbidites prevail in the upper part.

Four levels of clast supported conglomerates capped by normally graded pebbly mudstone are intercalated. The thickest conglomerate bed reaches 16 m and consists of large (up to 20x50 cm) densely packed calcilutite clasts (Pl. 28, fig. 3). Such two-component gravity-flow deposits represent a distal equivalent of disorganized debris breccias (Krause & Oldershaw, 1979). A possible correlation with the Sutomore section is shown in Fig. 2.2. Their paleogeographic relationship is given in Fig. 4.3a, Chapter 4.

Bar (upper tectonic unit): The Lower Member of the Bar Limestone is 140 m thick. It shows two distinct lithological associations. The lower half of the section does not exhibit typical turbidity-current features whereas the upper part is characterized by classical carbonate turbidites interbedded with thin layers of greenish marl.

The following observations concern the lower half of the succession. The characteristic lithology is thinly bedded limestone containing a pelagic fauna. Four levels of massive lime mudstone are interstratified. They display faint bedding, either parallel or oblique (lower two levels) to the general stratification of the sequence. They are interpreted as creep deposits and slides respectively. At the base of the first slide a lenticular, graded microconglomerate occurs. It is composed of radiolarian-wackestone clasts in a matrix of a radiolarian-filament mudstone. Rare ostracods and echinoderms are incorporated in the matrix. This microconglomerate layer may represent a turbidite which became deformed along the detachment of the overlying slide.

The described stratigraphic interval is characterized by the dominance of lime mud which is probably of periplatform origin. The dominance of peri-platform ooze facies associated with extensive submarine sliding is characteristic of the intercanyon highs on the upper slope in the base-of-slope apron model (Mullins & Cook, 1986).

Summary: The Lower Bar Limestone accumulated on the northeastern depositional slope of the Budva basin, passing to basin-plain (Petrovac section) (Fig. 4.3a in Chapter 4).

Two different depositional areas could be recognized along the basin axis. In the northwestern part of the Budva Zone medium-grained calcareous turbidites begin at the base of the lower member of the Bar Limestone (Bijela, Gornja Lastva sections). In the southeastern part, the lower member shows a vertical transition from lime-mud dominated facies in the lower half to classical turbidites in the upper half (Bar, Čanj sections).

Confined proximal (Sutomore) to distal (Čanj) mass-flow deposits have been observed locally but cannot be traced further north. They are interpreted as local collapse events possibly related to tectonic instability in the basin.

In the middle part of the Budva Zone no continuous sections can be found because of the rather complex tectonics. Thus it is difficult to reconstruct the lateral connection between these two areas.

2.3.3 Upper Bar Limestone Member

2.3.3.1 General description

The Upper Member of the Bar Limestone (Fig. 2.2) is characterized by thick oolitic beds comprised in megaturbidite sequences. Ooid packstone facies containing only about 10 % of other grains commonly occurs. In the calcarenites of the Lower Member, on the contrary, the ooids do not exceed 40 % of the total grain population. Oolites occur at the top of graded calcarenite units, as individual beds at the base of a coarse-grained turbidite sequence, or as independent deposits. Pure oolite beds show no grading and can be more than 20 m thick. Large replacement chert nodules still exhibiting the texture of oolites are common.

The Upper Bar Limestone Member is well exposed in the Bar section (Figs. 2.2; Pl. 28, figs. 1, 2). It consists of 220 m thick succession of carbonate gravity-flow deposits. The transition between the Lower and Upper Member is marked by several meters of light green marl. Four megacycles comprising thick coarse-grained conglomerates and oolite megabeds can be recognized. These are separated by 5 to 10 m thick sequences of fine resedimented carbonates. The uppermost portion is characterized by a 20 m thick thinning- and fining-upward sequence with a gradually increasing amount of replacement chert. The overlying Lastva Radiolarite is limefree.

Age: The Aalenian to Lower Bajocian foraminiferal assemblage (*Gutnicella cayeuxi* (LUCAS), *Spiraloconu-*

lus perconigi ALLEMAN & SCHROEDER (determination by M. Septfontaine)) was found in the first oolite bed at Sutomore. Chert samples 10 m above the lowest outcropping oolite at Čanj yielded lower to lower upper Bajocian radiolarians (Chapter 6). The Lower Bar Limestone Member is overlain by shales or marls. The transition between both members is often covered. The supposed age for the transition from the Lower to the Upper Member is lower Toarcian, based on the lithologic correlation with widely expanded clay-rich deposits of this period (Jenkyns & Clayton, 1986; Jenkyns, 1988).

The top was dated with radiolarians obtained from the overlying Lastva Radiolarite. They indicate an Oxfordian age (Bar, sample BM 102; Din Vrh, sample DIN 1.50 m; Chapter 6).

2.3.3.2 Composition

The description includes turbidites intercalated in basin plain Lastva Radiolarite Formation (see Chapter 2.4).

The unique lithological unit of the Upper Bar Limestone Member is the pure oolite megabeds. Otherwise the facies of both members are identical.

Oolitic packstone (Pl. 27, Figs. 1, 3) consists of 60–70% debris in a micrite matrix; it is generally recrystallized to microsparite, rarely to pseudosparite. Ooids comprise 60–90 % of all platform-derived clasts. They are large (1 mm in diameter), generally with a concentric, rarely radial structure. Completely micritized ooids are common.

Other clasts are echinoderms, molluscs, oncoids, codiacean algae, encrustacean algae (*Pseudolithocodium carpaticum* MIŠIK), peloids and rare large hollow sponge spicules. The following foraminifera were found (determination by M. Septfontaine; for the stratigraphically important species the position in the sections is indicated in brackets):

Amijiella amiji (HENSON)
Everticyclammina sp.
Gutnicella cayeuxi (LUCAS) (Sutomore 106.00 m, Sutomore 122.00 m, Gornja Lastva 225.70 m)
Lenticulina sp.
Mesoendothyra croatica GUŠIĆ
Nautiloculina oolitica MOHLER
Placopsilina sp.
Protopeneroplis striata WEYNSCHENK (Čanj 214.20 m, Čanj 228.00 m, Petrovac 65.60 m)
Siphovalvulina sp.
Spiraloconulus perconigi ALLEMAN & SCHROEDER (Sutomore 106.00 m, Gornja Lastva 225.70 m)
Trocholina sp.

Gutnicella and *Spiraloconulus* make their first appearance in the Aalenian (Septfontaine et al., 1991). They were found coexisting near the base of the Upper Member. Other taxa confirm the Middle Jurassic age.

The genera *Gutnicella*, *Protopeneroplis* and *Spiraloconulus* are restricted to the outer shelf margin, the others are ubiquitous (Septfontaine 1980, 1985, pers. comm. 1992). No typical inner-shelf foraminifera have been found.

2.3.4 Comparison between Lower and Upper Member, paleogeographic pelationship With The High Karst Platform

The Upper and Lower members differ in composition, facies associations and distributional patterns.

Composition: The grain constituents in both members of the Bar Limestone show the same origin of sediment supply: penecontemporaneous platform-derived debris mixed with semilithified coeval pelagic limeclasts. The higher proportion of ooids in the Upper Member (60 to 90 % vs. maximum 40 % of shallow-water grains in the Lower Member) reflects an increased production in the source area. The adjacent High Karst Platform was dominated by a system of oolitic bars in the Middle Jurassic, whereas during the Liassic only smaller discrete oolitic shoals were formed (Radoičić, 1982).

Facies association: The Upper Bar Limestone Member reveals dominant coarse-grained high-density turbidites associated with oolitic megabeds and about 10 % of fine resedimented carbonates. Oolitic sands locally filled in the pre-existing channels (Sutomore section).

Compared to the Lower Bar Limestone Member, the overall succession of the Upper Member exhibits a coarser grained composition, thicker bedding and proportionally less lime mudstone beds associated. The calculated sedimentation rate (Chapter 3, Fig. 3.2) is about 15 m per million years for the Lower and about 10 m for the Upper Member. Taking into account also the thicker bedding, a decrease in frequency of gravity-flow events can be inferred.

Lateral distribution: The Upper Bar Limestone Member is less extended laterally than the Lower Member (see Fig. 4.1, compare Figs. 4.3a and 4.3b, Chapter 4). The carbonate slope facies association characterizes only the upper tectonic unit (basin margin). Coeval deposits in the lower tectonic unit are lime-free radiolarites, occasionally punctuated by resedimented carbonates (basin plain). The antecedent topography could allow the base of the Upper Member to accumulate distally (Čanj section).

The Middle Jurassic platform margin is believed to have acted primarily as a barrier. The dominant component resedimented to the basin was the marginal oolitic sand, which was not cemented at an early stage. It moved downslope and triggered compound gravity flows, which travelled relativelly short distances and

produced depositional geometries with steeper slopes (see Kenter, 1990). The retreat of oolitic bars to the interior of the High Karst Platform starting at the end of the Liassic and continuing during the Dogger (Radoičić, 1982), amplified the shift of the slope-facies belts to the northeast. The main periods of lagoonal-mud off-bank transport could occur only when the platform was completely flooded. Less fine carbonate was dispersed seaward than during the Early Jurassic which allowed the lime-free radiolarite to accumulate in the basin.

The Middle Jurassic resedimented limestones of the upper tectonic unit around Kotor Bay are volumetrically subordinate to holosiliceous deposits (Cadet, 1978). This observation implies that the differences between the northwestern and southeastern depositional area as recorded during the accumulation of the Lower Bar Limestone Member, persisted to the Middle Jurassic.

In the Čanj section a 20 m thick unit of oolite, coarse-grained graded conglomerate and calcarenite is interstratified in the radiolarite. It represents a single compound gravity-flow deposit. The overlying radiolarite is Callovian in age. In the northwestern part of the basin (Bijela, Gornja Lastva), the resedimented carbonates of this age are abundant but single-event deposits do not display any exceptional thickness. Similarly to the Liassic resedimented carbonates, we can deduce that coarse-grained units are discontinuous, locally restricted, and dependent upon variations in basin margin topography.

2.4 Lastva Radiolarite

2.4.1 Definition

Type section: Lastva (location Fig. 1.2, p. 16, Figs. 1.4, 2.3) The formation is named after the type locality.

The Lastva Radiolarite is a sequence of rhythmically alternating chert and shale layers. Beds of silicified calcarenites are intercalated.

The radiolarites conformably overlie the Bar Limestone Formation. The base is abrupt. It is defined with the first thick sequence of variegated shale or radiolarian chert. The lithological change is generally well marked also by field morphology and vegetation, which allows an easily mappable distinction of both formations. At the upper boundary the Lastva Radiolarite is overlain by siliceous reddish limestone (Praevalis Limestone). A part of these two pelagic sequences can be displaced by platform-derived resedimented carbonates.

Age: The formation was dated by radiolarians. The oldest age obtained is Aalenian-lower Bajocian, 35 meters above the contact with the Bar Limestone in the Lastva section (sample GL 123, Chapter 6). A palynological study of the equivalent "Pelites de Kasteli" in the Pindos Zone revealed a Liassic age (Lyberis et al., 1980). On the basis of organic-matter enrichment, Jenkyns (1988) assumed the lower Toarcian for this lithologic unit. The youngest recorded age for the base of the formation is Oxfordian (Din Vrh, sample 1.50, Chapter 6). The top is upper Tithonian and synchronous in the continuous pelagic succession. When overlain by resedimented carbonates the topmost radiolarites can be as old as the Kimmeridgian.

As a consequence of the highly variable time span of the radiolarite accumulation, the thickness of the formation varies from about 20 meters (Din Vrh) to 150 meters (Gornja Lastva). In sequences attributed to the High Karst – Budva Zone transition, the Jurassic radiolarite is missing (D'Argenio et al., 1971; Radoičić & D'Argenio, 1988).

2.4.2 Facies description

Considering the colour, shale content and bedding style the following radiolarite facies can be distinguished from base to top (Fig. 2.3):

The **variegated** facies is divided in two parts. The first (V1) (Pl. 28, fig. 4) is characterized by a very high proportion of dark green or brownish shale alternating with thin beds of chert. Most chert beds are about 5 cm thick grey laminated siliceous sandstone consisting of sponge spicules and radiolarians. The high concentration of siliceous organisms and laminated structure suggests a bottom-current redeposition. The preservation of radiolarians is extremely poor. Centimeter-thick layers of dark variegated argilaceous chert are present. These contain rare moderately preserved radiolarians. Chert beds do not exceed 30 % of the sequence.

Higher in the sequence (V2) the shale constituent gradually decreases (Pl. 28, fig. 5). Dark reddish-green chert beds are thicker (5 to 10 cm), sometimes nodular, and are progressively less argilaceous. Siliceous sandstone beds disappear. Cherts represent 60 % to 90 % of the sequence. Moderately preserved radiolarians can be found in all chert beds. The slightly argilaceous chert occasionally contains a very well preserved and diverse fauna.

Green radiolarite (G) generally consists of thicker (average 10 cm) unevenly bedded, sometimes laminated greyish-green chert. Thin interlayers of slightly argilaceous yellowish-green chert are present at joints. They contain a small percentage of diagenetic pyrite (oxidized to limonite) in the form of scattered euhedral crystals. The content of chert varies from 95 % to 100 % of the sequence. The uppermost part of the green radiolarite in the Bar and Bijela sections is composed of thin, evenly bedded argilaceous chert with 20 % shale interlayers. The average preservation of radiolarians is very poor. Thinner yellowish interlayers, on the contrary, can yield pyritized Nassellaria-dominated fauna.

Greenish-red (GR) knobby radiolarite is characterized by 3 to 15 cm thick undulating chert beds alternating with a maximum 5 % shale. This facies is a few meters thick and always interstratified between green radiolarite and red knobby radiolarite. Chert beds are red in the middle part and green at the margins. The original colour was probably red, the margins owe their green colour to diagenesis. Radiolarians are abundant, diverse and well preserved.

Red knobby radiolarite (Rk) facies consists of decimeter-sized nodular chert beds with a high pinch to swell ratio. No shale is interlayered. At Čanj, where the facies is best exposed, it changes from orange-red through dark red to brick-red upsection. Radiolarians are well preserved.

Red ribbon (Rr) radiolarite displays a very regular alternation of dark brownish-red argilaceous chert (beds 3 to 6 cm) and centimeter-sized shale interlayers. The content of chert beds varies from 80 % to 90 %. In the Čanj section this facies is directly overlain by pelagic cherty limestone, the uppermost portion (3.5 meters) is brick red, containing some dispersed carbonate. Radiolarians are very abundant but moderately preserved and usually compressed because of the compaction of the relatively clay-rich sediment.

Besides radiolarians, sponge spicules and rhaxes occur through all the radiolarite succession. They are especially abundant in the lower variegated facies, where they predominate over radiolarians.

Carbonate gravity-flow deposits are intercalated throughout the Lastva Radiolarite. Calcarenite beds are silicified, generally 5–20 centimeters thick, rarely up to 30–40 centimeters. Occasionally thicker graded turbidites which escaped complete silification are interstratified. They were studied in thin section, for composition see Chapter 2.3.3.2. The frequency of calcarenite beds varies from absent to more than 50 % of the succession.

2.4.3 Radiolarian dating

The Lastva Radiolarite was systematically sampled at 5 m to 10 m intervals (Fig. 2.3). The biostratigraphic correlation among the sections studied was accomplished by means of the BioGraph computer program (Savary & Guex, 1991), based on the Unitary Association Method (Guex, 1977, 1991). The age assignment is based on published radiolarian zonations. Details on procedure and results are given in Chapter 6; radiolarian species present in each sample are indicated in the Appendix.

2.4.4 Relationship with older, time-equivalent, and younger formations

The oldest age obtained for the Lastva Radiolarite is Aalenian-lower Bajocian in the Gornja Lastva section. A relatively thick lime-free succession below the lowest radiolarian samples (Gornja Lastva, Bijela) suggests that the accumulation of radiolarite could start as early as Toarcian. The lower Dogger or earlier onset of radiolarites is a general characteristics of the Tethyan basins which had subsided in the Triassic (De Wever & Dercourt, 1985; Baumgartner, 1987; De Wever, 1989).

The Lastva Radiolarite interfingers with platform-derived resedimented carbonates (Upper Bar Limestone Member) which locally (Bar, Din Vrh) inhibited the accumulation of radiolarite as a normal basin-plain sediment. It is thus easy to explain the highly variable age of the base of the formation within the same basin. The maximal diachronism recorded ranges from the Aalenian-lower Bajocian (or maybe even Toarcian) to the Oxfordian. The same phenomenon of platform originating gravity-flow deposists, which displaced the autochthonous pelagic sediment, is observed for the top of the formation in the northwestern edge of the basin. The distance from the source area, type and rate of platform production, tectonics, slope morphology and slope to basin transition relief, which controlled the distribution of the resedimented carbonates, determined indirectly the distribution of the radiolarite deposition.

The radiolarite accumulation reached its maximum expansion in the Oxfordian and Kimmeridgian. At that time the High Karst Platform was rimmed by a reef (Radoičić, 1982). The reef facies occurs along the entire High Karst Platform margin facing now the Budva Basin (Grubić, 1983). The early lithified reef barriers blocked the transport of shallow water sediment off shore and therefore favored radiolarite deposition in the basin.

The development of a reef complex is a general characteristic of Dinaric carbonate platforms in the Upper Jurassic. Bosellini et al. (1981) interpreted the transition from oolitic barriers to reef-rimmed platform on the Friuli Platform, and suggested that the oolitic "factory" shut down because of a short eustatic drop in sea level in the Callovian proposed by Hallam (1978, R11 regression in Hallam, 1989, compare Fig. 4.2). The subsequent Oxfordian transgression flooded the cemented bottom and provided a suitable substratum for reefal organisms.

The radiolarite deposition was replaced by pelagic limestone in the Upper Tithonian. The increase of carbonate is abrupt (Čanj, Bar) except, where calcarenites and marls are intercalated (Lastva, Din Vrh).

Contemporary changes in lithology characterize the western Tethys and Atlantic sections. Weissert and Channell (1989) documented a progressive decrease of the carbon isotope curve starting at the Kimmeridgian-Tithonian boundary and achieving minimum values in the Upper Tithonian. They related this to other synchronous changes in the Tethys and Atlantic indicating a

N W

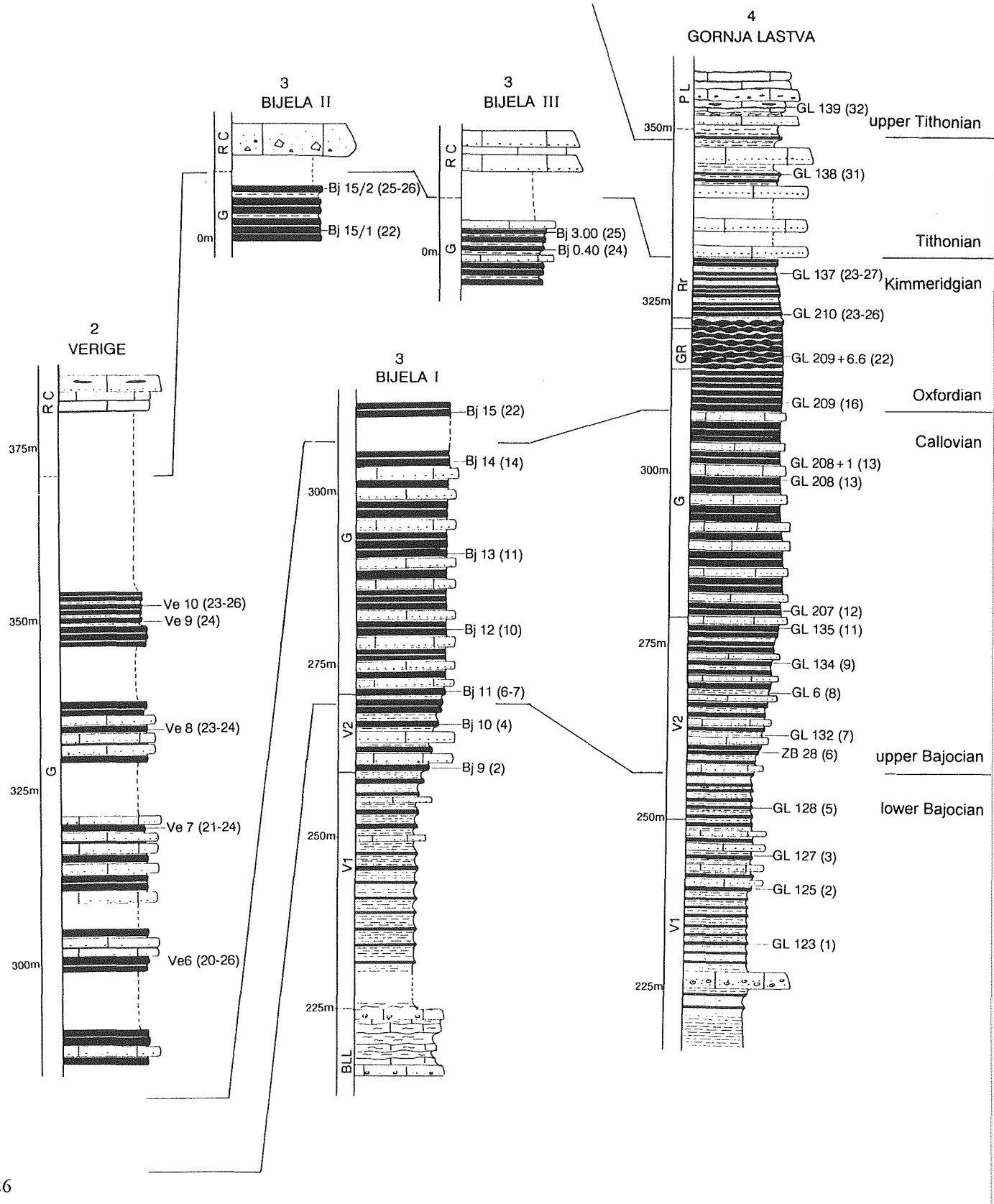
2
VERIGE
R C
G
375m
350m
325m
300m
Ve 10 (23-26)
Ve 9 (24)
Ve 8 (23-24)
Ve 7 (21-24)
Ve6 (20-26)
3
BIJELA II
R C
G
0m
Bj 15/2 (25-26)
Bj 15/1 (22)
3
BIJELA III
R C
G
0m
Bj 3.00 (25)
Bj 0.40 (24)
3
BIJELA I
G
V2
V1
BLL
300m
275m
250m
225m
Bj 15 (22)
Bj 14 (14)
Bj 13 (11)
Bj 12 (10)
Bj 11 (6-7)
Bj 10 (4)
Bj 9 (2)
4
GORNJA LASTVA
P L
Rr
GR
G
V2
V1
350m
325m
300m
275m
250m
225m
GL 139 (32)
GL 138 (31)
GL 137 (23-27)
GL 210 (23-26)
GL 209+6.6 (22)
GL 209 (16)
GL 208+1 (13)
GL 208 (13)
GL 207 (12)
GL 135 (11)
GL 134 (9)
GL 6 (8)
GL 132 (7)
ZB 28 (6)
GL 128 (5)
GL 127 (3)
GL 125 (2)
GL 123 (1)
upper Tithonian
Tithonian
Kimmeridgian
Oxfordian
Callovian
upper Bajocian
lower Bajocian

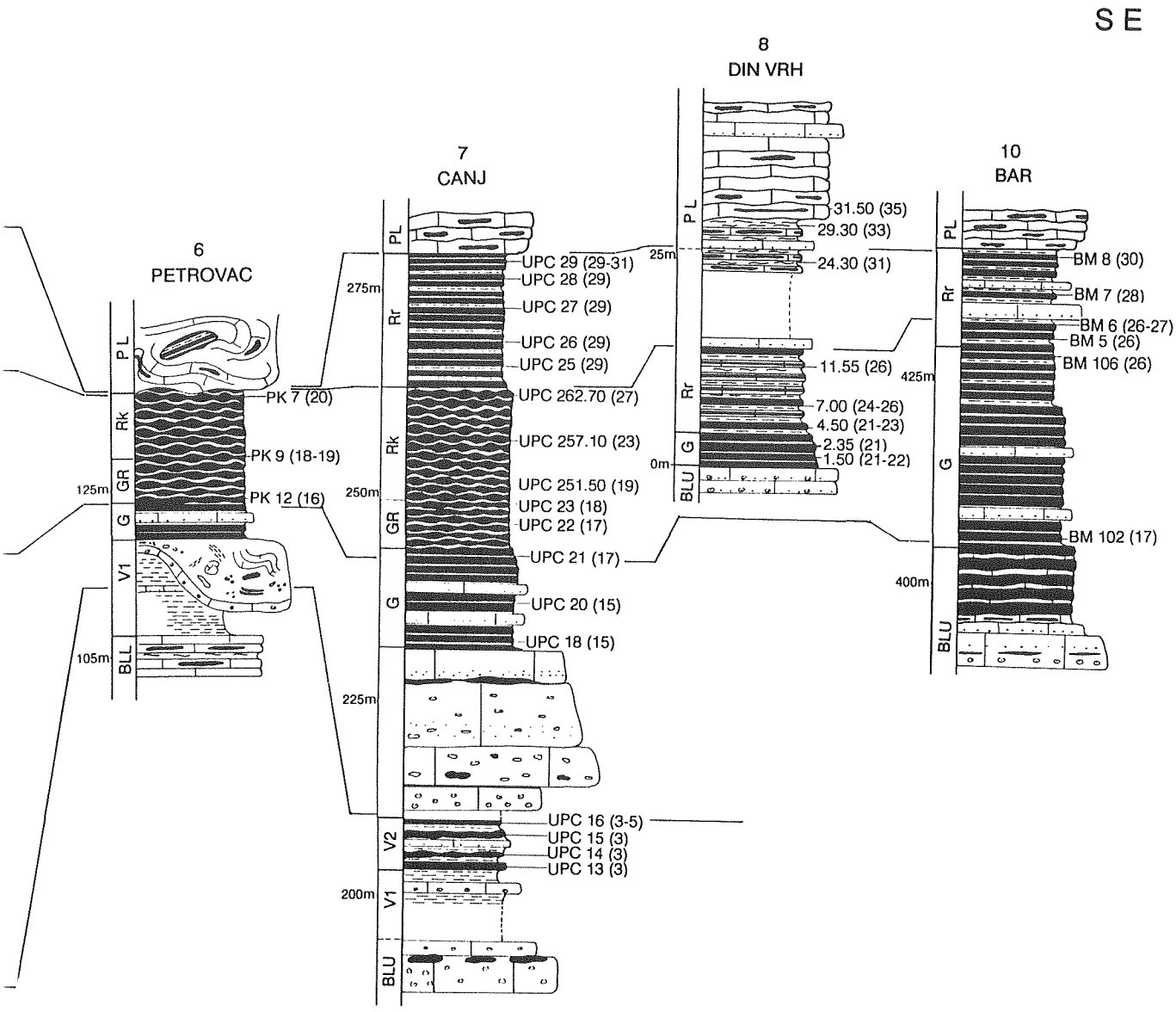

Fig. 2.3: Lithological columns of the Lastva Radiolarite Formation and position of samples. Number within brackets refers to corresponding unitary association. Main stratigraphic correlations are shown by solid lines. Legend: same as Fig. 1.4.
Abbreviations of different radiolarite facies: V1–lower variegated, V2–upper variegated, G–green, GR–greenish red knobby, Rk–red knobby, Rr–red ribbon.

modification in ocean chemistry. They concluded that drier climate conditions in the Upper Tithonian and Early Berriasian, as stated also by Hallam (1984, 1986), decreased water runoff on continents bordering the Tethys, diminished transfer of nutrients to the ocean and consequently reduced surface water productivity. Other scenarios explained changes in radiolarian versus nannoplankton sedimentation in terms of changes in upwelling conditions (Jenkyns & Winterer, 1982), decreased influence of a Late Jurassic equatorial current (Baumgartner, 1984, 1987), or establishment of a global equatorial current system through Central America (De Wever et al., 1986a; De Wever, 1989).

Most of the complete Tethyan sections deposited during the Tithonian-Berriasian show a rather gradual lithological transition to lime-rich facies (see Baumgartner, 1984). They are characterized by a significant amount of carbonate starting already in the Oxfordian. An abrupt change from radiolarite to limestone sedimentation has been observed in the Pindos (Fleury, 1980; Baumgartner, 1984; De Wever & Cordey, 1986) and in distal sequences of the Budva Zone. A progressive increase of carbonate in some sections (Lastva, Din Vrh) was probably related to local input of lime-mud from the adjacent platform.

2.4.5 Lateral and vertical relationship among different radiolarite facies

The relative abundance of interstratified calcarenites, proportion of shale interbeds, and colour change from green to red chert were plotted in a time-scale diagram (Fig. 2.4). Distinctive radiolarite facies show a regular distribution pattern.

Calcarenites and shales: The percentage of intercalated calcarenite beds differs laterally according to the proximity of the High Karst Platform. The major observed vertical shifts toward higher or lower values occur in parallel. A high frequency of resedimented carbonates is recorded through the Middle Jurassic. It abruptly passes to minimum values, characteristic of the Oxfordian and Kimmeridgian. A synchronous increase takes place at the Kimmeridgian-Tithonian boundary.

Changes in clay content occur more or less simultaneously in the whole basin. From the Toarcian to the Bathonian the clay constituent progressively decreases and reaches its minimum during the upper Bathonian to Oxfordian. An increase of the clay content is recorded in the Kimmeridgian. At the Čanj section it is slightly delayed.

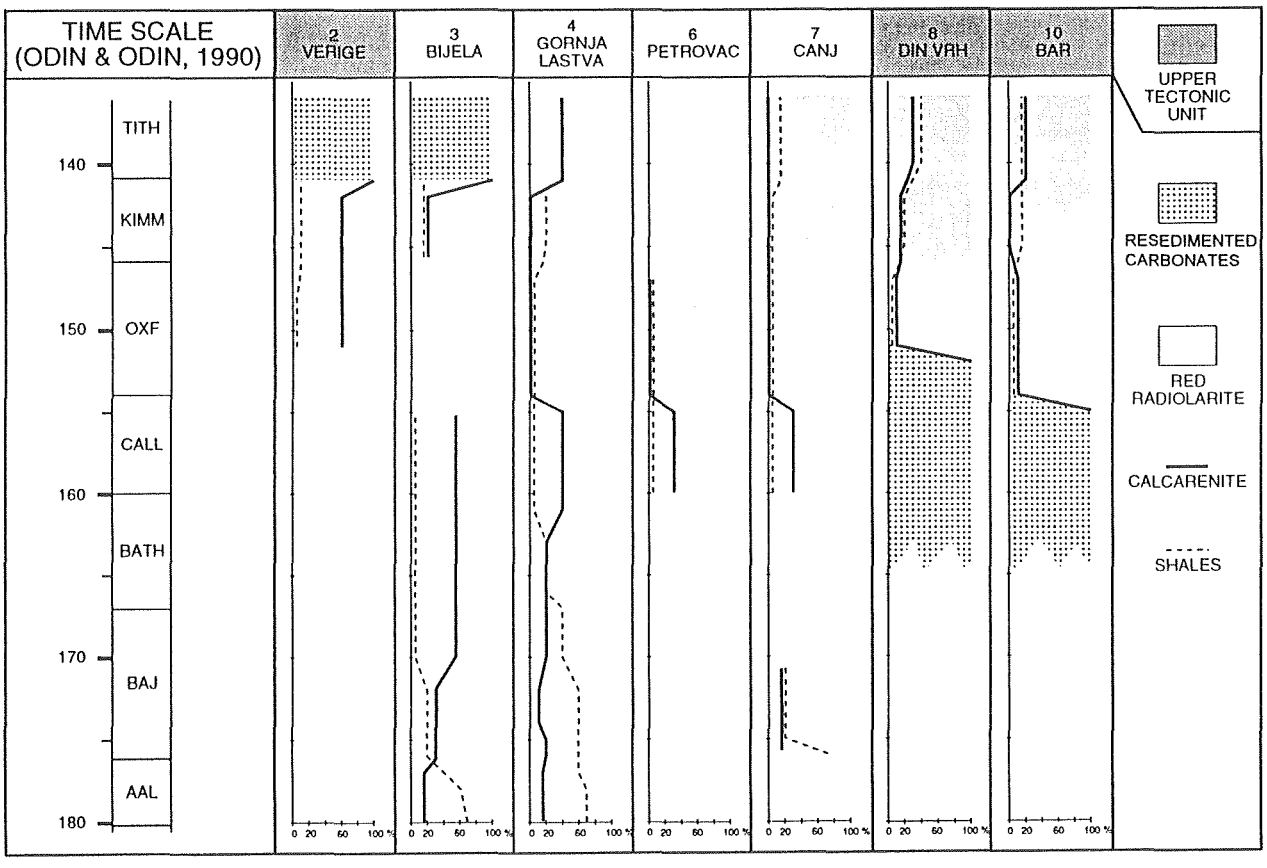

Fig. 2.4: Time-scale diagram showing variations in proportion of calcarenites and shales interstratified between cherts. Time span of accumulation of red radiolarites (GR, Rk and Rr facies) is also indicated.

The red knobby (Rk) chert, when present, is overlain by red ribbon (Rr) chert. This facies change is a consequence of an increased input of clay which reduced the permeability of the sediment. Therefore, it cannot be used as a stratigraphic marker even over relatively short distances (compare sections Gornja Lastva and Čanj in Figs. 2.3 and 4.1).

The pre-Oxfordian succession in the Gornja Lastva section shows a distinctive maximum frequency of resedimented carbonates through the upper Bathonian and Callovian (compare also Chapter 3, Fig. 3.1), coupled with minimum values of shale components. The Middle Jurassic High Karst Platform characterized by an oolitic-barrier rim and steep slopes can be compared to the tropical-water carbonate platforms with a pronounced highstand shedding (review in Schlager, 1992, Eberli, 1991a,b). The high volume of resedimented carbonates would thus imply a local sea-level highstand during the upper Bathonian and Callovian. On the other hand, the Middle Jurassic temporal variations in resedimented carbonates and shale abundance are poorly reproducible through the Budva Zone. On the basis of our data they cannot be directly interpreted in terms of sea-level oscilations.

The drastic reduction of resedimented carbonates at the Callovian-Oxfordian boundary coincides with the development of a protective reef on the platform margin (Radoičić, 1982) which efficiently dammed off-shore sediment transport. Hence, the Oxfordian and Kimmeridgian basinal facies were sedimented almost free of resedimented carbonates.

The Kimmeridgian addition of clay input can be correlated with the bauxite deposits in the interior of the High Karst Platform. The roof of the main bauxite deposits of Montenegro consists of lagoonal limestones with *Clypeina jurassica* FAVRE, assigned to the Tithonian (Bešić et al, 1965; Burić, 1966, Radoičić, 1982). The bed and wall rock show ages ranging from Upper Jurassic back to Upper Triassic (Bešić et al., 1965, Burić, 1966) which implies that some parts of the High Karst Platform were emerged during a longer period. The increased clay runoff might have been a consequence of the High Karst Platform emergence. A global sea-level highstand has been postulated for the Kimmeridgian (Haq et al., 1988; Hallam, 1988). The sea level drop on the High Karst Platform in this period was thus probably induced by local tectonics. Significant lateral differences in time of subaerial exposure between the different regions of the High Karst Platform would further corroborate with this hypothesis. The correlation between the clay input in the Budva Basin and bauxite deposits in the High Karst Platform remains, nevertheless, speculative since the provenance of clay in the Budva Zone has not been studied.

The Tithonian increment of the interstratified calcarenites postdates the increase of clay constituent. It is synchronous with reef-derived resedimented carbonates, which completely displaced the radiolarite in the northwestern part of the basin. The existence of resedimented carbonates also in the southern part of the basin suggests that both may be related to the same event (probably tectonic) which provoked a partial erosion of the platform margin (see Chapter 2.5).

The abundance of calcarenites as well as clay constituent in the Lastva Radiolarite reveals more or less synchronous changes in all parts of the Budva Basin. General controlling factors can thus be inferred. At least at the relatively coarse time-scale comparison the local topographic variations seem to play a subordinate role in determining the facies distribution.

Colour change: The green radiolarite facies (G) is widespread all over the basin in the Bathonian and Callovian. Upwards it can either pass to red knobby (Rk) or directly to red ribbon (Rr) facies. As shown in the diagram (Fig. 2.4) the colour change, signifying change from oxygen-depleted to relatively more oxygenated sea bottom conditions, does not appear synchronously. The oldest recorded red radiolarites are lower Oxfordian (Čanj section).

On the basis of the distribution of the resedimented carbonates, a relative distance from the platform can be established for the sections studied. The diachronous limit between green and red radiolarite follows the same pattern. Low-oxygen conditions persisted longer in near platform areas.

The Din Vrh section is an exception to the rule. Compared to the Bar section, the radiolarite sedimentation started later, which evokes a shorter distance from the platform. On the contrary, the green to red colour change occurred earlier. It should be noted that throughout the sequence some fine-carbonate beds are intercalated. The carbonate input provoked an increase of the pH of the bottom water and thus allowed the red facies to accumulate at a relatively lower Eh (Eh-pH diagrams of Garrels & Christ, 1965).

The landward side of the semi-enclosed basins with estuarine circulation acts as a nutrient trap enhancing organic productivity (De Boer, 1991). This model could provide a possible explanation for the oxygen-depleted conditions in near-coast areas of the Budva Basin. Organic matter enrichment due to faster burial rates or higher plankton production remains difficult to prove because the green facies does not systematically couple with higher sedimentation rates (see Chapter 3) nor with thicker chert beds. A higher productivity of nonskeletal organisms is nevertheless possible. The oxygenation of bottom water was furthermore a function of bathymetry and deep oceanic currents. The Budva Basin is comparable to the Recent Guaymas Basin, Gulf of California, with the basin sill situated below the core of oxygen

minimum layer (Ingle, 1981). The progressive change to more expanded oxygenated conditions through the Late Jurassic might have been a result of progressively increasing depth or bottom water circulation.

2.5 Jurassic-Lower Cretaceous resedimented carbonates

2.5.1 General description

Resedimented carbonates (Fig. 2.5) were deposited as a time-equivalent facies to a part of the radiolarites and Praevalis Limestone. They are composed mainly of turbidites, consisting of graded fine breccia or calcarenite, to calcisiltite sequences, occasionally with thin marl interbeds. Calcarenite beds are usually 50–70 cm thick, sometimes more than 2 m thick. Parallel lamination is a common sedimentary structure.

The most characteristic deposits are up to 12 m thick debris-flow breccia beds. These consist of pebble to cobble-sized angular reef-limestone clasts in a micritic matrix. Slump folds are present. The overall succession contains 15–25 % of replacement chert.

Age: Kimmeridgian age was determined in the highest radiolarite beds below the breccias. Upper Tithonian-Berriasian radiolarian assemblage was found below a fine-grained breccia bed containig stromatoporoids in the Gornja Lastva section. *Calpionellopsis oblonga* (CADISCH), which indicates an upper Berriasian to lower Valanginian age (Remane, 1985), occurs in the upper part of the Verige section in breccia matrix (Radoičić & D'Argenio, 1988). The carbonate gravity-flow deposition thus persisted at least through the Berriasian.

2.5.2 Composition and sources

Breccias and calcarenites consist of angular lithoclasts, usually densely packed, sometimes showing stylolitic contacts. Matrix is generally completely recrystallized. Subhedral dolomite crystals frequently occur. Rarely, matrix consists of pelagic carbonate mud or sand-size platform debris. Sorting is very poor.

Most of lithoclasts originated from shallow-water environments. Several microfacies were recognized: boundstone, oolitic grainstone, peloidal wackestone, and packstone with bivalves, foraminifera and intraclasts. Subrounded carbonate-mudstone clasts with pelagic fauna are very rare.

The skeletal debris was mainly transported incorporated in lithoclasts. Individual fossil remains can be found in the calcarenite fraction. The following fossils are abundant: stromatoporoids, chaetetids, binding organisms (*Tubiphytes*, *Pseudolithocodium*, *Baccinella*), oncoids, and echinoderms. Other fossils are foraminifera, thick-shelled molluscs, bryozoans and corallinacean algae.

Among the reef builders stromatoporoids and chaetetids occur throughout the sections. The following taxa were identified to a species level (determination D. Turnšek, position of samples indicated in brackets):

Astrostylopsis circoporea GERMOVŠEK (Bijela II 12 m, Fig. 2.3)

Chaetetes ehrenbergi FLÜGEL (Bijela II 12 m, Fig. 2.3)

Ellipsactinia polypora CANAVARI (Verige 430 m)

This assemblage is characteristic of the outer zone of the Oxfordian-Kimmeridgian reef body (Turnšek, 1969; Turnšek et al., 1981).

Foraminifera (determination by M. Septfontaine):

Labirinthina mirabilis WEYNSCHENK (Verige 386 m)

Alveosepta jaccardi (SCHROEDER) (Verige 386 m)

Both species are characteristic of the Oxfordian and Kimmeridgian (Septfontaine et al., 1991).

The majority of lithoclasts originated from a somewhat older reef-rimmed platform. Mainly the external zone of the reef complex seems to have been eroded. No *Cladocoropsis*, characteristic of the back-reef area, has been found in the extraclasts. Some debris represents time-equivalent pelagic origin and maybe also shallow water deposits.

2.5.3 Probable causes of platform erosion

A gradual narrowing of the Dinaric Tethys took place in the Late Jurassic and culminated in oceanic obduction at the end of the Jurassic (Dimitrijević, 1982; Pamić, 1982; Karamata, 1988) (see Fig. 1.1 for the present position of the ophiolite complex). The onset of flysch deposits containing reworked ophiolitic debris (Bosnian Flysch) has been dated as Tithonian?-Berriasian (Blanchet et al., 1969; Rampnoux, 1974; Blanchet, 1975) in the Bosnian Zone (see Fig. 1.1 for the tectonic position). An upper Tithonian-Lower Cretaceous erosion of obducted ophiolites has been documented also in the internal Albanides (Kodra et al., 1993) and in the Beotian Flysch in the Hellenides (Clément, 1971; Celet & Clément, 1971; Thiébault & Clément, 1992). The formation of bauxite horizons overlain by Tithonian deposits on the High Karst Platform (Bešić et al., 1965; Burić, 1966; Radoičić, 1982) could be ensued from regional compression-generated stresses provoking uplift, and associated with global humid climate (compare D'Argenio & Mindszenty 1991; 1992; see Chapter 2.4.5). It seems plausible that the tectonically induced uplift was responsible also for the partial erosion of the western High Karst Platform margin into the Budva Basin. Tectonic activity of the High Karst Platform as a major mechanism triggering Cretaceous carbonate gravity flows in the Budva Basin was inferred also by Obradović et al. (1988, 1989). A long-term eustatic sea-level

drop starting in the Tithonian and lasting to early Valanginian (Haq et al., 1988) might have further enhanced the erosional processes.

The onset of carbonate gravity-flow deposits marks a reef destruction event. Its Kimmeridgian-Tithonian age roughly corresponds to the extinction of most barrier reefs, which dominated the northern Dinaric Carbonate Platform margin during the lower Malm (Turnšek et al., 1981). In Montenegro, sphaeractinian reefs are supposed to range into the Lower Cretaceous (Radoičić, 1982; Grubić, 1983). Their stratigraphic distribution should probably be reevaluated. It seems likely that the reef buildups in the Tithonian and early Cretaceous, if they existed, must have had a much reduced areal extent with respect to the Oxfordian and Kimmeridgian.

2.5.4 Lateral distribution and local paleogeographic relationships

Continuous successions of upper Malm-Lower Cretaceous resedimented carbonates are confined to the northwestern edge of the Budva Zone (Fig. 4.3d). The sequence of the proximal facies (Verige section) is at least 300 m thick. The estimated thickness of the distal sequence (Bijela section) reaches 40 m. The latter terminates with a fining-upward portion grading to reddish cherty pelagic limestone. The abundance of resedimented carbonates decreases toward the southeast. In the same time interval, sections situated south of Kotor Bay show prevailing radiolarite and pelagic limestone facies with some calcarenites and rare fine breccias intercalated (Gornja Lastva, Din Vrh, Bar). These parts of the basin must have been more distant from the source area.

The observed distance of the Tertiary nappe overthrusting is greater in the southeast than in the northwest of the Budva Zone (Antonijević et al., 1969b; Mirković et al., 1968b), which partly explains the lack of outcropping slope facies. The southernmost reef-derived breccias and calcarenites are recorded in the area around Budva (Djenaš sequence in D'Argenio et al., 1971; Radoičić & D'Argenio, 1988).

In the northwestern realm the carbonate slope facies association is observed also in the antecedent (Middle Jurassic) basin-plain areas (Bijela section), whereas in the southeast, even proximal regions only occasionally received medium-grained resediments (Din Vrh, Bar) (compare Bijela and Bar sections in Fig. 4.1, Chapter 4). The pre-Tithonian bauxite deposits in the interior of the High Karst Zone are restricted to the area northwest of Podgorica (Bešić et al., 1965; Burić, 1966). The distribution of the bauxite deposits implies that the High Karst Platform was inclined toward southeast, probably due to more pronounced differential uplift in the northwestern area. For the same reason, the fracturing and erosion of the platform margin may have been more vigorous in the northwestern area. On the other hand, it seems possible that at least since the uppermost Jurassic the Budva Basin was narrower towards its present tectonic wedge-out in the northwest as already proposed by Antonijević et al. (1969b) and Radoičić (1982).

2.6 Praevalis Limestone

2.6.1 General description

Type section: Bar (location Fig. 1.2, p. 16, Fig. 2.5). The formation is named after the Roman province Praevalis, established by the emperor Diocletianus.

The sequence (Fig. 2.5) is composed of well stratified marly micrite (beds 10–20 cm) with replacement chert nodules and layers. The general colour of limestone is light red to violet red, rarely white to pale green, cherts are vivid red. Bedding planes are undulated. The amount of visible chert varies between 10 and 50 %. In the upper part of the sequence reddish marls are interlayered. Calcarenite beds are occasionally interstratified.

The limestone beds contain a maximum of 15 % calcified radiolarians in a mud matrix. Very rare calpionellids were found in the lower part of the sequence. Relativelly abundant and well preserved radiolarians were extracted from chert nodules.

Age: The Praevalis Limestone lies on the top of the Lastva Radiolarite. Radoičić (in D'Argenio et al., 1971; Radoičić & D'Argenio, 1988) found the upper Tithonian *Calpionella alpina* LORENZ near the base. Our radiolarian dating is not continuous all over the sequence. Berriasian-lower Valanginian, and upper Valanginian to Hauterivian assemblages were found in different sections. The base of the overlying Bijela Radiolarite is assigned to the Hauterivian-lower Barremian. In the Bar section the carbonate sedimentation continued to the upper Aptian-lower Albian, as confirmed by radiolarians and planktic foraminifera: *Hedbergella trocoidea* (GANDOLFI), *Ticinella* cf. *bejaouensis* SIGAL, *Ticinella* cf. *roberti* (GANDOLFI) (determination by L. O'Dogherty). The top of the Praevalis Limestone in the Petrovac section is also Aptian-Albian in age. A nannoplankton sample (at 184 m in the section) characterized by dissolution-resistant forms, yielded the following species (determination by J. Pavšič): *Eprolithus floralis* (STRADNER), *Rucinolithus irregularis* THIERSTEIN, *Stradneria crenulata* (BRAMLETTE & MARTINI), *Watznaueria barnesae* (BLACK), and *Zeugrhabdotus embergeri* (NOËL). The overlying radiolarite is upper Aptian-lower Albian at the base (sample PK1). Details about radiolarian dating are given in Chapter 6.

The maximum thickness for the late Tithonian to Hauterivian-Barremian interval does not exceed 50 m.

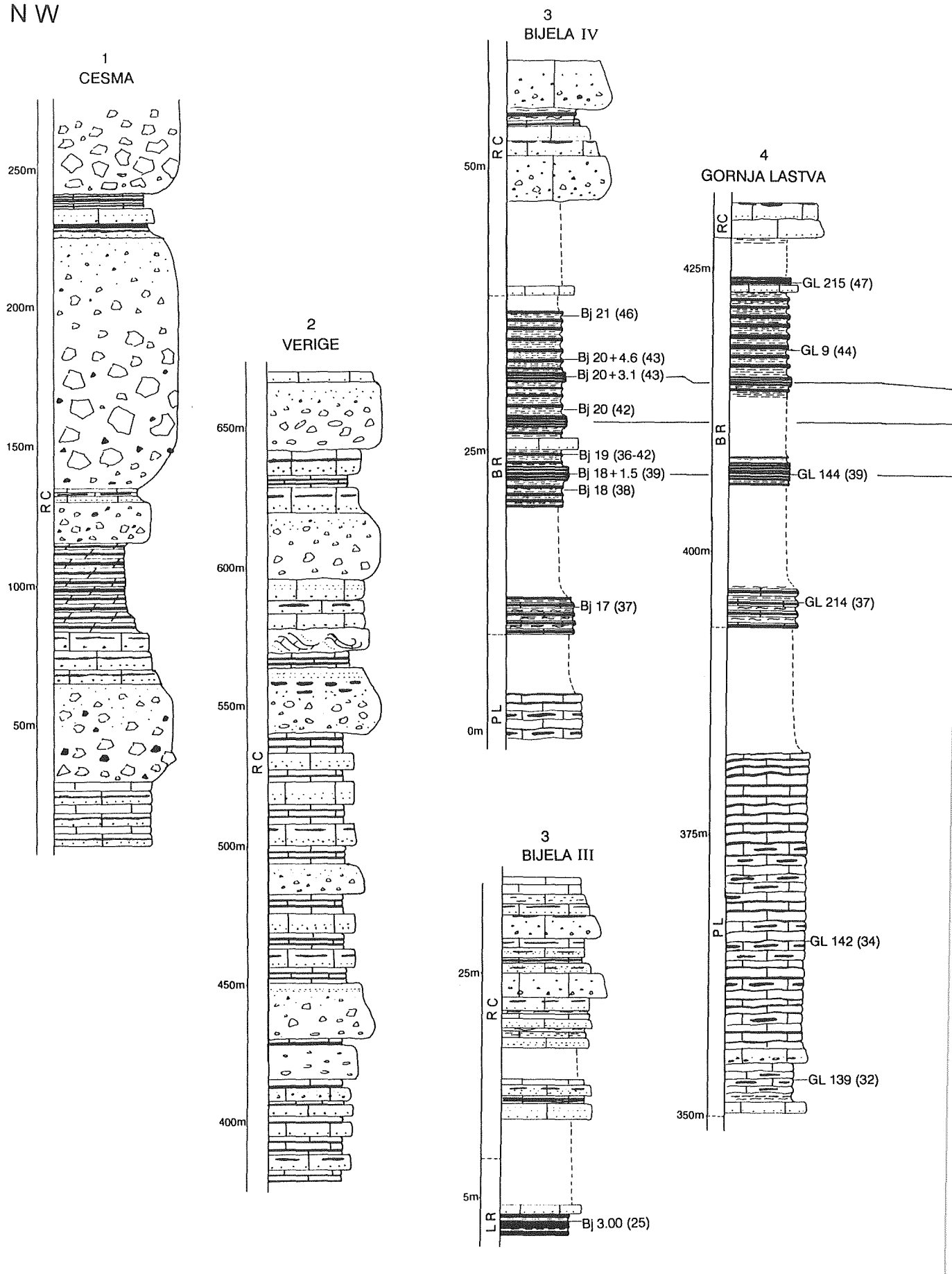
N W
1
CESMA
250m
200m
150m
100m
50m
RC
2
VERIGE
650m
600m
550m
500m
450m
400m
RC
3
BIJELA IV
50m
25m
0m
RC
BR
PL
Bj 21 (46)
Bj 20+4.6 (43)
Bj 20+3.1 (43)
Bj 20 (42)
Bj 19 (36-42)
Bj 18+1.5 (39)
Bj 18 (38)
Bj 17 (37)
3
BIJELA III
25m
5m
RC
LR
Bj 3.00 (25)
4
GORNJA LASTVA
425m
400m
375m
350m
RC
BR
PL
GL 215 (47)
GL 9 (44)
GL 144 (39)
GL 214 (37)
GL 142 (34)
GL 139 (32)

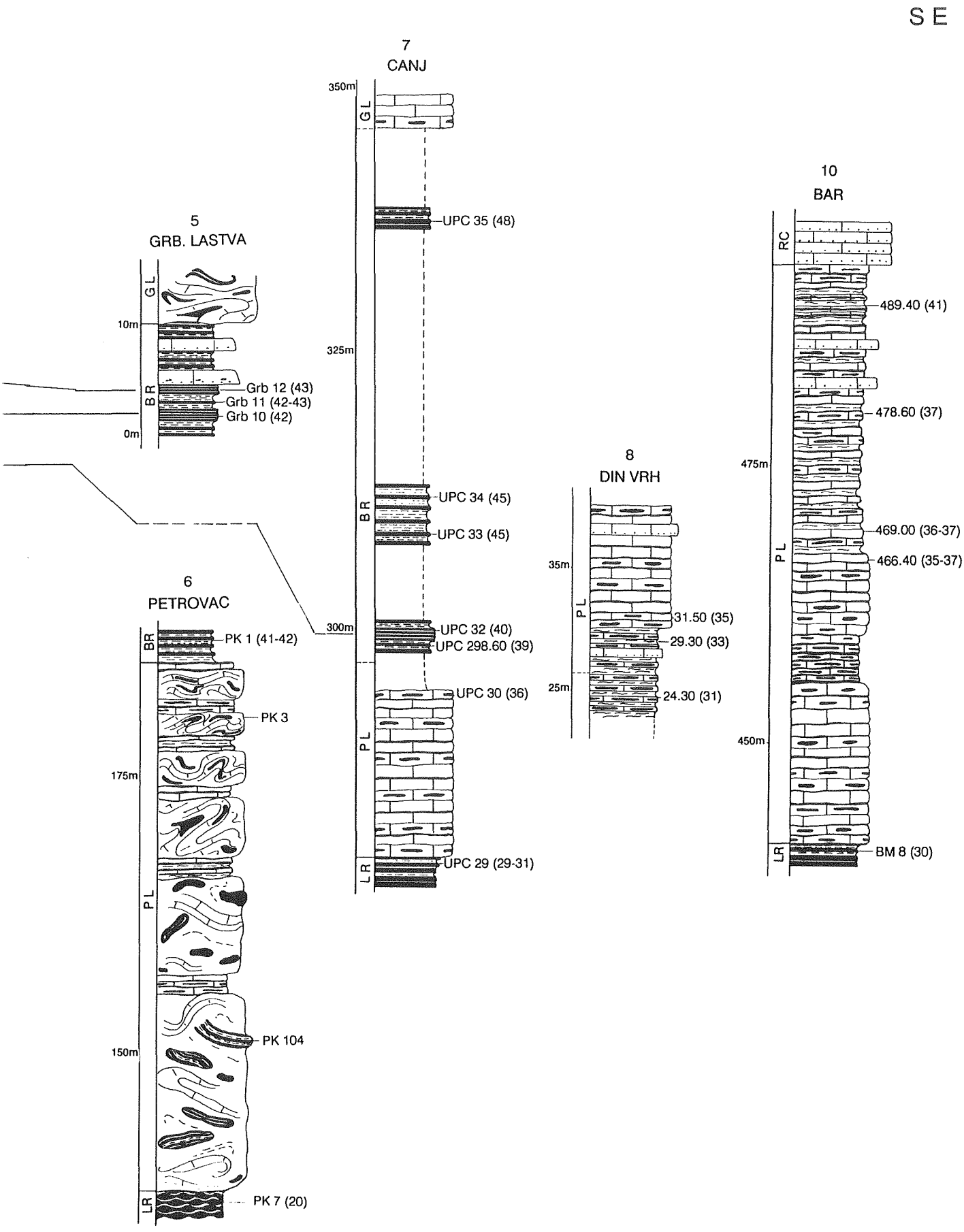

Fig. 2.5: Lithological columns of the Cretaceous formations and position of samples. Number within brackets refers to corresponding unitary association. Green levels of the Bijela Radiolarite are correlated by solid lines. Legend: same as Fig. 1.4. Note different scale for Česma and Verige sections.

2.6.2 Redeposited facies

In the Petrovac section (lower tectonic unit) (Fig. 2.5, Pl. 28, figs. 6, 7, 8) the whole lower Cretaceous succession consists of thick chaotic beds related to mass movements. They are 1 m to several meters thick, separated by a few tens of centimeters of undisturbed bedded limestone. The encompassed cherts show considerable deformation; they have a form of ruptured, folded layers or rotated nodules. Internal bedding, although extensively deformed, is usually still recognizable in the limestone portion.

In the lower part of the section up to 1 m large clasts of Tithonian ribbon radiolarite (sample PK 104, Appendix) are incorporated in these megabeds (Pl. 28, fig. 8). A chaotic bed near the top yielded a mixed Lower Cretaceous radiolarian assemblage (sample PK3) indicating a reworking of older strata. The base of the overlying radiolarite is assigned to the upper Aptian-lower Albian.

The described chaotic beds are interpreted as highly evolved slumps, which moved downslope incorporating underlying deposits. The accumulation of these debris-slump masses persisted till the Aptian-Albian, when pelagic deposition was interrupted by calcareous turbidites in the areas closer to the platform (Bar section).

2.6.3 Comparison with time-equivalent Tethyan formations

Lithologically, the Praevalis Limestone resembles the Lower Cretaceous Maiolica and Biancone facies in the Southern Alps and Apennines. The estimated sedimentation rates vary from about 6 m/Ma in the Lombardian Basin (Weissert, 1979) to about 10 m/Ma in the basinal sequences of Umbria-Marche (Baumgartner, 1990). In the Budva Zone, they show much lower values, reaching at most 2.5 m/Ma (Chapter 3). The amount of silica in the Maiolica facies is about 3–5 % (Weissert, 1979), whereas in the Budva Zone the average percentage of visible chert was estimated to 25 %.

The lithological contrasts between the Budva and other mentioned sequences could be due to lower production or more pronounced dissolution of calcareous nannoplankton and maybe also higher production of radiolarians in the Budva Basin. Lower values of carbonate content have been observed also in the Upper Jurassic deposits (Chapter 2.4).

2.7 Bijela Radiolarite

2.7.1 Description

Type section: Bijela (location Fig. 1.2, p. 16, Fig. 2.5). The formation is named after type locality. The lithological columns of the sections studied are given in Fig. 2.5.

The transition from the underlying siliceous Praevalis Limestone is gradual, marked by a progressive increase in clay and silica content. The base of the radiolarite is defined where the sequence has a typical radiolarite aspect of thin dark red siliceous beds alternating with clayey marls.

The predominant Bijela Radiolarite is dark red, characterized by a very high proportion of shale layers. Chert beds are thin (1–3 cm), generally representing 20–40 % of the sequence. In the lower and uppermost part of the sequence the chert beds are somewhat thicker (5–8 cm); they constitute 50–80 % of the sequence. At the base of the Bijela Radiolarite some dispersed carbonate is present, otherwise the overall facies is lime free. Several levels, ranging in thickness from 0.5 to 1.5 m, of green radiolarite are interstratified. The green facies is thin bedded (1–3 cm). The percentage of associated shales is lower than in red radiolarites (5–20 % vs. 20–80 %). On the basis of the vertical facies distribution and shale content it is relatively easy to distinguish the Cretaceous from the Jurassic radiolarite already in the field. The maximal estimated thickness of the Bijela Radiolarite is 60 m. Cherts yield abundant but moderately preserved radiolarians and sponge spicules. Details of radiolarian dating are given in Chapter 6, species inventory is listed in the Appendix.

Graded calcarenite beds up to 70 cm thick are interbedded in the sequence. The main component is debris of thick-shelled bivalves. Ooids, echinoderm plates and foraminifera (*Orbitolina* sp., Miliolidae, Textulariidae) occur. Angular clasts of peloidal wackestone are present in the coarser fraction. Calcarenite is occasionally capped by laminated radiolarian wackestone.

The radiolarite succession is overlain either by red *Globotruncana* limestone or by calcareous turbidites. The base of the Bijela Radiolarite is assigned to the Hauterivian-lower Barremian. The youngest age obtained for the top is Turonian.

2.7.2 Vertical facies changes

A gradual change from the Praevalis Limestone to Bijela Radiolarite indicates a transition of the sedimentary environment below the CCD. A progressive shallowing of the CCD through the Early Cretaceous period has been generally recognized in the central and southern Tethys and interpreted in terms of productivity changes (Weissert & Lini, 1991).

The estimates of silica accumulation rates in the Budva Basin show similar values in the lower Cretaceous carbonate and overlying lime-free facies (Chapter 3), thus providing no direct evidence of increasing radiolarian productivity. The lithological change seems to have occurred due to reduced production of calcareous plankton and/or enhanced dissolution of carbonate.

The upper Valanginian? to mid-Cretaceous time interval is further marked by an increase of clay components in pelagic deposits of the Budva Zone.

An important time-span of subaerial exposure and weathering in the interior of the High Karst Platform can be inferred from well documented bauxite deposits overlain by upper Cenomanian-Turonian limestone (Bešić et al., 1965; Burić, 1966; Radoičić, 1982). The bedrock consists of Upper Triassic, Lower Jurassic, Tithonian, or Lower Cretaceous carbonates (Burić, 1966). Bauxite deposits interstratified between the Tithonian and Valanginian (Grubić, 1964; Bešić et al., 1965), and Hauterivian-Barremian and Aptian (Grubić, 1964) are reported from some parts of the High Karst Zone. These might have originated from a redeposition of the pre-Tithonian bauxites (see Chapter 2.4.5). Nevertheless, it seems likely that at least some parts of the High Karst Platform were emerged during the entire early and middle Cretaceous.

We suppose that the increased proportion of clay in the Budva Basin was primarily induced by an elevated humidity. To a minor extent it may have been related to areal expansion of emergent continental-sediment sourceland. The increased clay input in the contemporaneous deposits of the Pindos Basin (Jaspes à radiolaires supérieurs, Marnes Rouges à Radiolaires, see Chapter 5) also suggest that the major factors controlling the amount of clay runoff were of regional importance.

Within the Bijela Radiolarite, which is predominantly of red colour, several levels of green radiolarite are intercalated. The interstratified green radiolarite reflects short episodes of reduced redox potential at the sediment-water interface or in the upper part of the interstitial water. A lower proportion of shale is characteristic of these levels. A reduced continental runoff might have been a consequence of a higher sea level. The oxygen deficiency was probably due to slower rate of deep-water renewal. At Bijela, three green levels occur in the sequence. The first one yielded lower Aptian radiolarians. The second green level is assigned to the upper Aptian-lower Albian. Lower-middle Albian radiolarians were found above the third green interval. An approximate correlation can be made with the green levels of the other sections studied (Fig. 2.5). The age of the first two green levels roughly corresponds to the oceanic anoxic events 1A and 1B of Arthur et al. (1990). The lower-middle Albian age of the third level suggests its position between the OAE 1B and OAE 1C. The mid-Cretaceous sedimentation in the Budva Zone reflects also global changes in oceanic conditions.

2.7.3 Lateral distribution

The Cretaceous radiolarite studied was deposited on the lower tectonic unit of the Budva Zone in the northwestern as well as southeastern depositional area (Fig. 4.3e). However, radiolarite sedimentation was not exclusively restricted to the lower tectonic unit. In the continuation of the Verige section, an approximately 30 m thick sequence of dark green bedded chert and shale is interstratified in carbonate gravity-flow deposits. At the top of this siliceous interval marly limestone and calcarenite contain *Hedbergella* sp. and orbitolinids (Radoičić & D'Argenio, 1988). The first overlying coarse-grained carbonate breccia yields rudist fragments (Čadjenović et al., 1988). This siliceous sequence is at least partly time-equivalent to the Bijela Radiolarite deposited in the lower tectonic unit. It was not studied for radiolarians in our work because the outcrop was very poorly exposed.

The southeastern depositional area was characterized by a contemporaneous deposition of radiolarites (lower tectonic unit) and pelagic limestones (upper tectonic unit). Reddish cherty limestones accumulated until upper Aptian-lower Albian in the Bar section. Marly intervals become more frequent beginning in the upper Valanginian?-Barremian. Calcarenite beds occur as intercalations in the Barremian?-Aptian and entirely displace pelagic deposits in the Albian. Lower Cretaceous pelagic sediments locally moved downslope where debris-slump chaotic beds were deposited distally (Petrovac).

Mid-Cretaceous carbonate sedimentation was thus restricted to areas which were influenced by a higher input of platform-derived lime mud and/or topographic highs.

The Cretaceous bauxites (similarly to Jurassic bauxites) are restricted to the area northwest of Podgorica (Burić, 1966). The most important deposits are known from Bijele Poljane, half way in a direct line from Kotor to Nikšić (see Fig. 1.2 for geographic position). On the basis of the distribution of bauxite deposits in the High Karst Zone we assumed that areal extent of the emerged hinterland was more important to the northwest. Consequently, the carbonate production and amount of fine-carbonate supplied to the adjacent basin were lower. The observed contrasts between holosiliceous deposits in the northwest (Verige) and carbonate deposits in the southeastern area (Bar) support the hypothesis of periplatform-ooze supply (see Baumgartner, 1987) as a major local factor determining the lateral distribution of radiolarite sedimentation in the mid-Cretaceous Budva Basin.

2.8 Middle-upper Cretaceous resedimented carbonates

2.8.1 General description

Medium-grained resedimented carbonates occasionally punctuated basin-plain facies (Fig. 2.5: Bijela, Grbaljska Lastva, Bar sections). Since the late Albian?-

Cenomanian, coarse-grained carbonate gravity-flow deposits entirely displaced pelagic sediments in the northwestern part of the basin (Fig. 2.5: Česma, Bijela, Gornja Lastva sections). The succession is composed of up to several meters thick inverse to normally graded breccias and calcarenites intercalated by marls and replacement chert layers.

2.8.2 Composition and age-diagnostic fossils

The fine-grained parts of breccia beds were studied in thin sections. These are composed of 70 to 80 % of clasts in a partly recrystalized mud matrix. Sorting is very poor. Among skeletal debris, thick-shelled bivalves prevail. *Orbitolina* sp. (samples: Grbaljska Lastva 5.10 m, Bijela IV 50 m, Bijela IV 60 m, Česma 270 m) and fragments of colonial corals, gastropods, echinoderms and ooids occur. Rock fragments comprise angular clasts of lime mudstone frequently containing Miliolidae, and wackestone and grainstone with peloids and large oncoids. Planktic foraminifera were found in the matrix, among them *Praeglobotruncana* cf. *stephani* (GANDOLFI) of upper Albian to Cenomanian age (sample Bijela IV 50 m, determination by G. Di Marco). Coarse-grained breccias overlying the Bijela Radiolarite in the Gornja Lastva section yielded *Orbitolina* sp. and globotruncanids of the Cenomanian-Turonian age (Cadet, 1978; Radoičić & D'Argenio, 1988).

Debris-flow breccias of similar composition (angular clasts derived from different shallow-water environments in a matrix composed of rudists and other shell debris) occur at the top of the Česma section (Fig. 2.5). The underlying medium-bedded silicified calcarenite contains *Rotalipora* cf. *appeninica* (RENZ) (sample Česma 236 m, determination by G. Di Marco), indicating an upper Albian to Cenomanian age. The 270 m thick section is characterized by three levels of coarse-breccia megabeds with lithoclasts reaching 2 m in diameter. Pebble-sized graded breccias and calcarenites with replacement chert are interstratified. Thinner beds are often completely dolomitized. The sequence was not dated. By correlation with other sections no older than Tithonian age is assumed for the lowermost breccia bed.

2.8.3 Local paleogeographic relationships

The composition of middle-upper Cretaceous resedimented carbonates documents a partial erosion of ancient platform margin and thus evokes genetic similarities with Tithonian-lowermost Cretaceous resedimented carbonates. Tectonic instability resulting in High Karst Platform uplift is believed to be the major cause for the return of coarse-grained carbonate gravity-flow deposits to the northwestern depositional area of the Budva Basin in the upper Albian?-Cenomanian since the global sea-level was relatively high in this time (Haq et al., 1988).

In comparison to the southeastern depositional area of the Budva Basin, the character of resedimented carbonates around Kotor Bay reveals a closer distance to the carbonate platform with the most proximal facies being recorded at Česma. The distinction may have, in addition, resulted from more intensive erosion and the presumably different nature of the platform margin (compare Chapter 2.5).

The variations between the two depositional environments are roughly correlative with those observed through the Tithonian and lowermost Cretaceous. The present dating is not precise enough to demonstrate an exact coincidence of Cretaceous turbiditic episodes through the entire Budva Basin.

3. SEDIMENTATION RATES

3.1 Introduction

Linear sedimentation rates of lithified sediment were calculated based on radiolarian dating (Figs. 3.1, 3.2). These were interpreted using the numerical time-scale proposed by Odin and Odin (1990).

The sedimentation rate of the total rock sequence was determined for all lithologies. In the radiolarites we then subtracted the interstratified calcarenite beds. To obtain the silica accumulation rate we finally eliminated the shale interlayers. The amount of clay dispersed in the chert layers was not taken into account.

3.2 Error margins

Comparison among time-equivalent sequences is subjected to about 10 % error in field measurements and 10 % error in assuming the proportion of shale or calcarenite interbeds in radiolarites and amount of visible replacement chert in limestones. An additional error can be caused by determining the position of the zonal limits on a measured section where the interval between two neighbouring samples is large. Differences up to 20 % for the total sedimentation rate and to 30 % for the accumulation rate of individual components are thus not considered significant. The estimates of silica accumulation rates for the calcarenite containing sequences can be further misleading, because the subtracted calcarenite beds are silicified.

The age assignment of the radiolarian assemblages from the Budva Zone is based on the correlation with other radiolarian zonations (Chapter 6). The calibration of the Jurassic and Cretaceous radiolarian zonations in general still allows a rather large interval of uncertainty when tied to the standard stages. Temporal variations in calculated sedimentation rates, especially when short time intervals are compared, are therefore to some degree affected by the subjective choice of the radiolarian zone boundary.

Temporal variations are further subject to the time-scale used. Average sedimentation rates through longer time-intervals (Fig. 3.2a,b) were calculated using two different absolute time-scales: Odin and Odin (1990) and Harland et al. (1990).

The presented sedimentation rates must be seen with all the above mentioned reservations. Short interval vertical correlations have the lowest confidence level.

3.3 Results

3.3.1 Sedimentation rates of the Lastva Radiolarite

The calculated sedimentation rates are graphically presented in Fig. 3.1.

Middle Jurassic: At the Gornja Lastva section a steadily decreasing sedimentation rate is observed from the Aalenian-lower Bajocian (3.5 m/Ma) to the Bathonian (2.5 m/Ma), because of a progressive decrease of shale interlayers. Almost doubled figures (4 m/Ma) in the upper Bathonian to Callovian are due to the input of resedimented carbonates. The silica accumulation rate through the same interval shows a gradual increase from 1.2 m/Ma to 2 m/Ma. The estimate is in accordance with the increase of average thickness of chert-beds (2–3 cm in the Aalenian, 5–10 cm in the Bajocian, 10 cm in the Callovian).

The Middle Jurassic sequence at Bijela expresses less variations in facies as well as sedimentation rate. The total sedimentation rate lies between 2 m/Ma and 2.6 m/Ma, or between 1.6 m/Ma and 1.3 m/Ma, if we ignore calcarenites and shales. Total sedimentation rates as well as silica accumulation rates for the upper Bajocian to Callovian are lower than in the contemporaneous Lastva section.

Sediment displacement in the axial NW–SE direction of the basin is inferred. With the diminished quantity of clay the sediment-capacity to fix the siliceous skeletons was reduced. Silica accumulation rate and bed-thickness increase at Gornja Lastva is a response to the intensified redistribution of siliceous skeletons rather than higher radiolarian production.

Oxfordian-Kimmeridgian: The average Oxfordian to Kimmeridgian silica accumulation rates obtained for the lower tectonic unit vary between 1.4 m/Ma (Gornja Lastva), 1.9 m/Ma (Petrovac) and 1.7 m/Ma (Čanj). For the upper tectonic unit sections, similar or even higher values were calculated: 1.5 to 2.0 m/Ma (Verige), 1.3 m/Ma (Din Vrh), 1.9 m/Ma (Bar). According to their paleogeographic position lower rates could be expected.

During the Oxfordian and Kimmeridgian the radiolarite sedimentation was most widely extended over the Budva Basin. The estimates of the silica accumulation rates remain within error margins. No regular pattern of sediment displacement can be recognized. It is, however, possible that the figures at least partly reflect topographic irregularities in the basin.

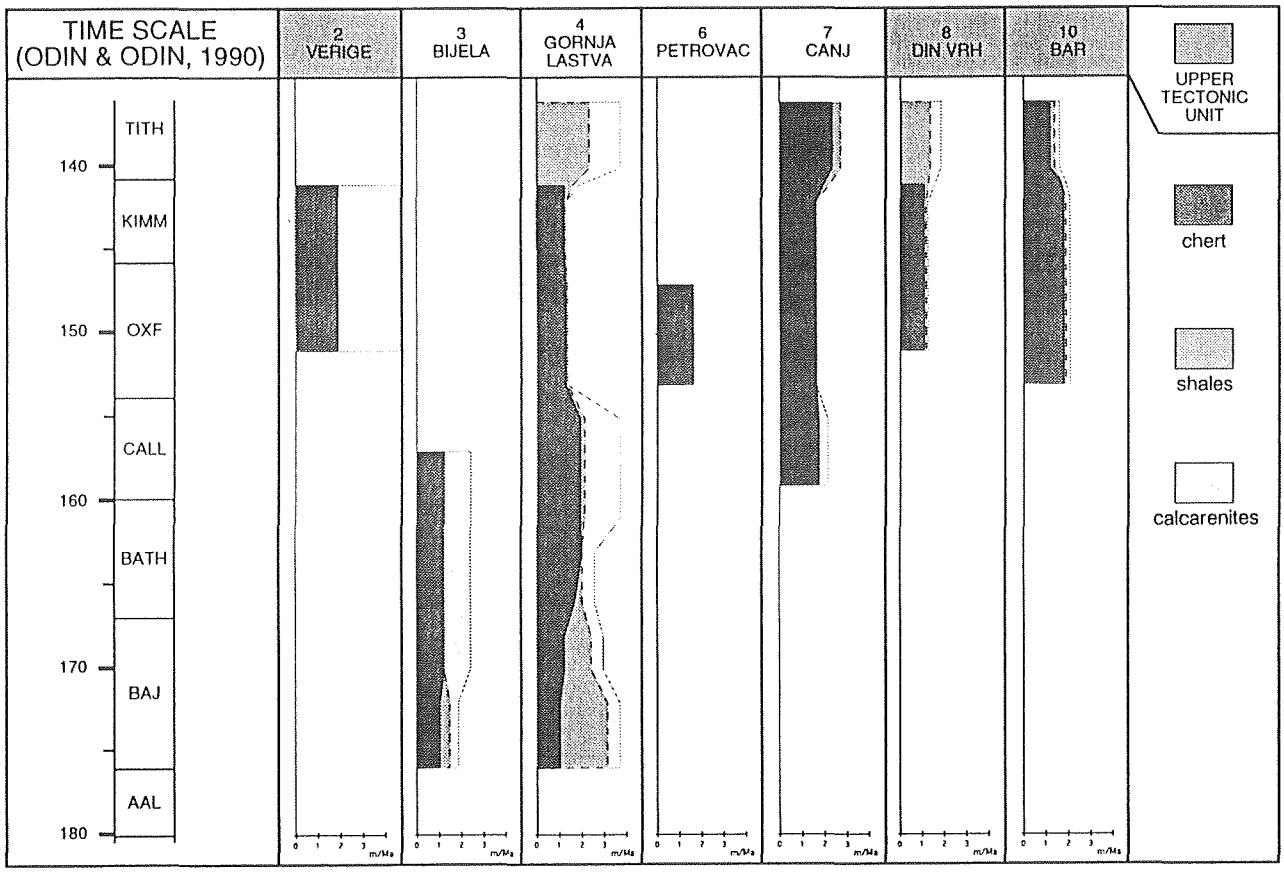

Fig. 3.1: Sedimentation rates of the Lastva Radiolarite.
Dotted lines – total rock sequence; dashed lines – shales and cherts; solid lines – cherts only.

Lower Tithonian: In the Tithonian the silica accumulation rate increased significantly in the Čanj section (2.5 m/Ma), whereas at the same time it decreased at Bar (1.3 m/Ma). Through the Oxfordian and Kimmeridgian both sections showed similar rates. This observation suggests a more important current activity in NE–SW direction, perpendicular to the basin axis. The intensified redeposition of autochthonous deposits coincides with the return of platform-derived carbonates in the basin. The higher current activity was also reflected by more oxygenated bottom water: only red radiolarites accumulated in the Tithonian.

No general direction of basin-sediment redistribution, characteristic of the entire Budva Basin could be recognized in the Lastva Radiolarite. Only nearby paleogeographic areas are mutually correlative.

3.3.2 Jurassic and Cretaceous sedimentation rates

Four most completely exposed sections were selected for the comparison of average sedimentation rates through longer time-intervals (Fig. 3.2a). Temporal variations in basin plain facies are described. Differences in sedimentation rate of the Lower and Middle Jurassic gravity-flow deposits were discussed in Chapter 2.3.4.

The lower Liassic radiolarite ("Passée Jaspeuse") sedimentation rates reach 3 m/Ma to 4 m/Ma. The silica accumulation rate of the "Passée Jaspeuse" is difficult to estimate because the carbonate and clay admixture are disseminated in chert beds.

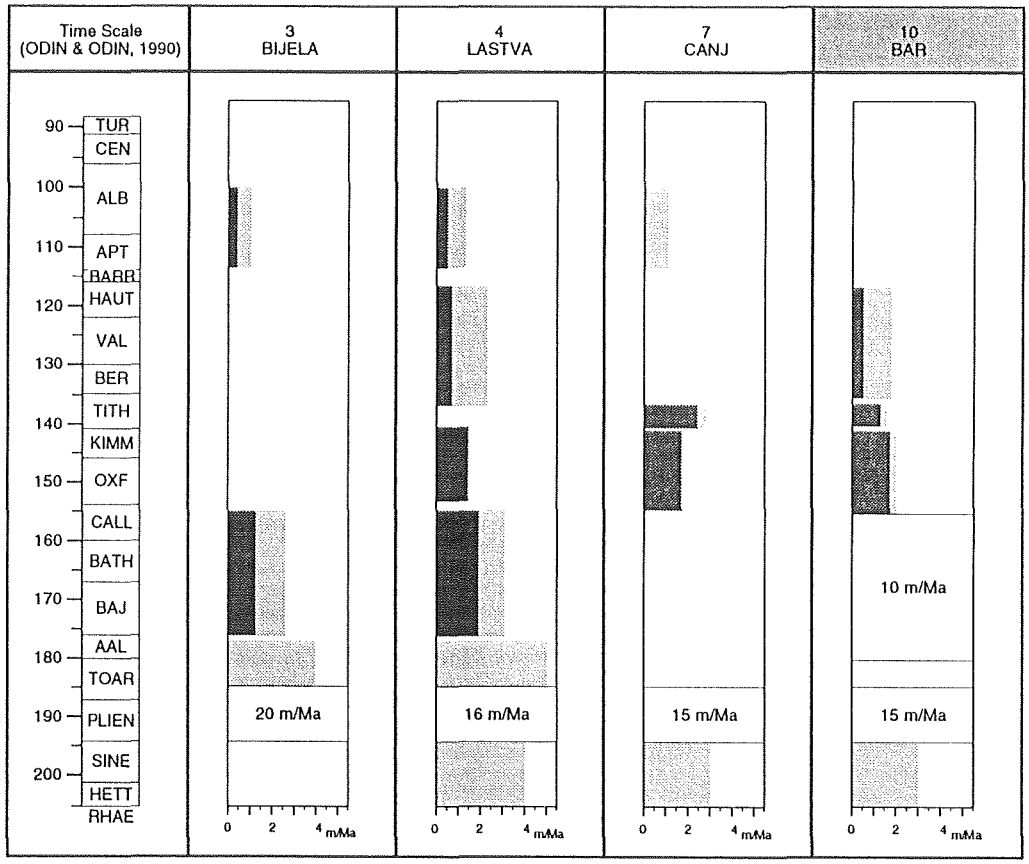

Fig. 3.2a

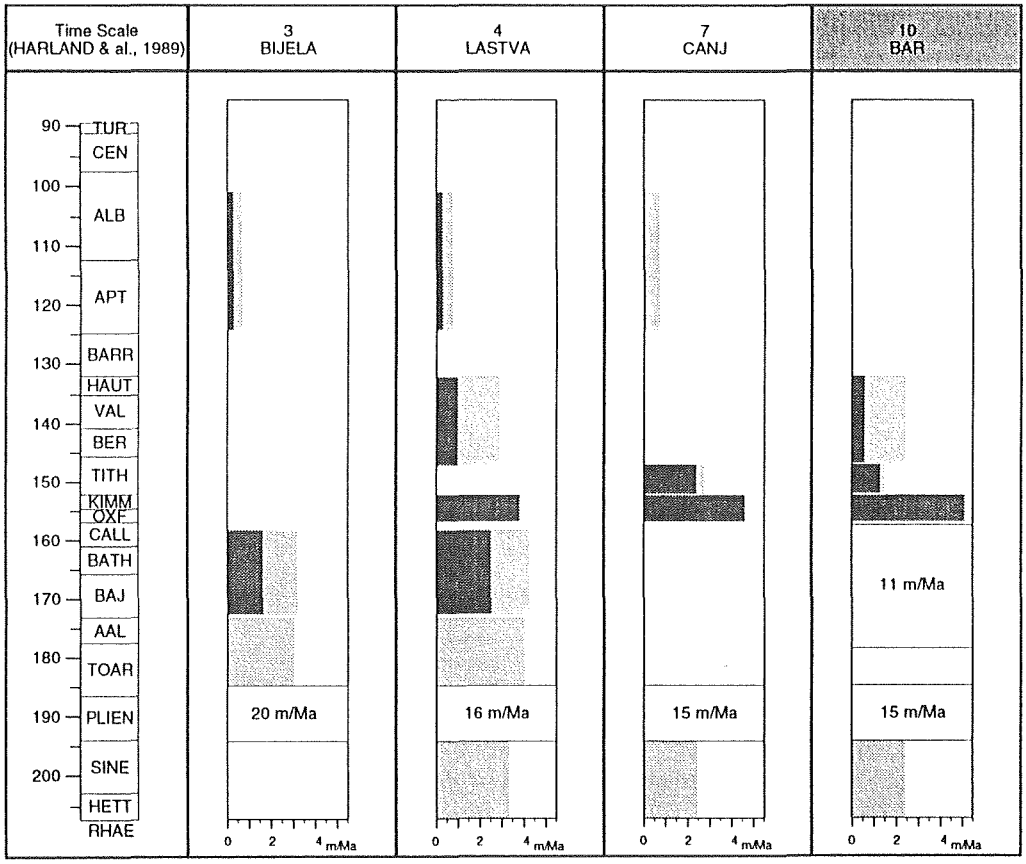

Fig. 3.2b

Fig. 3.2: Jurassic and Cretaceous average sedimentation rates of total rock sequences based on two different time-scales. Silica accumulation rates were calculated (darker rectangles) where the proportion of chert could be estimated. Sedimentation rates of turbiditic sequences are shown numerically.

Through the Middle and Upper Jurassic total sedimentation rates vary between 1.3 m/Ma and 5 m/Ma, depending on the amount of interstratified shales and calcarenites. The silica accumulation rates for this period vary between 1 m/Ma and 2 m/Ma, exceptionally 2.5 m/Ma. They contrast in the same order of magnitude vertically as they do laterally. In the previous paragraph, lateral differences were explained by sediment redistribution.

It is likely that the production of siliceous organisms was relatively constant through the whole Jurassic period. It should be recalled that a great part of silica in the "Passée Jaspeuse" Formation and lowermost Lastva Radiolarite originated from sponge spicules.

The lower Cretaceous cherty limestones have sedimentation rates similar to the underlying radiolarites, which implies a much lower silica accumulation rate. The mid-Cretaceous radiolarites have low sedimentation rates and silica accumulation rates only about 0.5 m/Ma. If we consider the Oxfordian-Kimmeridgian silica accumulation rates as a referential, because the most precise dating and lowest proportion of allochthonous components allow the best estimates, the mid-Cretaceous values are about three times lower.

The ecosystem of the Budva Basin probably underwent a major reorganization around the Jurassic-Cretaceous boundary, resulting in a low surface productivity which persisted through the middle Cretaceous.

Compared to Odin and Odin (1990), Harland et al. (1990) proposed a much shorter time-span for the Oxfordian and Kimmeridgian (Fig. 3.2b). Using their time-scale we could infer an exceptionally high opal supply for this time interval. In contrast, the Aptian-Albian silica accumulation rates appear even lower. The estimates suggest 10 to 20 times lower silica accumulation in the mid-Cretaceous than in the Upper Jurassic.

Sedimentation rates of the Jurassic radiolarite from the Pindos Zone were calculated (De Wever & Cordey, 1986; De Wever, 1989) on the basis of two different time-scales. The obtained average sedimentation rates range between 1.8–2 m/Ma and 1.4 m/Ma respectively and compare quite well with ours, if we consider that the Pindos Zone sections studied contain almost no resedimented carbonates and hence the sedimentation rates of total rock approximately correspond to the silica accumulation rates. The Cretaceous "Marne Rouge à Radiolaires" shows two to three times lower sedimentation rates than the Jurassic radiolarite sequence (De Wever & Origlia-Devos, 1982a), which is in accordance with the negative shift observed in the Budva Zone.

4. SEDIMENTARY EVOLUTION OF THE BUDVA BASIN

The facies evolution of the sections studied is given in Fig. 4.1. The relationship with the stratigraphic units of the High Karst Platform is synthetized in Fig. 4.2. A reconstruction of depositional environments is illustrated in Fig. 4.3.

4.1 Triassic

During the early Triassic the areas of the present Budva and High Karst Zones were occupied by a uniform sedimentation of red marine sandstones, dolomites and marly limestones. The differentiation of this paleogeographic realm started in the Anisian with the deposition of a thick clastic unit called "Anisian Flysch", which represents a syn-rift sedimentation.

These deposits are overlain by volcanic and volcanoclastic rocks associated with limestones and cherts. Different interpretations have been proposed to explain the cause of the Triassic magmatism. According to Channell et al. (1979) and Pamić (1984a, 1984b) it documents an intracontinental rifting stage, whereas Herak (1991) assumed a relation with late-Variscan convergent plate movements. Recently, Stampfli and Pillevuit (1993) suggested that the Budva Basin was an intracontinental rift, created by Pindos rifting, which cut the former margin of the Paleotethys.

The middle Triassic "flysch" and volcano-sedimentary facies associations characterized both the future Budva Basin as well as marginal regions of the later High Karst Platform. The adjacent swell was a site of condensed pelagic sedimentation of the Han Bulog type in the latest Anisian.

In the late Ladinian and Carnian, the High Karst Carbonate Platform became established and prograded over the marginal parts of the former trough.

The Triassic rift aborted. No volcanic activity has been known from the post-Triassic sequences of the Budva Zone. In a broader paleogeographic context of the Dinarides, the post-Triassic Budva Basin can be considered a rim basin (Stampfli et al., 1991) of an oceanic domain which is preserved as an obducted ophiolite belt in the Internal Dinarides. The High Karst Platform was a shoulder separating both pelagic realms. The evolution of the Budva rim basin was therefore closely dependent upon geodynamic events characterizing the Dinaric part of the Tethys.

4.2 Hettangian to Kimmeridgian

The paleogeographic relationship between the Budva Basin and the High Karst Platform (established in the Late Triassic) lasted through the Jurassic and Cretaceous. The sedimentary evolution of the Budva Basin was hence directly influenced by the sedimentary and tectonic activity of the High Karst Platform margin.

Carbonate gravity flows periodically diluted and displaced pelagic sediments. Occurrence and time-span of basin-plain deposits was thus determined by the abundance and distribution of coarse- to medium-grained resedimented carbonates. Variations in siliceous versus carbonate pelagic sedimentation are mainly explained by variable input of periplatform-ooze to the basin (see Baumgartner, 1987).

At the Triassic-Jurassic boundary the High Karst Platform underwent a tectonic restructurization (Radoičić, 1987a) resulting in the subsidence of its margins. As a response to the tectonic retreat of carbonate source area, the Budva Basin became starved in periplatform-ooze. In addition, it probably subsided to greater depth together with the platform margin. Subsequently, the lime-poor "Passée Jaspeuse" unit accumulated uniformly over the whole basin.

A progradation of carbonate accumulation in the upper Sinemurian-lower Pliensbachian marks the beginning of gravity-flow deposition (Bar Limestone Formation) which lasted until the end of the Middle Jurassic. The composition of resedimented carbonates reveals that they originated from penecontemporaneous platform and slope deposits. Their lateral distribution indicates a general direction of sediment transport from northeast to southwest.

Two major cycles of carbonate gravity-flow accumulation were recognized, with an interruption in the Toarcian. The Upper Member differs from the Lower Member of the Bar Limestone Formation by a higher proportion of ooids, coarser grain-size, thicker bedding and less lime-mudstone beds associated. Thick pure oolitic beds are present. Laterally, it is less expanded than the Lower Member. The differences in composition and lateral distribution were caused by a reorganization of the platform margin after the Toarcian. The Pliensbachian-early Toarcian (Fig. 4.3a) High Karst Platform was a low-relief limestone bank which supplied large volumes of detritus to the relatively gentle adjoining slope and to the basin. Smaller discontinuous oolitic shoals characterized the platform margin (Radoičić, 1982). The Middle Jurassic (Fig. 4.3b) platform margin, in contrast, was dominated by oolitic bars (Radoičić, 1982) which provided the major platform component displaced to the basin. In addition, they seem to have trapped and hampered the transport of lagoonal-mud off-shore. As a consequence, the gravity flows travelled shorter distances, produced steeper slopes, and allowed the accumulation of lime-free radiolarite (Lastva Radiolarite) distally.

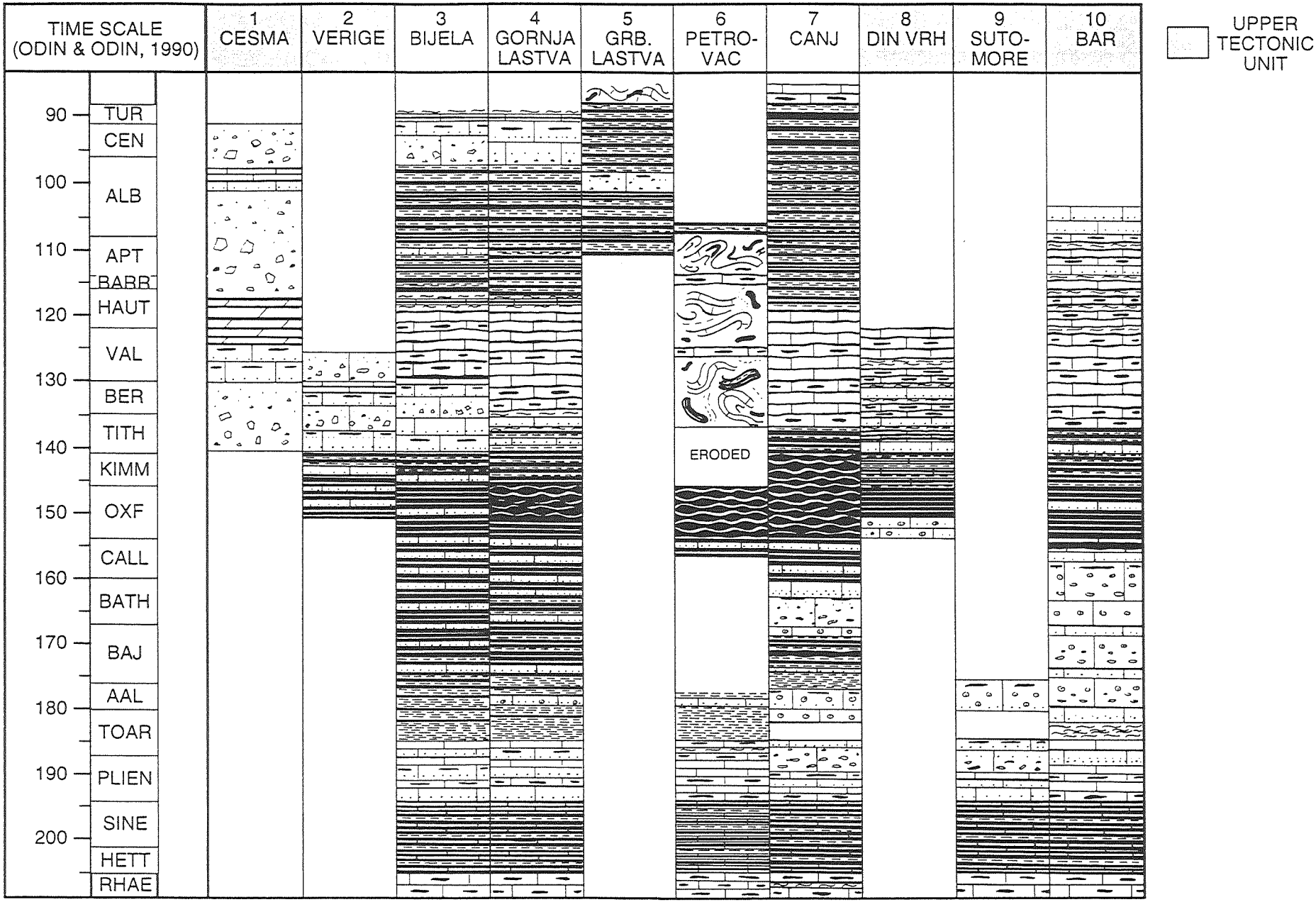

Fig. 4.1: Chronostratigraphic view of lithofacies in the 10 studied sections of the Budva Zone. Legend: same as Fig. 1.4.

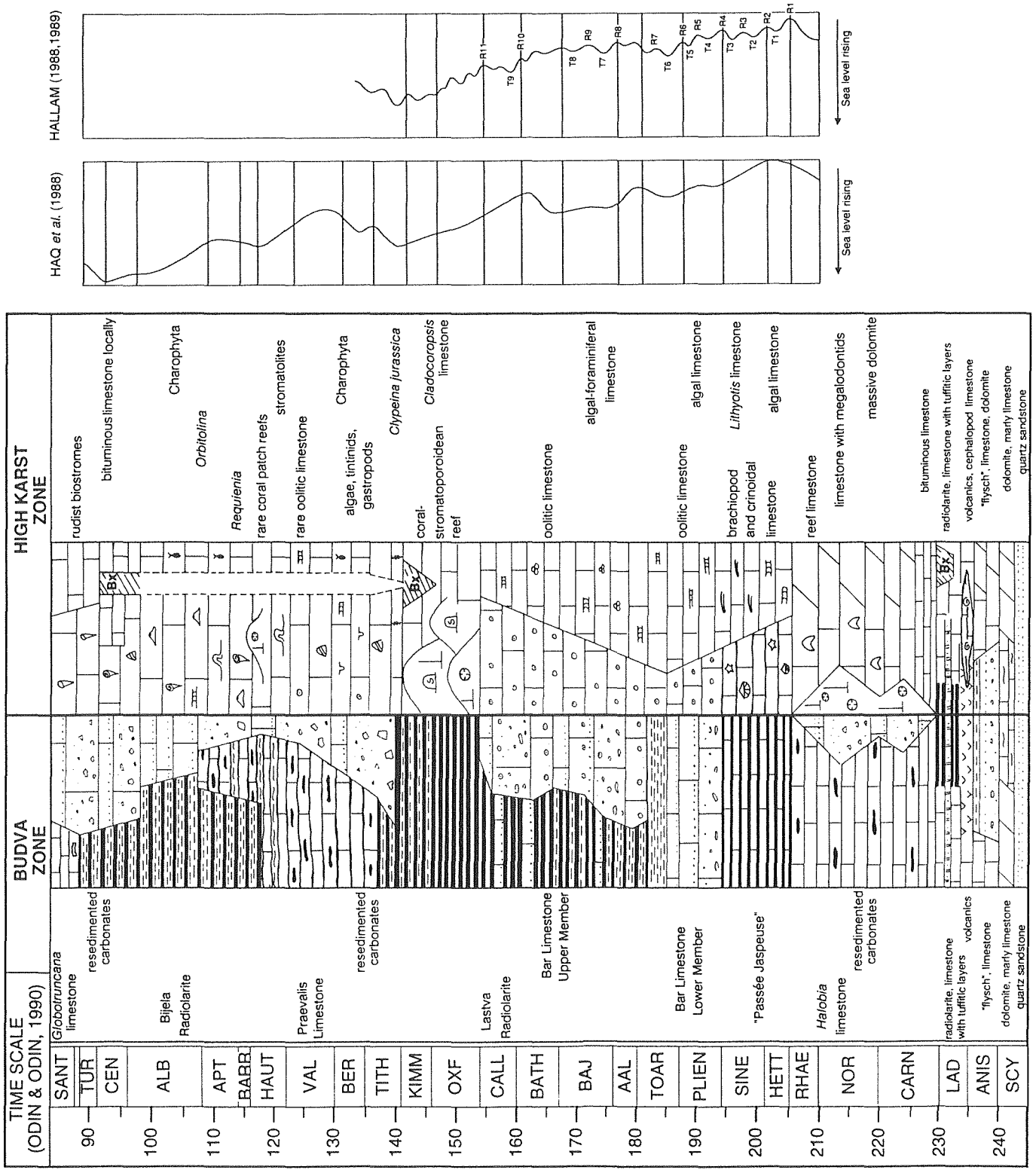

Fig. 4.2: Basin – platform facies relationship through time between the Budva Basin and the High Karst Platform. High Karst Zone and Triassic of the Budva Zone compiled according to Radoičić (1966, 1982, 1987b), Kalezić et al. (1976), Mirković (in press). Bx: bauxite deposits. Two alternative sea-level curves are given on the right.

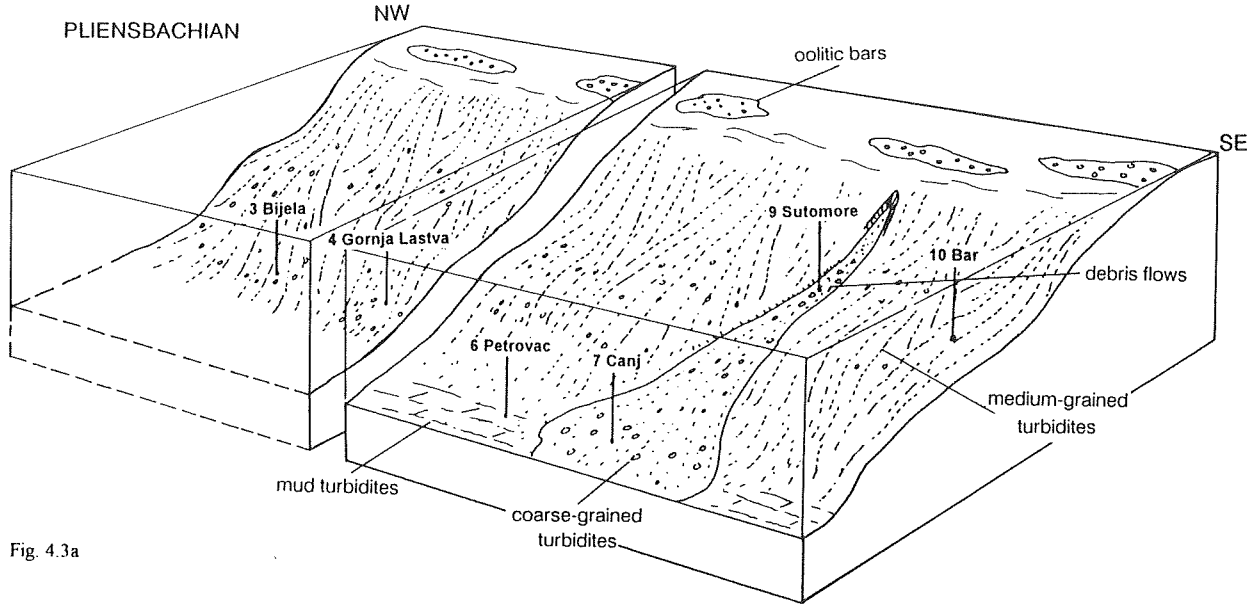

Fig. 4.3a

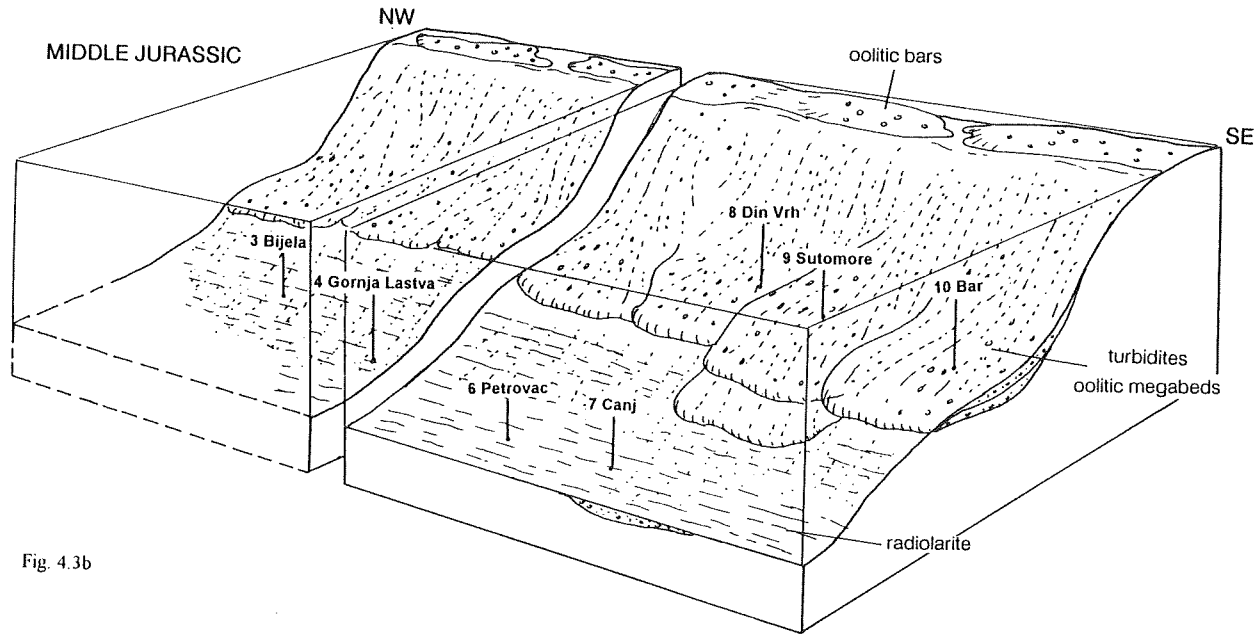

Fig. 4.3b

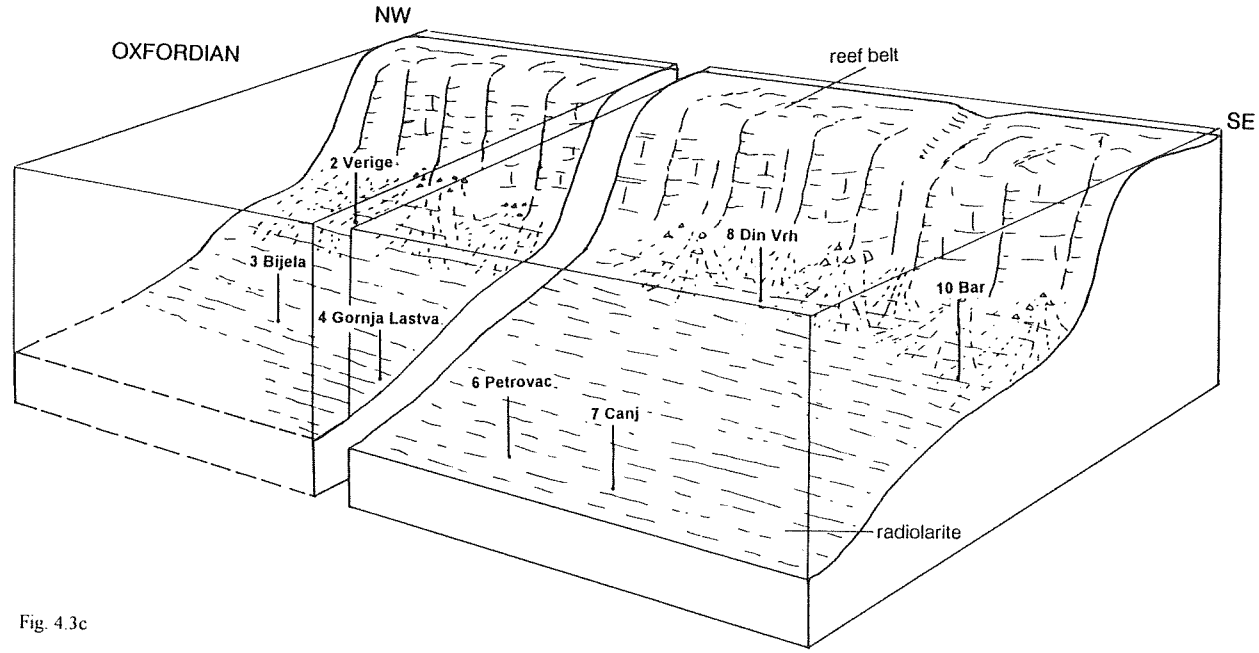

Fig. 4.3c

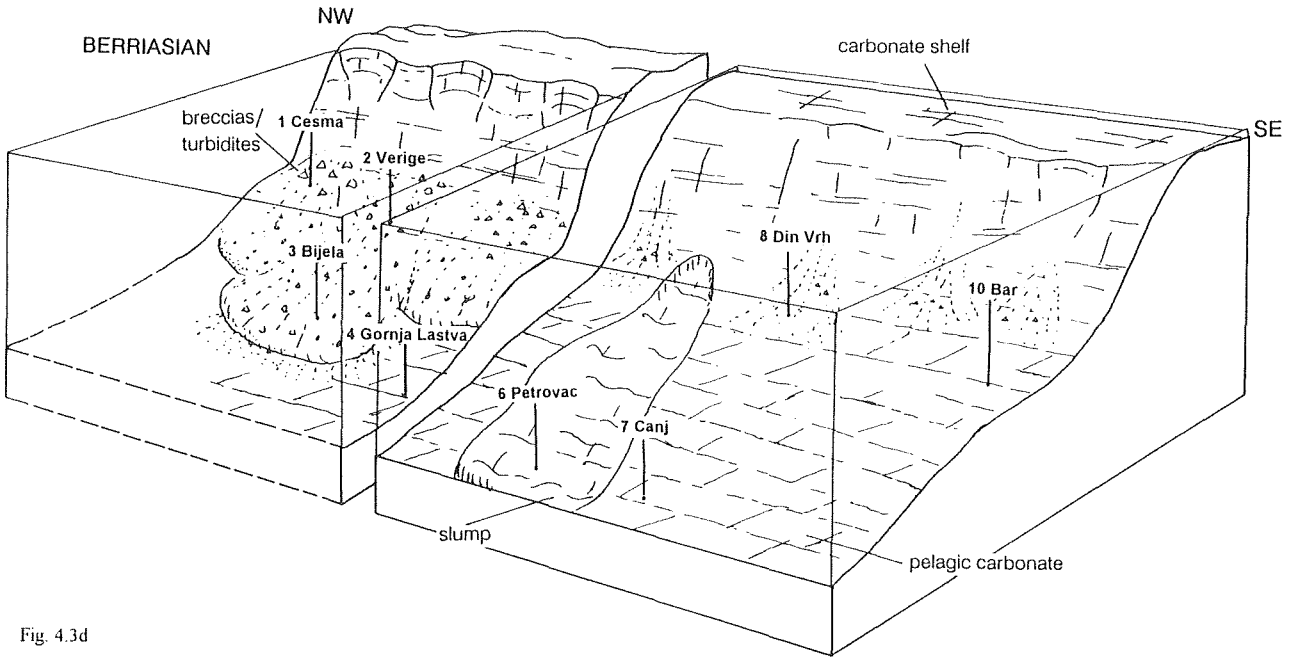

Fig. 4.3d

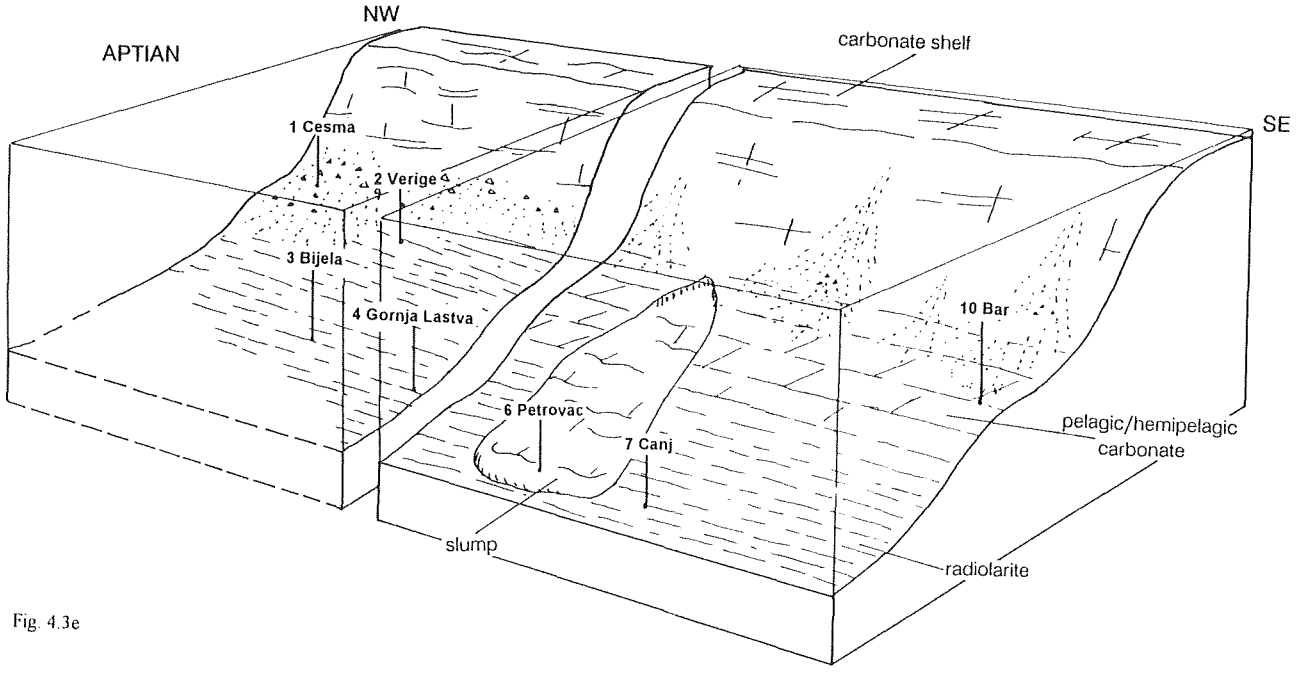

Fig. 4.3e

Fig. 4.3: Jurassic to mid-Cretaceous reconstruction of depositional environment of the northwestern and southeastern area of the Budva Basin and the adjacent High Karst Platform margin (not to scale). The position of the studied sections is indicated. See text for explanation.

A radical change in platform margin architecture took place at the beginning of the Late Jurassic (Fig. 4.3c) with the development of a coral-stromatoporoid reef complex (Radoičić, 1982). Early cementation velded the reef margin into a rigid wave-resistant mass, which efficiently blocked the off-shore sediment transport. The Oxfordian-Kimmeridgian time interval was therefore a period of most widely expanded radiolarite

sedimentation. Distal sequences, characterized by lime-free deposition since the Middle Jurassic, recorded a drastic reduction of interstratified calcarenites.

Green radiolarites, wide-spread in the Budva Basin before the Oxfordian, were replaced by red radiolarites in the Late Jurassic times. This facies change was diachronous. Oxygen depleted conditions persisted longer in near-platform areas. It is suggested that the relative age of the transition from green to red radiolarites in the Budva Zone can be used as an index of proximity to the margin.

An increase of shale interlayers was observed in the Kimmeridgian radiolarites. The higher input of clay was possibly related to the development of an emergent hinterland documented by bauxite deposits on the High Karst Platform (Bešić et al., 1965; Burić, 1966; see Chapter 2.4.5).

4.3 Tithonian and Cretaceous

The Tithonian–Berriasian (Fig. 4.3d) represents the time of platform-margin erosion. Coarse-grained breccias accumulated at the base of the steep marginal slopes. Finer-grained turbidites extended beyond the marginal slope into the adjoining basin. The turbidites and associated mass-flow deposits are composed mainly of lithoclasts of eroded ancient reef-fringed platform. Tectonic processes induced by closure of the Dinaric Tethys (see Chapter 2.5.4) are believed to have resulted in differential vertical motions and partial emergence of the High Karst Platform. An interaction of the tectonic uplift and a long term eustatic sea-level drop (Haq et al., 1988) was probably responsible for the erosional processes on the external part of the platform.

Another major episode of platform erosion documented in the northwestern depositional area of the Budva Zone began in the upper Albian-Cenomanian. A relatively high global sea level in this time (Haq et al., 1988) suggests that the erosion was primarily provoked by local tectonics.

Two different depositional realms could be recognized along the basin axis. Since the Tithonian, the discrepancies between the northwestern and southeastern realm were more pronounced. Geographically, only very closely situated sequences can be directly correlated.

Abundant coarse-grained resedimented carbonates characterized the northwestern realm during the Tithonian and Cretaceous (Figs. 4.3d, 4.3e). Their thickness and frequency decreases over short distances. On the other hand, the proximal sequences of the southeastern area contrast with their distal equivalents in the predominance of fine carbonates over holosiliceous deposits (Fig. 4.3e), possibly due to a higher supply of periplatform ooze. The pelagic sediments locally moved downslope where debris-slump chaotic beds were deposited distally (Petrovac section). The accumulation of these debris-slump masses persisted until the Aptian-Albian, when pelagic deposition was interrupted by calcareous turbidites in the areas closer to the platform margin (Bar section, see Fig. 4.1).

The differences between the two depositional areas reflect variations in platform production and slope morphology along the platform-basin transitional zone. It is in addition concluded that the Budva Basin narrowed toward northwest. The contrasts were amplified since the Tithonian, possibly due to accelerated High Karst Platform uplift in the northwestern area deduced from the distribution of bauxite deposits (Bešić et al., 1965; Burić, 1966).

Sedimentation in the distal sequences of the Budva Basin was to a minor degree determined by the platform margin dynamics, type and production rate. The facies development allows us to identify sedimentary events controlled by regional Tethyan paleoceanographic conditions. The transition from siliceous to carbonate facies (Praevalis Limestone) in the Late Tithonian and an opposite evolution in the Hauterivian-Barremian (Bijela Radiolarite) is correlative with synchronous shifts in the Southern Alps and Apennines (see Chapters 2.4.4 and 2.7.2). The radiolarite sedimentation continued until the Turonian.

A decrease of silica accumulation rate around the Jurassic-Cretaceous boundary would agree with reduced surface productivity inferred from other basinal successions of the western Tethys and Atlantic. In the Budva Basin lower silica accumulation rates persisted into the middle Cretaceous.

Pelagic deposits of the Budva Zone recorded an increase of clay components in the upper Valanginian? to mid-Cretaceous time interval. The increased clay input was probably to a great extent induced by an elevated humidity.

Short episodes of lower redox potential deduced from green levels interstratified in generally red Bijela Radiolarite most likely correspond to mid-Cretaceous oceanic anoxic events (see Chapter 2.7.2).

The Budva Basin, however, differs from other Tethyan basins by a relatively higher silica content in the Upper Jurassic and Cretaceous pelagic deposits. The low values of total-rock sedimentation rates through the Cretaceous suggest that these lithological differences are primarily due to a lower proportion of associated carbonate related to lower production and/or more pronounced dissolution of calcareous nannoplankton.

Triassic, Jurassic, and Cretaceous resediments in the Budva Basin were sourced from the High Karst Platform. There is no evidence of any sediment supply from the Dalmatian Platform in the Budva Basin outcropping today. We suppose that the Dalmatian-Budva transitional zone is covered by overthrusts of the Budva and High Karst Zones.

5. PALEOGEOGRAPHIC CONNECTION WITH OTHER TETHYAN BASINS

The position of tectonic units discussed in this chapter is indicated in Fig. 1.1 (Chapter 1). The relationship with the neighbouring paleogeographic units for the Middle Jurassic and early Late Cretaceous time is given in Fig. 5.2.

The Budva Zone continues southward to the Krasta-Cukali Zone in Albania and Pindos-Olonos Zone in Greece.

An extensive stratigraphic study of the **Pindos-Olonos Zone** was published by Fleury (1980) and Thiébault (1982). Supplementary dating was provided by De Wever & Thiébault (1981), De Wever & Origlia-Devos (1982a, 1982b), and De Wever & Cordey (1986).

The facies evolutions of the Pindos and Budva Zones are closely similar. The correlation of main lithostratigraphic units of both realms is outlined in Fig. 5.1.

The following two phenomena are confined to the Pindos Zone:

1. – The Jurassic as well as Cretaceous resedimented carbonates indicate a general western provenance of carbonate debris. An origin from the east was observed only in sequences close to the Parnassos Zone.

2. – Ophiolite debris-bearing clastics derived from the internal Hellenic zones are locally intercalated in lower and middle Cretaceous deposits.

The contrasts between the Budva and Pindos zones are due to the paleogeographic disposition of the eastern carbonate platform. Only fragments of a large High Karst Carbonate Platform existed south of the Scutari-Peć line in Albania.

The transitional zone between the western Dalmatian-Gavrovo-Tripolitza Carbonate Platform (supposed to be overlain by thrusts in Montenegro) is well exposed in the Pindos Zone.

The **Krasta-Cukali Zone** in Albania is characterized by a similar pelagic Mesozoic succession with prevail-

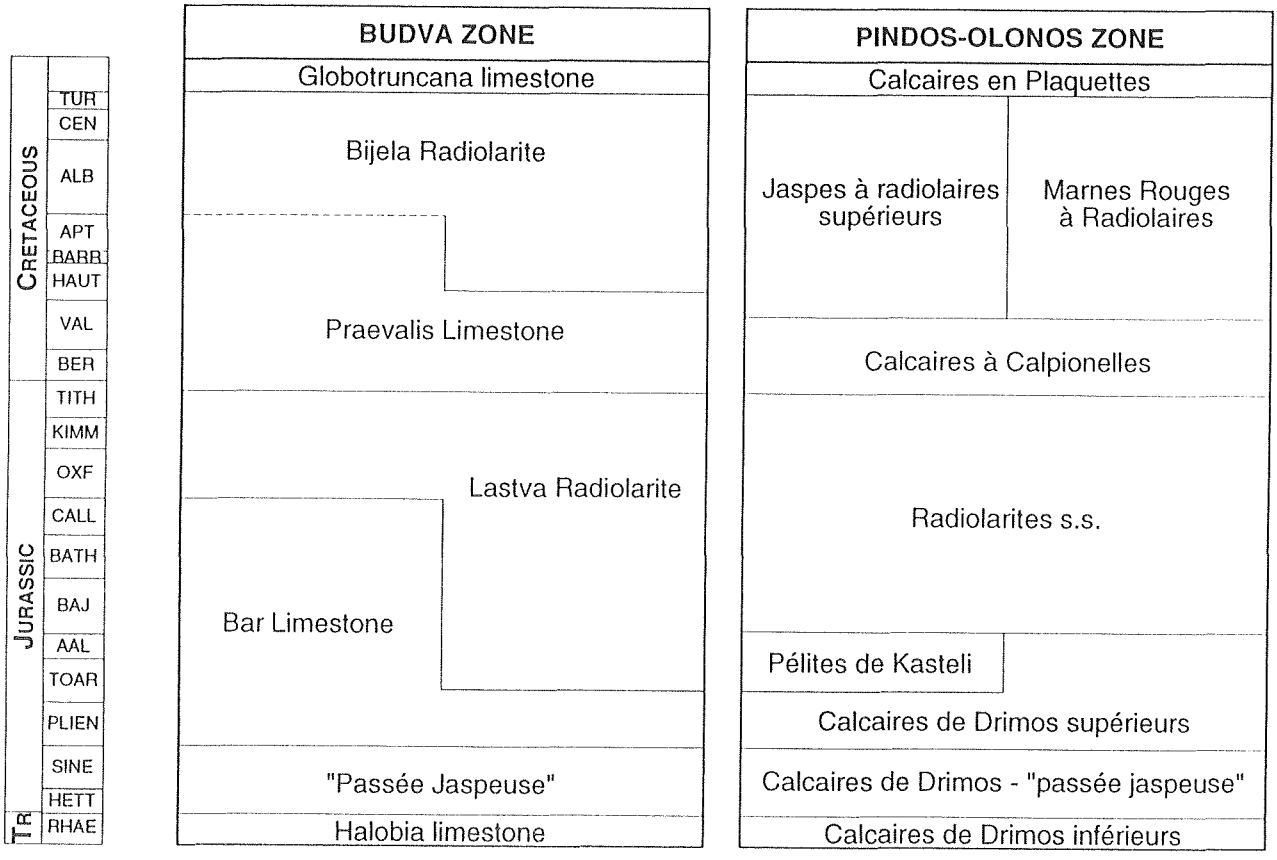

Fig. 5.1: Simplified correlation between the Budva Zone and Pindos Zone formations.

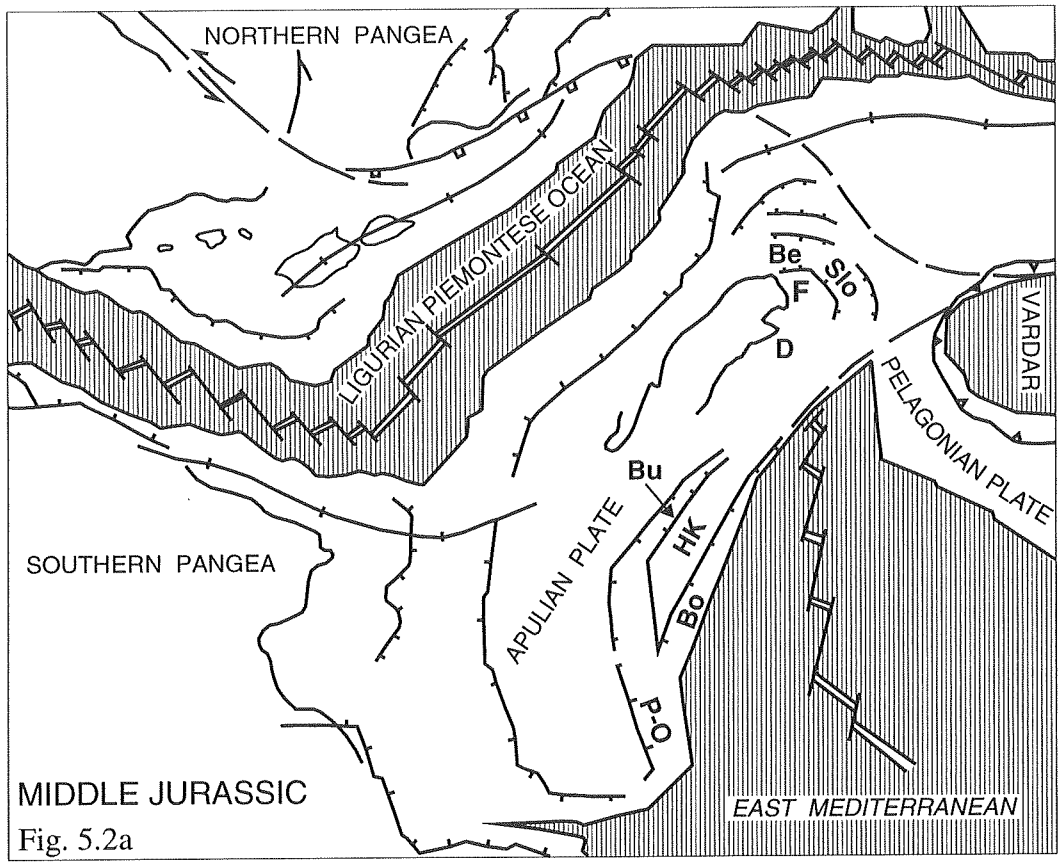

Fig. 5.2a

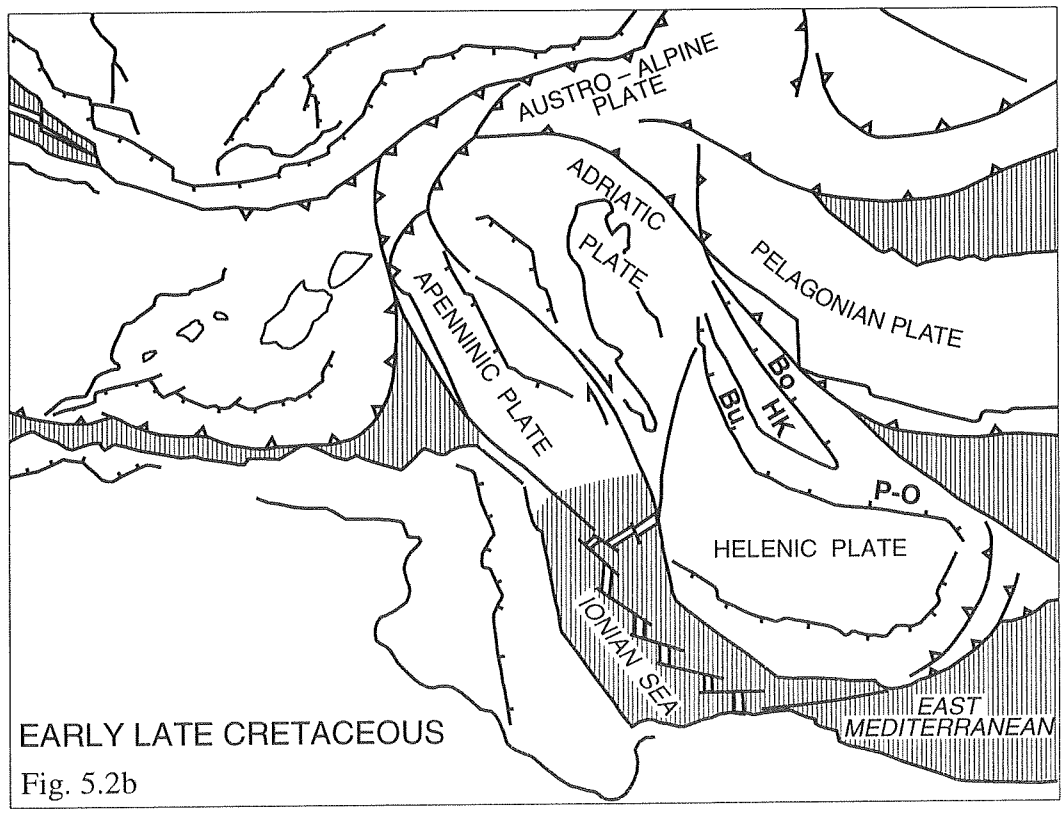

Fig. 5.2b

Fig. 5.2: Paleogeographic map of the Apulian Plate during the Middle Jurassic (Fig. 5.2a) and early Late Cretaceous (Fig. 5.2b) (after Marchant & Stampfli, in press).
Abbreviations: Be: Belluno Basin, Bo: Bosnian Basin, Bu: Budva Basin, D: Dinaric Platform, F: Friuli Platform, HK: High Karst Platform, P–O: Pindos–Olonos Basin, Slo: Slovenian Basin.

ing radiolarite facies (Dercourt, 1968; Papa, 1970). Condensed pelagic sequences of Toarcian to Upper Cretaceous age, overlying the Liassic massive limestone, are restricted to the northern part (Dercourt, 1968; Dodona & Farinacci, 1987). The recorded structural highs suggest a presence of intermediate submerged blocks between the High Karst – Albanian Alps Carbonate Platform and the basin (Dercourt, 1968).

The extension of the Budva Zone to the north is masked by its tectonic disappearance below the High Karst Thrust.

The study of facies distribution led us to conclude that the Budva Basin was narrower toward its present tectonic wedge-out, as already stated by Antonijević et al. (1969b) and Radoičić (1982). As a relatively narrow through it presumably continued about 200 km further north as far as Split (Chorowicz, 1975).

Herak (1986) proposed a paleogeographic connection between the Budva Basin and the **Tolmin Basin** in western Slovenia. According to this author the linking pelagic realm might have been partly overthrusted, partly eroded. The generally south verging thrusts and east–west oriented facies belts in the Tolmin region continue to central and eastern Slovenia; this would more likely imply a more direct relationship with the Bosnian Zone (Buser, 1987).

The Jurassic to Cretaceous sedimentary evolution of the **Belluno Basin** in northern Italy records an important carbonate debris supply from the east and therefore evokes certain affinities with the Budva Basin. The Middle Jurassic Vajont Limestone, an outstanding sequence of oolitic turbidites (Bosellini et al., 1981), is considered analogous to the Upper Bar Limestone Member. The relatively early initial formation of the Belluno as a Southern-Alps basin at the beginning of the Jurassic may be related to the formation of Dinaric basins (Sarti et al., 1992). During the Jurassic the Belluno and Budva area could be two discrete wedge shaped basins along the western margin of the same Friuli–Dinaric–High Karst Platform which is at present a continuous belt of Mesozoic shallow-water deposits.

6. RADIOLARIAN BIOCHRONOLOGY

6.1 Lower Jurassic biochronological correlation

This chapter deals with radiolarians obtained from the "Passée Jaspeuse" Formation. The position of the samples studied is indicated in Fig. 2.1 (Chapter 2). The radiolarian inventory is given in Fig. 6.1. In most cases, only a generic-level identification was possible.

The assemblage, collected at the base of the formation is characterized by the following radiolarians: *Pantanellium tanuense* PESSAGNO & BLOME, *Orbiculiforma*, *Canoptum* and *Droltus*. All the four genera existed in the uppermost Triassic and survived the Triassic-Jurassic boundary (Carter, 1993; Carter, in press). According to dating supported by ammonites, *Pantanellium tanuense* PESSAGNO & BLOME is regarded as a Hettangian index (Pessagno et al., 1987; Carter, in press).

Sample BM11, taken at the very base of the formation, yields an aberrant conodont, assignable to *Epigondolella* or *Paragondolella*, possibly of uppermost Triassic age (determination F. Hirsch). This conodont is associated with the above mentioned radiolarians. The "Passée Jaspeuse" is partly of fine-turbiditic origin. At present we cannot exclude the possibility that the conodont was reworked from some older strata.

Parahsuum, lacking in the lowermost part of the formation, is the most abundant genus in higher levels. It first appears in the latest Hettangian times (Carter, in press).

Wrangellium, supposed to make its first appearance in the Sinemurian (Pessagno et al., 1987), occurs in the middle and in the upper part of the formation.

The top of the formation contains *Katroma* associated with *Gigi*. These genera coexist in Subzone II of the *Parahsuum simplum* Assemblage-zone, assigned to the Sinemurian-? lower Pliensbachian (Hori, 1990). *Bagotum*, which does not extend below the Subzone II, was also found.

Sections	Gornja Lastva			Petrovac		Čanj	Bar		
Species \ Samples	GL 105	GL 109	GL 4	PK 26	PK 20	UPC 41.50	BM 11	BM 18	BM 21
Bagotum spp.					x				
Canoptum spp.	x	x	x		x		x	x	
Droltus spp.	x						x	x	
Gigi fustis					x				
Gigi sp. A			x		x	x			x
Gorgansium gongyloideum								x	
Katroma spp.			x	x	x				
Orbiculiforma spp.	x	x				x			x
Pantanellium tanuense	x	x					x		
Parahsuum ovale			x		x			x	
Parahsuum simplum			x		x	x		x	x
Paronaella spp.				x	x	x		x	x
Pseudoeucyrtis spp.	x	x	x		x				x
Wrangellium spp.			x	x					x

Fig. 6.1: Distribution of radiolarians in the "Passée Jaspeuse" Formation.

6.2 Middle Jurassic to Cretaceous biochronological correlation

6.2.1 Introduction

The continuous succession of radiolarian-bearing rocks in the Budva Zone from the beginning of the Middle Jurassic to the Turonian allowed us to establish a local radiolarian zonation for this time interval. The biochronological correlation was made by means of the BioGraph computer program (Savary & Guex,1991), based on the Unitary Association Method (Guex, 1977, 1991).

The U.A. Method defines maximal sets of actually or virtually coexisting taxa. Those sets are constructed from fragmentary biostratigraphic data collected in many localities where at least two taxa are found per sample. The resulting Unitary Associations differ from each other by containing mutually exclusive species. Considering the superposition among fossil species, the U.A.'s are arranged in a chronologic sequence. The U.A. Method generates discrete biochronological scales which will detect maximal intersections of the existence intervals for the co-occurring species.

The presence of a radiolarian taxon in a fossil sample is, to a great account, determined by redistribution of skeletons before burial and differential dissolution before and after deposition. As a consequence, the actual first and last appearances are highly diachronous among different localities. The deterministic U.A. Method, stacking all co-occurrence data in maximum relative stratigraphic ranges, has proven to be an efficient tool to construct reliable radiolarian zonations (Baumgartner, 1984; Jud, 1991; Carter, 1993).

6.2.2 Results

The radiolarian inventory of 95 samples from eight sections was studied. The Upper Jurassic part of the Bijela section was divided in three partial sections. The superpositional relationship of strata could not be determined in the field due to tectonic disruption and bad exposure. The species content of each sample is listed in the Appendix.

Based on distribution of 139 taxa, 48 different Unitary Associations were recognized. The resulting protoreferential is shown in Fig. 6.2.

Individual Unitary Associations, identified in separate sections, can differ in faunal content due to ecological, taphonomic or documentary factors. These usually have no chronological significance. Some of them must be merged to construct chronologically meaningful "zones". Such zones are characterized by a wide lateral traceability and a good mutual superpositional control (see Guex, 1991 for the details of the procedure). On the basis of the lateral reproducibility (Fig. 6.3) our U.A.'s were merged into 15 "zones". Faunal differences between the different U.A.'s encompassed in the same "zone", are ignored in the biochronological interpretation.

To enable a biostratigraphic correlation of sections, the assignment of each sample to a corresponding U.A., is indicated in the lithological columns showing the position of samples (Chapter 2, Figs. 2.3, 2.5)

6.2.3 Definition and age assignment of biochronologic units. Correlation with other zonations.

6.2.3.1 Jurassic

The determined biochronologic units were mostly calibrated through a correlation with published zonations, therefore age assignment and correlations are discussed simultaneously. Species or pairs of species defining individual U.A.'s, as well as mutually exclusive species defining their limits are evident from Fig. 6.2 and will not be systematically referred to in the text.

The union of **U.A.1 and U.A.2** occurs in two sections. U.A.1 was identified in the Gornja Lastva section, 5 m above a calcarenite bed containing *Gutnicella cayeuxi* (LUCAS), which is restricted to the Aalenian and lower Bajocian (Septfontaine et al., 1991).

Tonielli (1991) assigned an assemblage yielding *Parahsuum* (?) *magnum* TAKEMURA and *Ares cylindricus* (TAKEMURA) to uppermost Toarcian/Aalenian-lowermost Bajocian on the basis of ammonites. *Parahsuum* (?) *magnum* TAKEMURA associated with *Parahsuum* (?) *natorense* (EL KADIRI) and *Hexasaturnalis tetraspinus* (YAO) was found above middle Toarcian ammonites (El Kadiri, 1992).

U.A.2 is correlative with *Hsuum hisuikyoense* Assemblage Zone (Hori, 1990), based on the co-occurence of *Transhsuum hisuikyoense* (ISOZAKI & MATSUDA) and *Laxtorum* (?) *jurassicum* ISOZAKI & MATSUDA. The top of this zone is supposed to lie within upper Aalenian to lower Bajocian interval (Hori, 1990).

The coexistence of *Laxtorum* (?) *jurassicum* ISOZAKI & MATSUDA with *Transhsuum hisuikyoense* (ISOZAKI & MATSUDA) and *Unuma echinatus* ICHIKAWA & YAO allows the correlation with the upper part of the *Laxtorum* (?) *jurassicum* Interval Zone (Matsuoka & Yao, 1986).

U.A.1 and U.A.2 are assigned to the Aalenian-lower Bajocian. The superposed U.A.3 to U.A.5 not being younger than the lower upper Bajocian, an age comprising only the lower part of the lower Bajocian is probable.

The union of **U.A.3 to U.A.5** was identified in three sections. It is delimited from U.A.1 and U.A.2 by LAD of three and FAD of eight taxa, some of them (*Zartus*, *Ares*, *Turanta*) being known from the Liassic (Pessagno & Blome, 1980; De Wever, 1982a; Carter et al., 1988). This faunal change is partly preservation-controlled.

This union can be correlated with the lower Bajocian Zone 7 of Carter et al. (1988) on the basis of the coexisting *Emiluvia splendida* CARTER and *Zartus* spp. *Zartus* makes its last appearance in the lower part of the upper Bajocian (Zone 1D, Pessagno et al., 1987). The inferred age for U.A.3 to U.A.5 is lower to lower upper Bajocian.

U.A.'s 3 to 5 are probably partly time equivalent with *Tricolocapsa plicarum* Interval Zone (Matsuoka & Yao, 1986). The absence of the marker taxon and most of associated taxa in our material does not allow a direct correlation.

Trillus sp. and *Eucyrtidiellum* (?) *quinatum* TAKEMURA are restricted to U.A.0 in Baumgartner's (1984) zonation, which suggests the correlation of the U.A.0 with our U.A.'s 1 to 5.

The unions of **U.A.6 to U.A.7** and **U.A.8 to U.A.12** were identified in two sections.

The limit between these two chronologic units is marked by the mutual exclusion of *Unuma echinatus* ICHIKAWA & YAO with *Hagiastrum munitum* BAUMGARTNER and *Transhsuum maxwelli* (PESSAGNO) among others. It is concluded that the groups U.A.6 to U.A.7 and U.A.8 to U.A.12 are correlative with Zones A0 and A1 respectively of Baumgartner (1984). The limit between both unions of U.A.'s is placed in the upper part of the upper Bajocian, according to the updated calibration by O'Dogherty et al. (1989).

Both groups of U.A.'s are further correlative with the *Tricolocapsa conexa* Interval Zone (Matsuoka & Yao, 1986), which is defined by the FEAB of the marker species. *Cyrtocapsa mastoidea* YAO, restricted to the underlying *Tricolocapsa plicarum* Zone (Matsuoka & Yao, 1986) coexists with *Tricolocapsa conexa* MATSUOKA in our material.

The union of **U.A.13 to U.A.15** was identified in three sections. The faunal content of all the samples assigned to this chronologic unit is characterized by great many small nassellarians, spumellarians rarely occur. Due to different diagnostic pairs of species, a direct correlation with the zonation of Baumgartner (1984) is not possible.

The coexistence of *Stylocapsa* (?) *spiralis* MATSUOKA gr. with *Guexella nudata* (KOCHER) (see also taxonomic remarks on this species), *Stylocapsa catenarum* MATSUOKA and *Stichocapsa naradaniensis* MATSUOKA allows a correlation with the *Stylocapsa* (?) *spiralis* Zone (Matsuoka & Yao, 1986).

Stylocapsa tecta MATSUOKA and *Stylocapsa hemicostata* MATSUOKA have not been found in our material. All specimens of *Stylocapsa* (?) *spiralis* MATSUOKA gr. show an advanced evolutionary stage of surface ornamentation. We assume that the upper part of the *Tricolocapsa conexa* Zone and the lower part of the *Stylocapsa* (?) *spiralis* Zone have not been recorded in the Budva Zone due to widely spaced sampling in this interval and not to a stratigraphic gap.

The union of **U.A.16 to U.A. 18** was identified in four sections. The samples assigned to this chronologic unit generally contain a well preserved and diversified radiolarian fauna which is clearly reflected in the referential by the first appearance of many taxa.

The group U.A.16 to U.A.18 is separated from the underlying chronologic unit by mutually exclusive *Emiluvia orea* BAUMGARTNER with *Guexella nudata* (KOCHER) or *Higumastra imbricata* (OŽVOLDOVA) among others. On the basis of these species the boundary can be correlated to the limit between the A2 and B Zones of Baumgartner (1984). It is assigned to the Callovian-Oxfordian according to O'Dogherty et al. (1989).

The superposed **U.A.19 to U.A.22** were identified in six sections. The following group of U.A.23 to U.A.27 is assigned to the upper Oxfordian and Kimmeridgian. It is concluded that U.A.16 to U.A.18 and U.A.19 to U.A.22 lie within the Oxfordian.

The *Cinguloturris carpatica* Zone (Matsuoka & Yao, 1986) defines the interval between the LAD of *Tricolocapsa conexa* MATSUOKA and FAD of *Pseudodictyomitra primitiva* MATSUOKA & YAO, the latter being very rare in our material. On the basis of supplementary species like *Williriedellum carpathicum* DUMITRICA associated with *Williriedellum* sp. A sensu MATSUOKA and *Transhsuum maxwelli* (PESSAGNO) we correlated the *Cinguloturris carpatica* Zone to the interval of our U.A.16 to U.A.22.

The union of **U.A.23 to U.A. 27** is well represented in seven sections. *Podocapsa amphitreptera* FOREMAN makes its first appearance in this chronologic unit. The oldest datum known for this species is upper Oxfordian based on aptychi (Widz, 1991). *Pseudoeucyrtis reticularis* MATSUOKA & YAO is restricted to this unit. It is a common species in the Kimmeridgian ammonite-bearing sequence of Sierra de Ricote (O'Dogherty, personal communication). The concluded age for U.A.23 to U.A.27 is upper Oxfordian-Kimmeridgian.

The union of U.A.'s 23 to 27 is correlative to the *Pseudodictyomitra primitiva* Interval Zone (Matsuoka & Yao, 1986) on the basis of the following species common to both assemblages and defining U.A.23 to U.A.27: *Pseudoeucyrtis reticularis* MATSUOKA & YAO, *Podocapsa amphitreptera* FOREMAN, *Eucyrtidiellum ptyctum* (RIEDEL & SANFILIPPO) and *Cinguloturris carpatica* DUMITRICA. The top of the *Pseudodictyomitra primitiva* Interval Zone is defined with the FEAB of *Pseudodictyomitra carpatica* (LOZYNYAK) (Matsuoka, 1992), which first appers in U.A.31. The ancestral species *Pseudodictyomitra primitiva* MATSUOKA & YAO was found in U.A.29. Both species have not been observed in the same sample. Although on the basis of our data the above mentioned U.A.'s belong to the same

"zone", we cannot exclude a minor age difference between them. The upper limit of the *Pseudodictyomitra primitiva* Zone is thus placed within the interval of U.A.28 to U.A.31.

Baumgartner (1984) defined the boundary between B and C1 Zones on the basis of mutually exclusive *Bernoullius dicera* BAUMGARTNER or *Transhsuum maxwelli* (PESSAGNO) with *Acanthocircus dicranacanthos* (SQUINABOL). The same superposition was recorded in the Budva Zone. It is delimited with U.A.23 to U.A.27, where none of these species has been found.

U.A.28 to U.A.31 were identified in four sections. The samples assigned to this union of U.A.'s represent the top of the Jurassic Lastva Radiolarite. The assemblage was in addition compared to sample 89B–312R (sample courtesy of L. O'Dogherty) from the Betic Cordillera, dated as lower Tithonian with ammonites. The following species defining also our U.A.28 to U.A.31 have been determined: *Cinguloturris* sp. A and *Acanthocircus dicranacanthos* (SQUINABOL) associated with *Archaeodictyomitra minoensis* (MIZUTANI), *Syringocapsa* sp. A and *Protunuma japonicus* MATSUOKA & YAO. A lowermiddle Tithonian age seems plausible for U.A.28 to U.A.31.

Zones C1 and C2 of Baumgartner (1984) could not be distinguished in the Budva Zone.

U.A.'s 28 to 31 are differentiated from the underlying chronologic unit by the absence of a great number of taxa. The lack of some morphotypes is certainly related to moderate preservation and fewer number of examined sections in the upper unit. On the other hand, the disappearance of some dissolution-resistant forms, especially genera like *Parahsuum*, *Transhsuum* and *Tetratrabs* implies an extinction event. Whether or not this extinction is correlative to the high extinction rate detected in C1 and C2 Zones of Baumgartner (1984) could not be ascertained at present. For the time being, the observed faunal turnover is interpreted as local. It coincides with one of the major changes in sedimentary evolution of the Budva Basin.

The exposed comparison with the zonation of Baumgartner (1984) through the Middle and Upper Jurassic is based on correlation of a sequence of mutually exclusive species and assemblages of species. Both zonations were established by means of the Unitary Association Method. They monitor several contradictory concurrent ranges due to species coexisting in Baumgartner's samples, which have never been found together in the Budva Zone, and vice-versa. These contradictions point out the necessity to consider all available data in generating a globally applicable radiolarian zonation. The multi-worker Jurassic-Cretaceous Working Group is currently preparing an integrated radiolarian biochronologic scale for low-latitude radiolarians of Middle Jurassic to Cretaceous age. Our data have therefore not been merged with the database of Baumgartner and reinterpreted in this paper.

The age assignment of the radiolarian biochronologic units from the Budva Zone is essentially made through a correlation to Baumgartner's zonation. The calibration of this zonation has been updated by Baumgartner (1987) and more recently by O'Dogherty et al. (1989) based on ammonite-bearing sequences from the Betic Cordillera. Although these sequences provide a good age-control, the data remain limited to a rather small paleogeographic area. Considering the important diachronism of radiolarian species in a fossil record, further modifications of correlation to chronostratigraphic stages are possible. The previously mentioned contradictory concurrent ranges between Baumgartner's zonation and the one presented in this paper, further reduce the accuracy of our dating. We would like to stress that the stage assignment of the Jurassic radiolarian "zones" from the Budva Zone has relatively large intervals of uncertainty.

6.2.3.2 Cretaceous

The Cretaceous assemblages from the Budva Zone are generally characterized by a small number of identifiable taxa per sample. U.A.'s 32 to 36 comprising a long time interval from the upper Tithonian to possibly Hauterivian, in addition, demonstrate a low lateral reproducibility and weak superpositional control, because only very rare productive samples could be obtained from this sequence. Our own data are not self-sufficient to establish a chronologically meaningfull subdivision. Dating and also delineation among unitary associations is based on the existing zonations.

We followed the most accurate zonations available at present: Jud (1991) for the lower Cretaceous (U.A.32 to U.A.37 in our referential) and O'Dogherty (1994) for the middle-upper Cretaceous (U.A.38 to U.A.48 in our referential).

Pseudodictyomitra puga (SCHAAF) in association with *Cinguloturris* sp. A allow to assign **U.A.33 and U.A.34** to the Berriasian-lower Valanginian. **U.A.32** lacking *Pseudodictyomitra puga* (SCHAAF) can be as old as the upper Tithonian.

U.A.35 and U.A.36 are defined by the co-occurrence of *Mirifusus dianae* (KARRER) with *Cecrops septemporatus* (PARONA), which implies an upper Valanginian-Hauterivian age. The other species starting in U.A.35 or U.A.36 are either known from older strata in other regions or their stratigraphic range has not been well established yet, as is the case for *Hemicryptocapsa capita* (TAN). U.A.36 actually lacking *Cecrops septemporatus* (PARONA) is disconnected from the underlying U.A.31 in the section and can be of Berriasian to Hauterivian age.

The presence of *Acanthocircus variabilis*

(SQUINABOL) in the following **U.A.37** suggests that U.A.37 is not younger than the lower Barremian.

Sample PK/3, not included for the biochronological correlation, was collected in a slump-debris chaotic bed in the Petrovac section. It yields a rich well preserved radiolarian fauna with *Acanthocircus carinatus* FOREMAN and *Cinguloturris* sp. A among others. The association of these two species, which have clearly disconnected stratigraphic ranges, points out that the assemblage is mixed due to reworking. No differences in preservation have been observed for the reworked specimens.

U.A.38 to U.A.40 are characterized by a number of species which become extinct in the lower Aptian: *Acanthocircus carinatus* FOREMAN, *Parvicingula usotanensis* TUMANDA, *Sethocapsa uterculus* (PARONA), *Parvicingula boesii* (PARONA), *Archaeodictyomitra excellens* (TAN), and *Archaeodictyomitra* sp. A. *Acanthocircus carinatus* FOREMAN evolved from *Acanthocircus variabilis* (SQUINABOL) during the Barremian (Dumitrica & Jud, in prep.). The absence of species such as *Acanthocircus dicranacanthos* (SQUINABOL), *Cecrops septemporatus* (PARONA) and *Sethocapsa kaminogoensis* AITA, which do not extend above the Barremian, makes the lower Aptian age the most probable for U.A.38 to U.A.40.

Tricapsula costata WU defines **U.A.41 and U.A.42.** It is restricted to the upper Aptian and possibly lower Albian. The upper Aptian-lower Albian age is furthermore confirmed by foraminifera associated in sample BM 489.40 (Chapter 2.6.1).

U.A.45 to U.A.47 are assignable to the middle Albian-lowermost Cenomanian on the basis of co-occurring *Rhopalosyringium majuroense* SCHAAF, *Archaeocenosphaera* (?) sp. and *Novixitus weyli* SCHMIDT-EFFING with *Mita* sp. B sensu THUROW. *Pseudodictyomitra pseudomacrocephala* (SQUINABOL) is associated in U.A.47. The underlying **U.A.43 and U.A.44** lack the characteristic species of the zonation proposed by O'Dogherty (1994) and can therefore not be directly correlated. The superposition between U.A.43–U.A.44 and U.A.46–U.A.47 observed in two sections within a considerable rock-sequence, led us to assume a lower to lowermost middle Albian age for U.A.43 and U.A.44.

U.A.48 was identified in only one section. The assemblage comprising *Hemicryptocapsa polyhedra* DUMITRICA and *Afens liriodes* RIEDEL & SANFILIPPO indicates a lower Turonian or younger age. *Pseudodictyomitra pseudomacrocephala* (SQUINABOL), abundant in this sample, suggests that the sample is not younger than the Turonian (Pessagno, 1977b; Thurow, 1988). A long interval missing between U.A.47 and U.A.48 has not been sampled.

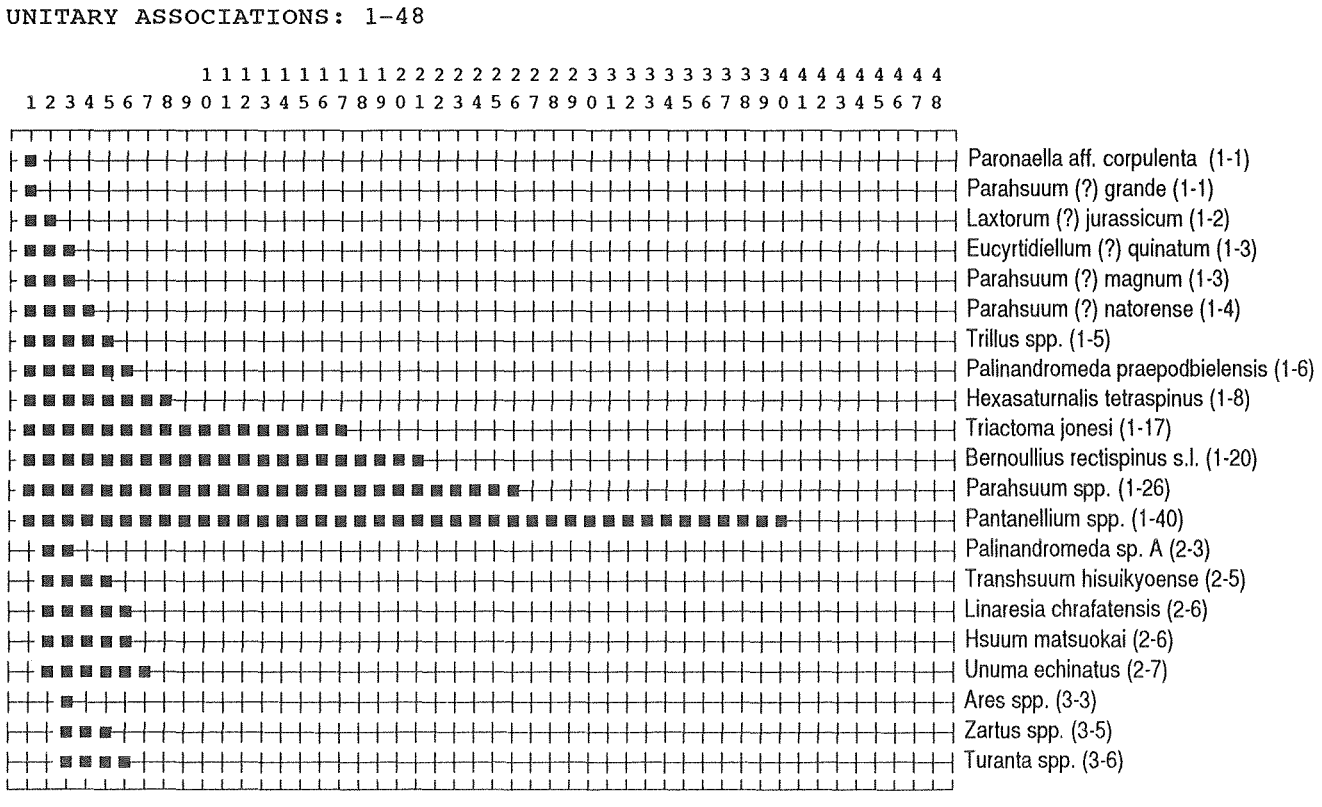

Fig. 6.2: Middle Jurassic to Turonian protoreferential (in brackets the ranges are presented numerically) (output of BioGraph program version 2.02, Savary & Guex, 1990). Correlation to standard chronostratigraphic stages is given in Fig. 6.3.

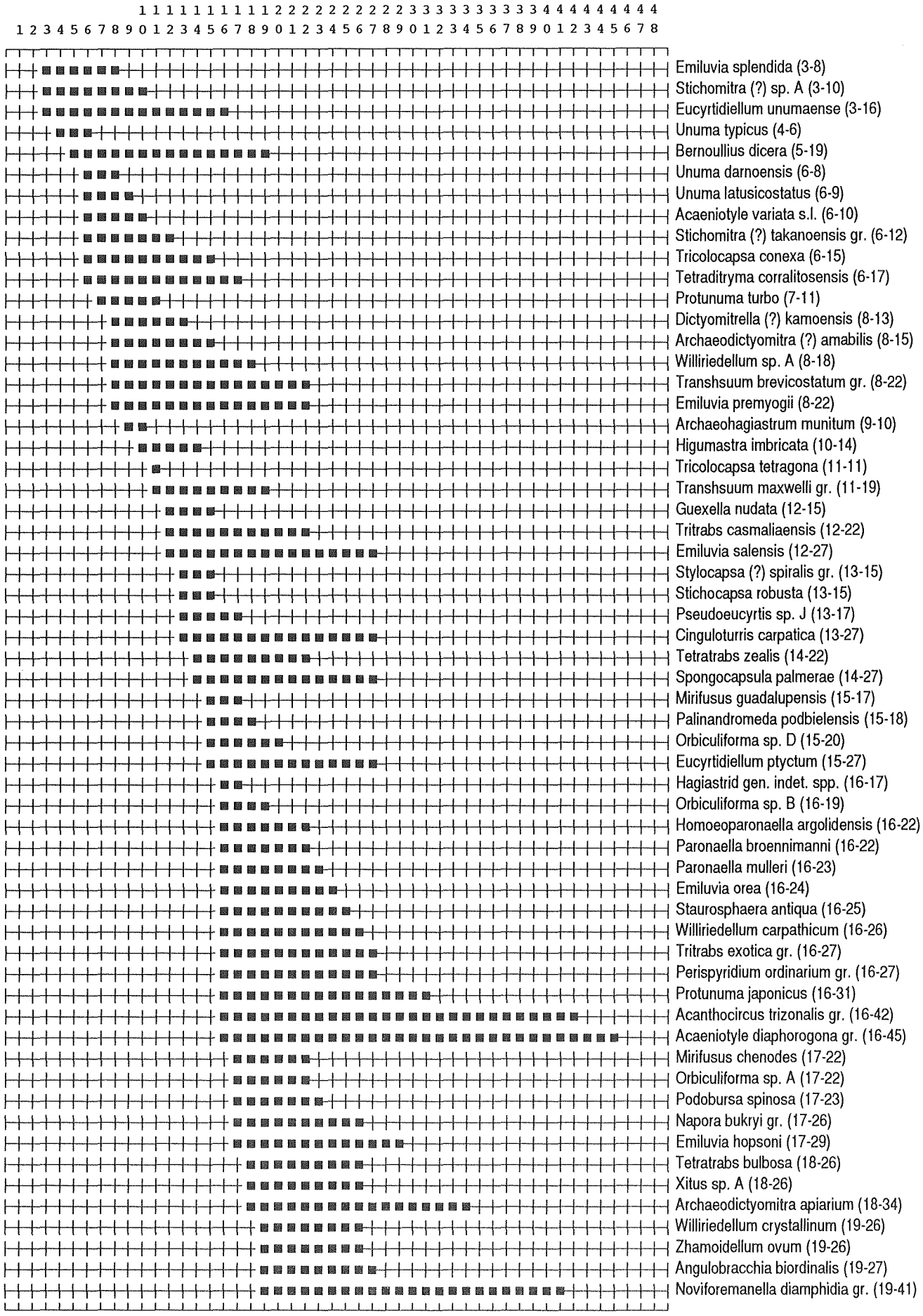

Fig. 6.2 continued

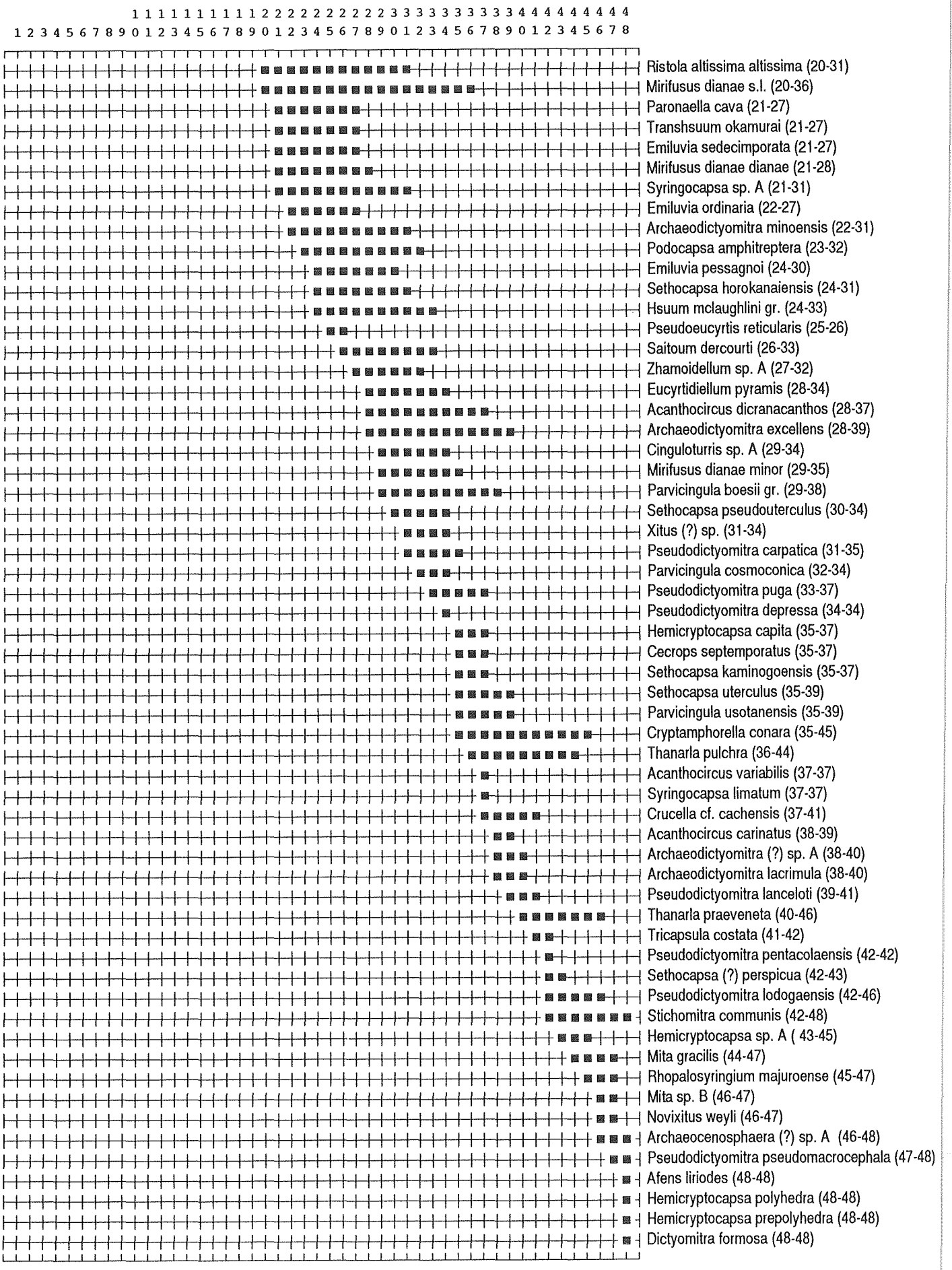

Fig. 6.2 continued

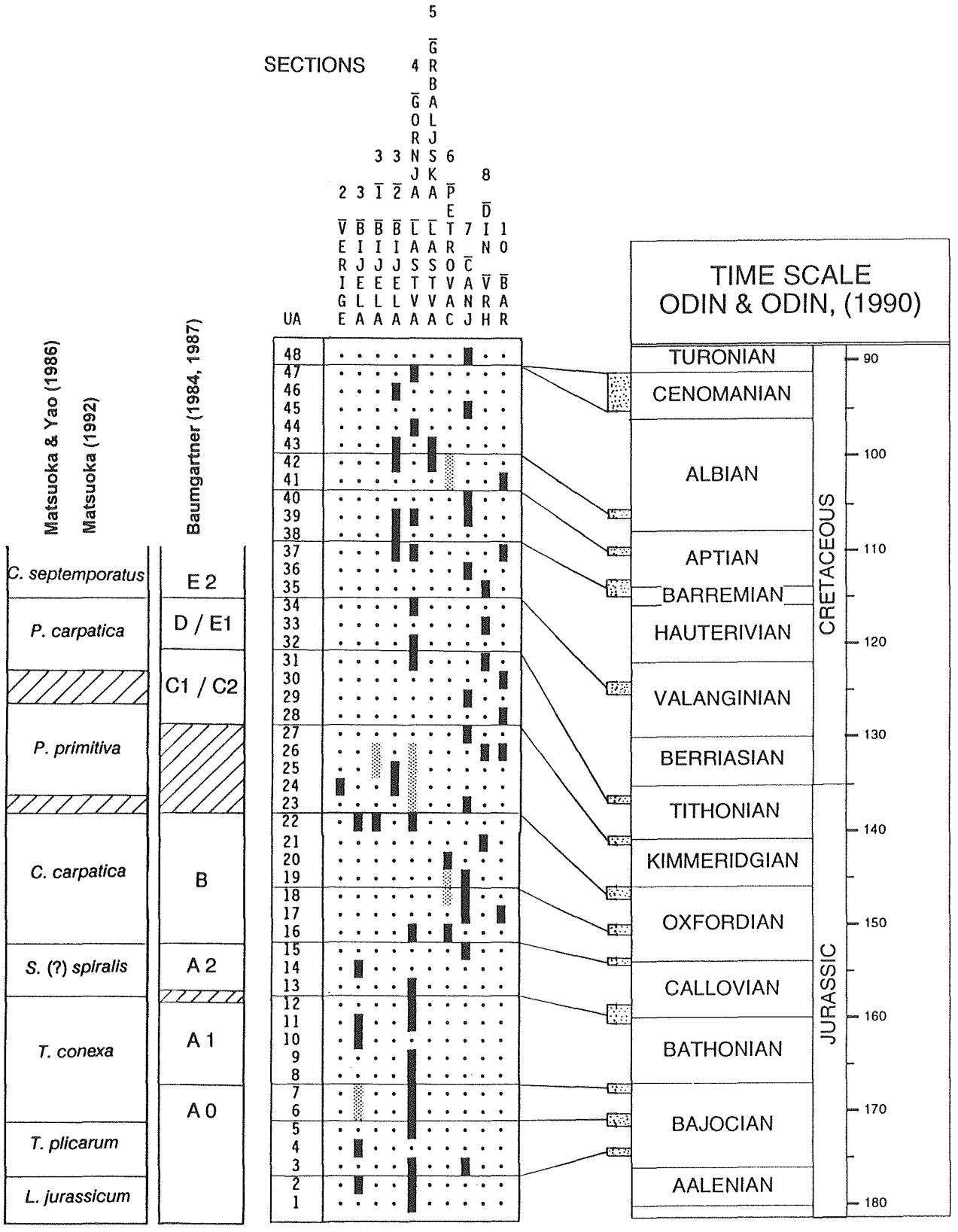

Fig. 6.3: Reproducibility table (output of BioGraph program version 2.02, Savary & Guex, 1990). Black and grey rectangles represent U.A.'s and unions of U.A.'s respectively, strictly identified in the sections studied. The proposed local "zones" are correlated to standard chronostratigraphic stages and radiolarian zonations proposed by Matsuoka & Yao (1986), Matsuoka (1992), and Baumgartner (1984, 1987). Cross-hatched fields indicate uncertain correlation.

7. SYSTEMATIC PALEONTOLOGY

7.1 Sample preparation

Radiolarians from chert samples were extracted using standard HF methods (Dumitrica, 1970; Pessagno & Newport, 1972; De Wever, 1982b).

The lower Cretaceous siliceous-limestone samples were first treated with acetic acid to remove the carbonate component. These residues were devoid of determinable radiolarians. Radiolarians were then isolated with diluted hydrofluoric acid.

7.2 General remarks on systematics

The main purpose of this work was the biostratigraphic research. The taxa are listed in alphabetical order of genera and species because they were not systematically studied on the suprageneric level. The generic assignment of species follows previous authors. Possible disagreements are discussed in the remarks or indicated by a question mark after the name of the genus.

The taxonomy is further adapted to the specific biostratigraphic problem. The long time-span investigated allowed us only a relatively low-resolution sampling. A broad definition of species is generally used to enable the correlation among the assemblages of different sections. Several morphotypes are often merged in groups, for example *Napora bukryi* PESSAGNO gr., *Acaeniotyle diaphorogona* FOREMAN gr. and others. Many taxa are treated on the generic level. Due to the clearly distinctive morphologic characters, their stratigraphic range is much more reliable than the range of individual species.

The taxonomic list and illustrations provide a precise definition of the taxa used in the database and resulting biochronological correlation. Morphotypes possessing high variability are illustrated with several figures to demonstrate at least the end members. The same principle is applied for the long ranging taxa, for which there is a picture of the oldest and the youngest form. Some transitional forms, not included in the database, are illustrated in order to clearly define the morphologic limits of a taxon. Each species is, in addition, provided with a critical synonymy as complete as possible.

Some of the listed species (marked with an asterisk) are not included in the zonation for the following reasons: 1: They were found only in one section and are therefore of no importance for correlation. 2: The presence of some radiolarians with delicate tests, especially spumellarians, is very discountinuous in our sections. Furthermore, ancestral and descendent forms are often similar in shape and external ornamentation. Such forms were not used for the correlation to avoid the introduction of possible homeomorphs. The illustrations of these species should complete the picture of the radiolarian assemblages from the Budva Zone and provide supplementary data for the correlation with other regions.

7.3 Taxonomic list

Species marked with an * asterisk are not included in the protoreferential.

Genus: **Acaeniotyle** FOREMAN 1973

Type species: Xiphosphaera umbilicata RÜST 1898

Acaeniotyle diaphorogona FOREMAN 1973 **gr.**
Pl. 2, figs. 10–11, 15

Acaeniotyle diaphorogona FOREMAN
Foreman 1973, p. 258, pl. 2, figs. 2–5.
Foreman 1975, pl. 2F, figs. 1–3, non figs 4–5; pl. 3, figs. 1–2.
Muzavor 1977, p. 34, pl. 1, fig. 1.
Mizutani 1981, p. 175, pl. 61, figs. 1–2.
De Wever & Thiébault 1981, p. 582, pl. 2, fig. 7.
Kanie et al. 1981, pl. 1, fig. 1.
Aoki 1982, pl. 1, fig. 1.
Schaaf 1984, p. 104–105, figs. 1–5.
Ožvoldova & Sykora 1984, p. 261, pl. 1, figs. 1–3.
Sanfilippo & Riedel 1985, p. 586, fig. 4.1a,b.
De Wever et al. 1986b, pl. 6, fig. 11.
Aita 1987, p. 63, pl. 12, fig. 12.
Ožvoldova & Peterčakova 1987, pl. 31, fig. 1.
Ožvoldova 1988, pl. 1, fig. 2.
Kawabata 1988, pl. 2, fig. 15
Thurow 1988, p. 396, pl. 9, fig. 8.
Tumanda 1989, p. 33, pl. 1, fig. 2, 3.
Baumgartner 1992, p. 317, pl. 3, fig. 1.
Matsuoka 1992, pl. 3, fig. 12.
Ožvoldova & Peterčakova 1992, pl. 1, fig. 16, ? 13.
Steiger 1992, p. 28, pl. 2, figs. 1, 2.
Taketani & Kanie 1992, Fig. 3.1.
Acaeniotyle sp. aff. A. *diaphorogona* FOREMAN
Foreman 1973, pl. 2, fig. 6, 7; pl. 16, fig. 16.
Foreman 1975, p. 607, pl. 1F, fig. 1.
Yao 1984, pl. 3, fig. 24.
Acaeniotyle diaphorogona FOREMAN s. l.
Baumgartner 1984, p. 753, pl. 1, figs. 1–2.
Widz 1991, p. 243, pl. 1, fig. 1.

* **Acaeniotyle umbilicata** (RÜST) 1898
Pl. 2, fig. 12

Xiphosphaera umbilicata RÜST
Rüst 1898, p. 7, pl. 1, fig. 9.

Dumitrica 1972, p. 832, pl. 1, fig. 1
Renz 1974, p. 799, pl. 2, figs. 9–11, 12; pl. 9, fig. 21.
Acaeniotyle umbilicata (RÜST)
Foreman 1973, p. 258, pl. 1, figs. 12–14, 16.
Foreman 1975, p. 607, pl. 2E, figs. 14–17; pl. 3, fig. 3.
Muzavor 1977, p. 26, pl. 1, fig. 3.
Nakaseko et al. 1979, pl. 4, fig. 7.
Baumgartner et al. 1980, p. 48, pl. 2, fig. 8.
Kocher 1981, p. 51, pl. 12, figs. 1–2.
Schaaf 1981, p. 431, pl. 6, fig. 11; pl. 15, fig. 3a,b.
Nakaseko & Nishimura 1981, p. 141, pl. 1, fig. 7; non pl. 14, fig. 2.
Kanie et al. 1981, pl. 1, fig. 2.
Baumgartner 1984, p. 754, pl. 1, fig. 5.
Ožvoldova & Sykora 1984, p. 261, pl. 1, figs. 4–5.
Schaaf 1984, p. 148–149, figs. 1, 2a,b, 3a,b.
Sanfilippo & Riedel 1985, p. 587, pl. 4.2a–d.
Aita & Okada 1986, p. 108, pl. 1, fig. 1.
De Wever et al. 1986b, pl. 6, figs. 8, 12–13.
Aita 1987, p. 63, pl. 12, fig. 2.
Igo et al. 1987, Fig. 2.11.
Pavšič & Goričan 1987, p. 22, pl. 2, fig. 5.
Kito 1987, pl. 1, fig. 7.
Ožvoldova 1988, pl. 1, fig. 1.
Thurow 1988, pl. 9, fig. 7.
Tumanda 1989, p. 33, pl. 1, fig. 4.
Kato & Iwata 1989, pl. 1, fig. 9.
Baumgartner 1992, p. 317, pl. 3, fig. 2.
Ožvoldova & Peterčakova 1992, pl. 1, figs. 8, 10.
Steiger 1992, p. 27, pl. 1, figs. 16, 17.
Taketani & Kanie 1992, Fig. 3.2.
Acaeniotyle tuberosa STEIGER
Steiger 1992, p. 27, pl. 1, figs. 18–20.

Acaeniotyle variata OŽVOLDOVA 1979 **s.l.**
Pl. 2, fig. 14

Acaeniotyle diaphorogona variata OŽVOLDOVA
Ožvoldova, 1979, p. 251, pl. I, fig. 2.
Conti & Marcucci 1991, pl. 1, fig. 2.
Matsuoka 1992, pl. 5, fig. 10.
Acaeniotyle (?) sp. 1
Kito 1989, p. 95, pl. 3, figs. 1–5, 8–9.
Acaeniotyle sp. B
Tonielli 1991, p. 21, pl. 1, fig. 20

Remarks: This species is characterized by massive nodes on the shell surface and branched spine-tips.

Genus: **Acanthocircus** SQUINABOL 1903

Type species: Acanthocircus irregularis SQUINABOL 1903

Acanthocircus carinatus FOREMAN 1973
Pl. 3, fig. 4

Acanthocircus carinatus FOREMAN
Foreman 1973, p. 260, pl. 5, fig. 2, non fig. 1.
non Riedel & Sanfilippo 1974, p. 775, pl. 2, figs. 1, 2.
Foreman 1975, p. 610, pl. 2C, fig. 8, pl. 4, fig. 12.
Schaaf 1981, p. 431, pl. 16, fig. 2.
Schaaf 1984, p. 159, fig. 7.

Acanthocircus dicranacanthos (SQUINABOL) 1914, emend. FOREMAN 1975

Saturnalis dicranacanthos SQUINABOL
Squinabol 1914, p. 289, pl. 22, figs. 4–7, pl. 23, fig. 8; text-fig. 1, p. 290.
Saturnalis novalensis SQUINABOL
Squinabol 1914, p. 268, 297, pl. 20, fig. 1; pl. 23, fig. 7.
Saturnulus sp.
Fischli 1916, p. 46, fig. 53.
Acanthocircus dizonius (RÜST) (?)
Foreman 1973, p. 260, pl. 4, fig. 4, 5.
Acanthocircus dizonius (RÜST)
Riedel & Sanfilippo 1974, p. 775, pl. 2, figs. 4, 5, non fig. 3.
Acanthocircus dicranacanthos (SQUINABOL)
emend. Foreman 1975, p. 610, pl. 2D, figs. 5, 6.
Muzavor 1977, p. 37, pl. 4, fig. 4.
Pessagno 1977a, p. 73, pl. 3, fig. 5.
Pessagno 1977b, p. 31, pl. 2, fig. 6.
Donofrio & Mostler 1978, p. 28, pl. 2, fig. 3; pl. 4, figs. 4, 7–9; pl. 5, figs. 10–11.
Nakaseko et al. 1979, p. 2, fig. 7.
Baumgartner et al. 1980, p. 49, pl. 1, fig. 11.
Holzer 1980, p. 156, text-fig. 2, pl. 1, figs. 1–12; pl. 2, fig. 7–9.
Okamura 1980, pl. 19, fig. 8.
Kanie et al. 1981, pl. 1, fig. 3.
Kocher 1981, p. 51, pl. 12, fig. 3.
Nakaseko & Nishimura 1981, p. 141, pl. 1, fig. 6.
Schaaf 1981, p. 431, pl. 7, fig. 1; pl. 16, fig. 3.
Aoki 1982, pl. 1, fig. 3.
Okamura & Uto 1982, pl. 4, figs. 12–14; pl. 5, fig. 17.
Baumgartner 1984, p. 754, pl. 1, fig. 7.
Ožvoldova & Sykora 1984, p. 261, pl. 1, figs. 6, 7.
Schaaf 1984, p. 106–107, figs. 1–5.
Sanfilippo & Riedel 1985, p. 591, pl. 5, 2a–c.
Aita & Okada 1986, p. 108, pl. 1, fig. 5.
De Wever et al. 1986b, pl. 6, figs. 3–4.
Pavšič & Goričan 1987, p. 22, pl. 2, fig. 2.
Ožvoldova & Peterčakova 1987, pl. 31, fig. 3.
Ožvoldova 1988, pl. 3, fig. 7.
Thurow 1988, p. 396, pl. 10, fig. 3.
Danelian 1989, p. 130, pl. 1, figs. 9–11.
Tumanda 1989, p. 34, pl. 2, fig. 12.
Ožvoldova & Peterčakova 1992, pl. 1, figs. 1, 2, 11.
Steiger 1992, p. 34, pl. 5, figs. 3–6.
Acanthocircus sp. cf. A. *dicranacanthos* (SQUINABOL)
Thurow 1988, p. 396, pl. 10, fig. 4.
Acanthocircus sp. B
Ožvoldova & Peterčakova 1992, p. 315, pl. 1, fig. 3.

Remarks: All morphotypes with a bifurcating spine at least at one end of the ring are included.

Acanthocircus trizonalis (RÜST) 1898 **gr.**
Pl. 3, figs. 1–2

Saturnulus dizonius RÜST
Rüst 1898, p. 8, pl. 2, fig. 3.
Saturnulus trizonalis RÜST
Rüst 1898, p. 9, pl. 2, fig. 4.
Fischli 1916, p. 47, fig. 52.
Saturnalis major SQUINABOL
Squinabol 1914, p. 288, pl. 22, fig. 3.
Saturnalis amissus SQUINABOL
Squinabol 1914, p. 296, pl. 23, figs. 2–5.
Acanthocircus amissus (SQUINABOL)
Donofrio & Mostler 1978, p. 23, pl. 1, figs. 1, 10; pl. 5, figs. 1–4, 6, 9; pl. 6, figs. 4, 6, 8, 11.
Ožvoldova 1988, pl. 3, fig. 8.
Ožvoldova 1990a, p. 139, pl. 5, fig. 2.
Ožvoldova 1990b, pl. 4, fig. 5.
Widz 1991, p. 243, pl. 1, fig. 2.
Steiger 1992, p. 34, pl. 5, fig. 7.
Acanthocircus trizonalis (RÜST)
Foreman 1973, p. 261, pl. 4, figs. 6–8.
Foreman 1975, p. 610, pl. 2D, figs. 1–4.
De Wever & Thiébault 1981, p. 584, pl. 2, fig. 16.
Schaaf 1981, p. 431, pl. 16, fig. 1.
Schaaf 1984, p. 155, fig. 5.
Sanfilippo & Riedel 1985, p. 592, figs. 5.1a–d.
Pavšič & Goričan 1987, p. 23, pl. 2, fig. 3.
Thurow 1988, p. 396, pl. 10, fig. 2.
Acanthocircus dizonius (RÜST)
Riedel & Sanfilippo 1974, p. 775, pl. 2, fig. 3, non figs. 4, 5.
Acanthocircus sp. A
Pessagno 1977a, p. 74, pl. 3, figs. 7–12.
Acanthocircus sp.
Schaaf 1981, p. 431, pl. 7, fig. 7.
Thurow 1988, p. 396, pl. 10, fig. 1.
Acanthocircus cf. *amissus* (SQUINABOL)
Dumitrica & Mello 1982, pl. 3, fig. 20.

Remarks: Distal peripheral spine is simple non-bifurcated and has a thickened saddle at its base.

Acanthocircus variabilis (SQUINABOL) 1914
Pl. 7, fig. 3

Saturnalis variabilis SQUINABOL
Squinabol 1914, p. 291, pl. 22, fig. 8, non fig. 9
Acanthocircus sp. aff. *S. variabilis* SQUINABOL
Foreman 1973, p. 261, pl. 5, figs. 4, 5.
Acanthocircus carinatus FOREMAN
Foreman 1973, p. 260, pl. 5, fig. 1, non fig. 2.
Riedel & Sanfilippo 1974, p. 775, pl. 2, fig. 1, non fig. 2.
Ožvoldova & Peterčakova 1992, pl. 1, fig. 5.
Acanthocircus variabilis (SQUINABOL)
non Pessagno 1977a, p. 74, pl. 3, fig. 6.
Donofrio & Mostler 1978, p. 32, pl. 3, figs. 6, 10, pl. 6, figs. 5, 7.
non Yang & Wang 1990, p. 204, pl. 2, fig. 8.

Genus: **Afens** RIEDEL & SANFILIPPO 1974

Type species: Afens liriodes RIEDEL & SANFILIPPO 1974

Afens liriodes RIEDEL & SANFILIPPO 1974
Pl. 26, figs. 1–2

Afens liriodes RIEDEL & SANFILIPPO
Riedel & Sanfilippo 1974, p. 775, pl. 11, fig. 11; pl. 13, figs. 14–16.
Sanfilippo & Riedel 1985, p. 624, Figs. 13.3a–c.
Thurow 1988, pl. 2, fig. 1.
Unnamed Nassellaria
Nakaseko & Nishimura 1981, pl. 13, fig. 6.

Genus: **Angulobracchia** BAUMGARTNER 1980

Type species: Paronaella (?) *purisimaensis* PESSAGNO 1977a

Angulobracchia biordinalis OŽVOLDOVA, in Ožvoldova & Sykora 1984
Pl. 6, figs. 2–3

Angulobracchia sp. aff. A. *digitata* BAUMGARTNER
Baumgartner 1980, p. 312, pl. 10, fig. 15.
Angulobracchia biordinale OŽVOLDOVA
Ožvoldova & Sykora 1984, p. 262, pl. 2, figs. 1–7; pl. 16, figs. 1, 2.
Ožvoldova 1988, pl. 1, fig. 10.
Widz 1991, p. 243, pl. 1, fig. 17.
Halesium digitatum (BAUMGARTNER)
De Wever et al. 1986b, pl. 8, fig. 10.
Halesium sp. aff. *Angulobracchia digitata* BAUMGARTNER
De Wever & Cordey 1986, pl. 1, fig. 15.

Angulobracchia digitata BAUMGARTNER 1980
Pl. 6, fig. 1

Angulobracchia digitata BAUMGARTNER
Baumgartner 1980, p. 310, pl. 10, figs. 18–22, pl. 12, fig. 11.
Kocher 1981, p. 55, pl. 12, fig. 11.
Danelian 1989, p. 140, pl. 2, fig. 12.
Ožvoldova 1990b, pl. 4, fig. 1.
Widz 1991, p. 243, pl. 1, fig. 8, 10.

*** Angulobracchia (?) sp. A**
Pl. 6, fig. 7

Angulobracchia (?) *portmanni* BAUMGARTNER
Steiger 1992, p. 50, pl. 12, figs. 7, 8 only.

Remarks: This species is characterized by a large triangular nodose central area. It differs from *Angulobracchia* (?) *portmanni* BAUMGARTNER (1984, p. 757, pl. 2, figs. 1–3) by having shorter rays and more expanded ray-tips.

Genus: **Archaeocenosphaera** PESSAGNO & YANG, in Pessagno et al. 1989

Type species: Archaeocenosphaera ruesti PESSAGNO & YANG, in Pessagno et al. 1989

Archaeocenosphaera (?) sp. A
Pl. 3, figs. 5–6

Cenosphaera? sp. A
Empson-Morin 1984, pl. 1, fig. 6.
Hemicryptocapsa polyhedra DUMITRICA
Thurow 1988, p. 401, pl. 1, fig. 1.
Hemicryptocapsa sp. cf. *H. polyhedra* DUMITRICA
Thurow 1988, p. 401, pl. 5, fig. 2.
Hemicryptocapsa sp.
Hernandez-Molina et al. 1991, Fig. 11.1.
Williriedellum sp. aff. *W. gilkeyi* DUMITRICA
Marcucci Passerini et al. 1991, fig. 4n.
Hemicryptocapsa sp. A
Marcucci Passerini & Gardin 1992, Fig. 31.

Remarks: Test covered by an irregular network of polygonal facets.

Neither a depression indicating an encased cephalis nor an aperture has been observed. This species probably belongs to Spumellariina.

Genus: **Archaeodictyomitra** PESSAGNO 1976, emend. PESSAGNO 1977b

Type species: Archaeodictyomitra squinaboli PESSAGNO 1976

Archaeodictyomitra (?) amabilis AITA 1987
Pl. 20, fig. 1

Thanarla sp. A
Aita 1982, pl. 1, fig. 5.
Kishida & Hisada 1986, pl. 2, fig. 9.
Thanarla sp. C
Aita 1982, pl. 1, fig. 16.
Archaeodictyomitra sp. R
Matsuoka 1982b, pl. 2, figs. 11a,b, 16.
Yao 1984, pl. 2, fig. 14.
Thanarla sp. A
Kishida & Hisada 1986, Fig. 2.9.
Archaeodictyomitra ? *amabilis* AITA
Aita 1985, fig. 6, 6.
Aita 1987, p. 70, pl. 1, figs. 13a,b; pl. 9, fig. 6.
Matsuoka 1990, pl. 1, fig. 5.
Maaté et al. 1993, Fig. 3.7, 3.8.
Thanarla (?) sp.
Kojima 1989, pl. 2, figs. 8a,b.
Mizutani & Kojima 1992, pl. 1, figs. 8a, 8b.
Archaeodictyomitra aff. *inexploratum* (BLOME)
Yao 1991, pl. 4, fig. 9.

Archaeodictyomitra apiarium (RÜST) 1885
Pl. 20, figs. 5–6, 12, 17–18

Lithocampe apiarium RÜST
Rüst 1885, p. 314, pl. 39 (14), fig. 8.
Dictyomitra apiarium (RÜST)
non Foreman 1975, p. 613, pl. 2G, figs. 7–8.
Dictyomitra excellens (TAN)
Baumgartner & Bernoulli 1976, p. 615, fig. 12k.
Archaeodictyomitra apiara (RÜST)
Pessagno 1977b, p. 41, pl. 6, fig. 6, 14.
non Kanie et al. 1981, pl. 1, fig. 8.
Nakaseko & Nishimura 1981, p. 145, pl. 6, figs. 2–4; pl. 15, figs. 2, 6, non fig. 1.
non Schaaf 1981, p. 432, pl. 18, fig. 2a,b.
Matsuyama et al. 1982, pl. 1, fig. 1.
Aoki 1982, pl. 2, fig. 11, ?12
Matsuoka & Yao 1985, pl. 2, fig. 4.
Tanaka et al. 1985, pl. 1, figs. 5, 6.
Conti & Marcucci 1986, pl. 1, fig. 3.
Kishida & Hisada 1986, fig. 2.8.
Matsuoka 1986c, pl. 2, fig. 14, pl. 3, fig. 13.
Kawabata 1988, pl. 2, fig. 9.
Wakita 1988, pl. 4, fig. 1.
Tumanda 1989, p. 36, pl. 2, fig. 9
Kiessling 1992, pl. 1, fig. 4, ?5.
Sano et al. 1992, pl. 2, fig. E.
Dictyomitra apiarum (RÜST)
Nakaseko et al. 1979, pl. 3, fig. 4, non fig. 3.
Archaeodictyomitra apiarium (RÜST)
Kocher 1981, 56, pl. 12, fig. 13.
Schaaf 1984, p. 92–93, figs. 1, 3a,b, 5a,b; non figs, 2, 4a,b.
Aita & Okada 1986, p. 108, pl. 1, fig. 11.
Igo et al. 1987, Fig. 2.14.
Pavšič & Goričan 1987, p. 24, pl. 2, fig. 11.
Danelian 1989, p. 142, pl. 3, figs. 1–2.
Widz 1991, p. 243, pl. 1, fig. 14.
Archaeodictyomitra apiaria (RÜST)
Ožvoldova & Sykora 1984, p. 263, pl. 3, fig. 6.
Baumgartner 1984, p. 758, pl. 2, figs. 5–6.
Ožvoldova 1990b, pl. 3, fig. 2; pl. 5, fig. 5.
Steiger 1992, p. 88, pl. 25, figs. 8, 9.
Archaeodictyomitra directiporata (RÜST)
? Ožvoldova 1988, pl. 4, fig. 3.

Remarks: See remarks under *Archaeodictyomitra minoensis* (MIZUTANI).

Archaeodictyomitra excellens (TAN) 1927
Pl. 20, figs. 2–4

Lithomitra excellens TAN
Tan 1927, p. 56, pl. 11, fig. 85.
Dictyomitra excellens (TAN)
Renz 1974, pl. 8, fig. 8, non fig. 7; pl. 11, fig. 35.
Dictyomitra apiarum (RÜST)
Nakaseko et al. 1979, pl. 3, fig. 3, non 4.
Archaeodictyomitra apiara (RÜST)
Schaaf 1981, p. 432, pl. 18, fig. 2a,b.
Nakaseko & Nishimura 1981, p. 145, pl. 6, fig. 1, non 3–4.
Kanie et al. 1981, pl. 1, fig. 8.
Okamura & Uto 1982, pl. 2, figs. 1–2.
Kito 1987, pl. 3, fig. 2.
Kato & Iwata 1989, pl. 2, fig. 4.
Taketani & Kanie 1992, Fig. 3.9.
Archaeodictyomitra excellens (TAN)
Baumgartner 1984, p. 758, pl. 2, figs. 7–8.
Pavšič & Goričan 1987, p. 24, pl. 2, fig. 10.
Tumanda 1989, p. 36, pl. 3, fig. 7; pl. 10, fig. 3.
Aguado et al. 1991, Fig. 1.4.
Matsuoka 1992, pl. 1, fig. 7.
Steiger 1992, p. 88, pl. 25, figs. 10, 11.
Archaeodictyomitra apiarium (RÜST)
Schaaf 1984, 92–93, figs. 2, 4a,b, non figs. 1, 3a,b, 5a,b.

Archaeodictyomitra lacrimula (FOREMAN) 1973
Pl. 21, figs. 5–6

Dictyomitra (?) *lacrimula* FOREMAN
Foreman 1973, p. 263, pl. 10, fig. 11.
Foreman 1975, p. 614, pl. 2G, figs. 5, 6, pl. 6, fig. 1.
Nakaseko et al. 1979, p. 22, pl. 4, fig. 1.
Archaeodictyomitra lacrimula (FOREMAN)
Schaaf 1981, p. 432, pl. 22, figs. 3a,b.
Nakaseko & Nishimura 1981, p. 146, pl. 6, figs. 5, 6; pl. 15, fig. 10.
Okamura & Uto 1982, pl. 7, fig. 4.
Sanfilippo & Riedel 1985, p. 598, Figs. 7.3a–c.
Okamura & Matsugi 1986, pl. 1, figs. 1, 2.
Kito 1987, pl. 3, fig. 3.
Tumanda 1989, p. 36, pl. 3, fig. 19.
Iwata et al. 1990, pl. 1, fig. 1, pl. 2, figs. 2, 6.
Aguado et al. 1991, Fig. 7.1.
Taketani & Kanie 1992, Fig. 3.10.
Thanarla lacrimula (FOREMAN) gr.
Vishnevskaya 1984, pl. 12, figs. 1, 4, 8.

Remarks: Only specimens with a closed or nearly closed, inversely conical distal part are included.

Archaeodictyomitra minoensis (MIZUTANI) 1981
Pl. 20, figs. 9, 14–15, 19, 20

Pseudodictyomitra minoensis MIZUTANI
Mizutani 1981, p. 178, pl. 58, fig. 4; pl. 63, figs. 9–10.
Adachi 1982, pl. 1, figs. 9, 10.
Yamamoto 1983, pl. 1, fig. 7.
Dictyomitra sp. aff. D. *minoensis* (MIZUTANI)
Yao 1984, pl. 3, fig. 5.
Archaeodictyomitra minoensis (MIZUTANI)
Matsuoka & Yao 1985, pl. 2, fig. 5.
Wakita 1988, pl. 5, fig. 2; pl. 6, fig. 10.
Yao 1991, pl. 4, fig. 25.
? Kiessling 1992, pl. 1, figs. 2–3.

Remarks: Archaeodictyomitra minoensis (MIZUTANI) is closely related to *A. apiarium* (RÜST). It differs from the latter by the circumferential ridges being larger with respect to intersegmental constrictions. Only narrow transverse ridges may develop with *A. apiarium*. The segmental division is externally more pronounced with *A. minoensis*.

Through time both species show a decrease in number of costae, which become thicker, especially where crossing the transverse ridges. Circular pores, systematically arranged on both sides of the ridge, become larger. Transitional forms (pl. 20, figs. 7, 8, 13) exist from the upper Oxfordian to the Tithonian.

The vertical costae of *A. minoensis* tend to disappear in the area of constrictions (pl. 20, fig. 9; illustrations by Mizutani, 1981). It is suggested that *A. minoensis* gave rise to *Pseudodictyomitra depressa* BAUMGARTNER.

Archaeodictyomitra (?) sp. A
Pl. 21, figs. 1–2

Stichocapsa decora RÜST
Nakaseko & Nishimura 1981, p. 162, pl. 17, fig. 9.
Stichocapsa sp. cf. S. *decora* RÜST
Schaaf 1981, p. 439, pl. 27, figs. 12a,b.
Mita (?) sp. E
Thurow 1988, p. 402, pl. 6, fig. 22.

Remarks: Proximal part conical, distal portion inflated, closed. Generally one row, sometimes two to three rows of pores between adjacent costae.

Genus: **Archaeohagiastrum** BAUMGARTNER 1984

Type species: Archaeohagiastrum munitum BAUMGARTNER 1984

Archaeohagiastrum munitum BAUMGARTNER 1984
Pl. 5, fig. 14

Crucella sp. A
Sashida et al. 1982, pl. 1, fig. 9.
Tetratrabs sp. B
Wakita 1982, pl. 5, fig. 4.
Archaeohagiastrum munitum BAUMGARTNER
Baumgartner 1984, p. 759, pl. 2, figs. 9–13.
Nagai 1985, pl. 2, fig. 5–5a.

Yamamoto et al. 1985, p. 34, pl. 3, fig. 7a,b.
Danelian 1989, p. 143, pl. 3, fig. 3.
Kito 1989, p. 116, pl. 7, fig. 8.
Tetraditryma sp. B
? Carter et al. 1988, p. 31, pl. 16, fig. 8.

Genus: **Ares** DE WEVER 1982a

Type species: Ares armatus DE WEVER 1982a

Remarks: Parares TAKEMURA (1986) is synonymized with *Ares* DE WEVER. The differences between these two genera (presence or absence of an external spine A and cylindrical or conical shape) are considered to be of specific rather than generic level.

Ares spp.
Pl. 26, figs. 13–14

Remarks: This morphotype is treated in the generic level.

Genus: **Bagotum** PESSAGNO & WHALEN 1982

Type species: Bagotum maudense PESSAGNO & WHALEN 1982

*** Bagotum sp.**
Pl. 17, fig. 11

Genus: **Bernoullius** BAUMGARTNER, in Baumgartner et al. 1980

Type species: Eucyrtis (?) *dicera* BAUMGARTNER, in Baumgartner et al. 1980

*** Bernoullius cristatus** BAUMGARTNER 1984
Pl 8, fig. 5

Eucyrtis (?) *dicera* BAUMGARTNER
Baumgartner et al. 1980, p. 54, pl. 6, fig. 6 (only).
Eucyrtis (?) sp. A
Kocher 1981, p. 68, pl. 13, figs. 19–20.
Bernoullius cristatus BAUMGARTNER
Baumgartner 1984, p. 760, pl. 2, figs. 14–15.
Danelian 1989, p. 144, pl. 3, fig. 4–6.
Kito 1989, p. 157, pl. 17, fig. 1.
Conti & Marcucci 1991, pl. 1, fig. 8.
Pessagno et al. 1993, p. 119, pl. 1, fig. 14.

Bernoullius dicera (BAUMGARTNER), in Baumgartner et al. 1980
Pl. 8, figs. 1–4

Lophophaena sp.
Ožvoldova 1979, p. 259, pl. 4, figs. 4–5.
Eucyrtis (?) *dicera* BAUMGARTNER
Baumgartner et al. 1980, p. 54, pl. 3, fig. 16, pl. 6, fig. 10, non fig. 6.
Kocher 1981, p. 68, pl. 13, figs. 17–18.
De Wever & Caby 1981, pl. 2, fig. 2I.
Bernoullius dicera (BAUMGARTNER)
Baumgartner 1984, p. 760, pl. 2, fig. 16.
Danelian 1989, p. 145, pl. 3, fig. 9.
Kito 1989, p. 157, pl. 17, fig. 2.
Widz 1991, p. 244, pl. 1, fig. 15.

*** Bernoullius furcospinus** KITO, DE WEVER, DANELIAN & CORDEY 1990
Pl. 8, fig. 19

Bernoullius sp. B
Danelian 1989, p. 145, pl. 3, fig. 12.
Bernoullius sp. 1
Kito 1989, p. 158, pl. 17, figs. 4, 5, 7, 10, 14.
Bernoullius furcospinus KITO, DE WEVER, DANELIAN & CORDEY
Kito et al. 1990, p. 344–347, pl. 2, fig. 1–3, 6, 8.
Spongiostoma ? *furcospinus* (KITO & DE WEVER)
Tonielli 1991, p. 26, pl. 1, fig. 3.

Bernoullius rectispinus KITO, DE WEVER, DANELIAN & CORDEY 1990 **s.l.**
Pl. 8, figs. 7–9, 11–18

Eucyrtis dicera BAUMGARTNER
Carayon et al. 1984, pl. 1, fig. 10.
Bernoullius sp. B.
De Wever et al. 1987, pl. A, fig. 3.
Goričan 1987, p. 181, pl. 1, fig. 18.
Bernoullius sp. A
Goričan 1987, p. 181, pl. 1, fig. 17.
Danelian 1989, p. 145, pl. 3, figs. 10–11.
Tonielli 1991, p. 22, pl. 1, fig. 11.
Conti & Marcucci 1991, p. 798, pl. 1, figs. 14, 16.
Widz 1991, p. 244, pl. 1, fig. 16.
Bernoullius sp. 2
Kito 1989, p. 158, pl. 17, figs. 8–9, 11–13, 15.
Bernoullius sp. 3
Kito 1989, p. 159, pl. 17, figs. 3, 6.
Bernoullius sp. C
Danelian 1989, p. 146, pl. 3, fig. 13.
Conti & Marcucci 1991, p. 798, pl. 1, fig. 13.
Bernoullius rectispinus KITO, DE WEVER, DANELIAN, CORDEY
Kito et al. 1990, p. 347–348, pl. II, fig. 4, 5, 7, 9, 10.
Bernoullius sp.
Yang & Wang 1990, p. 207, pl. 3, fig. 3.
Bernoullis leporinus leporinus CONTI & MARCUCCI
Conti & Marcucci 1991, p. 798, pl. 1, figs. 10, 12.
Bernoullius leporinus rotundus CONTI & MARCUCCI
Conti & Marcucci 1991, p. 799, pl. 1, fig. 11.
Spongiostoma? *rectispinus* (KITO & DE WEVER)

Tonielli 1991, p. 26, pl. 1, fig. 2.
Bernoullius chalouani EL KADIRI
El Kadiri 1992, p. 41, pl. 2, figs. 11, ?12.
Bernoullius brokenkettlensis PESSAGNO, BLOME & HULL
Pessagno et al. 1993, p. 119, pl. 1, figs. 5–7, 24, 28.
Bernoullius delnortensis PESSAGNO, BLOME & HULL
Pessagno et al. 1993, p. 120, pl. 1, figs. 4, 15, 26.
Bernoullius irwini PESSAGNO, BLOME & HULL
Pessagno et al. 1993, p. 120, pl. 1, figs. 1, 10, 13, 27.

Remarks: Included are all forms of *Bernoullius* with straight spines and pointed spine-tips. Specimens of different size and shape of the main body generally coexist.

It seems likely that morphotypes with well developed secondary grooves along the spines are restricted to the Middle Jurassic. They are not separated in the present range-chart.

Genus: **Canoptum** PESSAGNO, in Pessagno et al. 1979

Type species: Canoptum poissoni PESSAGNO, in Pessagno et al. 1979

*** Canoptum spp.**
Pl. 17, figs. 17–19

Genus: **Cecrops** PESSAGNO 1977b

Type species: Staurosphaera septemporata PARONA 1890.

Cecrops septemporatus (PARONA) 1890
Pl. 1, fig. 5

Staurosphaera septemporata PARONA
Parona 1890, p. 151, pl. 2, figs. 4, 5.
Foreman 1973, p. 259, pl. 3, fig. 4.
Riedel & Sanfilippo 1974, p. 780, pl. 1, figs. 6–8.
Foreman 1975, p. 609, pl. 2E, fig. 7, pl. 3, fig. 6.
Muzavor 1977, p. 53, 54, pl. 1, figs. 9, 10.
Nakaseko et al. 1979, p. 24, pl. 2, figs. 5, 6.
Kanie et al. 1981, pl. 1, fig. 5.
Schaaf 1981, p. 439, pl. 7, figs. 8a,b; pl. 16, figs. 10a,b.
Nakaseko & Nishimura 1981, p. 161, pl. 1, fig. 2.
Tumanda 1989, pl. 1, fig. 5.
Cecrops septemporatus (PARONA)
Pessagno 1977b, p. 33, pl. 3, fig. 11.
Baumgartner et al. 1980, p. 51, pl. 2, fig. 7.
Okamura & Uto 1982, pl. 7, fig. 19.
Baumgartner 1984, p. 761, pl. 2, figs. 17–18.
Schaaf 1984, p. 136–137, figs. 1a,b, 2a,b, 3a,b.
Thurow 1988, p. 398, pl. 9, fig. 18.
Ožvoldova & Peterčakova 1992, pl. 1, fig. 15.
Matsuoka 1992, pl. 1, fig. 1.
Cecrops septemporata (PARONA)
Kocher 1981, p. 59, pl. 12, fig. 25.
Sphaerostylus septemporatus (PARONA)
Sanfilippo & Riedel 1985, p. 590, Figs. 4.6a–d.
"Cecrops" septemporatus (PARONA)
Kito 1987, pl. 1, fig. 1.
Igo et al. 1987, Fig. 2.3.

Genus: **Cinguloturris** DUMITRICA, in Dumitrica & Mello 1982

Type species: Cinguloturris carpatica DUMITRICA, in Dumitrica & Mello 1982

Cinguloturris carpatica DUMITRICA, in Dumitrica & Mello 1982
Pl. 23, figs. 1, 6–11

Cinguloturris carpatica DUMITRICA
Dumitrica & Mello 1982, p. 23, pl. 4, figs. 7–11.
Yao 1984, pl. 2, fig. 28.
Matsuoka & Yao 1985, pl. 2, fig. 13.
Tanaka et al. 1985, pl. 1, fig. 12.
Aita 1985, fig. 7.12.
? Kishida & Hisada 1986, pl. 2, fig. 12.
Matsuoka 1986c, pl. 2, fig. 16, pl. 3, fig. 11a,b.
Matsuoka & Yao 1986, pl. 2, fig. 14.
Aita 1987, p. 64, pl. 10, fig. 12.
Ožvoldova 1988, pl. 6, fig. 8.
? Kawabata 1988, pl. 2, fig. 10.
Wakita 1988, pl. 4, fig. ? 16, pl. 5, fig. 8.
Kato & Iwata 1989, pl. 5, fig. 5; pl. 6, fig. 10.
Widz 1991, p. 244, pl. 1, fig. 11.
Yao 1991, pl. 4, fig. 11.
Matsuoka 1992, pl. 3, fig. 2; pl. 4, fig. 1.
Unnamed multicyrtoid nassellarian
? Adachi 1982, pl. 2, figs. 9, 10.
Yamamoto 1983, pl. 1, fig. 10.
Theoperidae gen. et sp. indet I
Aita 1982, pl. 2, fig. 18.
Theoperid gen. et sp. indet.
Aoki & Tashiro 1982, pl. 2, fig. 9.
Stichomitra sp. A
Yao et al. 1982, pl. 4, fig. 20.
Dictyomitra sp. B
Ishida 1983, pl. 5, figs. 3, 4.
Cinguloturris sp. aff. *C. carpatica* DUMITRICA
Yao 1984, pl. 3, fig. 19.
Cinguloturris sp. cf. *C. carpatica* DUMITRICA
Tanaka et al. 1985, pl. 1, fig. 7.

Remarks: See remarks under *Cinguloturris* sp. A.

Cinguloturris sp. A
Pl. 23, figs. 3–5

Cinguloturris sp. aff. C. *carpatica* DUMITRICA

Wakita 1988, pl. 6, fig. 14.
Cinguloturris sp.
Kato & Iwata 1989, pl. 2, fig. 7.

Remarks: Cinguloturris sp. A differs from other species of the genus by possessing well developed costae on the non-spongy part of the segments. Specimens having at least one segment with this structure are assigned to *Cinguloturris* sp. A.

Transitional forms between *Cinguloturris carpatica* DUMITRICA and *Cinguloturris* sp. A have the non-spongy part of the segments covered by equally spaced nodes, tending to form vertical costae (pl. 23, fig. 2). They are excluded from our biostratigraphic data, because in moderately preserved material they cannot be distinguished from *Cinguloturris* sp. A.

Genus: **Crolanium** PESSAGNO 1977b

Type species: Crolanium triquetrum PESSAGNO 1977b

* **Crolanium pythiae** SCHAAF 1981
Pl. 25, figs. 6–7

Dictyomira (?) sp.
Foreman 1975, p. 615, pl. 2H, fig. 4.
Crolanium pythiae SCHAAF
Schaaf 1981, p. 432, pl. 20, figs. 5a–c.
Schaaf 1984, p. 159, figs. 1, 2, 3a,b.
Sanfilippo & Riedel, 1985, p. 616, Fig. 13.1a–e.
Thurow 1988, p. 399, pl. 6, fig. 23.
Aguado et al. 1991, Fig. 7.7.
Matsuoka 1992, pl. 1, fig. 9.

Genus: **Crucella** PESSAGNO 1971

Type species: Crucella messinae PESSAGNO 1971

Crucella cf. cachensis PESSAGNO 1971
Pl. 6, fig. 11

Crucella cachensis PESSAGNO
cf. Pessagno 1971, p. 53, pl. 9, figs. 1–3.

Remarks: The Lower Cretaceous representatives of *Crucella* with a circular depression in the central area are included. They become extinct in the upper Aptian-lower Albian. Their stratigraphic continuity with nearly identical morphotypes from the Upper Cretaceous (typical *Crucella cachensis* PESSAGNO) has not been proven.

Genus: **Cryptamphorella** DUMITRICA 1970

Type species: Hemicryptocapsa conara FOREMAN 1968

Cryptamphorella conara (FOREMAN) 1968
Pl. 14, figs. 11, 12a,b

Hemicryptocapsa conara FOREMAN
Foreman 1968, p. 35, pl. 4, figs. 11a,b.
Cryptamphorella conara (FOREMAN)
Dumitrica 1970, p. 80, pl. 11, figs. 66a–c.
Dumitrica 1972, p. 842, pl. 1, figs. 2–5.
Dumitrica 1975, text-fig. 2, fig. 28.
Nakaseko et al. 1979, pl. 6, fig. 1.
Schaaf 1981, p. 433, pl. 1, figs. 6a,b; pl. 9, figs. 15a,b.
Nakaseko & Nishimura 1981, p. 148, pl. 5, figs. 11a,b.
Taketani 1982a, p. 67, pl. 7, figs. 6a,b, 7a,b.
Sanfilippo & Riedel 1985, p. 613, fig. 12.1a–c.
Thurow 1988, p. 399, pl. 1, fig. 2; pl. 5, fig. 1.
Marcucci Passerini et al. 1991, Fig. 31.
Cryptamphorella sp. cf. *C. conara* (FOREMAN)
Thurow 1988, p. 399, pl. 8, fig. 20.
Cryptamphorella sp.
Ožvoldova 1990a, p. 140, pl. 2, figs. 2, 7, 8.

Genus: **Cyrtocapsa** HAECKEL 1881

Type species: Cyrtocapsa ovalis RÜST 1885

* **Cyrtocapsa mastoidea** YAO 1979
Pl. 9, fig. 15

Cyrtocapsa mastoidea YAO
Yao 1979, p. 36, pl. 8, figs. 1–8.
Kido et al. 1982, pl. 4, fig. 7.
Matsuoka 1982b, pl. 1, fig. 7
Mizutani & Koike 1982, pl. 1, fig. 9.
Wakita 1982, pl. 3, fig. 9.
Yao et al. 1982, pl. 3, fig. 14.
Matsuoka 1983, p. 24, pl. 9, fig. 8.
Mizutani et al. 1984, pl. 1, fig. 10.
Matsuoka & Yao 1986, pl. 1, fig. 10.
Sato et al. 1986, fig. 17.13.
Yokota & Sano 1986, pl. 1, fig. 8.
Goričan 1987, p. 182, pl. 2, fig. 3.
Hattori 1987, pl. 13, fig. 13.
Yao 1991, pl. 3, fig. 4.
Sano et al. 1992, pl. 2, fig. Q.
Yaocapsa macroporata KOZUR
Kozur 1984, p. 57, pl. 7, fig. 4.
Grill & Kozur 1986, pl. 2, fig. 6.
Yaocapsa mastoidea (YAO)
Kozur 1991, pl. 2, fig. 3.

* **Cyrtocapsa aff. mastoidea** YAO 1979
Pl. 9, fig. 20

Stichocapsa sp. b
Kido et al. 1982, pl. 5, fig. 10.
Yaocapsa aff. *macroporata* KOZUR
Csontos et al. 1991, pl. 1, fig. 1.

Remarks: Cyrtocapsa aff. *mastoidea* differs from the type material by the median portion being more inflated, subspherical. The transition between thorax and abdomen is abrupt.

Genus: **Dibolachras** FOREMAN 1973

Type species: Dibolachras tytthopora FOREMAN 1973

*** Dibolachras tytthopora** FOREMAN 1973
Pl. 16, fig. 4

Dibolachras tytthopora FOREMAN
Foreman 1973, p. 265, pl. 11, fig. 4, pl. 16, fig. 15.
Foreman 1975, p. 617, pl. 2L, figs. 2, 3, pl. 6, fig. 16.
Schaaf 1981, p. 433, pl. 5, figs. 3a,b; pl. 26, figs. 1a,b, 4.
Schaaf 1984, p. 146–147, figs. 1a,b, 2, 3a,b.
Sanfilippo & Riedel 1985, p. 609, Fig. 11.4a,b.
Thurow 1988, p. 400, pl. 7, fig. 20.

Genus: **Dictyomitra** ZITTEL 1876, emend. PESSAGNO 1976

Type species: Dictyomitra multicostata ZITTEL 1876

Dictyomitra formosa SQUINABOL 1904
Pl. 22, figs. 1–3

Dictyomitra formosa SQUINABOL
Squinabol 1904, p. 232, pl. 10, fig. 4.
Pessagno 1986, p. 51, pl. 8, figs. 10–12.
Nakaseko et al. 1979, pl. 8, fig. 17.
De Wever & Thiébault 1981, p. 587, pl. 2, fig. 1.
Nakaseko & Nishimura 1981, p. 150, pl. 8, figs. 7, 8; pl. 16, figs. 4, 11.
Taketani 1982a, p. 58, pl. 4, figs. 6a,b; pl. 11, fig. 13.
Taketani 1982b, pl. 2, fig. 4.
Thurow 1988, p. 400, pl. 1, fig. 25.
Dictyomitra torquata FOREMAN
Foreman 1973, pl. 15, figs. 9–11.
Dictyomitra duodecimcostata (SQUINABOL)
Foreman 1975, p. 614, pl. 7, fig. 8.
Dictyomitra cf. *D. formosa* SQUINABOL
Thurow 1988, p. 400, pl. 1, fig. 23.

Genus: **Dictyomitrella** HAECKEL 1887

Type species: Eucyrtidium articulatum EHRENBERG 1875 (subsequent designation by Campbell 1954).

Dictyomitrella (?) kamoensis MIZUTANI & KIDO, in Kido et al. 1982
Pl. 24, fig. 1

"Dictyomitrella" sp. A
Mizutani et al. 1981, p. 197, fig. 2a.
Canoptum (?) sp.
Aita 1982, pl. 1, figs. 10–12b.
Dictyomitrella sp. A
Matsuoka 1982b, pl. 2, fig. 3a,b.
Dictyomitrella sp. D
Yao et al. 1982, pl. 3, fig. 21.
Dictyomitrella sp. E
Ishida 1983, pl. 4, figs. 4, 5; pl. 6, fig. 4.
Dictyomitrella (?) *kamoensis* MIZUTANI & KIDO
Kido et al. 1982, pl. 2, figs. 9–11.
Kojima 1982, pl. 1, fig. 3.
Owada & Saka 1982, pl. 1, fig. 14.
Mizutani & Kido 1983, p. 258, pl. 53, figs. 2–4b.
Mizutani et al. 1984, pl. 1, fig. 13.
Yao 1984, pl. 2, fig. 13.
Yamamoto et al. 1985, pl. 4, fig. 1.
Matsuoka & Yao 1986, pl. 2, fig. 7.
Aita 1987, p. 65, pl. 4, figs. 10a–11b; pl. 10, fig. 13.
Wakita 1988, pl. 4, fig. 13.
Matsuoka 1990, pl. 1, fig. 6, pl. 2, fig. 10.
Yao 1991, pl 4, fig. 10.
Matsuoka 1992, pl. 4, fig. 3.
Maaté et al. 1993, Fig. 3.5, 3.6.
"Dictyomitrella" kamoensis MIZUTANI & KIDO
Hattori & Yoshimura 1982, pl. 3, fig. 3.
Ristola kamoensis
Kishida & Hisada 1986, pl. 8, fig. 7.
Dictyomitrella (?) sp. A
Hattori 1987, pl. 18, fig. 15.
Dictyomitrella (?) sp. B
Hattori 1987, pl. 18, fig. 16.
Dictyomitrella (?) sp.
Hattori 1988b, pl. 2, figs. E, F, G.
"Dictyomitrella" spp.
Hattori 1989, pl. 32, figs. G, H.

Genus: **Droltus** PESSAGNO & WHALEN 1982

Type species: Droltus lyellensis PESSAGNO & WHALEN 1982

*** Droltus spp.**
Pl. 17, figs. 14, 20

Genus: **Emiluvia** FOREMAN 1973, emend. FOREMAN 1975, emend. PESSAGNO 1977a

Type species: Emiluvia chica FOREMAN 1973.

Emiluvia hopsoni PESSAGNO 1977a
Pl. 4, fig. 9

Emiluvia hopsoni PESSAGNO
Pessagno 1977a, p. 76, pl. 4, figs. 14–16; pl. 5, figs. 1–7; pl. 12, figs. 15–16.
Baumgartner et al. 1980, pl. 1, fig. 9.

Kocher 1981, p. 64, pl. 13, figs. 6–7.
Baumgartner 1984, p. 762, pl. 3, fig. 1.
De Wever et al. 1986b, pl. 6, fig. 22.
Ožvoldova & Peterčakova 1987, pl. 32, figs. 3, 4.
Conti & Marcucci 1991, pl. 1, figs. 20, 21.
Widz 1991, p. 246, pl. 1, fig. 25.
Matsuoka 1992, pl. 4, fig. 11.
Steiger 1992, p. 58, pl. 15, fig. 11.
Pessagno et al. 1993, p. 131, pl. 4, fig. 21.
Emiluvia cf. *hopsoni* PESSAGNO
Kato & Iwata 1989, pl. 3, fig. 10.

Emiluvia ordinaria OŽVOLDOVA, in Ožvoldova & Sykora 1984
Pl. 4, fig. 6

Emiluvia sp. A
Kocher 1981, p. 65, pl. 13, fig. 11.
Emiluvia sp. A KOCHER
De Wever & Cordey 1986, pl. 1, fig. 13.
Emiluvia sedecimporata salensis PESSAGNO
De Wever et al. 1986b, pl. 6, fig. 25.
Emiluvia ordinaria OŽVOLDOVA
Ožvoldova & Sykora 1984, p. 265, pl. 4, fig. 6–8, pl. 5, fig. 1–4, pl. 16, fig. 4.
Ožvoldova 1988, pl. 3, fig. 9.
Danelian 1989, p. 149, pl. 4, fig. 5–6.

Remarks: In the material studied *E. ordinaria* OŽVOLDOVA has the same stratigraphic range as *E. sedecimporata* (RÜST). These two morphotypes probably represent the variability of the same species.

Emiluvia orea BAUMGARTNER, in Baumgartner et al. 1980
Pl. 4, figs. 10–11

Emiluvia orea BAUMGARTNER
Baumgartner et al. 1980, p. 52, pl. 1, figs. 1–7.
Kocher 1981, p. 64, pl. 13, fig. 8.
Baumgartner 1984, p. 762, pl. 3, fig. 5
De Wever et al. 1986b, pl. 7, figs. 3, 9.
Aita 1987, p. 63, pl. 13, fig. 8.
Ožvoldova 1988, pl. 8, figs. 1–2.
Ožvoldova 1990b, pl. 3, fig. 4.
Danelian 1989, p. 150, pl. 4, figs. 7–9.
Emiluvia chica FOREMAN
Ožvoldova & Sykora 1984, p. 264, pl. 4, figs. 1–3.

Emiluvia pessagnoi FOREMAN 1973
Pl. 4, fig. 6

Emiluvia pessagnoi FOREMAN
Foreman 1973, p. 262, pl. 8, fig. 6.
Pessagno 1977a, p. 76, pl. 5, fig. 8.
Baumgartner et al. 1980, p. 53, pl. 1, fig. 10.
Baumgartner 1984, p. 762, pl. 3, fig. 3.
Aita & Okada 1986, p. 109, pl. 1, fig. 8.
De Wever et al. 1986b, pl. 7, figs. 8, 10.
Ožvoldova 1988, pl. 3, fig. 4.
Emiluvia pessagnoi pessagnoi FOREMAN
Steiger 1992, p. 54, pl. 14, figs. 8–11.
Emiluvia pessagnoi multipora STEIGER
Steiger 1992, pl. 15, figs. 1, 2.

Emiluvia premyogii BAUMGARTNER 1984
Pl. 4, figs. 1–2, 3a,b

Emiluvia chica FOREMAN
? Sato et al. 1982, pl. 3, fig. 14.
Emiluvia sp. B
Wakita 1982, pl. 6, fig. 8.
Emiluvia premyogii BAUMGARTNER
Baumgartner 1984, p. 762, pl. 3, figs. 6, 8–9, 11–12.
non De Wever & Miconnet 1985, p. 386, pl. 1, figs. 3–6.
Aita 1987, p. 63, pl. 1, fig. 3, pl. 8, fig. 5.
Goričan 1987, p. 182, pl. 3, fig. 8.
De Wever et al. 1987, pl. A, fig. 1.
Ožvoldova 1988, pl. 6, fig. 2; pl. 8, fig. 4.
Danelian 1989, p. 150, pl. 4, fig. 10–11.
Kito 1989, p. 112, pl. 6, fig. 8.
Ožvoldova 1990b, pl. 1, fig. 3.
Yang & Wang 1990, p. 205, pl. 2, figs. 5, 10.
Conti & Marcucci 1991, pl. 1, fig. 18.
Widz 1991, p. 246, pl. 1, fig. 18.
Pessagno et al. 1993, p. 132, pl. 4, figs. 7, 12.
Emiluvia aff. *premyogii* BAUMGARTNER
De Wever & Miconnet 1985, pl. 1, fig. 8.

Emiluvia salensis PESSAGNO 1977a
Pl. 4, figs. 7–8

Emiluvia salensis PESSAGNO
Pessagno 1977a, p. 77, pl. 5, figs. 9–11.
Kocher 1981, p. 65, pl. 13, fig. 10.
Emiluvia sedecimporata salensis PESSAGNO
Baumgartner 1984, p. 763, pl. 3, figs. 4, 7.
De Wever et al. 1986b, pl. 6, figs. 21, 25, 26; pl. 7, fig. 5.
Ožvoldova 1990b, pl. 3, fig. 5.
Widz 1991, p. 246, pl. 1, fig. 22.
Emiluvia salensis PESSAGNO gr.
Danelian 1989, p. 152, pl. 4, fig. 13.
Emiluvia sp. A
Danelian 1989, p. 154, pl. 4, figs. 16–18.
Emiluvia sp.
Conti & Marcucci 1991, pl. 1, fig. 19.

Emiluvia sedecimporata (RÜST) 1885
Pl. 4, fig. 4

Staurosphaera sedecimporata RÜST
Rüst 1885, p. 288, pl. 28(3), fig. 1.
Staurosphaera sedecimporata RÜST var. *elegans* WISNIOWSKI
Wisniowski 1889, p. 683, pl. 13, fig. 48.

Emiluvia sedecimporata elegans (WISNIOWSKI)
Baumgartner 1984, p. 763, pl. 3, fig. 2.
Ožvoldova 1988, pl. 1, fig. 7.
Widz 1991, p. 246, pl. 1, fig. 26.
Emiluvia sedecimporata (RÜST)
Ožvoldova & Sykora 1984, p. 264, pl. 3, figs. 5, 7.
Schaaf 1984, p. 152–153, fig. 8.
De Wever et al. 1986b, pl. 6, fig. 20.
Danelian 1989, p. 152, pl. 4, fig. 14–15.

Remarks: See remarks under *E. ordinaria* OŽVOLDOVA.

Emiluvia splendida CARTER, in Carter et al. 1988
Pl. 4, fig. 12

Emiluvia splendida CARTER
Carter et al. 1988, p. 35, pl. 16, figs. 5, 11.
Kito 1989, p. 113, pl. 6, figs. 13, 17.
Emiluvia sp. 2
Kito 1989, p. 115, pl. 6, figs. 14–16, 18–19; pl. 7, fig. 2.

Genus: **Eucyrtidiellum** BAUMGARTNER 1984

Type species: Eucyrtidium (?) *unumaensis* YAO 1979

*** Eucyrtidiellum nodosum** WAKITA 1988
Pl. 9, fig. 7

Eucyrtidium ? sp. B
Ishida 1983, pl. 9, fig. 8.
Eucyrtidiellum sp.
Baumgartner 1985, Fig. 38m.
Eucyrtidiellum sp. aff. *E. unumaense* (YAO)
Matsuoka 1986c, pl. 2, fig. 9, pl. 3, fig. 10.
Eucyrtidiellum sp. d
Nagai 1987, pl. 3, figs. 4a–c.
Eucyrtidiellum nodosum WAKITA
Nagai 1988, pl. 1, fig. 5; pl. 2, fig. 6.
Wakita 1988, p. 408, pl. 4, fig. 29; pl. 5, fig. 16.
Matsuoka 1990, pl. 2, fig. 8.
Matsuoka 1992, pl. 4, fig. 10.

Eucyrtidiellum ptyctum (RIEDEL & SANFILIPPO) 1974
Pl. 9, figs. 1–2

Eucyrtidium ptyctum RIEDEL & SANFILIPPO
Riedel & Sanfilippo 1974, p. 778, pl. 5, fig. 7; pl. 12, fig. 14, non fig. 15.
Baumgartner & Bernoulli 1976, p. 617, pl. 11e, g, non f.
Baumgartner et al. 1980, p. 53, pl. 3, fig. 13.
Aita 1982, pl. 2, figs. 8, 9a,b, non fig. 10.
Nishizono et al. 1982, pl. 2, fig. 12.
Yao 1984, pl. 2, fig. 30.
Sanfilippo & Riedel 1985, p. 618, fig. 12.4b, 4d, ? figs. 4a, 4c.
Eucyrtidium (?) *ptyctum* RIEDEL & SANFILIPPO
Pessagno 1977a, p. 94, pl. 12, fig. 7.
Mizutani 1981, p. 182, pl. 64, figs. 1a,b, 2.
Adachi 1982, pl. 3, figs. 7, 8.
Aoki & Tashiro 1982, pl. 3, figs. 1–3; pl. 4, fig. 10.
Okamura & Uto 1982, pl. 6, fig. 18.
Mizutani et al. 1982, p. 57, pl. 4, fig. 5.
Ishida 1983, pl. 9, fig. 4.
Yamamoto 1983, pl. 1, fig. 4.
Aita 1985, fig. 7.14.
Matsuoka & Yao 1985, pl. 2, fig. 8.
Tanaka et al. 1985, pl. 1, fig. 16.
Aita & Okada 1986, p. 109, pl. 6, figs. 14–17; pl. 7, figs. 3a,b.
Matsuoka & Yao 1986, pl. 2, fig. 10.
Iwata & Tajika 1989, pl. 5, fig. 1.
Matsuoka 1992, pl. 4, fig. 9.
Eucyrtidium ? *ptyctum* RIEDEL & SANFILIPPO
Dumitrica & Mello 1982, pl. 3, fig. 10, non fig. 9.
Nishizono & Murata 1983, pl. 4, fig. 7.
"Eucyrtidium" ptyctum RIEDEL & SANFILIPPO
Pessagno et al. 1984, p. 30, pl. 4, figs. 12–14.
Eucyrtidiellum ptyctum (RIEDEL & SANFILIPPO)
Baumgartner 1984, p. 764, pl. 4, figs. 1–3.
Baumgartner 1985, Fig. 38.1.
Matsuoka 1986c, pl. 2, fig. 10.
Nagai 1986, p. 14, pl. 2, fig. 7.
Aita 1987, p. 65, pl. 4, figs. 12a,b; pl. 10, fig. 14; pl. 14, fig. 3.
Nagai 1987, pl. 3, figs. 5a–c, 6.
Kawabata 1988, pl. 2, fig. 12.
Nagai 1988, pl. 2, figs. 4a,b.
Wakita 1988, pl. 4, fig. 28; pl. 5, fig. 17.
Kojima 1989, pl. 2, figs. 7a,b.
Nagai & Mizutani 1990, p. 595, figs. 3.5a,b.
Yao 1991, pl. 4, fig. 15.
Mizutani & Kojima 1992, Pl. 1, figs. 7a, 7b.
Sano et al. 1992, pl. 2, fig. K.
Eucyrtidiellum cf. *ozaiense* (AITA)
Widz 1991, p. 246, pl. 1, fig. 23.

Eucyrtidiellum pyramis (AITA), in Aita & Okada 1986
Pl. 9, figs. 3–4

Eucyrtidium sp.
Nishizono et al. 1982, pl. 2, fig. 11.
Eucyrtidium (?) sp.
Aoki 1982, pl. 2, fig. 20.
Eucyrtidium (?) *ptyctum* RIEDEL & SANFILIPPO
Okamura 1980, pl. 20, fig. 10.
Matsuyama et al. 1982, pl. 1, fig. 4.
Eucyrtidium sp. C
Nishizono & Murata 1983, pl. 4, fig. 12.
Eucyrtidium (?) *pyramis* AITA
Aita & Okada 1986, p. 109, pl. 6, figs. 8–13; pl. 7, figs. 1a,b.
Eucyrtidium (?) *ozaiense* AITA

Aita & Okada 1986, p. 109, pl. 6, figs. 1–5; pl. 7, figs. 2a,b.
Eucyrtidiellum ozaiense (AITA)
Nagai 1986, p. 16, pl. 2, fig. 8.
Aita 1987, p. 65, pl. 14, fig. 1.
Eucyrtidiellum pyramis (AITA)
Aita 1987, p. 65, pl. 14, fig. 2.
Kawabata 1988, pl. 2, fig. 13.
Nagai 1988, pl. 2, fig. 7.
Wakita 1988, pl. 6, figs. 21, 22, 23.
Sano et al. 1992, pl. 2, fig. L.
Eucyrtidiellum sp. aff. *E. pyramis* (AITA)
Wakita 1988, pl. 6, fig. 24.

Remarks: Specimens with a nodose thorax are also included under this species. *Eucyrtidiellum ozaiense* (AITA) is treated as a synonym of *E. pyramis* (AITA).

Eucyrtidiellum (?) quinatum TAKEMURA 1986
Pl. 9, figs. 8–12

Eucyrtidium (?) sp. A
Kishida & Sugano 1982, pl. 7, fig. 13.
Eucyrtidium (?) sp. C
Kishida & Sugano 1982, pl. 8, fig. 20.
Eostichomitra ? sp.
Kishida & Sugano 1982, pl. 10, figs. 15, 16.
Stichocapsa sp. aff. *S. japonica* YAO
Baumgartner 1984, p. 786, pl. 8, fig. 20.
Baumgartner 1985, Fig. 37k.
non Carter et al. 1988, p. 62, pl. 15, fig. 7.
Hori 1990, fig. 9.50.
Eucyrtidiellum quinatum TAKEMURA
Takemura 1986, p. 67, pl. 12, figs. 16–18.
Hattori 1988a, pl. 9, fig. A.
Hattori & Sakamoto 1989, pl. 9, figs. L, M; pl. 10, fig. A.
Eucyrtidiellum ? sp.
Takemura 1986, p. 68, pl. 12, fig. 19.
Eucyrtidiellum aff. *quinatum* TAKEMURA
Hattori 1987, pl. 12, figs. 18, 19.
Eucyrtidiellum sp.
Yao 1991, pl. 2, fig. 21.
? *Stichocapsa japonica* YAO
Pessagno et al. 1993, p. 160, pl. 8, fig. 23.

Remarks: Included are also specimens with only four segments, if the last segment has a nodose surface (pl. 9, figs. 8, 11).

Typical *Eucyrtidiellum quinatum* (pl. 9, figs. 9, 10) as described by Takemura (1986) coexists with forms showing a roughly nodose outer layer on the terminal segments (pl. 9, figs. 11, 12). Thickening of the shell-wall is considered to be an onthogenetic feature.

Eucyrtidiellum unumaense (YAO) 1979
Pl. 9, figs. 5–6

Eucyrtidium ptyctum RIEDEL & SANFILIPPO
Riedel & Sanfilippo 1974, pl. 12, fig. 15 (only).
Baumgartner & Bernoulli 1976, fig. 11f (only).
Eucyrtidium (?) *unumaensis* YAO
Yao 1979, p. 39, pl. 9, figs. 1–11.
Kocher 1981, p. 67, pl. 13, fig. 15.
Hattori & Yoshimura 1982, pl. 4, fig. 1.
Kido et al. 1982, pl. 4, fig. 9.
Kojima 1982, pl. 1, fig. 11.
Matsuoka 1982b, pl. 1, fig. 15.
Sashida et al. 1982, pl. 2, fig. 3.
Wakita 1982, pl. 3, fig. 1.
Yao et al. 1982, pl. 3, fig. 7.
Wakita & Okamura 1982, pl. 8, fig. 7.
Eucyrtidium sp.
Sashida et al. 1982, pl. 1, fig. 3.
Eucyrtidiellum unumaensis (YAO)
Baumgartner 1984, p. 765, pl. 4, fig. 6.
Yamamoto et al. 1985, p. 35, pl. 4, fig. 6.
Nagai 1986, p. 13, pl. 1, figs. 1a–c; pl. 2, fig. 1.
Takemura 1986, p. 67, pl. 12, figs. 10–12.
Goričan 1987, p. 182, pl. 3, figs. 9, 10.
Nagai 1988, pl. 2, fig. 1a,b.
Wakita 1988, pl. 3, fig. 15, pl. 4, fig. 25.
Hattori 1987, pl. 12, fig. 7.
Hattori 1988a, pl. 8, fig. I.
Hattori 1989, pl. 28, fig. F.
Eucyrtidium (?) *unumaense* YAO
Mizutani et al. 1984, pl. 1, fig. 8.
Aita 1985, figs. 7.15–16.
Matsuoka 1985, pl. 1, fig. 9.
Eucyrtidiellum unumaense (YAO)
Nagai 1987, pl. 2, figs. 1a–c.
Kojima 1989, pl. 2, figs. 5a,b.
Nagai 1989, pl. 1, figs. 1a–4c; pl. 2, figs. 1a–6d; pl. 3, figs. 2a–6b; pl. 4, figs. 1a–3, 6a,b.
Matsuoka 1990, pl. 1, fig. 8, pl. 2, fig. 7.
Nagai & Mizutani 1990, p. 579, figs. 4.6–7.
Yao 1991, pl. 3, fig. 6.
Sano et al. 1992, pl. 2, fig. J.
Monosera unumaensis (YAO)
Takemura & Nakaseko 1986, p. 1022, fig. 4.8 only.
Eucyrtidiellum pustulatum BAUMGARTNER
Baumgartner 1984, p. 765, pl. 4, figs. 4–5.
Baumgartner 1985, Fig. 43b.
Yamamoto et al. 1985, p. 35, pl. 4, figs. 4, 5.
Nagai 1986, p. 14, pl. 2, fig. 2.
Aita 1987, p. 65, pl. 4, figs. 13a–14b; pl. 10, figs. 15–16.
Nagai 1987, pl. 2, figs. 2a–c, 3a,b, 4a,b.
Nagai 1988, pl. 2, figs. 2a,b.
Wakita 1988, pl. 4, figs. 26–27.
Nagai & Mizutani 1990, p. 597, figs. 4.1a–5c.
Eucyrtidium (?) *unumaense* YAO
Aita 1985, fig. 7.15–16.
Eucyrtidiellum sp. A
Baumgartner 1985, Fig. 43c.

Remarks: Specimens with an entirely smooth abdomen were found together with specimens exhibiting a different degree of nodosity. *Eucyrtidiellum unumaense* (YAO) and *E. pustulatum* BAUMGARTNER are therefore considered as one species. *E. nodosum* WAKITA is treated separately.

Genus: **Gigi** DE WEVER 1982a

Type species: Gigi fustis DE WEVER 1982a

*** Gigi fustis** DE WEVER 1982a
Pl. 16, figs. 11–13

Gigi fustis DE WEVER
De Wever 1982a, p. 195, pl. 4, figs. 1–8.
De Wever 1982b, p. 340, pl. 57, figs. 1–6, 12.
De Wever & Origlia 1982b, pl. 1, fig. F.

*** Gigi (?) sp. A**
Pl. 16, figs. 14–15

Remarks: Test consisting of two segments. Thorax large, inflated, terminating with a short closed inversely conical tube. Thoracic wall of polygonal pore frames. Final tube covered by irregularly dispersed, small, generally closed circular pores.

This species is questionably assigned to *Gigi* because of the thoracic pore structure.

Gigi (?) sp. A differs from *Syringocapsa* sp. B of YAO (1982) by its smooth final tube.

Genus: **Gongylothorax** FOREMAN 1968, emend. DUMITRICA 1970

Type species: Dicolocapsa verbeeki TAN 1927

*** Gongylothorax sp. aff. G. favosus** DUMITRICA 1970
Pl. 13, figs. 9a–c, 11a–c

Gongylothorax favosus DUMITRICA
aff. Dumitrica 1970, p. 56, pl. 1, figs. 1a–c, 2.
Matsuoka 1986c, pl. 2, fig. 5, pl. 3, fig. 9.
Gongylothorax (?) sp. indet.
Aoki & Tashiro 1982, pl. 4, figs. 16a,b.
Gongylothorax sp. aff. *G. favosus* DUMITRICA
Matsuoka 1992, pl. 4, fig. 5.

Remarks: In comparison with the type material of Dumitrica (1970) this morphotype has a more elongated general shape with a larger cephalis and an ellipsoidal thorax. In addition, the sutural pore is composed of three small pores, situated in a distinct depression.

Typical forms of *G. favosus* have not been found in the material studied.

Genus: **Gorgansium** PESSAGNO & BLOME 1980

Type species: Gorgansium silviesense PESSAGNO & BLOME 1980.

*** Gorgansium gongyloideum** KISHIDA & HISADA 1985
Pl. 1, fig. 6

Gorgansium gongyloideum KISHIDA & HISADA
Kishida & Hisada 1985, p. 116, pl. 1, figs. 21–22.
Kishida & Hisada 1986, Fig. 4.4.
Hori 1990, pl. 1, fig. 6.

Genus: **Guexella** BAUMGARTNER 1984

Type species: Lithocampe nudata KOCHER 1981

Guexella nudata (KOCHER) 1981
Pl. 9, figs. 17–19

Lithocampe nudata KOCHER
Baumgartner et al. 1980, p. 55, pl. 6, fig. 3.
Kocher 1981, p. 75, pl. 14, figs. 18–19.
Lithocampe (?) *nudata* KOCHER
Yao et al. 1982, pl. 4, figs. 1–2.
Matsuoka 1982b, pl. 2, figs. 1–2.
aff. Aita 1982, pl. 1, fig. 19a–c.
Matsuoka 1983, p. 27, pl. 9, figs. 12–14.
Yao 1984, pl. 2, fig. 1.
Aita 1985, fig. 7.17.
Matsuoka & Yao 1986, pl. 2, fig. 3, pl. 3, fig. 17.
Guexella nudata (KOCHER)
Baumgartner 1984, p. 766, pl. 5, figs. 5–7.
Yamamoto et al. 1985, p. 35, pl. 4, fig. 7.
Matsuoka 1986c, pl. 3, fig. 15a,b.
Kishida & Hisada 1986, Fig. 8. 3.
Aita 1987, p. 65, pl. 5, figs. 5a–6b; pl. 10, fig. 17.
Matsuoka 1988, pl. 1, fig. 9.
Wakita 1988, pl. 3, fig. 13.
Danelian 1989, p. 167, pl. 5, fig. 3.
Matsuoka 1990, pl. 1, fig. 9.
Yao 1991, pl. 3, fig. 1.
Maaté et al. 1993, Fig. 3.13.
Gongylothorax sakawaensis MATSUOKA
Matsuoka 1982a, p. 74, pl. 1, figs. 1–10.
Matsuoka 1982b, pl. 3, figs. 1–2.
Yao et al. 1982, pl. 4, figs. 8–9.
Matsuoka 1983, p. 14, pl. 1, fig. 4, pl. 5, figs. 7a,b.
Yao 1984, pl. 2, figs. 19–20, 23.
Matsuoka & Yao 1986, pl. 2, fig. 4, pl. 3, fig. 10.
Aita 1987, p. 65, pl. 5, figs. 2a–3b.
Wakita 1988, pl. 4, fig. 14.
Yao 1991, pl. 4, fig. 7.
Matsuoka 1992, pl. 5, fig. 2.

Remarks: Gongylothorax sakawaensis MATSUOKA is synonymized with *Guexella nudata* (KOCHER). The

preservation of our material does not allow a transmitted light study to determine the number of segments.

Similar but much longer forms (*Guexella* aff. *nudata*, pl. 9, fig. 16) were found in the upper Bajocian.

Hagiastrid gen. indet. spp.
Pl. 5, figs. 1–2

Remarks: Strong external beams connected with diagonally arranged cortical bars forming two rows of alternating pores between adjacent beams. Only single rays were found in our material, the generic assignment is thus not possible.

Distally the rays bifurcate ending with two long strong spines, perforated at the base. A flat diverging spatula, perpendicular to the plane of spines, arises from each side of the ray at the point of bifurcation.

The spines can be rather straight, consisting of rounded ridges alternating with deep grooves (pl. 5, fig. 1). With some specimens they are curved, flattened, more sharply bladed, with a central ridge running from the base to the spine-tip (pl. 5, fig. 2).

This hagiastrid rarely occurs, different species have not been distinguished.

Genus: **Hemicryptocapsa** TAN 1927, emend. DUMITRICA 1970

Type species: Hemicryptocapsa capita TAN 1927

Hemicryptocapsa capita TAN 1927
Pl. 12, figs. 3–5

Hemicryptocapsa capita TAN
Tan 1927, p. 50, pl. 9, fig. 67.
non Dumitrica & Mello 1982, pl. 3, fig. 3.
Okamura & Uto 1982, pl. 2, fig. 20, pl. 6, fig. 4.
Igo et al. 1987, Fig. 2.12.
Kito 1987, pl. 2, fig. 7.
Tumanda 1989, p. 37, pl. 6, fig. 8, pl. 10, fig. 9
Aguado et al. 1991, Fig. 7.16, 20.
Matsuoka 1992, pl. 1, fig. 3.
Hemicryptocapsa spp. cf. *H. capita* TAN SIN HOK
Riedel & Sanfilippo, 1974, p. 779, pl. 6, figs. 2, 3, non figs. 1, 4.
Foreman 1975, p. 618, pl. 2I, fig. 20, non fig. 18.
Nakaseko et al. 1979, pl. 2, figs. 8, 9.
Nakaseko & Nishimura 1981, p. 153, pl. 4, fig. 5; pl. 14, fig. 7.
Hemicryptocapsa cf. *capita* TAN SIN HOK
Suyarl 1986, pl. 4, fig. 3

Remarks: Specimens with a nodose surface are excluded from the synonymy.

Hemicryptocapsa capita TAN differs from *Syringocapsa agolarium* FOREMAN (1973, p. 268, pl. 11, fig. 5; pl. 16, fig. 17) and from *Williriedellum* sp. A sensu MATSUOKA by having a large sutural pore.

Hemicryptocapsa polyhedra DUMITRICA 1970
Pl. 14, figs. 7–8

Hemicryptocapsa polyhedra DUMITRICA
Dumitrica 1970, p. 72, pl. 14, figs. 85a–c.
non Nakaseko et al. 1979, pl. 5, fig. 9.
non Nakaseko & Nishimura 1981, p. 153, pl. 4, fig. 2; ? pl. 14, fig. 5.
Yamauchi 1982, pl. 2, fig. 1.
Marcucci Passerini & Gardin 1992, Fig. 3f, 3g.

Remarks: See remarks under *H. prepolyhedra* DUMITRICA.

Hemicryptocapsa prepolyhedra DUMITRICA 1970
Pl. 14, fig. 4, 9

Hemicryptocapsa prepolyhedra DUMITRICA
Dumitrica 1970, p. 71, pl. 13, figs. 80a–c, 81, 82, 83a,b, 84; pl. 20, fig. 131.
Matsuyama et al. 1982, pl. 2, fig. 8.

Remarks: The polygonal structure of *Hemicryptocapsa prepolyhedra* DUMITRICA is made of rounded, pore-bearing rims, while it consists of sharp ridges with *H. polyhedra* DUMITRICA. Both species coexist (sample UPC 35). Transitional forms are illustrated in pl. 14, figs. 5, 6.

Hemicryptocapsa sp. A
Pl. 14, figs. 1, 2a,b, 3

Hemicryptocapsa polyhedra DUMITRICA
Nakaseko et al. 1979, pl. 5, fig. 9.
Nakaseko & Nishimura 1981, p. 153, pl. 4, fig. 2; ? pl. 14, fig. 5.

Remarks: Cephalo-thorax almost entirely encased in the inflated abdomen. The abdominal surface made of irregular polygonal facets, two to six pores present per facet. Sutural pore and aperture always present, both situated in a circular depression.

The presence of a thorax is assumed on the basis of the external similarity to *Hemicryptocapsa polyhedra* DUMITRICA and *H. prepolyhedra* DUMITRICA. The inner structure was not observed.

Hemicryptocapsa sp. A differs from *H. prepolyhedra* and *H. polyhedra* by more irregularly arranged ridges. Less pores are present per facet.

Genus: **Hexasaturnalis** KOZUR & MOSTLER 1983

Type species: Spongosaturnalis ? hexagonus YAO, 1972

Hexasaturnalis tetraspinus (YAO) 1972

Spongosaturnalis ? tetraspinus YAO

Yao 1972, p. 29, pl. 4, figs. 1–6; pl. 11, figs. 1–2.
Wakita 1982, pl. 4, fig. 12.
Mesosaturnalis tetraspinus (YAO)
Goričan 1987, p. 184, pl. 3, fig. 1.
Yao 1991, pl. 3, fig. 24.
Acanthocircus tetraspinus YAO
Hattori 1988a, pl. 2, fig. B.
Hexasaturnalis hexagonus (YAO)
Grill & Kozur 1986, pl. 2, fig. 5.
Mesosaturnalis hexagonus (YAO)
Carter et al. 1988, pl. 47, pl. 9, figs. 11, 12.
Mesosaturnalis squinaboli
Carayon et al. 1984, pl. 1, fig. 2.
Mesosaturnalis tetraspinus (YAO)
Carter & Jakobs 1991, p. 343, pl. 2, fig. 16.
Hexasaturnalis tetraspinus (YAO)
Tonielli 1991, p. 23, pl. 1, fig. 5.

Genus: **Higumastra** BAUMGARTNER 1980

Type species: Higumastra inflata BAUMGARTNER 1980

Higumastra imbricata (OŽVOLDOVA) 1979
Pl. 5, fig. 13

Crucella (?) *imbricata* OŽVOLDOVA
Ožvoldova 1979, p. 254, pl. 3, figs. 1, 4.
Higumastra imbricata (OŽVOLDOVA)
Kocher 1981, p. 71, pl. 14, fig. 8.
Baumgartner 1984, p. 767, pl. 4, fig. 13.
De Wever & Miconnet 1985, p. 387, pl. 1, fig. 10.
Aita 1987, p. 64, pl. 8, fig. 10.
Ožvoldova & Peterčakova 1987, p. 119, pl. 32, figs 6, 8.
Danelian 1989, p. 157, pl. 5, fig. 6.
Kito 1989, p. 134, pl. 13, fig. 1.
Yang & Wang 1990, p. 199, pl. 2, fig. 15.
Conti & Marcucci 1991, pl. 2, fig. 8.
non Steiger 1992, p. 43, pl. 10, fig. 4.
Pessagno et al. 1993, pl. 3, figs. 23, 24.
Higumastra sp. A
Ishida 1983, pl. 11, fig. 1.
Higumastra sp.
Yamamoto et al. 1985, pl. 4, figs. 8a,b.
Higumastra aff. *imbricata* OŽVOLDOVA
Kishida & Hisada 1986, Fig. 2. 24.

Genus: **Holocryptocanium** DUMITRICA 1970

Type species: Holocryptocanium tuberculatum DUMITRICA 1970

* **Holocryptocanium barbui** DUMITRICA 1970
Pl. 14, figs. 10 a,b, 13 a,b, 14 a,b

Holocryptocanium barbui DUMITRICA
Dumitrica 1970, p. 76, pl. 17, figs. 105–108b, pl. 21, fig. 136.
Dumitrica 1975, text-fig. 2, fig. 1.
Foreman 1975, p. 618, pl. 1F, fig. 9; pl. 6, fig. 13.
Pessagno 1977b, p. 40, pl. 6, fig. 18.
Nakaseko et. al. 1979, pl. 5, fig. 6.
Okamura 1980, pl. 21, fig. 2.
Schaaf 1981, p. 435, pl. 2, fig. 1a,b; pl. 10, fig. 6a,b.
Matsuyama et al. 1982, pl. 2, fig. 5
Taketani 1982a, p. 67, pl. 7, figs. 1a,b; pl. 13, figs. 18, 19.
Taketani 1982b, pl. 1, fig. 5
Yamauchi 1982, pl. 1, fig. 1
Murata et al. 1982, pl. 2, fig. 5.
Baumgartner 1984, p. 768, pl. 4, fig. 14
Yao 1984, pl. 5, fig. 1
Sanfilippo & Riedel 1985, p. 614, Figs. 12.2a–c.
Kito 1987, pl. 2, fig. 11.
Thurow 1988, p. 401, pl. 5, figs. 5–8.
Kato & Iwata 1989, pl. 4, fig. 10, pl. 8, fig. 5.
Tumanda 1989, p. 37, pl. 7, figs. 20–21.
Ožvoldova 1990a, p. 142, pl. 6, figs. 1–6.
Taketani & Kanie 1992, Fig. 3.16.
Holocryptocanium barbui barbui DUMITRICA
Nakaseko & Nishimura 1981, p. 153, pl. 3, figs. 1–4.
Holocryptocanium japonicum NAKASEKO & NISHIMURA
Nakaseko et al. 1979, pl. 5, figs. 8, 10
Okamura 1980, pl. 21, fig. 5
Aoki 1982, pl. 4, fig. 15.
Taketani 1982a, p. 67, pl. 7, figs. 2a,b, 3; pl. 13, fig. 21.
Yamauchi 1982, pl. 1, fig. 2
Holocryptocanium barbui japonicum NAKASEKO & NISHIMURA
Nakaseko & Nishimura 1981, p. 154, pl. 3, figs. 5–7b, pl. 14, fig. 10.
Holocryptocanium sp.
Okamura & Uto 1982, pl. 4, fig. 3, 4.
Suyarl 1986, pl. 4, fig. 9.
Holocryptocanium cf. *barbui* DUMITRICA
Goričan 1987, p. 183, pl. 3, fig. 17.
Holocryptocanium sp. C
Thurow 1988, p. 402, pl. 8, fig. 21.

Remarks: Holocryptocanium barbui DUMITRICA is not included in the zonation, because of its long stratigraphic range. It is especially frequent in the Bijela Radiolarite. Morphotypes with a smooth surface and polygonal pore frames generally coexist.

Genus: **Homoeoparonaella** BAUMGARTNER 1980

Type species: Paronaella elegans PESSAGNO 1977a

Homoeoparonaella argolidensis BAUMGARTNER 1980
Pl. 6, figs. 4–5

Hagiastrid cf. *Amphibracchium* sp.
Baumgartner & Bernoulli 1976, fig. 10h.
Homoeoparonaella argolidensis BAUMGARTNER

Baumgartner 1980, p. 288, pl. 2, figs. 1, 8–12; pl. 11, fig. 4.
Kocher 1981, p. 71, pl. 14, fig. 10.
Baumgartner 1984, p. 768, pl. 4, fig. 15.
De Wever et al. 1986b, pl. 8, figs. 5–7.
Danelian 1989, p. 158, pl. 5, figs. 7–8.
Kito 1989, p. 125, pl. 8, fig. 15.
Ožvoldova 1990b, pl. 4, fig. 2.
Widz 1991, p. 247, pl. 2, fig. 5.
Steiger 1992, p. 41, pl. 9, figs. 3, 4.

Homoeoparonaella sp. cf. *H. argolidensis* BAUMGARTNER
Baumgartner 1980, pl. 2, fig. 7.

Tritrabs ewingi (PESSAGNO)
Conti & Marcucci 1991, pl. 4, fig. 9.

* **Homoeoparonaella elegans** (PESSAGNO) 1977a
Pl. 6, fig. 8

Paronaella elegans PESSAGNO
Pessagno 1977a, p. 70, pl. 1, figs. 10–11.

Homoeoparonaella elegans (PESSAGNO)
Baumgartner 1980, p. 289, pl. 2, figs. 2–6; pl. 11, fig. 6.
Kocher 1981, p. 72, pl. 14, fig. 11.
Baumgartner 1984, p. 768, pl. 4, fig. 16.
Danelian 1989, p. 159, pl. 5, figs. 9–10.
Kito 1989, p. 126, pl. 9, figs. 12–16.
Widz 1991, p. 247, pl. 2, fig. 6.
Steiger 1992, p. 42, pl. 9, figs. 5, 6.

Genus: **Hsuum** PESSAGNO 1977a, emend. TAKEMURA 1986

Type species: Hsuum cuestaensis PESSAGNO 1977a

Hsuum matsuokai ISOZAKI & MATSUDA 1985
Pl. 19, figs. 9, 11–13

Hsuum sp. C
Hattori & Yoshimura 1982, pl. 3, fig. 8.

Hsuum sp. B
Kishida & Sugano 1982, pl. 7, figs. 14–16.

unnamed nassellaria
Wakita & Okamura 1982, pl. 7, fig. 3.

Hsuum sp.
Yao 1984, pl. 1, figs. 6, 7.
Matsuoka 1986a, pl. 2, figs. 1, 2, 3.

Hsuum (?) *matsuokai* ISOZAKI & MATSUDA
Isozaki & Matsuda 1985, p. 438, pl. 3, figs. 1–14.
Nagai 1988, pl. 1, fig. 9.
Sashida 1988, p. 19, pl. 4, figs. 16–18.
non Hattori 1988a, pl. 13, fig. E.
Hattori & Sakamoto 1989, pl. 16, fig. I.

Hsuum maxwelli PESSAGNO
De Wever & Miconnet 1985, pl. 4, fig. 3.

Hsuum primum TAKEMURA
Takemura 1986, p. 50, pl. 5, figs. 17–21.
Hattori 1987, pl. 17, figs. 11–13, non figs. 8–9.
Hattori & Sakamoto 1989, pl. 15, figs. I, J.

Hsuum aff. *mclaughlini* PESSAGNO & BLOME
Goričan 1987, p. 183, pl. 2, fig. 11.

? *Hsuum* (?) *matsuokai*
non Hattori 1988b, pl. 4, fig. E.

Hsuum matsuokai ISOZAKI & MATSUDA
Sashida 1988, p. 19, pl. 4, figs. 16–18.
Danelian 1989, p. 160, pl. 5, fig. 12.
Kito 1989, p. 179, pl. 21, figs. 1–4, 18.
Yao 1991, pl. 2, fig. 18.

Ogivus falloti EL KADIRI
El Kadiri 1992, p. 46, pl. 2, figs. 3, 4.

Hsuum mclaughlini PESSAGNO & BLOME **gr.**, in Pessagno et al. 1984
Pl. 19, figs. 1–5

Hsuum mclaughlini PESSAGNO & BLOME
Pessagno et al. 1984, p. 25, pl. 1, figs. 1–4, 12, 13, 17.

Protunuma sp. B
Steiger 1992, p. 90, pl. 27, fig. 6 only.

Remarks: A large variety of morphotypes, differing in size and outline are included. They are characterized by a thick irregular latticed structure on the proximal part. Straight continuous costae develop distally. The costate portion of the test is slightly inflated. The apical horn is small, circular in cross-section.

Hsuum mclaughlini gr. greatly resembles *Hsuum altile* HORI & OTSUKA (1989, p. 180. pl. 1, figs. 1–6). It is reported from the Zone 4 of Pessagno et al. (1987), it makes its first appearance in the Kimmeridgian in our sections while *H. altile* has not been found above the Aalenian (Hori, 1990).

Representatives of *Hsuum* with staggered costae along the entire test (pl. 19, figs. 6–8) coexist in the Kimmeridgian.

Genus: **Katroma** PESSAGNO and POISSON 1981, emend. DE WEVER 1982a

Type species: Katroma neagui PESSAGNO & POISSON 1981

* **Katroma spp.**
Pl. 16, figs. 9–10

Genus: **Laxtorum** BLOME 1984

Type species: Laxtorum hindei BLOME 1984

Laxtorum (?) jurassicum ISOZAKI & MATSUDA 1985
Pl. 23, figs. 12–13

Spongocapsula (?) sp. C
Yao et al. 1982, pl. 3, fig. 2.

Spongocapsula sp. C

Yao 1984, pl. 1, fig. 3, non figs. 4, 5.
Spongocapsula ? sp. A
Kishida & Sugano 1982, pl. 8, figs. 1, 2, 3?, 4, 5–7?.
Sato et al. 1986, Fig. 17.9.
Laxtorum (?) *jurassicum* ISOZAKI & MATSUDA
Isozaki & Matsuda 1985, p. 435, pl. 1, figs. 1–15.
Matsuoka & Yao 1986, pl. 1, fig. 6, pl. 3, fig. 3.
Hattori 1987, pl. 17, fig. 7.
Nagai 1988, pl. 1, fig. 6.
Sashida 1988, p. 24, pl. 4, figs. 11–15.
Hori 1990, fig. 9.51.
Yao 1991, pl. 2, fig. 17.

Genus: **Linaresia** EL KADIRI 1992

Type species: Linaresia beniderkoulensis EL KADIRI 1992

Linaresia chrafatensis EL KADIRI 1992
Pl. 19, fig. 10

Eucyrtid gen et sp. indet.
Baumgartner 1984, p. 763, pl. 3, figs. 13–16.
Baumgartner 1985, fig. 37n.
Goričan 1987, p. 182, pl. 2, fig. 9.
Canutus sp.
De Wever et al. 1985, pl. 1, figs. 9–11.
Hsuum sp. A
Takemura 1986, p. 50, pl. 5, fig. 22.
Danelian 1989, p. 161, pl. 5, figs. 14–16.
Linaresia chrafatensis EL KADIRI
El Kadiri 1992, p. 44, pl. 1, figs. 6–8, 14.
Ogivus rifensis EL KADIRI
El Kadiri 1992, p. 47, pl. 2, figs. 1, 5, 7.

Genus: **Mirifusus** PESSAGNO 1977a, emend. BAUMGARTNER 1984

Type species: Mirifusus guadalupensis PESSAGNO 1977a

Mirifusus chenodes (RENZ) 1974
Pl. 24, figs. 9–10

Lithocampe chenodes RENZ
Renz 1974, p. 793, pl. 7, fig. 30; pl. 12, fig. 14a–d.
Riedel & Sanfilippo 1974, p. 779, pl. 6, figs. 5–7; pl. 13, fig. 1.
Schaaf 1981, p. 435, pl. 5, fig. 2, pl. 25, figs. 5a,b, 7.
Kocher 1981, p. 74, pl. 74, pl. 14, fig. 17.
Aita & Okada 1986, pl. 2, fig. 12.
Kato & Iwata 1989, pl. 1, fig. 3.
Mirifusus chenodes (RENZ)
Baumgartner 1984, p. 770, pl. 5, figs. 9, 15.
Schaaf 1984, 98–99, figs. 1, 2, 3a,b, 4a,b.
non De Wever & Miconnet 1985, p. 387, pl. 5, figs. 1–2.
De Wever et al. 1986b, pl. 9, fig. 8.
Pavšič & Goričan 1987, p. 25, pl. 4, fig. 6.
Ožvoldova 1988, pl. 6, fig. 6.
Tumanda 1989, p. 38, pl. 1, fig. 15.
Ožvoldova & Peterčakova 1992, pl. 3, fig. 3.
Baumgartner 1992, p. 321, pl. 7, figs. 6, 7.
Matsuoka 1992, pl. 1, fig. 6.
Taketani & Kanie 1992, Fig. 4.1–2.

Mirifusus dianae (KARRER) 1867 **s.l.**

Lagena dianae KARRER
Karrer 1867, p. 365, pl. 3, fig. 8a,b.
Mirifusus mediodilatata (RÜST)
Nakaseko & Nishimura 1981, p. 155, pl. 8, fig. 15.
Mirifusus baileyi PESSAGNO
Okamura & Uto 1982, pl. 7, fig. 3.
Ishida 1983, pl. 5, fig. 7–8b.
Yamamoto 1983, pl. 1, figs. 1, 2.
Lithocampe mediodilatata RÜST
Riedel & Sanfilippo 1974, p. 779, pl. 7, figs. 1–3.
Mirifusus mediodilatatus (Rüst)
Aoki & Tashiro 1982, pl. 4, fig. 8.
Murata et al. 1982, pl. 1, figs. 11, 14.
Ožvoldova 1990b, pl. 1, fig. 10.
Yao et al. 1982, pl. 4, fig. 30.
Taketani & Kanie 1992, Fig. 4.3–4.
Mirifusus sp.
Okamura & Uto 1982, pl. 7, fig. 7.
Mirifusus dianae (KARRER)
Dumitrica & De Wever 1991, p. 553–557, figs. 1, 2a,b.

Remarks: See also synonymy under subspecies. Two subspecies are distinguished. The morphotype is treated also in the species level to enable specimens with a broken-off proximal part to be introduced in the database.

Mirifusus dianae dianae (KARRER) 1867
Pl. 24, figs. 18–19

Lagena dianae KARRER
Karrer 1867, p. 365, pl. 3, fig. 8a,b.
Lithocampe mediodilatata RÜST
Rüst 1885, p. 316, pl. 40, fig. 9.
Mirifusus (?) *mediodilatata* (RÜST)
Pessagno 1977a, p. 84, pl. 11, figs. 1–2.
Mirifusus mediodilatatus (RÜST)
Baumgartner et al. 1980, p. 56, pl. 5, figs. 9–11.
Nishizono et al. 1982, pl. 3, fig. 10.
Pessagno et al. 1984, p. 26, pl. 2, figs. 4, 5, 18, 19.
Yao 1984, pl. 3, fig. 22.
Sanfilippo & Riedel 1985, p. 608, figs. ?10.2a, 10.2c, non fig. 10.2b.
Matsuoka & Yao 1985, pl. 2, fig. 2.
Matsuoka & Yao 1986, pl. 2, fig. 18.
Aita 1987, p. 65, pl. 12, fig. 7.

Yao 1991, pl. 4, fig. 20.
Sano et al. 1992, pl. 2, fig. I.
Pessagno et al. 1993, p. 142, pl. 7, fig. 13.
Mirifusus mediodilatus mediodilatatus (RÜST)
Baumgartner 1984, p. 772, pl. 5, figs. 13, 19.
De Wever et al. 1986b, pl. 9, fig. 6.
Ožvoldova 1990b, pl. 5, fig. 1.
Steiger 1992, p. 64, pl. 18, figs. 1, 2.
Mirifusus baileyi PESSAGNO
Pessagno 1977a, p. 83, pl. 10, figs. 6–8, pl. 11, figs. 9–11.
Pessagno 1977b, p. 48, pl. 8, figs. 1, 8, 9, 26.
Mizutani 1981, p. 177, pl. 60, fig. 1.
Adachi 1982, pl. 1, fig. 1.4.
Pessagno et al. 1984, p. 26, pl. 2, figs. 1–3, 10, 13, 17, 21–23.
Wakita 1988, pl. 5, fig. 15.
Mirifusus mediodilatus baileyi (PESSAGNO)
Baumgartner 1984, p. 772, pl. 5, figs. 13, 19.
Mirifusus dianae (KARRER)
Dumitrica & De Wever 1991, p. 553–557, figs. 1, 2a,b.

Remarks: Mirifusus baylei PESSAGNO (1977a) is synonymized with *M. dianae dianae* (KARRER).

Mirifusus dianae minor BAUMGARTNER 1984
Pl. 24, fig. 20

Theoperid gen et sp. indet.
Foreman 1973, pl. 12, fig. 2.
Lithocampe mediodilatata RÜST
Riedel & Sanfilippo 1974, p. 779, pl. 7, fig. 1 only.
Foreman 1975, p. 616, pl. 2K, fig. 2; pl. 6, fig. 17.
Mirifusus mediodilatatus (RÜST)
Kanie et al. 1981, pl. 1, fig. 14.
Schaaf 1984, p. 122–123, figs. 1–4.
Aita & Okada 1986, pl. 2, fig. 1.
Kito 1987, pl. 3, fig. 12.
Igo et al. 1987, Fig. 2.1.
Kato & Iwata 1989, pl. 1, fig. 1.
Tumanda 1989, p. 38, pl. 1, fig. 14
Matsuoka 1992, pl. 1, fig. 5; pl. 2, fig. 5.
Mirifusus mediodilatatus (RÜST) gr.
Sanfilippo & Riedel 1985, fig. 10.2b only.
Mirifusus mediodilatatus minor BAUMGARTNER
Baumgartner 1984, p. 772, pl. 5, figs. 11, 14.
De Wever et al. 1986b, pl. 9, fig. 5.
Pavšič & Goričan 1987, p. 26, pl. 4, fig. 5.
Steiger 1992, p. 65, pl. 18, figs. 3, 4.
Mirifusus baileyi PESSAGNO
Ožvoldova & Sykora 1984, p. 267, pl. 10, fig. 7, 3.
Mirifusus mediodilatatus globosus STEIGER
Steiger 1992, p. 65, pl. 18, figs. 5, 6.

Mirifusus guadalupensis PESSAGNO 1977a
Pl. 24, fig. 17

Lithocampe mediodilatata RÜST
Ožvoldova 1979, p. 258, pl. 5, fig. 3.
Mirifusus guadalupensis PESSAGNO
Pessagno 1977a, p. 83, pl. 10, figs. 9–14.
Baumgartner et al. 1980, p. 55, pl. 5, figs. 12–14.
Kocher 1981, p. 75, pl. 14, fig. 20.
De Wever & Caby 1981, pl. 2, figs. 2 M, N.
Ishida 1983, pl. 5, figs. 6a,b.
Baumgartner 1984, p. 771, pl. 5, figs. 8, 22.
Pessagno et al. 1984, p. 26, pl. 2, figs. 12, 16, 24.
Yao 1984, pl. 2, fig. 29.
Baumgartner 1985, Fig. 38q.
De Wever et al. 1986b, pl. 9, fig. 7.
Kishida & Hisada 1986, Fig. 2. 2.
Ožvoldova & Peterčakova 1987, pl. 33, figs. 4, 5.
Ožvoldova 1988, pl. 2, fig. 3.
Yang & Wang 1990, p. 218, pl. 3, fig. 8, ?figs. 1, 14.
Conti & Marcucci 1991, pl. 2, fig. 12.
Pessagno et al. 1993, p. 140, pl. 6, fig. 9.
Mirifusus sp. A aff. *M. fragilis*
Conti & Marcucci 1991, p. 802, pl. 2, figs. 13–14, 17–18.

Genus: **Mita** PESSAGNO 1977b

Type species: Mita magnifica PESSAGNO 1977b

Mita gracilis (SQUINABOL) 1903
Pl. 21, figs. 14–17.

Sethoconus gracilis SQUINABOL
Squinabol 1903, p. 131, pl. 10, fig. 13.
Mita magnifica PESSAGNO
Schaaf 1981, p. 435, pl. 6, fig. 10; pl. 24, fig. 13a,b, non 3a,b.
Mita gracilis (SQUINABOL)
Taketani 1982a, p. 60, pl. 5, fig. 2a,b; pl. 12, fig. 3.
Schaaf 1984, p. 110, 111, figs. 1–3, 4a,b; 5a,b,c.
Goričan 1987, p. 184, pl. 3, figs. 22, 23.
non Thurow 1988, p. 402, pl. 3, fig. 2.

Mita sp. B sensu THUROW 1988
Pl. 21, figs. 11–12

Mita sp. B
Thurow 1988, p. 402, pl. 3, fig. 3.
Mita gracilis (SQUINABOL)
Thurow 1988, pl. 3, fig. 2.

* **Mita sp. C** sensu THUROW 1988
Pl. 21, fig. 10

Mita sp. C
Thurow 1988, p. 402, pl. 6, fig. 21.

Remarks: Mita sp. C differs from *Mita* sp. B by more irregular arrangement of pores and distinct transverse bars between costae. Similar large forms with a prominent segmentation of the inflated part occur in the upper Aptian–lower Albian (pl. 21, fig. 9).

Genus: **Napora** PESSAGNO 1977a

Type species: Napora bukryi PESSAGNO 1977a

Napora bukryi PESSAGNO 1977a **gr.**
Pl. 26, figs. 11–12

Napora bukryi PESSAGNO
Pessagno 1977a, p. 94, pl. 12, fig. 8.
Kocher 1981, p. 77, pl. 14, fig. 23.
De Wever & Caby 1981, pl. 2, fig. 2K.
Baumgartner 1984, p. 774, pl. 6, fig. 4.
De Wever et al. 1986b, pl. 11, fig. 14.
Pessagno et al. 1986, p. 37, pl. 9, figs. 5, 12–14.
Danelian 1989, p. 166, pl. 6, fig. 2.
Widz 1991, p. 247, pl. 2, fig. 21.
Napora lospensis PESSAGNO
Pessagno 1977a, p. 96, pl. 12, figs. 9–10
Baumgartner et al. 1980, p. 57, pl. 3, fig. 4.
Kocher 1981, p. 78, pl. 14, fig. 25.
Baumgartner 1984, p. 774, pl. 6, fig. 6.
Pessagno et al. 1984, p. 24, pl. 2, fig. 9.
De Wever et al. 1986b, pl. 11, figs. 13, 18, 22.
Pessagno et al. 1986, p. 42, pl. 9, fig. 11, 16.
Ožvoldova 1988, pl. 8, fig. 6.
Napora deweveri BAUMGARTNER
Baumgartner et al. 1980, p. 56, pl. 3, figs. 1–3, 5; pl. 6, fig. 9.
Kocher 1981, p. 78, pl. 14, fig. 24.
Baumgartner 1984, p. 774, pl. 6, fig. 3.
Danelian 1989, p. 167, pl. 6, fig. 3.
Conti & Marcucci 1991, pl. 3, figs. 1–2.
Napora deweveri BAUMGARTNER s.l.
Pessagno et al. 1986, p. 39, pl. 10, fig. 14.
Napora sp. cf. *N. lospensis* PESSAGNO
Danelian 1989, p. 168, pl. 6, fig. 4.

Remarks: Forms with a large hemispherical thorax assignable to *Napora lospensis* PESSAGNO, *N. bukryi* PESSAGNO or *N. deweveri* BAUMGARTNER are included. The preservation of the material studied generally does not allow a distinction among these three species.

Genus: **Noviforemanella** PESSAGNO, BLOME & HULL, in Pessagno et al. 1993

Type species: Paronaella (?) *hipposiderica* FOREMAN 1975

Noviforemanella diamphidia (FOREMAN) 1973 **gr.**
Pl. 7, figs. 1–3

Paronaella (?) *diamphidia* FOREMAN
Foreman 1973, p. 262, pl. 8, fig. 3–4.
Riedel & Sanfilippo 1974, pl. 12, fig. 4.
Foreman 1975, p. 612, pl. 5, fig. 4–5.
Baumgartner 1980, p. 302, pl. 4, fig. 4.
Schaaf 1981, p. 436, pl. 13, fig. 4.
Kito 1987, pl. 1, fig. 5.
Paronaella (?) sp. aff. P. (?) *diamphidia* FOREMAN
Foreman 1973, p. 262, pl. 8, fig. 5.
Paronaella (?) *hipposidericus* FOREMAN
Foreman 1975, p. 612, pl. 2E, fig. 1–2, pl. 5, fig. 3, 7, 10.
Baumgartner 1980, p. 302, pl. 4, figs. 1–3.
Baumgartner et al. 1980, p. 57, pl. 2, fig. 4.
Foremanella alpina MUZAVOR
Muzavor 1977, 67, pl. 3, fig. 8.
Foremanella diamphidia (FOREMAN)
Baumgartner 1984, p. 765, pl. 6, fig. 18.
Matsuoka & Yao 1985, pl. 2, fig. 9.
Sanfilippo & Riedel 1985, p. 593, fig. 5.4a,b.
Aita & Okada 1986, p. 112, pl. 1, fig. 10.
Aita 1987, p. 63, pl. 8, fig. 11.
Kito 1987, pl. 1, fig. 5.
Pavšič & Goričan 1987, p. 25, pl. 3, fig. 4.
Dostzaly 1988, pl. 1, fig. 1.
Matsuoka 1992, pl. 2, fig. 11.
Steiger 1992, p. 46, pl. 10, fig. 15.
Foremanella hipposidericus (FOREMAN)
Baumgartner 1984, p. 765, pl. 6, fig. 19.
Sanfilippo & Riedel 1985, p. 593, fig. 5.3.
Aita 1987, p. 63, pl. 12, fig. 8.
Ožvoldova & Peterčakova 1987, pl. 34, figs. 2, 3.
Ožvoldova 1990b, pl. 1, fig. 5.
Widz 1991, p. 246, pl. 1, fig. 27.
Paronaella (?) sp.
Yao 1984, pl. 3, fig. 25.
Foremanella sp.
Yao 1991, pl. 4, fig. 27.
Foremanella diamphidia diamphidia FOREMAN
Baumgartner 1992, p. 321, pl. 7, fig. 1.
Foremanella sp. B.
Steiger 1992, p. 46, pl. 10, fig. 17.
Noviforemanella sp. aff. *N. hipposiderica* (FOREMAN)
Pessagno et al. 1993, p. 123, pl. 2, figs. 9, 23; ?figs. 8, 22.

Genus: **Novixitus** PESSAGNO 1977b

Type species: Novixitus mclaughlini PESSAGNO 1977b

Novixitus weyli SCHMIDT-EFFING 1980
Pl. 25, figs. 8–9

? *Stichomitra elegans* (SQUINABOL)
Dumitrica 1975, text-fig. 2, fig. 11.
Novixitus sp. A
Pessagno 1977b, p. 54, pl. 9, fig. 6.
Dictyomitra (?) sp. C
Nakaseko et al. 1979, pl. 7, fig. 3, non fig. 4.
Dictyomitra (?) sp. A
Nakaseko et al. 1979, pl. 7, fig. 5.
Dictyomitra (?) sp. H
Nakaseko et al. 1979, pl. 7, fig. 6.

Novixitus weyli SCHMIDT-EFFING
Schmidt-Effing 1980, p. 252, fig. 33.
Nakaseko & Nishimura 1981, p. 155, pl. 10, figs. 1, 2; pl. 16, ?fig. 10.
Matsuyama et al. 1982, pl. 2, fig. 4.
Taketani 1982a, p. 62, pl. 5, figs. 9a,b; pl. 12, fig. 11.
Taketani 1982b, pl. 1, fig. 11.
Kato & Iwata 1989, pl. 3., ? fig. 3; pl. 8, fig. 9.
Thurow 1988, p. 402, pl. 4, fig. 1.
Novixitus mclaughlini PESSAGNO
Okamura 1980, pl. 21, fig. 8, non fig. 12.
Novixitus cf. *weyli* SCHMIDT-EFFING
Mizutani et al. 1982, pl. 5, fig. 3.
Novixitus sp. A
Yamauchi 1982, pl. 1, fig. 10.
Novixitus sp.
Kato & Iwata 1989, pl. 8, fig. 10.

Genus: **Orbiculiforma** PESSAGNO 1973

Type species: Orbiculiforma quadrata PESSAGNO 1973

Orbiculiforma sp. A sensu WIDZ 1991
Pl. 3, figs. 14–15

Orbiculiforma sp. A
Widz 1991, p. 247, pl. 2, fig. 12.
Cenodiscus (?) sp.
Pessagno et al. 1993, p. 135, pl. 5, fig. 5.

Remarks: This species differs from other representatives of the genus by its regular meshwork of large polygonal pore-frames.

Orbiculiforma sp. B sensu WIDZ 1991
Pl. 3, figs. 8–9

Orbiculiforma sp. B
Widz 1991, p. 248, pl. 2, fig. 14.

Remarks: Outer layer consisting of small polygonal pore-frames with tiny nodes on vertices. One rim of thicker nodes around central cavity. Nine sturdy pyramidal bladed spines on the periphery.

Orbiculiforma sp. D sensu WIDZ 1991
Pl. 3, figs. 10–12

Orbiculiforma sp.
Ožvoldova 1988, pl. 2, figs. 1–2.
Ožvoldova 1990b, p. 302, pl. 3, fig. 1.
Orbiculiforma sp. D
Widz 1991, p. 248, pl. 2, figs. 15–16.

Remarks: This species is characterized by an irregular pore-pattern of the outer layer. The pores are large around the central cavity and become smaller on the periphery.

Genus: **Palinandromeda** PESSAGNO, BLOME & HULL, in Pessagno et al. 1993

Type species: Andromeda crassa BAUMGARTNER 1980

Palinandromeda podbielensis (OŽVOLDOVA) 1979
Pl. 15, fig. 6

Anthocorys podbielensis OŽVOLDOVA
Ožvoldova 1979, p. 257, pl. 4, figs. 1–3.
Andromeda violae BAUMGARTNER
Baumgartner et al. 1980, p. 50, pl. 4, figs. 10–14, pl. 6, fig. 11.
Sato et al. 1982, pl. 4, fig. 9.
Nishizono et al. 1982, pl. 2, fig. 15.
Pessagno et al. 1984, p. 30, pl. 4, figs. 16, 18, 19.
Sato et al. 1986, Fig. 17.19.
Acanthocorys podbiliensis OŽVOLDOVA
Steiger 1981, pl. 14, fig. 9.
Andromeda podbielensis (OŽVOLDOVA)
Kocher 1981 p. 54, pl. 12, figs. 8–9.
Baumgartner 1984, p. 755, pl. 1, figs. 11–12.
De Wever & Miconnet 1985, p. 384, pl. 3, figs. 1–2, 6–7, 9.
? De Wever et al. 1986b, pl. 9, figs. 10–11, 17.
Kishida & Hisada 1986, Fig. 2. 20.
Ožvoldova & Peterčakova 1987, pl. 31, figs. 4, 5.
Ožvoldova 1988, pl. 6, fig. 5.
Danelian 1989, p. 138, pl. 2, fig. 11.
Kito 1989, p. 217, pl. 25, fig. 2, 12–14.
Andromeda depressa DE WEVER & MICONNET
De Wever et al. 1987, pl. A, fig. 5.
Andromeda crassa BAUMGARTNER
Kito 1989, p. 216, pl. 25, fig. 8, non fig. 7.
"Andromeda" violae BAUMGARTNER
Yang & Wang 1990, p. 212, pl. 5, figs. 7, 8.

Palinandromeda praepodbielensis (BAUMGARTNER) 1984
Pl. 15, figs. 4–5

Andromeda praepodbielensis BAUMGARTNER
Baumgartner 1984, p. 756, pl. 1, figs. 13–15.
Baumgartner 1985, fig. 37j.
Goričan 1987, p. 181, pl. 2, fig. 7.
Takemura 1986, p. 63, pl. 11, figs. 4–7.
Kito 1989, p. 216, pl. 25, figs. 9–11, 15.
Tonielli 1991, p. 21, pl. 1, figs. 4, 13.
Yao 1991, pl. 3, fig. 15.
Andromeda praecrassa BAUMGARTNER
Kito 1989, p. 216, pl. 25, figs. 4–6, ? 16.

Palinandromeda sp. A
Pl. 27, figs. 1–3

Andromeda (?) sp.
Takemura 1986, p. 63, pl. 11, fig. 8.
Andromeda sp. 1
Kito 1989, p. 217, pl. 25, figs. 1–3.

Andromeda aff. A. *praepodbielensis* BAUMGARTNER
Conti & Marcucci 1991, p. 797, pl. 1, fig. 7.

Remarks: This species differs from other representatives of the genus by higher number of segments. The test is slenderly conical, increasing gradually in height and width.

Genus: **Pantanellium** PESSAGNO 1977a

Type species: Pantanellium riedeli PESSAGNO 1977a

Remarks: Several very similar morphotypes occur through the Jurassic and Cretaceous. *Pantanellium tanuense* PESSAGNO & BLOME and *P. oligoporum* (VINASSA) are determined to the species level in the present study. In the zonation *Pantanellium* is treated as a genus.

*** Pantanellium oligoporum** (VINASSA) 1899
Pl. 1, figs. 7–9

Ellipsoxiphus oligoporus VINASSA
Vinassa 1899, p. 228, pl. 17, fig. 44.
Form ancestral to *Sphaerostylus lanceola*
Riedel & Sanfilippo 1974, p. 780, pl. 1, figs. 4, 5; pl. 12, fig. 1.
Sphaerostylus sp. A
Matsuoka & Yao 1985, pl. 2, fig. 14.
Sphaerostylus oligoporus (VINASSA)
Sanfilippo & Riedel 1985, p. 590, Fig. 4.5
Matsuoka 1992, pl. 3, fig. 4.
Spherostylus lanceola (PARONA)
Kawabata 1988, pl. 2, fig. 16.
Pachyoncus (?) sp.
Kato & Iwata 1989, pl. 5, fig. 3.

Remarks: Pantanellium oligoporum (VINASSA) can easily be distinguished from other species of *Pantanellium* by its wide spines, few pores and strong nodes on vertices.

*** Pantanellium tanuense** PESSAGNO & BLOME 1980
Pl. 1, figs. 14–18

Pantanellium tanuense PESSAGNO & BLOME
Pessagno & Blome 1980, p. 247, pl. 4, figs. 3, 4, 24.
Ellipsoxiphus tanuensis (PESSAGNO & BLOME)
Kozur & Mostler 1990, p. 214, pl. 14, figs. 10, 11.

Remarks: Our specimens have longer spines than the type material.

Genus: **Parahsuum** YAO 1982

Type species: Parahsuum simplum YAO 1982

Remarks: Middle and Upper Jurassic forms of *Parahsuum* s.s. are included in the database on the generic level.

Parahsuum (?) grande HORI & YAO 1988
Pl. 18, figs. 9–11

Archaeodictyomitra sp. A
? Yao et al. 1980, pl. 3, figs. 7–9.
Archaeodictyomitra sp. a
Kido 1982, pl. 4, fig. 7.
Parahsuum (?) *grande* HORI & YAO
Hori & Yao 1988, 54, pl. 2, figs. 7a–e, 8–12.
Hori 1990, Fig. 9.45.
Yao 1991, pl. 2, fig. 13.
Sano et al. 1992, pl. 2, fig. B.

Remarks: Our specimens differ from the type material by having a dome-shaped rather than conical apical portion.

Intersegmental constrictions are developed on the distalmost part, or they comprise more than a half of the test. The circumferential ridges nevertheless lack thickened discontinuous costal elements, characteristic of *Transhsuum hisuikyoense* (ISOZAKI & MATSUDA). *Parahsuum* sp. D of Yao et al. (1982, pl. 2, fig. 19) and Matsuoka & Yao (1986, pl. 1, fig. 7), assigned to *P.* (?) *grande* by Hori & Yao (1988), is therefore included in *Transhsuum hisuikyoense.*

Parahsuum (?) magnum TAKEMURA 1986
Pl. 19, figs. 15–17

Parvicingula sp. G
Kishida & Sugano 1982, pl. 10, fig. 1.
Parahsuum (?) *magnum* TAKEMURA
Takemura 1986, p. 49, pl. 5, figs. 12–15.
Kito 1989, p. 175, pl. 20, fig. 6.
Yao 1991, pl. 3, fig. 17.
El Kadiri 1992, p. 47, pl. 2, figs. 2, 6, 8, 9, 13.
Parahsuum cruciferum TAKEMURA
Tonielli 1991, p. 26, pl. 1, fig. 8.

Remarks: Included are also specimens with a pointed horn (pl. 19, fig. 15).

Parahsuum (?) natorense (EL KADIRI) 1992
Pl. 19, figs. 14, 18

Parahsuum (?) sp. 5
Kito 1989, p. 178, pl. 19, figs. 21–22.
Canutus (?) *natorensis* EL KADIRI
El Kadiri 1992, p. 41, pl. 1, fig. 11–13.

Remarks: This species is questionably assigned to *Parahsuum* because of its distinct inflated distal part.

*** Parahsuum officerense** (PESSAGNO & WHALEN) 1982
Pl. 17, fig. 8

Lupherium officerense PESSAGNO & WHALEN

Pessagno & Whalen 1982, p. 135, pl. 6, figs. 5, 3, 18; pl. 12, fig. 5.
Grill & Kozur 1986, pl. 1, figs. 4, 5.
Goričan 1987, p. 184, pl. 2, fig. 10.
Hattori & Sakamoto 1989, pl. 18, figs. A,B.
Parahsuum officerense (PESSAGNO & WHALEN)
Yao 1991, pl. 3, fig. 16.

* **Parahsuum ovale** HORI & YAO 1988
Pl. 17, fig. 13

Parahsuum (?) sp. C
Yao 1982, pl. 4, figs. 9–11.
Yao et al. 1982, pl. 2, fig. 10.
Hori 1986, fig. 6.3
Matsuoka 1986a, pl. 1, fig. 2.
Matsuoka & Yao 1986, pl. 1, fig. 3.
Parahsuum directiporata (Rüst)
Sato et al. 1986, fig. 17.11.
Bagotum sp. A
Sashida et al. 1986, fig. 5.18.
Parahsuum ovale HORI & YAO
Hori & Yao 1988, p. 51, pl. 1, figs. 3a–e, 4a–c, 6–8, 9a,b.
Hori 1990, fig. 8.16.
Yao 1991, pl. 2, fig. 2.
Parahsuum takarazawaense SASHIDA
Sashida 1988, p. 19, pl. 1, figs. 6–13, 18, 19.

* **Parahsuum simplum** YAO 1982
Pl. 17, figs. 9–10, 12

Parahsuum simplum YAO
Yao 1982, p. 61, pl. 4, figs. 1–8.
Imoto et al. 1982, pl. 1, figs. 1, 2.
Yao et al. 1982, pl. 2, fig. 9.
Ishida 1983, pl. 2, figs. 1–2.
Matsuoka & Yao 1986, pl. 1, fig. 2.
Goričan 1987, p. 185, pl. 1, fig. 3.
Hori & Yao 1988, p. 51, pl. 1, figs. 1a–d.
Sashida 1988, p. 19, pl. 1, figs. 1–5, 16, 17.
Hori 1990, pl. 8, fig. 15.
Yao 1991, pl. 2, fig. 1.
? Sano et al. 1992, pl. 2, fig. A.

Genus: **Paronaella** PESSAGNO 1971, emend. BAUMGARTNER 1980

Type species: Paronaella solanoensis PESSAGNO 1971.

Paronaella broennimanni PESSAGNO 1977a
Pl. 6, figs. 6–7, 9–10

Paronaella bronnimanni PESSAGNO
Pessagno 1977a, p. 69, pl. 1, figs. 4–5.
Paronaella broennimanni PESSAGNO
Baumgartner 1980, p. 300, pl. 9, fig. 6.
Kocher 1981, p. 80, pl. 15, fig. 5.
Baumgartner 1984, p. 777, pl. 6, fig. 17.
Danelian 1989, p. 172, pl. 6, fig. 11.
Paronaella sp.
Ožvoldova 1990b, p. 302, pl. 4, fig. 8.
Paronaella pristidentata BAUMGARTNER
? Widz 1991, p. 250, pl. 2, fig. 23.
Paronaella sp. C
Widz 1991, p. 250, pl. 3, fig. 2, non fig. 3.

Remarks: Specimens with finer meshwork and less differentiated structure on the ray-tips than with the type material are also included (pl. 6, fig. 7).

Paronaella cava (OŽVOLDOVA) 1990b
Pl. 7, figs. 4–6

Paronaella (?) sp.
Ožvoldova & Sykora 1984, p. 268, pl. 8, figs. 2, 3; pl. 9, fig. 7.
Angulobracchia (?) *cava* OŽVOLDOVA
Ožvoldova 1990b, p. 300, pl. 2, figs. 1, 2, 3, 5.

Paronaella aff. corpulenta DE WEVER 1981
Pl. 7, figs. 14–16

Paronaella corpulenta DE WEVER
Aff. De Wever 1981b, p. 33, pl. 2, figs. 7–9.
Kito 1989, p. 142, pl. 14, figs. 11, 13.
Paronaella sp. 2
Kito 1989, p. 143, pl. 14, figs. 14, 15.

Remarks: This species differs from the typical *P. corpulenta* DE WEVER by having a finer, denser spongy meshwork. It further differs from *P. porosa* CARTER (Carter et al., 1988) by the rays not being enlarged at the tips.

The width of rays is highly variable.

* **Paronaella kotura** BAUMGARTNER 1980
Pl. 7, fig. 12

Paronaella kotura BAUMGARTNER
Baumgartner 1980, p. 302, pl. 9, figs. 15–19; pl. 12, fig. 8.
Kocher 1981, p. 80, pl. 15, fig. 7.
Baumgartner 1984, p. 777, pl. 6, fig. 20.
De Wever et al. 1986b, pl. 9, fig. 2.
Ožvoldova & Peterčakova 1987, pl. 34, figs. 7, 9.
Ožvoldova 1988, pl. 6, fig. 4.
Conti & Marcucci 1991, pl. 3, fig. 5.
Widz 1991, p. 248, pl. 2, fig. 17.

Paronaella mulleri PESSAGNO 1977a
Pl. 7, figs. 8–10

Paronaella mulleri PESSAGNO
Pessagno 1977a, p. 71, pl. 2, figs. 2–3.
Baumgartner 1980, p. 304, pl. 9, fig. 8.

Kocher 1981, p. 80, pl. 15, fig. 8.
Baumgartner 1984, p. 778, pl. 6, fig. 21.
? Nagai 1985, pl. 4, figs. 2, 2a.
De Wever et al. 1986b, pl. 8, fig. 8.
De Wever & Cordey 1986, pl. 1, fig. 20.
Ožvoldova 1988, pl. 4, fig. 10.
Danelian 1989, p. 173, pl. 6, fig. 12–15.
Widz 1991, p. 250, pl. 2, figs. 26–27.
Paronaella sp. cf. *P. mulleri* PESSAGNO
Baumgartner 1980, p. 304, pl. 9, fig. 5; pl. 12, figs. 4–7.
Paronaella denudata (RÜST)
Ožvoldova 1990b, pl. 1, fig. 7.

* **Paronaella pygmaea** BAUMGARTNER 1980
Pl. 7, fig. 13

Paronaella pygmaea BAUMGARTNER
Baumgartner 1980, p. 306, pl. 9, figs. 2, 9.
Aita 1987, p. 64, pl. 1, fig. 7; pl. 8, fig. 12.
? Ožvoldova 1990b, pl. 3, fig. 6.
Widz 1991, p. 250, pl. 2, fig. 23.

Genus: **Parvicingula** PESSAGNO 1977a

Type species: Parvicingula santabarbarensis PESSAGNO 1977a

Parvicingula boesii (PARONA) 1890 **gr.**
Pl. 24, figs. 11, 14–15

Dictyomitra boesii PARONA
Parona 1890, p. 170, pl. 6, fig. 9.
Foreman 1975, p. 613, pl. 2H, figs. 10–11; pl. 7, fig. 9.
Riedel & Sanfilippo 1974, p. 778, pl. 4, fig. 6, non fig. 5.
Parvicingula boesii (PARONA)
Pessagno 1977b, p. 48, pl. 8, fig. 5.
Okamura 1980, pl. 20, figs. 3, 9.
Aoki 1982, pl. 2, fig. 8
Okamura & Uto 1982, pl. 3, figs. 5, 6, 7, 9, 10.
Suyarl 1986, pl. 3, fig. 1.
Pavšič & Goričan 1987, p. 27, pl. 4, fig. 11.
non Ožvoldova & Peterčakova 1987, pl. 34, fig. 4.
Ožvoldova 1988, pl. 4, fig. 2; non pl. 7, fig. 7.
Thurow 1988, p. 403, pl. 6, fig. 9.
Tumanda 1989, p. 38, pl. 4, figs. 1, 2.
Ožvoldova & Peterčakova 1992, pl. 3, fig. 12.
Matsuoka 1992, pl. 1, fig. 11; pl. 2, fig. 4.
Steiger 1992, p. 86, pl. 23, figs. 1–7.
Taketani & Kanie 1992, Fig. 4.8–9.
Parvicingula boesii (PARONA) group
non Baumgartner et al. 1980, p. 58, pl. 5, fig. 15, pl. 6, fig. 8.
Ristola boesii (PARONA) s.l.
Pessagno et al. 1984, p. 28, pl. 3, fig. 9.
? Widz 1991, p. 250, pl. 3, fig. 6.
Ristola boesii (PARONA)
Aita & Okada 1986, pl. 2, figs. 2, 3.
Kito 1987, pl. 3, fig. 9.
Kato & Iwata 1989, pl. 1, fig. 4, pl. 4, fig. 6.
Igo et al. 1987, Fig. 2.2.

Parvicingula cosmoconica (FOREMAN) 1973
Pl. 24, figs. 2–3

Dictyomitra cosmoconica FOREMAN
Foreman 1973, p. 263, pl. 9, fig. 11; pl. 16, fig. 3.
Foreman 1975, p. 614, pl. 2H, fig. 3; pl. 7, fig. 1.
Parvicingula cosmoconica (FOREMAN)
Baumgartner et al. 1980, p. 58, pl. 5, fig. 16; pl. 6, fig. 7.
Baumgartner 1984, p. 778, pl. 7, fig. 1.
Ožvoldova & Sykora 1984, p. 268, pl. 9, fig. 5.
Schaaf 1984, p. 153, fig. 6.
Aita & Okada 1986, pl. 2, fig. 4.
non De Wever & Cordey 1986, pl. 1, fig. 3.
non Kito 1987, pl. 3, fig. 5.
Pavšič & Goričan 1987, p. 27, pl. 4, fig. 10.
Matsuoka 1992, pl. 2, fig. 8.
Steiger 1992, p. 86, pl. 24, figs. 4–6.
Taketani & Kanie 1992, Fig. 4.10.

* **Parvicingula dhimenaensis** BAUMGARTNER 1984
Pl. 24, figs. 12–13

Amphipyndax sp.
Baumgartner & Bernoulli 1976, p. 611, figs 12 e,i,m.
Parvicingula boesii (PARONA)
De Wever & Caby 1981, pl. 2, fig. 2C.
Kocher 1981, p. 81, pl. 15, fig. 11.
Parvicingula sp. C
Aita 1982, pl. 1, figs. 13–14.
Amphipyndax ? sp.
Nishizono et al. 1982, pl. 3, fig. 16.
Parvicingula dhimenaensis BAUMGARTNER
Baumgartner 1984, p. 778, pl. 7, figs. 2–4.
De Wever & Miconnet 1985, p. 389, pl. 4, figs. 4, 6–8.
Yamamoto et al. 1985, p. 36, pl. 6, fig. 1.
Conti 1986, pl. 1, fig. 1.
Matsuoka 1986c, pl. 2, fig. 12.
Aita 1987, p. 66, pl. 2, figs. 3a,b, 5a,b; pl. 9, fig. 12–13.
Goričan 1987, p. 185, pl. 3, figs. 13–14.
Wakita 1988, pl. 4, fig. 10, pl. 5, fig. 7.
Matsuoka 1990, pl. 1, fig. 7.
Parvicingula spinosa AITA
Aita 1985, figs. 6.12, 6.13.
Eoxitus baloghi KOZUR
Kozur 1985, p. 216, fig. 2c.
Eoxitus elongatus KOZUR
Kozur 1985, p. 217, fig. 1h.
Eoxitus nodosus KOZUR
Kozur 1985, p. 217, fig. 2a,b,d.
Parvicingula dhimenaensis BAUMGARTNER gr.
Kishida & Hisada 1986, Fig. 2.4; Fig. 8. 2.

Parvicingula usotanensis TUMANDA 1989
Pl. 24, fig. 16

Dictyomitra boesii PARONA
Riedel & Sanfilippo 1974, p. 778, pl. 4, fig. 5, non. fig. 6.
Parvicingula boesii (PARONA)
Schaaf 1981, p. 436, pl. 3, figs. 13a,b, pl. 18, figs. 6a,b.
Okada et al. 1982, pl. 1, fig. 5.
Parvicingula sp.
SuyarI 1986, pl. 3, fig. 2
Parvicingula usotanensis TUMANDA
Tumanda 1989, p. 30, pl. 4, fig. 4, pl. 10, figs. 11a,b.

Genus: **Parvivacca** PESSAGNO & YANG, in Pessagno et al. 1989

Type species: Parvivacca blomei PESSAGNO & YANG 1989

* **Parvivacca blomei** PESSAGNO & YANG, in Pessagno et al. 1989
Pl. 2, figs. 2–3

Parvivacca blomei PESSAGNO & YANG
Pessagno et al. 1989, p. 344, pl. 10, figs. 13, 14, 16, 18, 28.

Genus: **Perispyridium** DUMITRICA 1978

Type species: Trilonche (?) *ordinaria* PESSAGNO 1977a

Perispyridium ordinarium (PESSAGNO) 1977a **gr.**
Pl. 26, fig. 16

Trilonche (?) *ordinaria* PESSAGNO
Pessagno 1977a, p. 79, pl. 6, fig. 14.
Perispyridium ordinarium (PESSAGNO)
Dumitrica 1978, p. 35, pl. 3, figs. 1, 2, 5; pl. 4, fig. 9.
Kocher 1981, p. 83, pl. 15, fig. 15.
Pessagno & Blome 1982, p. 294, pl. 6, figs 4, 12, 15.
Nishizono et al. 1982, pl. 2, fig. 9.
Aita 1982, pl. 3, fig. 23.
Baumgartner 1984, p. 779, pl. 7, figs. 5–6.
Pessagno et al. 1984, p. 24, pl. 1, fig. 7.
De Wever et al. 1985, pl. 1, fig. 25.
De Wever & Cordey 1986, pl. 1, fig. 18.
De Wever et al. 1986b, pl. 6, fig. 9.
Aita 1987, p. 66, pl. 6, figs. 1a,b; pl. 12, fig. 13.
Yang & Wang 1990, p. 212, pl. 5, fig. 5.
Matsuoka 1992, pl. 3, fig. 8; pl. 4, fig. 12.
Trigonocyclia sp.
Ožvoldova 1979, p. 253, pl. 3, fig. 2.
Perispyridium (?) *ordinarium* (PESSAGNO)
De Wever & Caby 1981, pl. 2, fig. 2A.
Perispyridium cf. *tamanense* PESSAGNO & BLOME
Ožvoldova 1988, p. 385, pl. 1, fig. 6.
Perispyridium aff. *tamanense* PESSAGNO & BLOME
Widz 1991, p. 252, pl. 3, fig. 5.
Perispyridium sp. A
Widz 1991, p. 252, pl. 3, fig. 4.

Genus: **Podobursa** WISNIOWSKI 1889, emend. FOREMAN 1973

Type species: Podobursa dunikowskii WISNIOWSKI 1889

Podobursa spinosa (OŽVOLDOVA) 1975
Pl. 16, fig. 5

Podobursa pantanellii (PARONA)
Riedel & Sanfilippo 1974, p. 779, pl. 8, fig. 5, pl. 13, fig. 6.
Muzavor 1977, p. 108, pl. 7, fig. 5.
Sanfilippo & Riedel 1985, p. 611, fig. 11.2a,b.
Heitzeria spinosa OŽVOLDOVA
Ožvoldova 1975, p. 78, pl. 101, fig. 2.
Podobursa berggreni PESSAGNO
Pessagno 1977a, p. 90, pl. 12, figs. 1–5.
Podobursa spinosa (OŽVOLDOVA)
Ožvoldova 1979, p. 256, pl. 2, fig. 4.
Baumgartner et al. 1980, p. 60, pl. 3, fig. 10.
Kocher 1981, p. 85, pl. 15, fig. 18.
Baumgartner 1984, p. 779, pl. 7, fig. 8.
Ožvoldova 1988, pl. 8, fig. 5.
Ožvoldova 1990b, pl. 2, fig. 6.
Conti & Marcucci 1991, p. 802, pl. 3, fig. 6.
Ožvoldova 1992, pl. 5, fig. 10.
Pessagno et al. 1993, p. 157, pl. 8, fig. 1.
Podobursa spinosa (OŽVOLDOVA) gr.
De Wever et al. 1986b, pl. 10, figs. 5, 6, 8, 10.

Genus: **Podocapsa** RÜST 1885, emend. FOREMAN 1973

Type species: Podocapsa guembeli RÜST 1885, (subsequent designation by Campbell 1954).

Podocapsa amphitreptera FOREMAN 1973
Pl. 16, figs. 1–3

Podocapsa amphitreptera FOREMAN
Foreman 1973, p. 267, pl. 13, fig. 11.
Foreman 1975, p. 617, pl. 6, fig. 15.
Muzavor 1977, p. 112, pl. 7, fig. 4.
Baumgartner et al. 1980, p. 61, pl. 3, figs. 8–9.
Kocher 1981, p. 86, pl. 15, fig. 20.
De Wever & Caby 1981, p. 470, pl. II, fig. 2L.
Yao et al. 1982, pl. 4, fig. 29.
Baumgartner 1984, p. 780, pl. 7, figs. 9–10.
Schaaf 1984, p. 90–91, figs. 1–3b.
Ožvoldova & Sykora 1984, p. 269, pl. 11, figs. 2, 3, 6.
Yao 1984, pl. 3, fig. 14.
Matsuoka & Yao 1985, pl. 2, fig. 10.
De Wever & Miconnet 1985, p. 390, pl. 2, fig. 6.

Sanfilippo & Riedel 1985, p. 612, fig. 11.5
Matsuoka & Yao 1986, pl. 2, fig. 17.
De Wever et al. 1986b, pl. 10, figs. 2–3.
Aita & Okada 1986, p. 114, pl. 3, figs. 6–7.
Aita 1987, p. 66, pl. 12, fig. 3.
Ožvoldova & Peterčakova 1987, pl. 34, fig. 8.
Ožvoldova 1988, pl. 4, fig. 1.
Dostzaly 1988, pl. 1, fig. 2
Yao 1991, pl. 4, fig. 26.
Widz 1991, p. 252, pl. 3, fig. 14.
Baumgartner 1992, p. 324, pl. 10, fig. 9.
Matsuoka 1992, pl. 2, fig. 6.
Steiger 1992, p. 61, pl. 17, fig. 1.
Nassellaria gen et sp. indet.
Nakaseko & Nishimura 1981, pl. 8, fig. 12a,b.

Genus: **Praeconocaryomma** PESSAGNO 1976

Type species: Praeconocaryomma universa PESSAGNO 1976

* **Praeconocaryomma sp.**
Pl. 2, fig. 13

Genus: **Protunuma** ICHIKAWA & YAO 1976

Type species: Protunuma fusiformis ICHIKAWA & YAO 1976

Protunuma japonicus MATSUOKA & YAO 1985
Pl. 10, figs. 1–2

Protunuma fusiformis ICHIKAWA & YAO
Mizutani 1981, p. 181, pl. 63, figs. 1, 8; pl. 64, fig. 3.
Adachi 1982, pl. 3, figs. 9–10.
Ožvoldova & Sykora 1984, p. 270, pl. 8, figs. 6, 7.
? Nishizono & Murata 1983, pl. 4, fig. 15.
Steiger 1992, p. 90, pl. 27, figs. 2, 3.
Protunuma (?) sp.
Imoto et al. 1982, pl. 3, fig. 10.
Protunuma sp. D.
Yao et al. 1982, pl. 4, fig. 24.
Yao 1984, pl. 3, figs. 12, 17.
Protunuma costata (HEITZER)
Baumgartner 1984, p. 781, pl. 7, fig. 15.
Protunuma japonicus MATSUOKA & YAO
Matsuoka & Yao 1985, p. 130, pl. 1, figs. 11–15; pl. 3, figs. 6–9.
Matsuoka 1986c, pl. 2, fig. 7.
Matsuoka & Yao 1986, pl. 3, fig. 22.
? Wakita 1988, pl. 5, fig. 13, pl. 6, fig. 19.
Kito 1989, p. 213, pl. 24, fig. 15.
Yao 1991, pl. 4, fig. 24.
Kiessling 1992, pl. 1, fig. 10.
Matsuoka 1992, pl. 3, fig. 5.
Protunuma spp.
Widz 1991, p. 253, pl. 3, figs. 15, 16.

Protunuma turbo MATSUOKA 1983
Pl. 10, figs. 5a,b, 6

Protunuma sp. J
Yao et al. 1982, pl. 4, fig. 5.
Matsuoka 1982b, pl. 2, fig. 5a,b.
Protunuma turbo MATSUOKA
Matsuoka 1983, p. 24, pl. 4, figs. 4–7; pl. 8, figs. 16–18; pl. 9, figs. 1–2.
Aita 1987, p. 66, pl. 6, figs. 4a,b, 5a,b.
Maaté et al. 1993, Fig. 3.16, 3.17.
Protunuma sp. cf. *P. turbo*
Matsuoka 1990, pl. 1, fig. 4.

Genus: **Pseudocrucella** BAUMGARTNER 1980

Type species: Crucella sanfilippoae PESSAGNO 1977a

* **Pseudocrucella adriani** BAUMGARTNER 1980
Pl. 6, figs. 13–14

Pseudocrucella adriani BAUMGARTNER
Baumgartner 1980, p. 291, pl. 8, figs. 4, 8, 12, 15, 16.
Kocher 1981, p. 88, pl. 15, fig. 23.
Baumgartner 1984, p. 781, pl. 7, fig. 16.
De Wever et al. 1986b, pl. 8, fig. 3.
Ožvoldova 1988, pl. 3, fig. 6.
Pseudocrucella sp. A
Baumgartner 1980, p. 292, pl. 1. fig. 13, pl. 8, figs. 3, 5, 7, 9, 13, pl. 11, figs. 11, 12, 14.
Ishida 1983, pl. 11, fig. 2.
Goričan 1987, p. 185, pl. 1, fig. 9.

* **Pseudocrucella sp. B** sensu BAUMGARTNER 1980
Pl. 6, fig. 12

Pseudocrucella sp. B
Baumgartner 1980, p. 292, pl. 8, figs. 2, 6.
Nagai 1985, pl. 3, fig. 3a.

Genus: **Pseudodictyomitra** PESSAGNO 1977b

Type species: Pseudodictyomitra pentacolaensis PESSAGNO 1977b

Pseudodictyomitra carpatica (LOZYNYAK) 1969
Pl. 22, fig. 17

Dictyomitra carpatica LOZYNYAK
Lozynyak 1969, p. 38, pl. 2, figs. 11–12.
Foreman 1973, p. 263, pl. 10, figs. 1–3; pl. 16, fig. 5.
Foreman 1975, p. 614, pl. 2G, figs. 12–14, non fig. 11; pl. 7, fig. 7, non fig. 6.

Pseudodictyomitra sp. C
Pessagno 1977b, p. 52, pl. 8, fig. 6.
Pseudodictyomitra carpatica (LOZYNYAK)
Schaaf 1981, p. 436, pl. 3, fig. 2, non figs. 1a–c; pl. 20, ? fig. 4a,b.
Nakaseko & Nishimura 1981, p. 158, pl. 9, figs. 6, 11.
non De Wever & Thiébault 1981, p. 590, pl. 2, fig. 2.
Matsuyama et al. 1982, pl. 1, fig. 7.
Yao 1984, pl. 4, fig. 14.
Baumgartner 1984, p. 782, pl. 8, fig. 1.
Schaaf 1984, p. 94–95, fig. 1, non figs 2a,b; ? fig. 3.
Aita & Okada 1986, pl. 1, figs. 13, 14; pl. 7, fig. 10.
Suyarl 1986, pl. 1, figs. 1, ?2, 3, 4.
Kito 1987, pl. 3, fig. 4.
Kawabata 1988, pl. 2, fig. 7.
Iwata & Tajika 1989, pl. 4, fig. 12.
Matsuoka 1992, pl. 2, figs. 2, 3.
Ožvoldova & Peterčakova 1992, pl. 4, fig. 13.
Steiger 1992, p. 87, pl. 25, figs. 1–3, 7.
Taketani & Kanie 1992, Fig. 4.12.
Pseudodictyomitra sp. cf. *P. carpatica* (LOZYNYAK)
Nishizono et al. 1982, pl. 3, fig. 9.
Matsuoka 1986a, pl. 4, figs. 9–11.
Sano et al. 1992, pl. 2, fig. F.
Pseudodictyomitra aff. *carpatica* LOZYNYAK
De Wever et al. 1986b, pl. 11, fig. 3.
Pseudodictyomitra sp.
Kanie et al 1981, pl. 1, fig. 18.

Remarks: Forms with segments rectangular rather than trapeziodal in outline, and prominent depressions between adjacent costae (see De Wever & Thiébault, 1981) are assigned to *Pseudodictyomira lanceloti* SCHAAF.

Pseudodictyomitra depressa BAUMGARTNER 1984
Pl. 20, fig. 10

Pseudodictyomitra sp.
Okamura 1980, pl. 20, figs. 6, 11.
Archaeodictyomitra carpatica (LOZYNYAK)
Okamura & Uto 1982, pl. 2, fig. 3, non figs. 4, 5, 10.
Pseudodictyomitra carpatica (LOZYNYAK)
Okamura & Uto 1982, pl. 8, fig. 7a,b.
Aoki 1982, pl. 2, figs. 14, 15
Tumanda 1989, p. 38, pl. 3, fig. 8
Pseudodictyomitra depressa BAUMGARTNER
Baumgartner 1984, p. 782, pl. 8, figs. 2, 7–8, 11.
? Suyarl 1986, pl. 1, fig. 7.
Taketani & Kanie 1992, Fig. 4.13.
Steiger 1992, p. 87, pl. 25, figs. 4–5.

Remarks: Pseudodictyomitra depressa BAUMGARTNER should probably be assigned to archaeodictyomitrids. See remarks under *Archaeodictyomitra minoensis* (MIZUTANI).

See also remarks under *Pseudodictyomitra puga* (SCHAAF).

Pseudodictyomitra lanceloti SCHAAF 1981
Pl. 22, figs. 10–11

Pseudodictyomitra lanceloti SCHAAF
Schaaf 1981, p. 436, pl. 18, figs. 9a,b.
Pseudodictyomitra sp.
Matsuyama et al. 1982, pl. 1, fig. 9.
Pseudodictyomitra rigida WU
Wu 1986, p. 358, pl. 2, figs. ? 15, 22.
Pseudodictyomitra carpatica (LOZYNYAK)
De Wever & Thiébault 1981, p. 590, pl. 2, fig. 2.
Thurow 1988, p. 404, pl. 6, fig. 12.
Aguado et al. 1991, pl. 7, fig. 2.

Remarks: See remarks under *Pseudodictyomira carpatica* (LOZYNYAK).

Pseudodictyomitra lodogaensis PESSAGNO 1977b
Pl. 22, figs. 5–7

Dictyomitra sp.
Dumitrica 1975, Fig. 2.8.
Pseudodictyomitra lodogaensis PESSAGNO
Pessagno 1977b, p. 50, pl. 8, figs. 4, 21, 28.
Nakaseko & Nishimura 1981, p. 159, pl. 9, fig. 5.
Schaaf 1981, p. 437, pl. 3, fig. 5.
Yao 1984, pl. 5, fig. 14.
Goričan 1987, p. 186, pl. 3, fig. 20.
Thurow 1988, p. 405, pl. 3, fig. 12.
Taketani & Kanie 1992, Fig. 5.1.
Dictyomitra urakawaensis TAKETANI
Taketani 1982a, p. 59, pl. 4, figs. 8a,b, pl. 11, fig. 16.
Taketani 1982b, pl. 1, fig. 13.
Tumanda 1989, p. 37, pl. 8, figs. 4, 5.

Remarks: Pseudodictyomitra lodogaensis PESSAGNO differs from *P. pentacolaensis* PESSAGNO by finer, more densely packed costae. The porous intersegmental constrictions with respect to segments are lower than with *P. pentacolaensis*.

Pseudodictyomitra pentacolaensis PESSAGNO 1977b
Pl. 22, figs. 12–13

Pseudodictyomitra pentacolaensis PESSAGNO
Pessagno 1977b, p. 50, pl. 8, figs. 3, 17, 23; pl. 12, fig. 10.
Thurow 1988, p. 405, pl. 3, fig. 17.
Pseudodictyomitra sp. D
Pessagno 1977b, 52, pl. 8, fig. 13.
Pseudodictyomitra cf. *pentacolaensis* PESSAGNO
Taketani & Kanie 1992, Fig. 5.2.

Remarks: See remarks under *Pseudodictyomitra lodogaensis* PESSAGNO.

*** Pseudodictyomitra primitiva** MATSUOKA & YAO 1985
Pl. 22, fig. 16

Dictyomitra sp. B
Yao et al. 1982, pl. 4, fig. 27.
Yao 1984, pl. 3, figs. 1, 3, non fig. 2.
Unnamed multicyrtoid nassellaria
Adachi 1982, pl. 2, fig. 4.
Pseudodictyomitra primitiva MATSUOKA & YAO
Matsuoka & Yao 1985, p. 131, pl. 1, figs. 1–6; pl. 3, figs. 1–4.
Matsuoka 1986a, pl. 4, figs. 8, ? 7.
Matsuoka & Yao 1986, pl. 2, fig. 19.
Kawabata 1988, pl. 2, fig. 8.
Ožvoldova 1988, pl. 2, fig. 6.
Wakita 1988, pl. 5, fig. 3, pl. 6, figs. 6–7.
Danelian 1989, p. 184, pl. 7, fig. 14.
Yao 1991, pl. 4, fig. 18.
Matsuoka 1992, pl. 3, fig. 1.
Sano et al. 1992, pl. 2, fig. D.
Hsuum sp.
? Iwata & Tajika 1989, pl. 5, fig. 8.

Pseudodictyomitra pseudomacrocephala (SQUINABOL) 1903
Pl. 22, fig. 4

Dictyomitra pseudomacrocephala SQUINABOL
Squinabol 1903, p. 139, pl. 10, fig. 2.
Foreman 1975, p. 614, pl. 7, fig. 10.
Dumitrica 1975, Fig. 2. 19.
Dictyomitra sp.
Foreman 1973, pl. 14, fig. 16.
Dictyomitra macrocephala SQUINABOL
Riedel & Sanfilippo 1974, p. 778, pl. 4, figs. 10, 11; pl. 14, fig. 11.
Dictyomitra (?) *pseudomacrocephala* SQUINABOL
Pessagno 1976, p. 53, pl. 3, figs. 2–3.
Nakaseko et al. 1979, pl. 6, fig. 13–14.
Pseudodictyomitra pseudomacrocephala (SQUINABOL)
Pessagno 1977b, p. 51, pl. 8, figs. 10, 11.
Okamura 1980, pl. 21, fig. 6.
Schmidt-Effing 1980, p. 247, fig. 8.
Nakaseko & Nishimura 1981, p. 159, pl. 9, figs. 1–4; pl. 16, figs. 5–8.
Schaaf 1981, p. 437, pl. 24, fig. 1a,b.
De Wever & Thiébault 1981, p. 592, pl. 1, fig. 5.
Matsuyama et al. 1982, pl. 2, fig. 3.
Mizutani et al. 1982, pl. 4, figs. 10–11.
Taketani 1982a, p. 61, pl. 5, figs. 4a,b; pl. 12, figs. 7–8.
Taketani 1982b, pl. 1, fig. 8.
Schaaf 1984, p. 130–131, figs. 1–5, 6a–c.
Yao 1984, pl. 5, figs. 11, 12, 16.
Sanfilippo & Riedel 1985, p. 608, Figs. 10.1a–e.
Thurow 1988, p. 405, pl. 1, fig. 13; pl. 3, fig. 16.
Kato & Iwata 1989, pl. 8, fig. 9.
Tumanda 1989, p. 38, pl. 8, fig. 3.
Hernandez-Molina et al. 1991, Fig. 11.3.
Marcucci Passerini et al. 1991, Fig. 3h.
Pseudodictyomitra sp. A
Okamura 1980, pl. 22, fig. 6.

Pseudodictyomitra puga (SCHAAF) 1981
Pl. 24, figs. 4–5

Dictyomitra (?) sp.
Dumitrica 1972, pl. 4, figs. 4, 7.
Dictyomitra carpatica LOZYNYAK
Nakaseko et al. 1979, p. 21, pl. 3, fig. 9
Archaeodictyomitra puga SCHAAF
Schaaf 1981, p. 432, pl. 3, fig. 7, pl. 21, figs. 11a,b.
Schaaf 1984, p. 157, fig. 1.
Thurow 1988, p. 398, pl. 6, fig. 15
Ožvoldova 1990b, p. 140, pl. 3, fig. 8, 9, pl. 4, fig. 7.
Pseudodictyomitra puga (SCHAAF)
Nakaseko & Nishimura 1981, p. 160, pl. 9, fig. 8.
Murata et al. 1982, pl. 2, fig. 14.
SuyarI 1986, pl. 1, figs. 5, 6, 9.
Igo et al. 1987, Fig. 2.4.
Pavšič & Goričan 1987, p. 28, pl. 4, fig. 12.
Tumanda 1989, p. 39, pl. 2, fig. 6.
Taketani & Kanie 1992, Fig. 5.3.
Pseudodictyomitra sp.
Okamura & Uto 1982, pl. 5, fig. 1.
Wrangellium (?) *medium* WU
Wu 1986, p. 358, pl. 3, figs. 2, 7, 19, 23.
Dictyomitrella (?) *puga* (SCHAAF)
Matsuoka 1992, pl. 2, fig. 1.

Remarks: Pseudodictyomitra puga (SCHAAF) differs from *P. depressa* BAUMGARTNER by having narrower circumferential ridges with the two rows of pores situated closer to each other.

The disposition of relict pores in the constrictions suggests that *Pseudodictyomitra puga* should be related to parvicingulids rather than pseudodictyomitrids.

*** Pseudodictyomitra sp. A**
Pl. 22, figs. 8–9

Remarks: Costae more irregularly distributed than with *Pseudodictyomitra lodogaensis* PESSAGNO or *P. pentacolaensis* PESSAGNO. Finer secondary costae present.

*** Pseudodictyomitra sp. C** sensu YAO 1982
Pl. 22, figs. 14–15

Dictyomitra sp. C
Yao et al. 1982, pl. 4, fig. 28.
Yao 1984, pl. 1, fig. 4.
Unnamed multicyrtoid nassellarian

Adachi 1982, pl. 2, figs. 5, 6.
Dictyomitra sp.
Kato & Iwata 1989, pl. 3, fig. 6
Pseudodictyomitra primitiva MATSUOKA & YAO
Kiessling 1992, pl. 1, fig. 8.

Remarks: This species differs from *Pseudodictyomitra primitiva* MATSUOKA & YAO by the segments not being trapezoidal in outline and by having only very rare faint costae. It closely resembles *P. nuda* (SCHAAF) (*Archaeodictyomitra nuda* SCHAAF 1981, p. 432, pl. 3, fig. 6). It differs from the latter by more lobate, distally constricted outline.

Genus: **Pseudoeucyrtis** PESSAGNO 1977b

Type species: Eucyrtis (?) *zhamoidai* FOREMAN 1973

*** Pseudoeucyrtis hanni** TAN 1927
Pl. 16, fig. 16

Lithocampe hanni TAN
Tan 1927, p. 64, pl. 13, fig. 109.
Eucyrtis elido SCHAAF
Schaaf 1981, p. 434, pl. 5, fig. 6; pl. 25, figs 3a,b.
Eucyrtis hanni (TAN SIN HOK)
Riedel & Sanfilippo 1974, p. 779, pl. 5, figs. 9–12, ?13–14; pl. 12, fig. 18, ? 16–17.
Schaaf 1984, p. 157, fig. 8.
Sanfilippo & Riedel 1985, p. 618, Fig. 13.7.
Baumgartner 1992, p. 320, pl. 6, fig. 5.

Pseudoeucyrtis reticularis MATSUOKA & YAO 1985
Pl. 16, figs. 21–22

Ellipsoxiphus elongatus HEITZER
? Heitzer 1930, p. 389, pl. 27, fig. 18.
Pseudoeucyrtis sp.
Mizutani 1981, pl. 61, figs. 5, 6.
Ožvoldova & Sykora 1984, p. 270, pl. 10, figs. 5, 6, 8; pl. 13, fig. 2.
Wakita 1988, pl. 6, fig. 15.
Pseudoeucyrtis sp. A
Yao et al. 1982, pl. 4, fig. 25.
Yao 1984, pl. 3, fig. 18.
Widz 1991, p. 253, pl. 3, fig. 21.
Pseudoeucyrtis reticularis MATSUOKA & YAO
Matsuoka & Yao 1985, p. 132, pl. 1, figs. 16–21, pl. 3, figs. 14–17.
Matsuoka & Yao 1986, pl. 3, fig. 15.
Danelian 1989, p. 184, pl. 7, fig. 15.
Yao 1991, pl. 4, fig. 21.
Eucyrtis aff. *tenuis* (RÜST)
De Wever et al. 1986b, pl. 11, fig. 10.
Pseudoeucyrtis sp.
Wakita 1988, pl. 6, fig. 15.

*** Pseudoeucyrtis sp. B** sensu WIDZ 1991
Pl. 16, figs. 19–20

Eucyrtis sp.
Aita 1987, pl. 12, fig. 6.
Pseudoeucyrtis sp.B
Widz 1991, p. 253, pl. 3, fig. 22.

Remarks: This morphotype differs from *Pseudoeucyrtis* sp. J sensu CONTI & MARCUCCI by a less expressed segmental division externally and by having no spines or tubercles on the shell surface. It further differs from *P. reticularis* MATSUOKA & YAO by the middle inflated part being more individualized.

On the basis of the stratigraphic position it is assumed that *Pseudoeucyrtis* sp. B represents the intermediate form between *Pseudoeucyrtis* sp. J and *P. reticularis*.

Pseudoeucyrtis sp. J sensu CONTI & MARCUCCI 1991
Pl. 17, figs. 17–18

Pseudoeucyrtis sp.
Wakita 1988, pl. 4, fig. 24.
Pseudoeucyrtis tenuis (RÜST)
Yang & Wang 1990, p. 213, pl. 5, figs. 9, 11, non fig. 1.
Eucyrtis sp. J aff. *E. micropora* (SQUINABOL)
Conti & Marcucci 1991, p. 800, pl. 2, figs. 1, 2.

*** Pseudoeucyrtis sp.**
Pl. 16, fig. 23

Remarks: Test elongated, spindle-shaped, without strictures. Shell wall thick, multi-layered, with small irregular pore frames.

Genus: **Rhopalosyringium** CAMPBELL & CLARK 1944

Type species: Rhopalosyringium magnificum CAMPBELL & CLARK 1944

Rhopalosyringium majuroense SCHAAF 1981
Pl. 26, figs. 7–10

Artostrobium urna FOREMAN
Schmidt-Effing 1980, p. 244, fig. 4.
Rhopalosyringium majuroensis SCHAAF
Schaaf 1981, p. 437, pl. 6, figs. 2, 3; pl. 23, fig. 5.
Nakaseko & Nishimura 1981, p. 161, pl. 8, fig. 16; pl. 17, fig. 7.
Taketani 1982a, p. 70, pl. 8, figs. 7a,b.
Schaaf 1984, p. 120–121, figs. 1a,b, 2, 3, 4a,b, 5, 6, 7a,b.
Thurow 1988, p. 405, pl. 4, fig. 5.
Tumanda p. 39, pl. 7, fig. 13.
Rhopalosyringium obiraensis TAKETANI
Taketani 1982a, p. 70, pl. 8, figs. 4a,b.
Taketani 1982b, pl. 3, figs. 2a,b.

Rhopalosyringium sp. cf. *R. majuroensis* SCHAAF
Yao 1984, pl. 5, fig. 5.

Remarks: Specimens lacking a thick ring at the lumbar stricture are also included, *Rhopalosyringium obiraense* TAKETANI is thus synonymized with *R. majuroense* SCHAAF.

*** Rhopalosyringium sp. A**
Pl. 26, fig. 6

Remarks: This species differs from *Rhopalosyringium majuroense* SCHAAF by having a cylindrical thorax, not tapering distally. The cephalis is characterized by the same pore-pattern as the thorax.

Genus: **Ristola** PESSAGNO & WHALEN 1982, sensu BAUMGARTNER 1984

Type species: Parvicingula (?) *procera* PESSAGNO 1977a

Ristola altissima altissima (RÜST) 1885
Pl. 24, figs. 6–7

Lithocampe altissima RÜST
Rüst 1885, p. 315(45), pl. 40, fig. 2.
Parvicingula altissima (RÜST)
emend. Pessagno 1977a, p. 85, pl. 8, figs. 9–10.
Nakaseko et al. 1979, p. 23, pl. 1, figs. 9, 10.
Kocher 1981, p. 81, pl. 15, fig. 9.
Nakaseko & Nishimura 1981, p. 156, pl. 8, fig. 14.
Adachi 1982, pl. 1, fig. 8.
Yao 1982, pl. 4, fig. 19.
Parvicingula (?) *altissima* RÜST
Baumgartner et al. 1980, p. 58, pl. 5, figs. 4–7.
Ožvoldova & Sykora 1984, p. 268, pl. 11, figs. 4, 7, 8; pl. 15, fig. 3.
Yao 1984, pl. 2, fig. 25.
De Wever et al. 1986b, pl. 9, fig. 9.
Ristola altissima (RÜST)
Baumgartner 1984, p. 783, pl. 8, fig 3, non figs. 4, 9.
Pessagno et al. 1984, p. 28, pl. 3, fig. 10.
Aita & Okada 1986, p. 114, pl. 2, figs. 5, 6.
Aita 1987, p. 66, pl. 12, fig. 11; non pl. 11, fig. 9.
Kito 1987, pl. 3, fig. 11.
Ožvoldova 1988, pl. 4, fig. 5.
Wakita 1988, pl. 5, fig. 14.
Danelian 1989, p. 186, pl. 7, fig. 16, non figs. 17–18.
Yao 1991, pl. 4, fig. 12.
Kiessling 1992, pl. 1, fig. 11.
Sano et al. 1992, pl. 2, fig. M.
Ristola altissima (RÜST) ssp. A
Widz 1991, p. 253, pl. 3, fig. 24.
Ristola altissima (RÜST) spp. B
Widz 1991, p. 253, pl. 3, fig. 25.

Remarks: Ristola altissima altissima (RÜST) is characterized by a well individualized bulbous proximal part. The outer layer shows equally spaced strong nodes. This subspecies corresponds to the morphotype A of *Ristola altissima* described by Danelian (1989).

*** Ristola cretacea** (BAUMGARTNER), in Baumgartner et al. 1980
Pl. 24, fig. 8

Lithocampe altissima RÜST
Muzavor 1977, p. 102, pl. 8, fig. 7.
Parvicingula cretacea BAUMGARTNER
Baumgartner et al. 1980, p. 59, pl. 5, figs. 1–3, pl. 6, fig. 4.
Ristola cretacea (BAUMGARTNER)
Baumgartner 1984, p. 783, pl. 8, figs. 5, 10.
Aita & Okada 1986, p. 114, pl. 2, fig. 7.
Kato & Iwata 1989, pl. 1, fig. 6.
Steiger 1992, p. 87, pl. 24, figs. 7–8.

Genus: **Saitoum** PESSAGNO 1977a

Type species: Saitoum pagei PESSAGNO 1977a

Saitoum dercourti WIDZ & DE WEVER 1993
Pl. 26, figs. 3–5

Saitoum sp.
Mizutani 1981, p. 183, pl. 63, figs. 2, 3.
Saitoum sp. A
Widz 1991, p. 254, pl. 3, fig. 26.
Widz & De Wever 1993, p. 85, pl. 1, fig. 18.
Saitoum dercourti WIDZ & DE WEVER
Widz & De Wever 1993, p. 85, pl. 1, fig. 17.

Remarks: This species differs from *Saitoum cepeki* SCHAAF (1981, p. 437, pl. 6, fig. 15; pl. 21, fig. 8) by the cephalis being hemispherical, less constricted distally.

Genus: **Sethocapsa** HAECKEL 1881

Type species: Sethocapsa cometa (PANTANELLI) in Rüst 1885 (subsequent designation by Foreman 1973)

*** Sethocapsa accincta** STEIGER 1992
Pl. 15, fig. 8

Sethocapsa accincta STEIGER
Steiger 1992, p. 64, pl. 17, figs. 15, 16.

Sethocapsa horokanaiensis KAWABATA 1988
Pl. 15, figs. 9–10

Gen. et spec. indet.
Okamura & Uto 1980, pl. 2, fig. 17.
Sethocapsa (?) sp.

Matsuyama et al. 1982, pl. 1, fig. 6.
Sethocapsa horokanaiensis KAWABATA
Kawabata 1988, p. 4, pl. 1, figs. 9–12; pl. 3, fig. 3.

Sethocapsa kaminogoensis AITA, in Aita & Okada 1986
Pl. 15, fig. 7

Sethocapsa sp.
Okamura & Uto 1982, pl. 3, fig. 12.
Kito 1987, pl. 2, fig. 3.
Tricolocapsa sp.
Okamura & Uto 1982, pl. 9, figs. 1a,b.
Sethocapsa kaminogoensis AITA
Aita & Okada 1986, p. 114–115, pl. 4, figs. 5–8, pl. 5, figs. 1–8, pl. 7, figs. 4a–c.
Aita 1987, pl. 14, fig. 5.
Tumanda 1989, p. 39, pl. 4, figs. 13, 14, pl. 10, fig. 12.

Sethocapsa (?) perspicua (SQUINABOL) 1903
Pl. 21, fig. 13

Cyrtocapsa perspicua SQUINABOL
Squinabol 1903, p. 142, pl. 10, fig. 16.
Schaaf 1984, p. 163, fig. 10.
Cyrtocapsa (? *Sethocapsa*) *perspicua* SQUINABOL
Thurow 1988, pl. 3, fig. 5.
Stichocapsa perspicua SQUINABOL
Aguado et al. 1991, Fig. 7.8.
Baumgartner 1992, p. 326, pl. 13, figs. 4, ?5.

Sethocapsa pseudouterculus AITA, in Aita & Okada 1986
Pl. 15, figs. 16–17

Sethocapsa pseudouterculus AITA
Aita & Okada 1986, p. 116, pl. 3, fig. 12; pl. 4, figs. 1–4; pl. 7, figs. 5a,b, 12a,b.
Aita 1987, pl. 14, fig. 6.
Sethocapsa sp. A
Aita & Okada 1986, p. 118, pl. 3, fig. 13.
Aita 1987, pl. 14, fig. 8.
Sethocapsa uterculus (PARONA)
Matsuoka 1992, pl. 2, fig. 9 only.
Steiger 1992, p. 63, pl. 17, fig. 14.

Remarks: Sethocapsa pseudouterculus (AITA) differs from *P. uterculus* (PARONA) by 1) the conical proximal part of the test being less depressed in the last segment, 2) lacking a flattened top of the last segment, which, in addition, 3) is not rimmed by larger pores.

Sethocapsa uterculus (PARONA) 1890, sensu FOREMAN 1975
Pl. 15, figs. 11–15

?*Theocapsa uterculus* PARONA
Parona 1890, p. 168, pl. 5, fig. 17.
?*Sethocapsa crucigera* RÜST
Rüst 1898, p. 46, pl. 14, fig. 10.
Sethocapsa sp. cf. *Theocapsa uterculus* PARONA
Foreman 1975, p. 617, pl. 2I, figs. 21, 22.
Kanie et al. 1981, pl. 1, fig. 12.
Sethocapsa uterculus (PARONA)
Schaaf 1981, p. 437, pl. 5, figs. 8a,b; pl. 26, figs. 5a,b.
Okamura & Uto 1982, pl. 3, fig. 15.
Baumgartner 1984, p. 784, pl. 8, fig. 15.
Schaaf 1984, p. 151, figs. 1a,b, 3a,b, 4, non figs. 2a–c.
Yao 1984, pl. 4, fig. 1.
Suyarl 1986, pl. 4, figs. 1, 2.
Igo et al. 1987, Fig. 2.19.
Kito 1987, pl. 2, fig. 1.
Tumanda 1989, p. 39, pl. 5, fig. 7.
Aguado et al. 1991, Fig. 7.12.
Matsuoka 1992, pl. 2, fig. 4; non pl. 2, fig. 9.
non Steiger 1992, p. 63, pl. 17, fig. 14.
Taketani & Kanie 1992, Fig. 5.4.
Sethocapsa cf. *uterculus* (PARONA)
Igo et al. 1987, Fig. 2.8.
Taketani & Kanie 1992, Fig. 5.5.

Remarks: See remarks under *Sethocapsa pseudouterculus* AITA.

Genus: **Spongocapsula** PESSAGNO 1977a

Type species: Spongocapsula palmerae PESSAGNO 1977a

Spongocapsula palmerae PESSAGNO 1977a
Pl. 23, figs. 17–19

Spongocapsula palmerae PESSAGNO
Pessagno 1977a, p. 88, pl. 11, fig. 12–14.
Kocher 1981, p. 93, pl. 16, fig. 17.
Baumgartner 1984, p. 785, pl. 8, fig. 16.
Widz 1991, p. 254, pl. 4, fig. 1.
Steiger 1992, p. 66, pl. 18, fig. 8.
Pessagno et al. 1993, p. 157, pl. 7, fig. 18.
Spongocapsula cf. *perampla* (RÜST)
Ožvoldova 1988, p. 387, pl. 8, fig. 3.
Spongocapsa palmerae PESSAGNO
Yang & Wang 1990, p. 209, pl. 4, figs. 8, 14.

* **Spongocapsula perampla** (RÜST) 1885
Pl. 23, fig. 20

Lithocampe perampla RÜST
Rüst 1885, p. 315, pl. 39, fig. 11.
Riedel & Sanfilippo 1974, p. 779, pl. 8, figs. 1–4.
Spongocapsula sp. aff. *S. perampla* (RÜST)
Pessagno 1977a, p. 90, pl. 11, fig. 15.
Spongocapsula perampla (RÜST)
? Kocher 1981, p. 94, pl. 16, fig. 18.

Baumgartner 1984, p. 785, pl. 8, fig. 17.
De Wever et al. 1986b, pl. 10, figs. 16, 20.
Ožvoldova 1988, p. 2, fig. 7.
Steiger 1992, p. 66, fig. 9.
Spongocapsula sp. A
Yao 1984, pl. 3, fig. 20.
Matsuoka & Yao 1985, pl. 2, fig. 3.

Genus: **Staurosphaera** HAECKEL 1881

Type species: Staurosphaera crassa DUNIKOWSKI 1882

Staurosphaera antiqua (RÜST) 1885
Pl. 4, figs. 13–15

Staurosphaera antiqua RÜST
Rüst 1885, p. 289, pl. 28, fig. 2.
non Muzavor 1977, p. 52 pl. 1, fig. 8.
Baumgartner 1984, p. 785, pl. 8, fig. 18.
Ožvoldova 1990b, pl. 3, fig. 8.
Conti & Marcucci 1991, pl. 4, fig. 3.
Widz 1991, p. 254, pl. 4, fig. 5.
Emiluvia antiqua (RÜST)
Pessagno 1977a, p. 76, pl. 4, figs. 9–10.
Kocher 1981, p. 63, pl. 13, fig. 4.
Emiluvia (?) *antiqua* (RÜST)
Baumgartner 1985, fig. 38g.
Staurosphaera sp. A
Widz 1991, p. 254, pl. 4, fig. 4.
Staurosphaera sp. B
Widz 1991, p. 256, pl. 4, fig. 3.

Genus: **Stichocapsa** HAECKEL 1881

Type species: Stichocapsa jaspidea RÜST 1885

* **Stichocapsa naradaniensis** MATSUOKA 1984
Pl. 11, fig. 6

Stichocapsa sp. C
Yao et al. 1982, pl. 4, figs. 15–16.
Matsuoka 1982b, pl. 3, fig. 6.
Stichocapsa naradaniensis MATSUOKA
Matsuoka 1984, p. 145, pl. 1, figs. 1–5. pl. 2, figs. 1–6.
Matsuoka 1986c, pl. 3, fig. 18.
Matsuoka & Yao 1986, pl. 2, fig. 12, pl. 3, fig. 19.
Aita 1987, p. 67, pl. 6, figs. 9a–10b.
Yao 1991, pl. 4, fig. 13.
Stichocapsa cf. *naradaniensis* MATSUOKA
Wakita 1988, pl. 4, fig. 18.

Stichocapsa robusta MATSUOKA 1984
Pl. 13, figs. 12, 13 a,b

Stichocapsa convexa YAO
Aita 1982, pl. 1, figs. 6–7b.
Stichocapsa sp.
Sato et al. 1982, pl. 4, fig. 1.
Stichocapsa robusta MATSUOKA
Matsuoka 1984, p. 146, pl. 1, figs. 6–13, pl. 2, figs. 7–12.
Kishida & Hisada 1986, fig. 2.16.
Aita 1987, p. 67, pl. 7, fig. 1a,b, pl. 11, figs. 11–12.
Matsuoka 1986c, pl. 1, fig. 12.
Matsuoka 1988, pl. 1, fig. 8.
Danelian 1989, p. 193, pl. 8, fig. 6–7.
Matsuoka 1990, pl. 1, fig. 10.
Yao 1991, pl. 4, fig. 8.
Matsuoka 1992, pl. 5, fig. 3.
Sano et al. 1992, pl. 2, fig. P.

Genus: **Stichomitra** CAYEUX 1897

Type species: No type species has yet been designated for *Stichomitra* in the sense in which this generic name is now used world-wide.

Stichomitra communis SQUINABOL 1903
Pl. 25, figs. 1–5

Stichomitra communis SQUINABOL
Squinabol 1903, p. 141, pl. 8, fig. 40.
Nakaseko et al. 1979, p. 24, pl. 7, fig. 10.
Nakaseko & Nishimura 1981, p. 162, pl. 11, fig. 11; pl. 16, fig. 14.
Taketani 1982a, p. 54, pl. 3, fig. 9; pl. 11, fig. 5.
Taketani 1982b, pl. 1, fig. 12.
Schaaf 1984, p. 162, fig. 8a,b.
Goričan 1987, p. 186, pl. 3, fig. 21.
Thurow 1988, p. 406, pl. 4, fig. 10.
Stichomitra sp.
Dumitrica 1975, Fig. 2.21.
Parvicingula? tekschaensis (ALIEV)
Schaaf 1981, p. 436, pl. 3, fig. 12; pl. 20, figs. 3a,b.
Stichomitra sp. cf. *S. communis* SQUINABOL
Thurow 1988, p. 406, pl. 4, fig. 10.
Stichomitra gr. *asymbatos* FOREMAN
Hernandez-Molina et al. 1991, Fig. 11.4.
Stichomitra asymbatos FOREMAN
Marcucci Passerini et al. 1991, Fig. 3e.
Marcucci Passerini & Gardin 1992, Fig. 4o.

Stichomitra (?) takanoensis AITA 1987 **gr.**
Pl. 23, fig. 16

Macrocephalic multicyrtid theoperid gen et sp. indet.
Baumgartner 1985, figs. 43 l,m.
Nassellaria gen. et sp. ind.
Conti 1986, pl. 1, figs. 2, 3.
Stichomitra (?) *takanoensis* AITA
Aita 1987, p. 73, pl. 3, figs. 10a–12; pl. 10, figs. 6–7.
Maaté et al. 1993, Fig. 3.4, 3.10.
Macrocephalic multicyrtid nassellarian

Goričan 1987, p. 184, pl. 2, figs. 16, 17.
Spongocapsa takanoensis (AITA)
Yang & Wang 1990, p. 209, pl. 4, fig. 1.

Remarks: Generally no horn. Spongy structure visible only distally, when present.

Stichomitra (?) sp. A
Pl. 23, figs. 14–15

unidentified cyrtoid
Baumgartner 1985, Fig. 37o.
g. et sp. indet.
De Wever & Miconnet 1985, pl. 4, fig. 13.
macrothoracic multicyrtid nassellarian
Goričan 1987, p. 184, pl. 2, figs. 18, 19.

Remarks: In the general shape, especially in the shape of cephalis, this morphotype resembles *Stichomitra* (?) *tairai* AITA (1987, p. 72, pl. 3, figs. 7a–9; pl. 10, figs. 3–4). It differs from the latter in the wall-structure of the postcephalic segments, which can be well compared with that of *Stichomitra takanoensis* AITA.

Genus: **Stylocapsa** PRINCIPI 1909, emend. TAN 1927

Type species: Stylocapsa exagonata PRINCIPI 1909

*** Stylocapsa catenarum** MATSUOKA 1982a
Pl. 11, figs. 3–5

Stylocapsa catenarum MATSUOKA
Matsuoka 1982a, p. 75, pl. 2, figs. 1–11.
Matsuoka 1982b, pl. 3, figs. 3–4.
Yao et al. 1982, pl. 4, fig. 10.
Matsuoka 1983, p. 18, pl. 2, fig. 10; pl. 7, figs. 1–2.
Yao 1984, pl. 2, fig. 17–18.
Matsuoka 1986c, pl. 3, fig. 17.
Matsuoka & Yao 1986, pl. 2, fig. 11.
Wakita 1988, pl. 4, fig. 20.
Matsuoka 1990, pl. 2, fig. 4.
Yao 1991, pl. 4, fig. 6.
Stylocapsa (?) *catenarum* MATSUOKA
Aita 1987, p. 67, pl. 7, figs. 4a,b; 5a,b.

Stylocapsa (?) spiralis MATSUOKA 1982a **gr.**
Pl. 11, figs. 1 a–c, 2

Stylocapsa (?) *spiralis* MATSUOKA
Matsuoka 1982a, p. 77, pl. 3, figs. 1–8.
Matsuoka 1982b, pl. 3, figs. 8–9.
Yao et al. 1982, pl. 4, figs. 11–12.
Yao 1984, pl. 2, figs. 15–16.
Matsuoka 1986c, pl. 1, figs. 6, 7.
Matsuoka & Yao 1986, pl. 2, fig. 6, pl. 3, fig. 20.
Sato et al. 1986, Fig. 17.20.
Aita 1987, p. 67, pl. 7, figs. 7a,b.
Wakita 1988, pl. 4, fig. 19.
Iwata & Tajika 1989, pl. 5, figs. 4, 5.
Yao 1991, pl. 4, fig. 5.
Matsuoka 1992, pl. 5, fig. 1.
Stylocapsa (?) *spiralis* MATSUOKA group
Matsuoka 1983, p. 18, pl. 2, figs. 5–9, pl. 6, figs. 14–15.

Genus: **Suna** WU 1986

Type species: Suna geometrica WU 1986

*** Suna hybum** (FOREMAN) 1975
Pl. 2, fig. 1

Triactoma hybum FOREMAN
Foreman 1975, p. 609, pl. 2F, figs. 6, 7, pl. 3, figs. 7, 9.
Schaaf 1981, p. 440, pl. 12, fig. 7.
Thurow 1988, p. 407, pl. 9, fig. 11.
Tumanda 1989, p. 35, pl. 1, fig. 6.
Taketani & Kanie 1992, Fig. 3.8.
Triactoma sp. cf. *T. echiodes* FOREMAN
Foreman 1973, pl. 3, fig. 2, non fig. 3.
Suna geometrica WU
Wu 1986, p. 357, pl. 2, fig. 12, 13.
Triactoma cfr. *echinodes* FOREMAN
Igo et al. 1987, Fig. 2.10.

Genus: **Syringocapsa** NEVIANI 1900

Type species: Theosyringium robustum VINASSA 1900

Syringocapsa limatum FOREMAN 1973
Pl. 16, fig. 8

Syringocapsa limatum FOREMAN
Foreman 1973, p. 268, pl. 11, figs. 6, 7, pl. 16, fig. 8
Foreman 1975, p. 617, pl. 2K, fig. 7
non Aita 1987, p. 68, pl. 12, fig. 1.
non Kito 1989, p. 202, pl. 23, fig. 5.
Syringocapsa limata FOREMAN
Tumanda 1989, p. 40, pl. 2, fig. 2
Morosyringium limatum (FOREMAN)
? Steiger 1992, p. 85, pl. 22, fig. 12.

Syringocapsa sp. A
Pl. 16, figs. 6–7

Podobursa (?) *polylophia* FOREMAN
Aita & Okada 1986, p. 112, pl. 3, figs. 4–5.
Syringocapsa limatum FOREMAN
Aita 1987, p. 68, pl. 12, fig. 1.
Kito 1989, p. 202, pl. 23, fig. 5.
Syringocapsa sp.
De Wever et al. 1986b, pl. 10, fig. 1.
Syringocapsa sp. A
Widz 1991, p. 256, pl. 4, fig. 6.

Helocingulum polylophium (FOREMAN)
Steiger 1992, pl. 22, figs. 10, 11.

Remarks: This species differs form other similar species like *Podobursa* (?) *polylophia* FOREMAN (1973, p. 266, pl. 11, figs. 8–9) or *Syringocapsa limatum* FOREMAN by a shorter proximal part, rather abrupt transition to the inflated median portion and a shorter apical horn. It differs from *Syringocapsa lucifer* BAUMGARTNER (1984, p. 786, pl. 9, fig. 5) by having a longer, larger and porous terminal tube.

Genus: **Tetraditryma** BAUMGARTNER 1980

Type species: Tetraditryma pseudoplena BAUMGARTNER 1980

Remarks: Saldorfus PESSAGNO, BLOME & HULL (Pessagno et al., 1993) is not considered a different genus.

Tetraditryma corralitosensis (PESSAGNO) 1977a
Pl. 5, figs. 15–16

Crucella (?) *corralitosensis* PESSAGNO
Pessagno 1977a, p. 72, pl. 2, figs. 10–13.
Tetraditryma corralitosensis (PESSAGNO)
Baumgartner 1980, p. 296, pl. 7, figs. 12–15, pl. 11, fig. 13.
Kocher 1981, p. 98, pl. 16, fig. 31.
De Wever & Caby 1981, pl. 2, fig. 2G.
Baumgartner 1984, p. 787, pl. 9, figs. 6–7.
Aita 1985, fig. 6.1.
De Wever & Miconnet 1985, p. 390, pl. 1, fig. 9.
Nagai 1985, pl. 3, fig. 4–4a.
Aita 1987, p. 64, pl. 9, fig. 1.
De Wever et al. 1987, pl. 1, fig. A4.
Ožvoldova 1988, pl. 6, fig. 3.
Danelian 1989, p. 194, pl. 8, fig. 8.
Steiger 1992, p. 44, pl. 10, fig. 6.
Tetraditryma sp. cf. *T. corralitosensis* (PESSAGNO)
Wakita 1982, pl. 5, figs. 9–10.
Yang & Wang 1990, p. 200, pl. 1, fig. 16.
Tetraditryma corralitosensis bifida CONTI & MARCUCCI
Conti & Marcucci 1991, p. 804, pl. 4, fig. 4–5.
Saldorfus coldspringensis PESSAGNO, BLOME & HULL
Pessagno et al. 1993, p. 126, pl. 3, figs. 1, 4, 7.
Saldorfus corralitosensis (PESSAGNO)
Pessagno et al. 1993, p. 126, pl. 3, fig. 13.
Saldorfus oregonensis PESSAGNO, BLOME & HULL
Pessagno et al. 1993, p. 127, pl. 3, figs. 11, 12, 18.

Remarks: Saldorfus coldspringensis PESSAGNO, BLOME & HULL and *Saldorfus oregonensis* PESSAGNO, BLOME & HULL are not distinguished from *Tetraditryma corralitosensis* (PESSAGNO).

* **Tetraditryma pseudoplena** BAUMGARTNER 1980
Pl. 5, fig. 12

Hagiastrum plenum RÜST
Pessagno 1977a, p. 72, pl. 2, fig. 14.
Tetraditryma pseudoplena BAUMGARTNER
Baumgartner 1980, p. 297, pl. 1, fig. 9; pl. 7, figs. 1–11.
Baumgartner et al. 1980, p. 63, pl. 2, fig. 1.
Kocher 1981, p. 98, pl. 16, figs. 32–33.
Sato et al. 1982, pl. 3, fig. 7.
Ishida 1983, pl. 11, fig. 7.
Baumgartner 1984, p. 788, pl. 9, figs, 12, 14.
Carayon et al. 1984, pl. 1, fig. 5.
? Baumgartner 1985, Fig. 38. f.
Nagai 1985, pl. 4, figs. 1, 1a; ? pl. 3, figs. 5, 5a;
Goričan 1987, p. 187, pl. 1, fig. 10.
? Ožvoldova & Peterčakova 1987, pl. 35, fig. 4.
Ožvoldova 1990b, pl. 3, fig. 7.
Yang & Wang 1990, p. 200, pl. 1, fig. 9.
Widz 1991, p. 256, pl. 4, fig. 9.
Tetraditryma cf. *pseudoplena* BAUMGARTNER
De Wever et al. 1986b, pl. 8, fig. 1.

Genus: **Tetratrabs** BAUMGARTNER 1980

Type species: Tetratrabs gratiosa BAUMGARTNER 1980

Tetratrabs bulbosa BAUMGARTNER 1980
Pl. 5, fig. 7

Tetratrabs bulbosa BAUMGARTNER
Baumgartner 1980, p. 295, pl. 5, fig. 1; pl. 6, figs. 1–3, 8.
Baumgartner et al. 1980, p. 63, pl. 2, fig. 5.
Kocher 1981, p. 99, pl. 16, fig. 34.
Baumgartner 1984, p. 788, pl. 9, fig. 11.
De Wever et al. 1986b, pl. 7, fig. 13.
Tetratrabs aff. *zealis* (OŽVOLDOVA)
De Wever et al. 1986b, pl. 7, figs. 14, 15.

Tetratrabs zealis (OŽVOLDOVA) 1979
Pl. 5, figs. 10–11

Crucella zealis OŽVOLDOVA
Ožvoldova 1979, p. 34, pl. 2, fig. 1.
Tetratrabs gratiosa BAUMGARTNER
Baumgartner 1980, p. 295, pl. 1, fig. 11; pl. 5, figs. 2–7; pl. 6, fig. 4–7, 9–14; pl. 11, figs. 7–9.
Baumgartner et al. 1980, p. 63, pl. 2, fig. 6.
Ishida 1983, pl. 11, fig. 9.
Tetratrabs zealis (OŽVOLDOVA)
Kocher 1981, p. 99, pl. 17, fig. 1.
Matsuoka 1992, pl. 5, fig. 12.

Genus: **Thanarla** PESSAGNO 1977b

Type species: Dictyomitra veneta SQUINABOL 1903

*** Thanarla elegantissima** (CITA) 1964, sensu SANFILIPPO & RIEDEL 1985
Pl. 21, fig. 8

Lithocampe elegantissima CITA
Cita 1964, p. 148, pl. 12, figs. 2, 3
Riedel & Sanfilippo 1974, p. 779, pl. 6, figs. 8–10, pl. 13, figs. 2–4
Nakaseko et al. 1979, p. 23, pl. 7, fig. 1
Lithocampe (?) *elegantissima* CITA
Pessagno 1976, p. 55, pl. 3, fig. 6
Thanarla elegantissima (CITA)
Pessagno 1977b, p. 46, pl. 7, fig. 10
?Okamura 1980, pl. 21, fig. 1
Schmidt-Effing 1980, p. 246, figs. 2, 21, 22.
Matsuyama et al. 1982, pl. 2, fig. 2.
Mizutani et al. 1982, pl. 5, fig. 2.
Taketani 1982a, p. 59, pl. 4, fig. 12, pl. 11, figs. 17, 18.
Taketani 1982b, pl. 1, fig. 3.
Yamauchi 1982, pl. 1, fig. 16.
Schaaf 1984, p. 162, figs. 11a,b.
Sanfilippo & Riedel 1985, p. 600, Fig. 8.1a–e.
Thurow 1988, p. 407, pl. 4, fig. 11.
Kato & Iwata 1989, pl. 8, fig. 1.
Marcucci Passerini et al. 1991, Fig. 3a, 3b.
Thanarla pulchra (SQUINABOL)
Nakaseko & Nishimura 1981, p. 163, pl. 7, figs. 4, 7 only.
Murata et al. 1982, pl. 2, fig. 9.
Kato & Iwata 1989, pl. 8, fig. 2.
Tumanda 1989, p. 40, pl. 3, fig. 17.

Thanarla praeveneta PESSAGNO 1977b
Pl. 21, figs. 3–4

Thanarla praeveneta PESSAGNO
Pessagno 1977b, p. 46, pl. 7, fig. 11, 16, 18, 23, 27.
De Wever & Thiébault 1981, p. 593, pl. 1, fig. 7.
Goričan 1987, p. 187, pl. 3, fig. 18.
Tumanda 1989, p. 40, pl. 8, fig. 1.
Taketani & Kanie 1992, Fig. 5.10.
non Steiger 1992, p. 89, pl. 26, fig. 7.
Archaeodictyomitra sp. aff. *praeveneta* (PESSAGNO)
Yao 1984, pl. 5, fig. 7.

Thanarla pulchra (SQUINABOL) 1904, sensu SANFILIPPO & RIEDEL 1985
Pl. 21, fig. 7

Sethamphora pulchra SQUINABOL
Squinabol 1904, p. 213, pl. 5, fig. 8.
Dictyomitra pulchra (SQUINABOL)
Dumitrica 1975, p. 87, fig. 2.7.
Lithocampe elegantissima CITA
Foreman 1975, p. 616, pl. 2G, figs. 3, 4.
Muzavor 1977, p. 100, pl. 8, fig. 1.
Aoki 1982, pl. 3, figs. 11–12.
Thanarla pulchra (SQUINABOL)
Pessagno 1977b, p. 46, pl. 7, figs. 7, 21, 26.
Nakaseko & Nishimura 1981, p. 163, pl. 15, fig. 11 only.
Schaaf 1981, 439, pl. 4, fig. 10; pl. 19, figs. 7a,b.
Taketani 1982a, p. 59, pl. 11, fig. 19.
Baumgartner 1984, p. 788, pl. 9, fig. 15.
Schaaf 1984, p. 133, figs. 1, 5a,b; 7a,b only.
Sanfilippo & Riedel 1985, p. 600, Fig. 8.2a–e.
SuyarI 1986, pl. 2, fig. 1, non fig. 2.
Pavšič & Goričan 1987, p. 29, pl. 4, fig. 13.
Thurow 1988, p. 407, pl. 7, fig. 9.
Marcucci Pesserini et al. 1991, Fig. 3c.
Matsuoka 1992, pl. 1, fig. 12.
Taketani & Kanie 1992, Fig. 5.11–12.
Lithocampe (?) *elegantissima* FOREMAN
Nakaseko et al. 1979, p. 23, pl. 4, fig. 2
Thanarla pacifica NAKASEKO & NISHIMURA
Nakaseko & Nishimura 1981, p. 163, pl. 7, figs. 3a,b, 6, 9; pl. 15, fig. 14.
Thanarla sp. cf. *T. pulchra* (SQUINABOL)
Okamura & Uto 1982, pl. 5, fig. 6
Yao 1984, pl. 4, fig. 10
Thanarla – Archaeodictyomitra gr.
Okamura & Uto 1982, pl. 1, fig. 12 only.
Thanarla conica (ALIEV)
Kito 1987, pl. 3, pl. 1.

Genus: **Theocapsomma** HAECKEL 1887, emend. FOREMAN 1968

Type species: Theocapsa linnaei HAECKEL 1887

*** Theocapsomma cordis** KOCHER 1981
Pl. 9, fig. 13

Theocapsomma cordis KOCHER
Kocher 1981, p. 100, pl. 17, figs. 2–4.
Baumgartner 1984, p. 789, pl. 9, figs. 16–17.
Yamamoto et al. 1985, p. 38, pl. 8, fig. 2, 3a,b.
Danelian 1989, p. 196, pl. 8, fig. 17.
Matsuoka 1990, pl. 2, fig. 3.

Genus: **Transhsuum** TAKEMURA 1986

Type species: Transhsuum medium TAKEMURA 1986

Transhsuum brevicostatum (OŽVOLDOVA) 1975 **gr.**
Pl. 18, figs. 6–8

Dictyomitra sp. D.
Baumgartner & Bernoulli 1976, p. 617, fig. 12j.
Lithostrobus brevicostatus OŽVOLDOVA
Ožvoldova 1975, p. 84, pl. 102, fig. 1.
? Ožvoldova 1979, p. 259, pl. 5, fig. 2.
Hsuum brevicostatum (OŽVOLDOVA)
Kocher 1981, p. 73, pl. 14, fig. 13.

Baumgartner 1984, p. 769, pl. 5, figs. 1–2.
De Wever & Miconnet 1985, p. 387, pl. 4, fig. 12.
De Wever et al. 1986b, pl. 11, fig. 2.
non Matsuoka 1986a, pl. 2, fig. 10.
Ožvoldova & Peterčakova 1987, pl. 33, fig. 3.
Ožvoldova 1988, pl. 6, fig. 1, 11.
Wakita 1988, pl. 3, fig. 12, pl. 4, fig. 6.
Matsuoka 1990, pl. 1, fig. 2.
Ožvoldova 1990b, pl. 5, fig. 3.
Matsuoka 1992, pl. 5, fig. 7.
Widz 1991, p. 247, pl. 2, fig. 9.
? Pessagno et al. 1993, p. 136, pl. 6, figs. 3, 4, 21, 23.

Hsuum maxwelli PESSAGNO
Mizutani 1981, p. 176, pl. 59, fig. 5.
Mizutani et al. 1982, pl. 4, fig. 4.

Remarks: Various morphotypes are included. They have discontinuous costae limited to one segment, the segmental division is thus appearant in outline. No apical horn.

Transhsuum hisuikyoense (ISOZAKI & MATSUDA) 1985
Pl. 18, figs. 12–14

Hsuum sp. A
Kojima 1982, pl. 1, fig. 6.
Hsuum sp. a group
Kido et al. 1982, pl. 2, fig. 4.
Hsuum sp. B
? Yao et al. 1982, pl. 3, fig. 1.
Yao 1984, pl. 1, fig. 2, ?1.
Kishida & Hisada 1986, text-fig. 7.2, 3.
Matsuoka 1986a, pl. 2, fig. 6.
Hsuum sp. G.
Kishida & Sugano 1982, pl. 8, figs 13–14, non fig. 15.
? Nishizono & Murata 1983, pl. 5, fig. 5.
Sato et al. 1986, Figs. 17.15, 17.16.
Parahsuum sp. D
Yao et al. 1982, pl. 2, fig. 19.
Matsuoka & Yao 1986, pl. 1, fig. 7.
Hsuum spp.
Baumgartner 1985, Fig. 37p,q,r; Fig. 38s.
Hsuum hisuikyoense ISOZAKI & MATSUDA
Isozaki & Matsuda 1985, p. 437, pl. 2, figs. 10–18.
Sashida 1988, p. 18, pl. 4, figs. 3, 6–8, 19, 20.
Matsuoka & Yao 1986, pl. 1, fig. 8; pl. 3, fig. 4.
Hattori 1988a, pl. 13, fig. G.
Nagai 1988, pl. 1, fig. 8.
Hattori & Sakamoto 1989, pl. 15, figs. C,E, non fig. D.
Kito 1989, p. 179, pl. 20, figs. 7–13.
Hori 1990, Fig. 9.54.
Yao 1991, pl. 2, fig. 16.
Sano et al. 1992, pl. 2, fig. C.
Hsuum bipartitum GRILL & KOZUR
Grill & Kozur 1986, p. 256, pl. 5, figs. 1–6; pl. 7, fig. 6.
Transhsuum medium TAKEMURA
Takemura 1986, p. 51, pl. 5, fig. 25 (only).
Hsuum brevicostatum (OŽVOLDOVA)
Yokota & Sano 1986, pl. 1, fig. 9.
Transhsuum aff. *T. medium* TAKEMURA
Hattori 1987, pl. 17, figs. 5, 6, non fig. 15.
Hsuum sp. aff. *H. hisuikyoense* ISOZAKI & MATSUDA
Hattori & Sakamoto 1989, pl. 15, figs. F,H, non fig. G.
Hsuum sp. 1
Kito 1989, p. 180, pl. 20, figs. 14, 15, ?16, 21, 22.

Remarks: Included are specimens with a *Parahsuum*-like wall structure on the proximal part of the test and strong short discontinuous costae distally.

Transhsuum fuchsi (GRILL & KOZUR)(*Hsuum fuchsi* GRILL & KOZUR 1986, p. 255, pl. 6, figs. 1–3) with blunt discontinuous costae on the whole test and a perforate wall structure similar to that of *Transhsuum okamurai* (MIZUTANI), is considered a different species.

See also remarks under *Parahsuum* (?) *grande* HORI & YAO.

Transhsuum okamurai (MIZUTANI) 1981
Pl. 18, fig. 5

Pseudodictyomitra okamurai MIZUTANI
Mizutani 1981, p. 178, pl. 60, figs. 3–5.
Aoki & Tashiro 1982, pl. 2, fig. 10.
? Wakita 1988, pl. 5, fig. 5; pl. 6, fig. 11.
Unnamed multicyrtoid nassellarian
Adachi 1982, pl. 3, fig. 4.
Hsuum okamurai (MIZUTANI)
Kiessling 1992, pl. 1, fig. 6.

Transhsuum maxwelli (PESSAGNO) 1977a **gr.**
Pl. 18, figs. 1–4

Hsuum maxwelli PESSAGNO
Pessagno 1977a, p. 81, pl. 7, figs. 14–16.
Kocher 1981, p. 73, pl. 14, fig. 14.
Dumitrica & Mello 1982, pl. 4, figs. 1–3.
Pessagno et al. 1984, p. 25, pl. 1, fig. 6.
De Wever & Cordey 1986, pl. 1, fig. 1.
Kishida & Hisada 1986, fig. 2.10.
Matsuoka 1986a, pl. 2, figs. 11, 14, 16.
Matsuoka 1986c, pl. 2, fig. 15.
Matsuoka & Yao 1986, pl. 2, fig. 16.
Wakita 1988, pl. 4, figs. 4, 5; pl. 5, fig. 11.
Matsuoka 1990, pl. 1, fig. 12.
Widz 1991, p. 247, pl. 2, figs. 10–11.
Yao 1991, pl. 3, fig. 22.
Matsuoka 1992, pl. 4, fig. 4.
Hsuum sp. aff. *H. maxwelli* PESSAGNO
Pessagno 1977a, p. 82, pl. 8, figs. 1–2.
Baumgartner 1985, fig. 43g.
Hsuum maxwelli PESSAGNO gr.
Baumgartner 1984, p. 769, pl. 5, figs. 3–4.

Ožvoldova 1988, pl. 3, fig. 3; pl. 6, fig. 10.
Hsuum sp. A
Yamamoto et al. 1985, p. 35, pl. 5, fig. 2.
Hsuum sp. B
Yamamoto et al. 1985, p. 36, pl. 5, fig. 3.
Transhsuum maxwelli (PESSAGNO) gr.
Danelian 1989, p. 197, pl. 8, fig. 18–19.
Hsuum maxwelli PESSAGNO s.l.
Pessagno et al. 1993, p. 136, pl. 6, fig. 1.

Remarks: Distinction from other species same as by Baumgartner (1984).

Genus: **Triactoma** RÜST 1885

Type species: Triactoma tithonianum RÜST 1885

* **Triactoma blakei** (PESSAGNO) 1977a
Pl. 2, fig. 5–6

Tripocyclia blakei PESSAGNO
Pessagno 1977a, p. 80, pl. 6, figs. 15–16.
Ishida 1983, pl. 4, fig. 15.
Triactoma blakei (PESSAGNO)
Kocher 1981, p. 101, pl. 17, fig. 5 (only).
non Mizutani 1981, p. 175, pl. 57, figs. 5–6.
non Adachi 1982, pl. 5, fig. 3.
non Baumgartner 1984, p. 789, pl. 10, fig. 3.
non Yamamoto et al. 1985, p. 39, pl. 8, fig. 5.
De Wever et al. 1986b, pl. 6, fig. 23, non fig. 15.
non Ožvoldova & Peterčakova 1987, pl. 35, fig. 5.
non Wakita 1988, pl. 5, fig. 23.
Pessagno et al. 1989, p. 206, pl. 7, figs. 17, 19, 24.
Ožvoldova 1990b, pl. 1, fig. 1.
Widz 1991, p. 256, pl. 4, fig. 13.

Triactoma jonesi (PESSAGNO) 1977a
Pl. 2, figs. 8–9

Tripocyclia jonesi PESSAGNO
Pessagno 1977a, p. 80, pl. 7, figs. 1–5.
Triactoma jonesi (PESSAGNO)
Kocher 1981, p. 102, pl. 17, fig. 10.
Baumgartner 1984, p. 790, pl. 10, fig. 4.
non Ožvoldova & Sykora 1984, p. 272, pl. 11, fig. 5, pl. 10, fig. 4.
non De Wever et al. 1986b, pl. 6, fig. 16.
Kishida & Hisada 1986, fig. 2.22.
Goričan 1987, p. 187, pl. 1, fig. 16.
Conti & Marcucci 1991, pl. 4, figs. 7–8.
Tripocyclia trigonum RÜST
Sashida et al. 1982, pl. 1, fig. 5.
Ishida 1983, pl. 4, fig. 14.
Tripocyclia jonesi PESSAGNO emend. PESSAGNO & YANG
Pessagno et al. 1989, p. 222, pl. 7, figs. 5, 11, 21.
Yang & Wang 1990, p. 206, pl. 2, fig. 9.
Pessagno et al. 1993, p. 134, pl. 5, figs. 3, 21.
Tripocyclia sp. B.
Widz 1991, p. 257, pl. 4, fig. 12.

* **Triactoma parablakei** YANG & WANG 1990
Pl. 2, fig. 4

Triactoma blakei (PESSAGNO)
Baumgartner 1984, p. 789, pl. 10, fig. 3.
Yamamoto et al. 1985, p. 39, pl. 8, fig. 5.
Ožvoldova & Peterčakova 1987, pl. 35, fig. 5.
Triactoma sp.
? De Wever & Miconnet 1985, pl. 4, fig. 15.
Triactoma parablakei YANG & WANG
Yang & Wang 1990, p. 206, pl. 3, figs. 9, 15.

* **Triactoma cf. southforkensis** PESSAGNO & YANG, in Pessagno et al. 1989
Pl. 2, fig. 7

Triactoma southforkensis PESSAGNO & YANG
cf. Pessagno et al. 1989, p. 224, pl. 5, figs. 1–3, 16, 21.

Remarks: The illustrated specimen differs from the type material by having narrow shallow secondary grooves on the ridges of the spines.

Genus: **Tricapsula** WU 1986

Type species: Tricapsula costata WU 1986

Remarks: Tricolocapsa plicarum YAO was originally designated as the type species of *Tricapsula* (Wu, 1986). In this paper *Tricolocapsa plicarum* YAO and *Tricapsula costata* WU are assigned to different genera, *Tricapsula costata* is considered the type species of the genus *Tricapsula*.

Tricapsula costata WU
Pl. 10, figs. 3–4

Theocorys antiqua SQUINABOL
Riedel & Sanfilippo 1974, p. 781, pl. 10, fig. 9, non figs. 10, 11.
Sanfilippo & Riedel 1985, p. 623, fig. 14.6d only.
Tricapsula costata WU
Wu 1986, p. 359, pl. 3, figs. 6, 16, 17.
Protunuma sp.
Tumanda 1989, pl. 6, fig. 19.
Ožvoldova 1990a, p. 143, pl. 2, figs. 4, 5.
Cyrtophormis (?) *costata* SQUINABOL
Aguado et al. 1991, Fig. 7.15.

Remarks: Longitudinal rows of pores are present between the adjacent plicae as well as on their surface.

Genus: **Tricolocapsa** HAECKEL 1881

Type species: Tricolocapsa theophrasti HAECKEL 1887 (subsequent designation by Campbell 1954).

Tricolocapsa conexa MATSUOKA 1983
Pl. 11, figs. 7 a,b, 8–9, 10 a,b

Tricolocapsa plicarum YAO
Sashida et al. 1982, pl. 1, fig. 2.
Ishida 1983, pl. 8, fig. 9.
Tricolocapsa sp. a
Kido et al. 1982, pl. 5, fig. 5.
Tricolocapsa aff. *plicarum*
Matsuoka 1982b, pl. 3, fig. 15.
Tricolocapsa sp. E
Aita 1982, pl. 2, figs. 5a,b, non fig. 4.
Gongylothorax ? sp.
Kishida & Sugano 1982, pl. 8, fig. 22, non fig. 21.
Tricolocapsa conexa MATSUOKA
Matsuoka 1983, p. 20, pl. 3, figs. 3–7; pl. 7, figs. 11–14.
Yao 1984, pl. 2, figs. 2–4.
Yamamoto et al. 1985, p. 39, pl. 8, figs. 7a,b.
Kishida & Hisada 1986, fig. 2.17.
Matsuoka 1986b, fig. 3d–f.
Matsuoka 1986c, pl. 1, figs. 9, 10.
Matsuoka & Yao 1986, pl. 1, fig. 17, pl. 3, fig. 18.
Aita 1987, p. 68, pl. 7, figs. 9a,b.
Matsuoka 1988, pl. 1, figs. 3–5.
Ožvoldova 1988, pl. 7, figs. 9, 10.
Danelian 1989, p. 204, pl. 9, figs. 7–10.
Matsuoka 1990, pl. 1, fig. 13, pl. 2, fig. 13.
Kozur 1991, pl. 3, fig. 1.
Yao 1991, pl. 3, fig. 2.
Sano et al. 1992, pl. 2, fig. T.

Remarks: Some specimens display only very faint transverse ridges between adjacent longitudinal plicae (pl. 11, fig. 7a,b).

*** Tricolocapsa (?) fusiformis** YAO 1979
Pl. 9, fig. 14

Tricolocapsa (?) *fusiformis* YAO
Yao 1979, p. 33, pl. 4, figs. 12–18, pl. 5, figs. 1–4.
Wakita & Okamura 1982, pl. 7 fig. 10.
Kojima 1982, pl. 2, fig. 2.
Wakita 1982, pl. 3, fig. 4.
Kido et al. 1982, pl. 5, fig. 3.
Matsuoka 1982b, pl. 1, figs. 17–19.
Matsuoka 1983, p. 19, pl. 2, fig. 11; pl. 8, fig. 1.
Matsuoka & Yao 1986, pl. 1, fig. 14, pl. 3, fig. 8.
Yokota & Sano 1986, pl. 1, fig. 7.
Kojima 1989, pl. 2, figs. 4a,b.
Yao 1991, pl. 3, fig 2.
Japonocapsa fusiformis (YAO)
Grill & Kozur 1986, pl. 2, fig. 2.
Protunuma fusiformis ICHIKAWA & YAO
Sano et al. 1992, pl. 2, fig. R.

Tricolocapsa tetragona MATSUOKA 1983
Pl. 13, figs. 8, 10

Tricolocapsa sp. N
Matsuoka 1982b, pl. 2, figs. 13, 17.
Tricolocapsa sp. E
Aita 1982, pl. 2, fig. 4, non figs. 5a,b.
Tricolocapsa tetragona MATSUOKA
Matsuoka 1983, p. 22, pl. 3, figs. 8–12, pl. 8, figs. 4–10.
Yao 1984, pl. 2, figs. 5, 6.
Matsuoka & Yao 1986, pl. 1, fig. 18, fig. 18.
Aita 1987, p. 68, pl. 7, figs. 11a,b.
Sato et al. 1986, Fig. 17.18.
Yao 1991, pl. 3, fig. 3.
Maaté et al. 1993, Fig. 3.18.

*** Tricolocapsa sp. A**
Pl. 11, figs. 11a,b, 12a,b, 13a,b

Remarks: This species is characterized by an irregular network of ridges, generally encompassing one, rarely more (pl. 11, fig. 13) circular pores. A large aperture and a deep perforate depression present at the base.

Tricolocapsa sp. A differs from *T. conexa* MATSUOKA by lacking distinct longitudinal plicae. It differs from *Stylocapsa lacrimalis* MATSUOKA (1983, p. 16, pl. 1, figs 12–13; pl. 7, figs. 3–10) by the number of segments and larger size.

Genus: **Trillus** PESSAGNO & BLOME 1980

Type species: Trillus seidersi PESSAGNO & BLOME 1980

Trillus spp.
Pl. 1, fig. 1

Remarks: The taxon is treated on the generic level.

Genus: **Tritrabs** BAUMGARTNER 1980

Type species: Paronaella (?) *casmaliaensis* PESSAGNO 1977a

Tritrabs casmaliaensis (PESSAGNO) 1977a
Pl. 5, figs. 8–9

Paronaella (?) *casmaliaensis* PESSAGNO
Pessagno 1977a, p. 69, pl. 1, figs. 6–8.
Tritrabs casmaliaensis (PESSAGNO)
Baumgartner 1980, p. 293, pl. 1, fig. 10; pl. 4, fig. 11; pl. 11, fig. 10.
Kocher 1981, p. 105, pl. 17, fig. 18.
Ishida 1983, pl. 10, fig. 6.
Baumgartner 1984, p. 791, pl. 10, fig. 9.

Baumgartner 1985, fig. 43a.
Ožvoldova 1988, pl. 8, fig. 8.
Danelian 1989, p. 206, pl. 9, fig. 13–14.
Kito 1989, pl. 8, fig. 1.
Ožvoldova 1990b pl. 1, fig. 8.
Conti & Marcucci 1991, pl. 4, fig. 11.
Widz 1991, p. 257, pl. 4, fig. 17.
Steiger 1992, p. 41, pl. 8, fig. 1, non figs. 2–3.

Tritrabs sp. A
Ishida 1983, pl. 10, fig. 8.

Tritrabs aff. *casmaliaensis* (PESSAGNO)
De Wever et al. 1986b, pl. 8, fig. 12.

Tritrabs rhododactylus BAUMGARTNER
Conti & Marcucci 1991, pl. 4, fig. 10.

Tritrabs exotica PESSAGNO 1977a **gr.**
Pl. 5, figs. 3–6

Paronaella (?) *exotica* PESSAGNO
Pessagno 1977a, p. 70, pl. 1, figs. 12–13.

Tritrabs exotica (PESSAGNO)
Baumgartner 1980, p. 294, pl. 4, fig. 16.
Kocher 1981, pl. 17, fig. 20.
Baumgartner 1984, p. 791, pl. 10, fig. 11.
De Wever et al. 1986b, pl. 8, fig. 19.
Kito 1989, p. 121, pl. 13, figs. 16–17.
Ožvoldova 1990b, pl. 1, fig. 4; pl. 4, fig. 3.
Steiger 1992, p. 39, pl. 7, figs. 8–10.

Tritrabs rhododactylus BAUMGARTNER
Baumgartner 1980, p. 294, pl. 4, figs. 12–15; pl. 11, fig. 15.
? Ishida 1983, pl. 10, fig. 10.
Baumgartner 1984, p. 791, pl. 10, fig. 13.
De Wever et al. 1986b, pl. 8, fig. 11.
Danelian 1989, p. 208, pl. 10, figs. 2–5.
Kito 1989, p. 122, pl. 13, figs. 12–14.
Steiger 1992, p. 39, pl. 7, fig. 7.

Tritrabs rhododactyla BAUMGARTNER
Kocher 1981, p. 106, pl. 17, fig. 22.

Tritrabs cf. *exotica* (PESSAGNO)
De Wever et al. 1986b, pl. 8, fig. 14.
Danelian 1989, p. 208, pl. 10, fig. 1.

Tritrabs sp. aff. T. *rhododactylus* BAUMGARTNER
Conti & Marcucci 1991, pl. 4, fig. 12.

Remarks: Tritrabs rhododactylus BAUMGARTNER is considered a synonym of *Tritrabs exotica* (PESSAGNO). Equal or unequal interradial angles may develop with otherwise identical specimens. No difference in the stratigraphic range of these two morphotypes has been observed in our material.

Genus: **Turanta** PESSAGNO & BLOME 1982

Type species: Turanta capsensis PESSAGNO & BLOME 1982

Turanta spp.
Pl. 26, fig. 15

Remarks: Representatives of the genus *Turanta* rarely occur, therefore they are not distinguished in the species level.

Genus: **Unuma** ICHIKAWA & YAO 1976

Type species: Unuma (Unuma) typicus ICHIKAWA & YAO 1976

Unuma darnoensis KOZUR 1991
Pl. 10, figs. 7–8, 9a,b

Unuma (Unuma) sp.
Owada & Saka 1982, pl. 2, fig. 4.

Unuma sp. A
? Wakita 1982, pl. 4, fig. 1.

Protunuma sp.
Hattori & Sakamoto 1989, pl. 19, fig. J.

Unuma darnoensis KOZUR
Kozur 1991, pl. 2, fig. 2.

Remarks: Unuma darnoensis KOZUR differs from *U. typicus* ICHIKAWA & YAO by a more inflated last segment, smaller hemispherical apertural cap and more plicae visible laterally. Compared to *U. latusicostatus* AITA it shows no abrupt change in width between the conical and the inflated portion of the test and no spines on the plicae.

The species name is tentatively used in this paper, since the original assignment by Kozur (1991) lacks a description.

Unuma echinatus ICHIKAWA & YAO 1976
Pl. 10, figs. 10–11

Unuma echinatus ICHIKAWA & YAO
Ichikawa & Yao 1976, p. 112, pl. 1, figs. 5–6; pl. 2, figs. 5–7.
Yao et al. 1982, pl. 3, fig. 5
Mizutani & Koike 1982, pl. 2, fig. 6.
Wakita 1982, pl. 3, figs. 11–12.
Matsuoka 1982b, pl. 1, fig. 1a,b, 21.
Nishizono et al. 1982, pl. 2, fig. 20.
Kishida & Sugano 1982, pl. 11, figs. 6–8.
Ishida 1983, pl. 4, figs. 7–8.
Baumgartner 1984, p. 792, pl. 10, figs. 14–15.
Yao 1984, pl. 1, fig. 13.
Baumgartner 1985, Fig. 37 l,m.
De Wever & Cordey 1986, pl. 1, fig. 12.
Grill & Kozur 1986, pl. 1, fig. 1.
Matsuoka & Yao 1986, pl. 1, fig. 3; pl. 3, fig. 11.
Takemura 1986, p. 58, pl. 8, figs. 14–15.
Goričan 1987, p. 188, pl. 2, fig. 5.
Hattori 1987, pl. 14, figs. 2, 3.
Hattori 1988a, pl. 8, fig. B.

Hattori & Sakamoto 1989, pl. 8, figs. L, M; pl. 9, fig. A.
Kito 1989, p. 213, pl. 24, fig. 11–12, ? fig. 10
Yao 1991, pl. 3, fig. 8.
Sano et al. 1992, pl. 2, fig. N.
Unuma sp. cf. *U. echinatus* ICHIKAWA & YAO
Kido et al. 1982, pl. 3, fig. 10.
Unuma typicus ICHIKAWA & YAO
Nishizono et al. 1982, pl. 2, fig. 19.
Unuma sp. aff. *U. echinatus* ICHIKAWA & YAO
Hattori 1988a, pl. 8, fig. C.
Unuma sp. B
Hattori 1987, pl. 14, fig. 4.

Unuma latusicostatus (AITA) 1987
Pl. 10, fig. 12

Unuma ? sp. C
Ishida 1983, pl. 8, fig. 4.
Unuma sp.B
Ishida 1983, pl. 8, fig. 5.
Tricolocapsa laticostata AITA
Aita 1985, fig. 7.8–9.
Tricolocapsa latusicostata AITA
Aita 1987, p. 76, pl. 4, figs. 7a–8b; pl. 10, figs. 8–9.
Csontos et al. 1991, pl. 1, fig. 2.
Unuma latusicostatus (AITA)
Maaté et al. 1993, Fig. 3.20, 3.21.

Unuma typicus ICHIKAWA & YAO 1976
Pl. 10, fig. 13

Unuma typicus ICHIKAWA & YAO
Ichikawa & Yao 1976, p. 112, pl. 1, figs. 1–3.
non Nishizono et al. 1982, pl. 2, fig. 19.
Yao et al. 1982, pl. 3, fig. 6.
Ishida 1983, pl. 4, fig. 9.
Matsuoka & Yao 1986, pl. 1, fig. 12; pl. 3, fig. 12.
Sato et al. 1986, Fig. 17.14.
Takemura 1986, p. 58, pl. 8, fig. 16.
Goričan 1987, p. 188, pl. 2, fig. 4.
non Hattori 1987, pl. 14, fig. 6.
Hattori 1988a, pl. 8, fig. A.
Hattori & Sakamoto 1989, pl. 8, fig. J, non fig. K.
non Kito 1989, p. 214, pl. 24, figs. 7–9.
Yao 1991, pl. 3, fig. 9.
? Pessagno et al. 1993, p. 161, pl. 8, fig. 20.

Genus: **Williriedellum** DUMITRICA 1970

Type species: Williriedellum crystallinum DUMITRICA 1970

Williriedellum carpathicum DUMITRICA 1970
Pl. 12, figs. 6 a,b, 7–8

Williriedellum carpathicum DUMITRICA
Dumitrica 1970, p. 70, pl. 9, fig. 56a,b, 57–59; pl. 10, fig. 61.
Aita 1982, pl. 3, fig. 6.
Aoki & Tashiro 1982, pl. 4, figs. 15a,b; pl. 5, figs. 5a,b, 11, 12a,b.
Ožvoldova 1990b, pl. 5, figs. 2, 4.
Widz & De Wever 1993, p. 88, pl. 2, figs. 4–6.
Tricolocapsa sp. O
Yao et al. 1982, pl. 4, fig. 21.
Yao 1984, pl. 2, figs. 31–32.
Matsuoka & Yao 1986, pl. 2, fig. 13.
Tricolocapsa yaoi MATSUOKA
Matsuoka 1986c, p. 106, pl. 2, figs. 1–4. pl. 3, figs. 1–8.
Yao 1991, pl. 4, fig. 16.
Matsuoka 1992, pl. 4, fig. 6.
Tricolocapsa cf. *yaoi* MATSUOKA & YAO
? Wakita 1988, pl. 5, fig. 18.
Tricolocapsa sp. B
Ožvoldova 1988, p. 389, pl. 2, fig. 4; pl. 7, ? fig. 4.
Ožvoldova 1992, p. 115, pl. 2, fig. 9.

Williriedellum crystallinum DUMITRICA 1970
Pl. 12, figs. 1, 2 a–c

Williriedellum crystallinum DUMITRICA
Dumitrica 1970, p. 69, pl. 10, figs. 60a–c, 62, 63.
Widz 1991, p. 257, pl. 4, figs. 21, 22.
Williriededellum cf. *crystallinum* DUMITRICA
Adachi 1982, pl. 4, figs. 8, ?9.
Yamamoto 1983, pl. 1, fig. 6.
Wakita 1988, pl. 5, fig. 25; pl. 6, fig. 18.
Kiessling 1992, pl. 1, fig. 14.

Williriedellum sp. A sensu MATSUOKA 1983
Pl. 12, figs. 9 a–c, 10 a–c, 11 a,b

Hemicryptocapsa capita TAN SIN HOK
Dumitrica & Mello 1982, pl. 3, fig. 3.
Tricolocapsa sp. I
Matsuoka 1982b, pl. 2, fig. 14; pl. 3, fig. 14.
Yao et al. 1982, pl. 4, fig. 14.
Williriedellum sp. A gr. MATSUOKA
Matsuoka 1983, p. 23, pl. 4, figs. 1–3; pl. 8, figs. 11–15.
Goričan 1987, p. 188, pl. 3, figs. 15, 16.
Wakita 1988, pl. 4, fig. 22.
Williriedellum sp. A
Matsuoka 1985, pl. 1, fig. 6.
Matsuoka 1986c, pl. 1, fig. 8; pl. 2, fig. 6.
Aita 1987, p. 68, pl. 7, fig. 15a,b.
Matsuoka 1992, pl. 4, fig. 7.
Maaté et al. 1993, Fig. 3.19.
Williriedellum sp.
Yamamoto et al. 1985, p. 40, pl. 9, fig. 8.

Remarks: The specimens included vary by the degree of encasement of the cephalo-thorax in the abdomen and by the number of larger pores at the basal appendage.

Genus: **Wrangellium** PESSAGNO & WHALEN 1982

Type species: Wrangellium thurstonense PESSAGNO & WHALEN 1982

*** Wrangellium sp.**
Pl. 17, fig. 16

Genus: **Xitus** PESSAGNO 1977b

Type species: Xitus plenus PESSAGNO 1977b

*** Xitus gifuensis** MIZUTANI 1981
Pl. 25, figs. 11–12

Xitus gifuensis MIZUTANI
Mizutani 1981, p. 180, pl. 59, figs. 1, 2a,b, 3, 4.
Adachi 1982, pl. 3, figs. 1–2.
Yamamoto 1983, pl. 1, fig. 5.
Wakita 1988, pl. 5, ? fig. 9; pl. 6, fig. 20.

Remarks: Similar but somewhat higher forms with weaker nodes were found stratigraphically bellow *Xitus gifuensis* MIZUTANI (*Xitus* cf. *gifuensis*, pl. 25, fig. 16).

Xitus sp. A sensu WIDZ 1991
Pl. 25, figs. 13–15

Xitus cf. *spicularius* (ALIEV)
De Wever et al. 1986b, pl. 11, fig. 4.
Xitus aff. *spicularius* (ALIEV)
De Wever et al. 1986b, pl. 11, fig. 5.
Xitus sp. A
Widz 1991, p. 257, pl. 4, fig. 26.

Remarks: This species differs from *Xitus spicularius* (ALIEV) (*Dictyomitra spicularia* ALIEV 1965, p. 39, pl. 6, fig. 9) by having equally sized instead of alternating small and large nodes.

Xitus (?) sp. sensu STEIGER 1992
Pl. 25, fig. 10

Gen. et sp. indet.
Schaaf 1984, p. 152–153, fig. 2.
Xitus sp.
Steiger 1992, p. 89, pl. 26, figs. 12, 13.

Remarks: For description see Steiger (1992). This species differs from *Eucyrtidium* ? *monokawaense* TUMANDA (1989, p. 32, pl. 4, figs. 9–10; pl. 10, figs. 1–b), to which it is appearently related, by the test increasing less rapidly in width, having a narrowed prolongation of the last segment and lacking pores on the blunt ridges.

Genus: **Yamatoum** TAKEMURA 1986

Type species: Yamatoum elegans TAKEMURA 1986

*** Yamatoum spp.**
Pl. 10, figs. 14–15

Remarks: Forms with two horizontally arranged rows of spines are included. The terminal portion is usually broken off, which makes the distinction among *Yamatoum komaniense* TAKEMURA (1986, p. 56, pl. 7, figs. 19–22), *Y. spinosum* TAKEMURA (1986, p. 56, pl. 8, figs.1–3) and *Y. caudatum* TAKEMURA (1986, p. 57, pl. 8, figs. 7–9) impossible.

*** Yamatoum (?) sp. A**
Pl. 10, fig. 16

Stichocapsa sp. A
Mizutani & Koike 1982, pl. 2, figs. 1, 2a,b.
Stichocapsa (?) sp. A
Wakita 1982, pl. 3, fig. 8.
Stichocapsa sp. B
Yamamoto et al. 1985, p. 38, pl. 7, fig. 6.
Stichocapsa (?) sp. D
Hattori 1987, pl. 13, fig. 11.

Genus: **Zartus** PESSAGNO & BLOME 1980

Type species: Zartus jonesi PESSAGNO & BLOME 1980

Zartus spp.
Pl. 1, figs. 2–4

Remarks: The taxon is treated on the generic level.

Genus: **Zhamoidellum** DUMITRICA 1970

Type species: Zhamoidellum ventricosum DUMITRICA 1970

Zhamoidellum ovum DUMITRICA 1970
Pl. 13, figs. 3–4, 5 a,b, 6–7

Zhamoidellum ovum DUMITRICA
Dumitrica 1970, p. 79, pl. 9, figs. 52a,b, 53, 54.
Aoki & Tashiro 1982, pl. 3, fig. 8, non fig. 10; pl. 5, figs. 13, 17a,b.
Dumitrica & Mello 1982, pl. 3, fig. 13.
Ožvoldova 1988, pl. 7, fig. 3.
Widz 1991, p. 257, pl. 4, fig. 19.
Kiessling & Zeiss p. 191, pl. 2, fig. 7.
Zhamoidellum sp. A
Aita 1982, pl. 3, figs. 7–8b.
Tricolocapsa sp. A
? Yao 1984, pl. 3, figs, 10, 11.
Zhamoidellum mikamense AITA
Aita 1985, fig. 7:10–11.
Aita 1987, p. 74, pl. 4, figs. 9a,b; pl. 10, figs. 10, 11.
Iwata & Tajika 1989, pl. 5, fig. 2.

Matsuoka 1992, pl. 3, fig. 3; pl. 4, fig. 8.

Tricolocapsa sp.

? Wakita 1988, pl. 5, fig. 19.

Complexopora tirolica KIESSLING

Kiessling & Zeiss 1992, p. 191, pl. 1, figs. 1–9; pl. 2, figs. 1–2.

Complexopora sp. A

Kiessling & Zeiss 1992, p. 1, figs. 10–11.

Complexopora sp. B

Kiessling & Zeiss 1992, p. 191, pl. 1, fig. 12.

Remarks: This species as defined by Dumitrica (1970) shows a large variability of the shape of the abdomen. Pore frames are usually well developed. *Zhamoidellum mikamense* AITA is thus considered a younger synonym of *Zhamoidellum ovum*.

Forms with a circular sutural pore or depression are also included. *Complexopora tirolica* KIESSLING is synonymized with *Zhamoidellum ovum*.

Zhamoidellum sp. A

Pl. 13, figs. 1–2

Remarks: This morphotype differs from *Zhamoidellum ovum* DUMITRICA by a more elongate overall shape, the thorax being almost entirelly encased in the abdomen, and a large widely open sutural pore.

Acknowledgements

I wish to thank my supervisor Peter O. Baumgartner for the guidance of this study, for having visited the outcrops and for the critical reading of the manuscript. Jean Guex, Gérard M. Stampfli and Patrick De Wever also read the manuscript, Drago Skaberne and Dragica Turnšek reviewed some chapters. Their corrections and important suggestions were extremely helpful. I would like to thank Elisabeth S. Carter for her comments and for editing the English text.

I wish to express my sincere thanks to Katica Drobne for having provided me with valuable advice and encouragement.

Luis O'Dogherty gave me free access to his unpublished data and radiolarian residues. Discussions with him, Pascale Dalla Piazza and Alain Pillevuit were always useful and stimulating.

Mirko Mirković is gratefully acknowledged for his guidance in the field and for having introduced me to the geology of the Budva Zone.

The benthic foraminifera were determined by Michel Septfontaine, reef organisms by Dragica Turnšek, planktic foraminifera by Luis O'Dogherty and Gianni Di Marco, nannoplankton by Jernej Pavšič, and conodonts by Francis Hirsch. I am much obliged to them all.

Milojka Huzjan accompanied me in the field during the first year of the study. Kata Cvetko prepared the thin sections, Alain Pillevuit and Iztok Sajko realized the computer-made figures, Gianni Di Marco contributed to the hand-drawn figures, Markus Bill took the transmitted light photographs, Edouard Sottas processed the scanning electron micrographs. Iztok Sajko prepared the final, camera-ready computer print-out of the text. I greatly appreciate their help.

This research was financially supported by the Centre of Scientific Research of the Slovenian Academy of Sciences and Arts and aided by grants from the Ministry of Science and Technology of Slovenia, University of Lausanne and Société Académique Vaudoise. The publication was partially funded by the Fondation Dr. Joachim de Giacomi, the Faculty of Science, University of Lausanne, Société Académique Vaudoise, and Société Vaudoise des Sciences Naturelles.

I equally wish to thank the Institute of Geology and Paleontology of the Lausanne University for inviting me to study here in Lausanne and for making available the use of their facilities. I would like to thank everyone at the Institute for their friendship and their generous assistance over the last four years.

REFERENCES

ADACHI M. 1982: Some considerations on the Mirifusus baileyi assemblage in the Mino terrain, central Japan. — News of Osaka Micropaleontologists, Spec. vol. 5, pp. 211–225.

AGUADO, R., O'DOGHERTY, L., REY, J. and VERA, J.A. 1991: Turbiditas calcáreas del Cretácico al norte de Vélez Blanco (Zona Subbética): biostratigrafía y génesis. — Rev. Soc. Geol. España, vol. 4, no. 3–4, pp. 272–304.

AITA, Y. 1982: Jurassic radiolarian biostratigraphy in Irazuyama district, Kochi Prefecture, Japan – a preliminary report. — News of Osaka Micropaleontologists, Spec. vol. 5, pp. 255–270.

AITA, Y. 1985: Jurassic radiolarian biostratigraphy of the Irazuyama Formation (Takano Section), Shikoku, Japan. — Scientific and Technical Reports of the Mining College, Akita University, no. 6, pp. 33–41.

AITA, Y. 1987: Middle Jurassic to Lower Cretaceous radiolarian biostratigraphy of Shikoku with reference to selected sections in Lombardy Basin and Sicily. — Science Reports of the Tokohu University, Sendai, Second Series (Geology), vol. 58, no. 1, pp. 1–91.

AITA, Y. and OKADA, H. 1986: Radiolarians and calcareous nannofossils from the uppermost Jurassic and lower Cretaceous strata of Japan and Tethyan regions. — Micropaleontology, vol. 32, no. 2, pp. 97–128.

ALIEV, K.S. 1965: Radiolarians of the Lower Cretaceous deposits of northeastern Azerbaidzhan and their stratigraphic significance. — Izdat. Akad. Azerbaidz. SSR, Baku, pp. 3–124.

ANTONIJEVIĆ, R., PAVIĆ, A. and KAROVIĆ, J. 1969a: Osnovna geološka karta 1:100 000, listovi Kotor i Budva.— Savezni geološki zavod, Beograd.

ANTONIJEVIĆ R., PAVIĆ, A., KAROVIĆ, J., DIMITRIJEVIĆ, M., RADOIČIĆ, R., PEJOVIĆ, D., PANTIĆ, S. and ROKSANDIĆ, M. 1969b: Osnovna geološka karta 1:100 000, Tumač za listove Kotor i Budva (Explanatory text for Kotor and Budva sheets).— Savezni geološki zavod, Beograd, pp. 1–64.

AOKI, T. 1982: Upper Jurassic to Lower Cretaceous radiolarians from the Tsukimiyama and Tei Melanges of the northern Shimanto Belt in Kochi Prefecture, Shikoku. — News of Osaka Micropaleontologists, Spec. vol. 5, pp. 339–351.

AOKI, T. and TASHIRO, M. 1982: Stratigraphic study of the Shimanto Belt (Cretaceous Kamigumi Formation equivalent to the Doganaro Formation) near Kamigumi, Kagami-cho, Kagami-gun, Kochi Prefecture. — Sci. Rept. Kochi Univ., vol. 31, pp. 1–24.

ARTHUR, M.A., BRUMSACK, H.-J., JENKYNS, H.C. and SCHLANGER, S.O. 1990: Stratigraphy, geochemistry, and paleoceanography of organic carbon-rich Cretaceous sequences. — In: GINSBURG, R.N. and BEAUDOIN, B. (Eds.): Cretaceous Resources, Events and Rhythms, Kluwer Academic Publishers & NATO Scientific Affairs Division, Series C, vol. 304, pp. 75–119.

AUBOUIN, J. 1960: Essai sur l'ensemble italo-dinarique et ses rapports avec l'arc alpin. — Bull. Soc. Géol. France, sér. 7, vol. 2, no. 4, pp. 487–526.

BAUMGARTNER, P.O. 1980: Late Jurassic Hagiastridae and Patulibracchiidae (Radiolaria) from the Argolis Peninsula (Peleponnesus, Greece). — Micropaleontology, vol. 26, no. 3, pp. 274–322.

BAUMGARTNER, P.O. 1984: A Middle Jurassic-Early Cretaceous low latitude radiolarian zonation based on unitary associations and age of Tethyan radiolarites. — Eclogae geologicae Helvetiae, vol. 77, no. 3, pp. 729–841.

BAUMGARTNER, P.O. 1985: Jurassic sedimentary evolution and nappe emplacement in the Argolis Peninsula (Peloponnesus, Greece). — DenkschriftenderSchweizerischenNaturforschenden Gesellschaft, vol. 99, pp. 1–111.

BAUMGARTNER, P.O. 1987: Age and genesis of Tethyan Jurassic radiolarites. — Eclogae geologicae Helvetiae, vol. 80, no. 3, pp. 831–879.

BAUMGARTNER, P.O. 1990: Genesis of Jurassic Tethyan radiolarites. — The example of Monte Nerone (Umbria-Marche Apennines). — In: PALLINI, G., CECCA, F., CRESTA, S. and SANTANTONIO, M. (Eds.): Atti II Conv. Int., Fossili, Evoluzione, Ambiente. Pergola, pp. 19–32.

BAUMGARTNER, P.O. 1992: Lower Cretaceous radiolarian biostratigraphy and biogeography off Northwestern Australia (ODP Sites 765 and 766 and DSDP Site 261), Argo Abyssal Plain and Lower Exmouth Plateau. — In: GRADSTEIN, F.M., LUDDEN, J.N., et al. (Eds.): Proceedings of the Ocean Drilling Program, Scientific Results, vol. 123, pp. 299–342.

BAUMGARTNER, P.O. and BERNOULLI D. 1976: Stratigraphy and radiolarian fauna in a Late Jurassic-Early Cretaceous section near Achladi (Evvoia, Eastern Greece). — Eclogae geologicae Helvetiae, vol. 69, no. 3, pp. 601–626.

BAUMGARTNER, P., DE WEVER, P. and KOCHER, R. 1980: Correlation of Tethyan Late Jurassic – Early Cretaceous radiolarian events. — Cahiers de Micropaléontologie, vol. 2, pp. 23–86.

BEŠIĆ, Z. 1975: Geologija Crne Gore. Stratigrafija i facijalni sastav Crne Gore, Vol. I/1. — Društvo za nauku i umjetnost Crne Gore, Titograd, Posebna izdanja vol. 2, pp. 1–415.

BEŠIĆ, Z. 1980: Geologija Crne Gore. Stratigrafija i facijalni sastav Crne Gore, Vol. I/2. — Crnogorska akademija nauka i umjetnosti, Titograd , Posebna izdanja vol. 9, pp. 1–365.

BEŠIĆ, Z. 1983: Geologija Crne Gore. Geotektonika i paleogeografija Crne Gore, Vol. III. — Crnogorska akademija nauka i umjetnosti, Titograd, Posebna izdanja vol. 16, pp. 1–212.

BEŠIĆ, Z., VUKOVIĆ, V. and CICOVIĆ, B. 1965: Boksiti Crne Gore (Bauxites du Monténégro, Yougoslavie). — Rudnici boksita Nikšić (Mines des bauxites – Nikšić), Nikšić, pp. 1–168.

BLANCHET, R. 1975: De l'Adriatique au bassin Pannonique, essai d'un modèle de chaîne alpine. — Mém. Soc. Géol. France, vol. 120, pp. 1–172, pl. 1–4.

BLANCHET, R., CADET, J.-P., CHARVET, J. and RAMPNOUX, J.-P. 1969: Sur l'existence d'un important domaine de flysch tithonique-crétacé inférieur en Yougoslavie: l'unité du flysch bosniaque. — Bull. Soc. géol. France, sér 7, vol. 11, pp. 871–880.

BLOME, C.D. 1984: Upper Triassic Radiolaria and Radiolarian Zonation from Western North America. — Bulletins of American Paleontology, vol. 85, no. 318, pp. 1–88.

BOSELLINI, A., MASETTI, D. and SARTI, M. 1981: A Jurassic "Tongue of the ocean" infilled with oolitic sands: the Belluno Trough, Venetian Alps, Italy. — Marine Geology, vol. 44, pp. 59–95.

BUKOWSKI, G. 1903: Blatt Budua (Zone 36, Kol XX, SW) der geologischen Detailkarte von Süddalmatien 1:25 000. — Geologische Reichanstalt, Lieferung 5, Wien.

BUKOWSKI, G. 1904: Blatt Budua (Zone 36, Kol. XX, SW.–Grupe). Erläuterungen zur geologischen Detailkarte von Süddalmatien 1:25 000. — Geologische Reichsanstalt, Wien, pp. 1–66.

BUKOWSKI, G. 1909a: Blatt Spizza (Zone 37, Kol. XX). Südhälfte. Geologische Detailkarte von Süddalmatien 1:25 000. — Geologische Reichsanstalt, Wien.

BUKOWSKI, G. 1909b: Blatt Spizza (Zone 37, Kol. XX). Nordhälfte. Geologische Detailkarte von Süddalmatien 1:25 000. — Geologische Reichsanstalt, Wien.

BUKOWSKI, G. 1912: Blatt Spizza (Zone 37, Kol. XX). Erläuterungen zur geologischen Detailkarte von Süddalmatien. — Geologische Reichsanstalt, Wien, pp.1–104.

BUKOWSKI, G. 1927: Geologische Detailkarte des Gebirges um Budua in Süddalmatien. — Jahrbuch der geologischen Bundesanstalt, Wien, vol. 57, no. 1–2, pp. 195–204, 1 Karte 1:25 000.

BURIĆ, P. 1966: Geologija ležišta boksita Crne Gore (Géologie des gites de bauxite du Monténégro (Yougoslavie)). — Geološki glasnik, Sarajevo, Posebna izdanja vol. 8, pp. 1–277.

BUSER, S. 1987: Development of the Dinaric and Julian Carbonate Platforms and of the intermediate Slovenian Basin (NW Yugoslavia). — Mem. Soc. Geol. It., vol. 40, pp. 313–320.

CADET, J.-P. 1970: Esquisse géologique de la Bosnie-Herzégovine et du Monténégro occidental (Yougoslavie). — Bull. Soc. Géol. France, ser 7, vol. 12, pp. 973–985.

CADET, J.-P. 1978: Essai sur l'évolution alpine d'une paléomarge continentale: les confins de la Bosnie-Herzégovine et du Monténégro (Yougoslavie). — Mém. Soc. Géol. France, vol. 133, pp. 1–83, pl. 1–4.

ČADJENOVIĆ, D., STIJOVIĆ, V. and MIRKOVIĆ, M. 1988: Kredni alohtoni karbonati, Budva zona. — In: MIRKOVIĆ, M. and VUJISIĆ, P. (Eds.): Vodič ekskurzije 6. skupa sedimentologa Jugoslavije, Crnogorsko geološko društvo, Titograd, pp. 26–32.

CAFIERO, B. and DE CAPOA BONARDI, P. 1980: Stratigraphy of the pelagic Triassic in the Budva-Kotor area (Crna Gora, Montenegro Yugoslavia). — Boll. Soc. Paleont. Ital., vol. 19, no. 2, pp. 179–204.

CAFIERO, B. and DE CAPOA BONARDI, P. 1981: I conodonti dei calcari ad Halobia del Trias superiore del Montenegro (Crna Gora, Jugoslavia). — Riv. Ital. Paleont., vol. 86, no. 3, pp. 563–576.

CAMPBELL, A.S. 1954: Radiolaria. — In: MOORE, R.C. (Ed.): Treatise on invertebrate paleontology, Part D, Protista 3, Geological Society of America and University of Kansas Press, Lawrence, pp. D11–D195.

CAMPBELL, A.S. and CLARK, B.L. 1944: Radiolaria from Upper Cretaceous of Middle California. — Geological Society of America, Special Papers, no. 57, pp. i–viii and 1–61.

CARAYON, V., DE WEVER, P. and RAOULT, J.-F. 1984: Etude des blocs calcaires contenus dans les séries franciscaines du Sud-Ouest de l'Oregon (U.S.A.): conséquences sur l'âge des mélanges franciscains. — C. R. Acad. Sc. Paris, t. 298, sér. II, no. 16, pp. 709–714.

CARTER, E.S. 1993: Biochronology and paleontology of uppermost Triassic (Rhaetian) radiolarians, Queen Charlotte Islands, British Columbia, Canada. — Mémoires de Géologie (Lausanne), vol. 11, pp. 1–175.

CARTER, E.S. (in press): Evolutionary trends in latest Norian through Hettangian radiolarians from the Queen Charlotte Islands, British Columbia.

CARTER, E.S., CAMERON, B.E.B. and SMITH, P.L. 1988: Lower and Middle Jurassic radiolarian biostratigraphy and systematic paleontology, Queen Charlotte Islands, British Columbia. — Bulletin – Geological Survey of Canada, vol. 386, pp. 1–109.

CARTER, E.S. and JAKOBS, G.K. 1991: New Aalenian Radiolaria from the Queen Charlotte Islands, British Columbia: implications for biostratigraphic correlation. — Geological Survey of Canada, Current Research, Part A, Paper 91–1A, pp. 337–351.

CAYEUX, L. 1897: Contribution à l'étude micrographique des terrains sédimentaires. 1. Etude de quelques dépôts siliceux secondaires et tertiaires du Bassin de Paris et de la Belgique. 2. Craie du Bassin de Paris. — Mémoires Soc. Géol. Nord, Lille, vol. 4, no. 2, pp. 1–591, pl. 1–10.

CELET, P. 1977: The Dinaric and Aegean arcs: the geology of the Adriatic. — In: NAIRN, A.E.M., KANES, W. H. and STEHLI, F. G. (Eds.): The ocean basins and margins. Plenum Press, New York, London, pp. 215–261.

CELET, P. and CLÉMENT, B. 1971: Sur la présence d'une nouvelle unité paléogéographique et structurale en Grèce continentale du sud: l'unité du flysch béotien. — C. R. somm. Soc. géol. Fr. 1, 43–47.

CHANNELL, J.E.T., D'ARGENIO, B. and HORVATH, F. 1979: Adria, the African Promontory, in Mesozoic Mediterranean Palaeogeography. — Earth Science Reviews, vol. 15, pp. 213–292.

CHOROWITZ, J. 1975: Le devenir de la zone de Budva vers le Nord-Ouest de la Yougoslavie. — Bull. Soc. Géol. France, sér. 7, vol. 17, no. 5, pp. 699–707.

CITA, M.B. 1964: Ricerche micropaleontologiche e stratigrafiche sui sedimenti pelagici del Giurassico superiore e del Cretaceo inferiore nella catena del Monte Baldo. — Rivista italiana di paleontologia e stratigrafia, Memoria 10, pp. 1–182.

CLÉMENT, B. 1971: Découverte d'un flysch éocrétacé en Béotie (Grèce continentale). — C. R. Acad. Sci. Paris, t. 272, pp. 791–792.

CONTI, M.,1986: New data on the biostratigraphy of the Tuscan cherts at Monte Cetona (Southern Tuscany, Italy). — Marine Micropaleontology, vol. 11, no. 1–3, pp. 107–112.

CONTI, M. and MARCUCCI, M. 1986: The onset of radiolarian deposition in the ophiolite sequences of the Northern Apennine. — Marine Microplaleontolgy, vol. 11, no. 1–3, pp. 129–138.

CONTI, M. and MARCUCCI, M. 1991: Radiolarian assemblage in the Monte Alpe Cherts at Ponte di Lagoscuro, Val Graveglia (Eastern Liguria, Italy). — Eclogae Geologicae Helvetiae, vol. 84, no. 3, pp. 791–817.

CSONTOS, L., DOSZTÁLY, L. and PELIKÁN, P. 1991: Radiolariák a Bükk Hegységből (Radiolarians from the Bükk Mts.). — Magyar Állami Földtani Intézet, Budapest, pp. 357–381.

D'ARGENIO, B., RADOIČIĆ, R. and SGROSSO, I. 1971: A Paleogeographic Section through the Italo-dinaric External Zones during Jurassic and Cretaceous Times. — Nafta, Zagreb, vol. 22, no. 4–5, pp. 195–207.

D'ARGENIO, B. and MINDSZENTY, A. 1991: Karst bauxites at regional unconformities and geotectonic correlation in the Cretaceous of the Mediterranean. — Boll. Soc. Geol. It., vol. 110, pp. 85–92.

D'ARGENIO, B. and MINDSZENTY, A. 1992: Tectonic and climatic control on paleokarst and bauxites. — Giornale de Geologia, ser. 3, vol. 54, no. 1, pp. 207–218.

DANELIAN, T. 1989: Radiolaires jurassiques de la Zone Ionienne (Epire, Grèce). Paléontologie–stratigraphie, implications paléogéographiques. — Mém. Sc. Terre Univ. Curie, Paris, no. 89–25, pp. 1–269.

DE BOER, P. L. 1991: Pelagic Black Shale-Carbonate Rhythms: Orbital Forcing and Oceanographic Response. — In: EINSELE, G., RICKEN, W and SEILACHER, A. (Eds.): Cycles and Events in Stratigraphy. Springer-Verlag, Berlin, Heidelberg, New York, pp. 63–78.

DERCOURT, J. 1968: Sur l'accident de Scutari-Peć, la signification paléogéographique de quelqes séries condensées en Albanie septentrionale. — Ann. Soc. Géol. Nord, vol. 88, no. 3, pp. 109–117.

DERCOURT, J., FLAMENT, J. M., FLEURY, J.-J. and MEILLIEZ, F. 1973: Stratigraphie des couches situées sous les radiolarites de la zone du Pinde-Olonos (Grèce): le Trias supérieur et le Jurassique inférieur. — Ann. géol. Pays hellén., vol. 25, pp. 397–406.

DE WEVER, P. 1981: Hagiastridae, Patulibracchiidae et Spongodiscidae (Radiolaires polycystines) du Lias de Turquie. — Revue de Micropaléontologie, vol. 24, no. 1, pp. 27–50.

DE WEVER, P. 1982a: Nassellaria (Radiolaires Polycystines) du Lias de Turquie. — Revue de Micropaléontologie, vol. 24, no. 4, pp. 189–232.

DE WEVER, P. 1982b: Radiolaires du Trias et du Lias de la Tethys (Systématique, Stratigraphie). — Société Géologique du Nord, Publication no. 7, pp. 1–599.

DE WEVER, P. 1989: Radiolarians, Radiolarites, and Mesozoic Paleogeography of the Circum-Mediterranean Alpine Belts. — In: HEIN, J.R. and OBRADOVIĆ, J. (Eds.): Siliceous Deposits of the Tethys and Pacific regions. Springer-Verlag, New York, Berlin, Heidelberg, pp. 31–49.

DE WEVER, P. and CABY, R. 1981: Datation de la base des schistes lustrés postophiolitiques par des radiolaires (Oxfordien supérieur-Kimmeridgien moyen) dans les Alpes Cottiennes (Saint-Veran, France). — C. R. Acad. Sc. Paris, vol. 292, pp. 467–472.

DE WEVER, P. and THIÉBAULT, F. 1981: Les Radiolaires d'âge Jurassique supérieur à Crétacé supérieur dans les radiolarites du Pinde-Olonos (Presqu'île de Koroni; Péloponnèse Méridional, Grèce). — Geobios, vol. 14, no. 5, pp. 577–609.

DE WEVER, P. and ORIGLIA-DEVOS, I. 1982a: Datations nouvelles par les Radiolaires de la série des Radiolarites s.l. du Pinde-Olonos (Grèce). — C. R. Acad. Sc. Paris, Ser. 2, vol. 294, no. 6, pp. 399–404.

DE WEVER, P. and ORIGLIA-DEVOS, I. 1982b: Datation par les Radiolaires des niveaux siliceux du Lias de la série du Pinde-Olonos (formation de Drimos, Péloponnèse et Grèce continentale). — C. R. Acad. Sc. Paris, Sér 2, vol. 294, no. 19, pp. 1191–1198.

DE WEVER, P. and DERCOURT, J. 1985: Les radiolaires triasico-jurassiques marqueurs stratigraphiques et paléogéographiques dans les chaînes alpines périméditerranéen-

nes; une revue. — Bull. Soc. géol. France, Sér. 8, vol. 1, no. 5, pp. 653–662.

DE WEVER, P., DUEE, G. and EL KADIRI, K. 1985: Les séries stratigraphiques des klippes de Chrafate (Rif septentrional, Maroc). Temoins d'une marge continentale subsidente au cours du Jurassique-Crétacé. — Bull. Soc. géol. France, Sér. 8, vol. 1, no. 3, pp. 363–379.

DE WEVER, P. and MICONNET, P. 1985: Datations directes des radiolarites du bassin du Lagonegro (Lucanie, Italie méridionale) Implications et conséquences. — Revist. Española Micropaleont., vol. 17, no. 3, pp. 373–402.

DE WEVER, P. and CORDEY, F. 1986: Datation par les Radiolaires de la Formation des Radiolarites s.s. de la Série du Pinde-Olonos (Grèce): Bajocien (?)-Tithonique. — Marine Micropaleontology, vol. 11, no. 1–3, pp. 113–127.

DE WEVER, P., RICOU, L.-E. and FOURCADE, E. 1986a: La fin brutale de l'optimum radiolaritique au Jurassique terminal: l'effet de la circulation océanique. — C. R. Acad. Sc. Paris, t. 302, sér. II, no. 9, pp. 665–670.

DE WEVER, P., GEYSSANT, J.R., AZÉMA, J., DEVOS, I., DUÉE, G., MANIVIT, H. and VRIELYNCK, B. 1986b: La coupe de Santa Anna (zone de Sciacca, Sicile): Une synthèse biostratigraphique des apports des macro-, micro- et nannofossiles du Jurassique supérieur et Crétacé inférieur. — Revue de Micropaléontologie, vol. 29, no. 5, pp. 141–186.

DE WEVER, P., BAUMGARTNER, P.O. and POLINO, R. 1987: Précision sur les datations de la base des Schistes Lustrés postophiolitiques dans les Alpes Cottiennes. — C. R. Acad. Sc. Paris, Sér. 2, vol. 305, pp. 487–491.

DIMITRIJEVIĆ, M.D. 1982: Dinarides: An Outline of the Tectonics. — Earth Evolution Sciences, vol. 2, no 1, pp. 4–23.

DIMITRIJEVIĆ, M.N. 1967: Sedimentološko-stratigrafski problemi srednjotriaskog fliša u terenima između Skadarskog jezera i Jadranskog mora (Sedimentologic problems of Middle Triassic flysch in the terrains between Scutari Lake and the Adriatic Sea). — Geološki glasnik, Titograd, vol. 5, pp. 224–311.

DJORDJEVIĆ, P. and KNEŽEVIĆ, V. 1969: Trijaski vulkaniti na području Budva–Sutomore (Crnogorsko Primorje) (The Triassic rocks of the Montenegrin littoral between Sutomore and Budva were formed in two phases). — Geološki anali Balkanskog poluostrva, Beograd, vol. 34, pp.489–507.

DODONA, E. and FARINACCI, A. 1987: Le radiolariti nella serie lacunosa di Spiten, un altofondo non subsidente del Mesozoico d'Albania. — Bolletino della Societa Paleontologica Italiana, vol. 26, no. 1–2, pp. 39–46.

DONOFRIO, D. and MOSTLER, H. 1978: Zur Verbreitung der Saturnalidae (Radiolaria) im Mesozoikum der Nördlichen Kalkalpen und Südalpen. — Geologisch-Paläontologische Mitteilungen Innsbruck, vol. 7, no. 5, pp. 1–55.

DOSZTALY, L. 1988: A paleontological study of the "Öregszirt" radiolarites in the Pilis Mountains. — M. Áll. Földtani Intézet Evi Jelentese az 1986, Budapest, pp. 229–239.

DUMITRICA, P. 1970: Cryptocephalic and cryptothoracic Nassellaria in some Mesozoic deposits of Romania. — Revue roumaine de géologie, géophysique et géographie, Série de géologie, vol. 14, no. 1, pp. 45–124.

DUMITRICA, P. 1972: Cretaceous and Quaternary Radiolaria in deep sea sediments from the northeast Atlantic Ocean and Mediterranean Sea. — In: RYAN, W.B.F., HSÜ, K.J., et al. (Eds.): Initial Rep. Deep Sea Drill. Proj., vol. 13, pp. 829–901.

DUMITRICA, P. 1975: Cenomanian Radiolaria at Podul Dimbovitei. — Micropaleontological guide to the Mesozoic and Tertiary of the Romanian Carpathians. Institute of Geology and Geophysics, Bucharest, pp. 87–89.

DUMITRICA, P. 1978: Family Eptingiidae n. fam., extinct Nassellaria (Radiolaria) with sagittal ring. — Dari de seama, Inst. Geol. Geofiz., Bucuresti, vol. 64 (1976–1977), pp. 27–38.

DUMITRICA, P. and MELLO, J. 1982: On the age of the Meliata Group and the Silica Nappe radiolarites (localities Držkovce and Bohunovo, Slovak Karst, ČSSR). — Geologicke prace, vol. 77, pp. 17–28, pl. 1–4.

DUMITRICA, P. and DE WEVER, P. 1991: Assignation to radiolaria of two Upper Jurassic species previously described as Foraminifera: systematic consequences. — C. R. Acad. Sci. Paris, t. 312, Ser. II, pp. 553–558.

DUMITRICA, P. and JUD, R. (in prep.): Aurisaturnalis carinatus (Foreman), an example of phyletic gradualism among saturnalid-type radiolarians.

DUNIKOWSKI, E. v. 1882: Die Spongien, Radiolarien und Foraminiferen der unterliassichen Schichten vom Schafberg bei Salzburg. — Denkschr. (kais.) Akad. Wiss. Wien, math.-natw. Kl. 45, pp. 163–194.

EBERLI, G.P. 1991a: Growth and Demise of Isolated Carbonate Platforms: Bahamian Conroversies. — In: MÜLLER, D.W. MCKENZIE, J.A. and WEISSERT, H. (Eds.): Controversies in Modern Geology: Evolution of Geological Theories in Sedimentology, Earth History and Tectonics. Academic Press, London, San Diego, New York, pp. 231–248.

EBERLI, G.P. 1991b: Calcareous Turbidites and Their Relationship to Sea-Level Fluctuations and Tectonism. — In: EINSELE, G., RICKEN, W and SEILACHER, A. (Eds.): Cycles and Events in Stratigraphy. Springer-Verlag, Berlin, Heidelberg, New York, pp. 340–359.

EL KADIRI, K. 1992: Description de nouvelles espèces de radiolaires jurassiques de la Dorsale calcaire externe (Rif, Maroc). — Revista Española de Paleontologia, Extra, pp. 37–48.

EMPSON-MORIN, K. 1984: Depth and latitude distribution of Radiolaria in Campanian (Late Cretaceous) tropical and subtropical oceans. — Micropaleontology, vol. 30, no. 1, pp. 87–115.

FISCHLI, H. 1916: Beitrag zur Kenntnis der fossilen Radiolarien in der Riginagelfluh. — Mitteilungen der Naturwissenschaftlichen Gesellschaft in Winterthur, Jahrgang 1915–1916, no. 11, pp. 44–47.

FLEURY, J.J. 1980: Les zones de Gavrovo-Tripolitza et du Pinde-Olonos (Grèce continentale et Péloponnèse du Nord). Evolution d'une plate-forme et d'un bassin dans leur cadre alpin. — Soc. Géol. Nord, Lille, vol. 4, pp.1–651, pl. 1–10.

FOREMAN, H.P. 1968: Upper Maestrichtian Radiolaria of California. — The Palaeontological Association, Special Papers in Palaeontology, London, no. 3, pp. iv + 1–82.

FOREMAN, H.P. 1973: Radiolaria from DSDP Leg 20. — In: HEEZEN, B.C., MACGREGOR, J.D., et al. (Eds.): Initial Rep. Deep Sea Drill. Proj., vol. 20, pp. 249–305.

FOREMAN, H.P. 1975: Radiolaria from the North Pacific, Deep Sea Drilling Project, Leg 32. — In: LARSON, R.L., MOBERLY, R., et al. (Eds.): Initial Rep. Deep Sea Drill. Proj., vol. 32, pp. 579–676.

GARRELS, R.M. and CHRIST, C.L. 1965: Solutions, minerals and equilibrium. — Harper & Row, New York, pp. 1–450.

GORIČAN, Š. 1987: Jurassic and Cretaceous radiolarians from the Budva zone (Montenegro, Yugoslavia). — Revue de Micropaléontologie, vol. 30, no. 3, pp. 177–196.

GRILL, J. and KOZUR, H. 1986: The first evidence of the Unuma echinatus radiolarian zone in the Rudabanya Mts. (northern Hungary). — Geologisch-Paläontologische Mitteilungen Innsbruck, vol. 13, no. 11, pp. 239–275.

GRUBIĆ, A. 1964: Les bauxites de la province dinarique (Yougoslavie). — Bull. Soc. Géol. France, sér. 7, vol. 6, pp. 382–388.

GRUBIĆ, A. 1980: Yougoslavie. — In: Géologie des pays européens; Espagne, Grèce, Italie, Portugal, Yougoslavie. 26e Congrès Géologique International, Comité National Francais de Géologie ,Paris, pp. 288–342.

GRUBIĆ, A. 1983: Rezultati paleontoloških i biostratigrafskih ispitivanja sferaktinida iz Srbije i Crne Gore (Results of paleontological and biostratigraphic study of sphaeractiniids from Serbia and Montenegro). — Razprave zavoda za geološka i geofizička istraživanja, Beograd, vol. 21, pp. 1–51.

GUEX, J. 1977: Une nouvelle méthode d'analyse biochronologique. — Bull. Géol. Lausanne, no. 224, pp. 309–322.

GUEX, J. 1991: Biochronological Correlations. — Springer-Verlag, Berlin, Heidelberg, New York, pp. 1–250.

HAECKEL, E. 1881: Entwurf eines Radiolarien-Systems auf Grund von Studien der Challenger – Radiolarien. — Jenaische Zeitschrift für Naturwissenschaft, vol. 15 (new series, vol. 8, pt. 3), pp. 418–472.

HAECKEL, E. 1887: Report on the Radiolaria collected by H.M.S. Challenger during the years 1873–1876. — Report on the Scientific Results of the Voyage of the H.M.S. Challenger, Zoology, vol. 18, 2 parts, Atlas, clxxxviii + 1803 pp.

HALLAM, A. 1978: Eustatic cycles in the Jurassic. — Palaeogeography, Palaeoclimatology, Palaeoecology, vol. 23, pp. 1–32.

HALLAM, A. 1984: Continental humid and arid zones during the Jurassic and Cretaceous. — Palaeogeography, Palaeoclimatology, Palaeoecology, vol. 47, pp. 195–223.

HALLAM, A. 1986: Role of climate in affecting late Jurassic and early Cretaceous sedimentation in the North Atlantic. — In: SUMMERHAYES, C.P. and SHACKLETON, N.J. (Eds.): North Atlantic Palaeoceanography. Geological Society, Special Publication, vol. 21, pp. 277–281.

HALLAM, A. 1988: A reevaluation of Jurassic eustasy in the light of new data and the revised Exxon curve. — In: WILGUS, C.K. et al. (Eds.): Sea level changes – an integrated approach. Spec. Publs. Soc. econ. Paleont. Miner., Tulsa, vol. 42, pp. 261–273.

HALLAM, A. 1989: The case for sea-level change as a dominant causal factor in mass extinction of marine invertebrates. — Phil. Trans. R. Soc. Lond. B 325, pp. 437–455.

HAQ, B.U., HARDENBOL, J. and VAIL, P.R. 1988: Mesozoic and Cenozoic chronostratigraphy and cycles of sea-level change. — In: WILGUS, C.K. et al. (Eds.): Sea level changes – an integrated approach. Spec. Publs. Soc. econ. Paleont. Miner., Tulsa, vol. 42, pp. 71–108.

HARLAND, W.B., ARMSTRONG, R.L., COX, A.V., CRAIG, L.E., SMITH, A.G. and SMITH, D.G. 1990: A geologic time scale 1989. — Cambridge University Press, Cambridge, pp. 1–263.

HATTORI, I. 1987: Jurassic radiolarian fossils from the Nanjo Massif, Fukui Prefecture, Central Japan. — Bulletin of the Fukui Museum of Natural History, Fukui, vol. 34, pp. 29–101.

HATTORI, I. 1988a: Radiolarian fossils from manganese nodules at the upper reach of the Turamigawa in the Nanjo Massif, Fukui Prefecture, central Japan, and the tectonic significance of the northwestern Mino Terrane. — Bull. Fukui municip. Mus. nat. Hist., vol. 55, pp. 55–101.

HATTORI, I. 1988b: Surface texture of radiolarians and extraction method of radiolarians. — Jour. Faculty Education Fukui Univ., Part II (Natural Sci.), vol. 38, pp. 71–85.

HATTORI, I. 1989: Jurassic radiolarians from manganese nodules at three sites in the western Nanjo Massif, Fukui Prefecture, Central Japan. — Jour. Faculty Education Fukui Univ., Part II (Natural Sci.), vol. 39, pp. 47–134.

HATTORI, I. and YOSHIMURA, M. 1982: Lithofacies distribution and radiolarian fossils in the Nanjo area in Fukui Prefecture, central Japan. — News of Osaka Micropaleontologists, Spec. vol. 5, pp. 103–116.

HATTORI, I. and SAKAMOTO, N. 1989: Geology and Jurassic Radiolarians from manganese nodules of the Kanmuriyama – Kanakusadake Area in the Nanjo Massif, Fukui Prefecture, Central Japan. — Bulletin of the Municipal Museum of Natural History, vol. 36, pp. 25–79.

HEITZER, I. 1930: Die Radiolarienfauna der mitteljurassischen Kieselmergel im Sonnwendgebirge. — Jb. geol. Bundesanst. Wien, vol. 80, no. 3–4, pp. 381–406, pl. 27–29.

HERAK, M. 1986: A new concept of geotectonics of the Dinarides. — Acta geologica, Zagreb, vol. 16, no. 1, pp. 1–42.

HERAK, M. 1991: Dinaridi. Mobilistički osvrt na genezu i strukturu (Dinarides. Mobilistic view of the genesis and structure). — Acta geologica, Zagreb, vol. 21, no. 2, pp. 35–117.

HERNÁNDEZ-MOLINA, F.J., SANDOVAL, J., AGUADO, R., O'DOGHERTY, L., COMAS, M.C. and LINARES, A. 1991: Olistoliths from the Middle Jurassic in Cretaceous materials of the Fardes formation. Biostratigraphy (Subbetic Zone, Betic Cordillera). — Rev. Soc. Geol. España, vol. 4, no. 1–2, pp. 79–104.

HOLZER, H.L. 1980: Radiolaria aus Ätzrückständen des Malm und der Unterkreide der Nördlichen Kalkalpen (Österreich). — Annalen des Naturhistorischen Museums in Wien, vol. 83, pp. 153–167.

HORI, R. 1986: Parashuum simplum assemblage (Early Jurassic radiolarian assemblage) in the Inuyama area, central Japan. — News of Osaka Micropaleontologists, Spec. vol. 7, pp. 45–52.

HORI, R. 1990: Lower Jurassic Radiolarian Zones of SW Japan. — Trans. Proc. Palaeont. Soc. Japan., vol. 159, pp. 562–586.

HORI, R. and YAO, A. 1988: Parahsuum (Radiolaria) from the Lower Jurassic of the Inuyama area, central Japan. — Journal of Geosciences, Osaka City University, vol. 31, pp. 47–61.

HORI, R. and OTSUKA, T. 1989: Early Jurassic radiolarians from the Mt. Norikuradake area, Mino Terrane, central Japan. — Journal of Geosciences, Osaka City University, vol. 32, pp. 175–198.

ICHIKAWA, K. and YAO, A. 1976: Two new genera of Mesozoic cyrtoid radiolarians from Japan. — In: TAKAYANAGI, Y. and SAITO, T.: Progress in Micropaleontology. Micropaleontology Press, The American Museum of Natural History, New York, pp. 110–117.

IGO, H., SASHIDA, K. and UENO, H. 1987: Early Cretaceous radiolarians from the Esashi Mountains, northern Hokkaido. — Annual Report of the Institute of Geoscience, University of Tsukuba, no. 13, pp. 105–109.

IMOTO, N., TAMAKI, A., TANABE, T. and ISHIGA, H. 1982: An age determination on the basis of radiolarian biostratigraphy of a bedded manganese deposit at the Yumiyama Mine in the Tamba district, Southwest Japan. — News of Osaka Micropaleontologists, Spec. vol. 5, pp. 227–253.

INGLE, J.C. Jr. 1981: Origin of Neogene diatomites around the North Pacific Rim. — In: GARRISON, R.E. and DOUGLAS, R.G. et al. (Eds.): The Monterey Formation and Related Siliceous Rocks of California. Spec. Publ. Pac. Sect. Soc. econ. Paleont. Miner., Los Angeles, pp. 159–179.

ISHIDA, K. 1983: Stratigraphy and radiolarian assemblages of the Triassic and Jurassic siliceous sedimentary rocks in Konose Valley, Tokushima Prefecture, Southwest Japan. — Journal of Science, University of Tokushima, vol. 16, pp. 111–141.

ISOZAKI, Y. and MATSUDA, T. 1985: Early Jurassic radiolarians from bedded chert in Kamiaso, Mino Belt, central Japan. — Earth Science; Journal of the Association for the Geological Collaboration in Japan, vol. 39, no. 6, pp. 429–442.

IWATA, K. and TAJIKA, J. 1989: Jurassic and Cretaceous radiolarians from the pre-Tertiary system in the Hidaka Belt, Maruseppu region, Northeast Hokkaido. — Jour. Faculty Sci., Hokkaido Univ., Ser. IV, vol. 22, no. 3, pp. 453–466.

IWATA, K., HARIYA, Y., HO-CHOI, J., YAGI, E. and MIURA, T. 1990: Radiolarian age of the manganese deposits of the Tokoro belt, Northeast Hokkaido. — Jour. Faculty Sci., Hokkaido Univ., Ser. IV., vol. 22, no. 4, pp. 565–576.

JENKYNS, H.C. 1988: The Early Toarcian (Jurassic) anoxic event: stratigraphic, sedimentary, and geochemical evidence. — American Journal of Science, vol. 288, pp. 101–151.

JENKYNS, H. and WINTERER, E. 1982: Palaeoceanography of Mesozoic ribbon radiolarites. — Earth and Planetary Science Letters, vol. 60, pp. 351–375.

JENKYNS, H.C. and CLAYTON, C.J. 1986: Black shales and carbon isotopes in pelagic sediments from the Tethyan Lower Jurassic. — Sedimentology, vol. 33, pp. 87–106.

JUD, R. 1991: Biochronology and systematics od Early Cretaceous Radiolaria of the Western Tethys. — Doct. Thesis, Faculty Sci., Univ. Lausanne (unpubl.).

KALEZIĆ, M., ŠKULETIĆ, D. and PEROVIĆ, Z. 1976: Geološki sastav i tektonika priobalnog dijela Jadrana na teritoriji SR Crne Gore (Geological composition and tectonic of the coastal area of the Adriatic on the territory of S. R. Montenegro). — Geološki glasnik, Titograd, vol. 8, pp. 7–42.

KANIE, Y., TAKETANI, Y., SAKAI, A. and MIYATA, Y. 1981: Lower Cretaceous deposits beneath the Yezo group in the Urakawa area, Hokkaido. — Journal of the Geological Society of Japan, vol. 87, pp. 527–533.

KARAMATA, S. 1988: "The Diabase-Chert Formation", some genetic aspects. — Bulletin de l'Academie Serbe des Sci-

ences et des Arts, Classe des Sciences naturelles et mathématiques, Beograd, vol. 95, no. 28, pp. 1–11.

KATO, Y. and IWATA, K. 1989: Radiolarian biostratigraphic study of the pre-Tertiary system around the Kamikawa Basin, central Hokkaido, Japan. — Journal of the Faculty of Science, Hokkaido University, Series IV, vol. 22, no. 3, pp. 425–452.

KAWABATA, K. 1988: New species of Latest Jurassic and Earliest Cretaceous radiolarians from the Sorachi Group in Hokkaido, Japan. — Bulletin of the Osaka Museum of Natural History, vol. 43, pp. 1–13.

KENTER, J.A.M. 1990: Carbonate platform flanks: slope angle and sediment fabric. — Sedimentology, vol. 37, pp. 777–794.

KIDO, S. 1982: Occurrence of Triassic chert and Jurassic siliceous shale at Kamiaso, Gifu Prefecture, central Japan. — News of Osaka Micropaleontologists, Spec. vol. 5, pp. 135–151.

KIDO, S., KAWAGUCHI, I., ADACHI, M. and MIZUTANI, S. 1982: On the Dictyomitrella(?) kamoensis-Pantanellium foveatum assemblage in the Mino area, central Japan. — News of Osaka Micropaleontologists, Spec. vol. 5, pp. 195–210.

KIESSLING, W. 1992: Paleontological and facial features of the Upper Jurassic Hochstegen Marble (Tauern Window, Eastern Alps). — Terra Nova, vol. 4, pp. 184–197.

KIESSLING, W. and ZEISS, A. 1992: New paleontological data from the Hochstegen Marble (Tauern Window, Eastern Alps). — Geol. Paläont. Mitt. Innsbruck, vol. 18, pp. 187–202.

KISHIDA, Y. and SUGANO, K. 1982: Radiolarian zonation of Triassic and Jurassic in outer side of southwest Japan. — News of Osaka Micropaleontologists, Spec. vol. 5, pp. 271–300.

KISHIDA, Y. and HISADA, K. 1985: Late Triassic to Early Jurassic radiolarian assemblages from the Ueno-mura area, Kanto Mountains, central Japan. — Memoirs of Osaka Kyoiku University, ser. III, vol. 34, no. 2, pp. 103–129.

KISHIDA, Y. and HISADA, K. 1986: Radiolarian assemblages of the Sambosan Belt in the western part of the Kanto Mountains, central Japan. — News of Osaka Micropaleontologists, Spec. vol. 7, pp. 25–34.

KITO, N. 1987: Stratigraphic relation between greenstones and clastic sedimentary rocks in the Kamuikotan Belt, Hokkaido, Japan. — Journal of the Geological Society of Japan, vol. 93, no. 1, pp. 21–35.

KITO, N. 1989: Radiolaires du Jurassiques Moyen et Supérieur de Sicile (Italie): Biostratigraphie et Taxonomie. — Mém. Sc. Terre Univ. Curie, Paris, n. 89–7, pp. 1–239.

KITO, N., DE WEVER, P., DANELIAN, T. and CORDEY, F. 1990: Middle to Late Jurassic radiolarians from Sicily (Italy). — Marine Micropaleontology, vol. 15, no. 3–4, pp. 329–349.

KNEŽEVIĆ, V. 1975: Trijaske magmatske stene Crne Gore (Triassic igneous rocks of Montenegro). — Acta geologica, Zagreb, vol. 41, pp. 107–147.

KNEŽEVIĆ, V. 1976: Karakter magmatizma i variacije u njegovom hemizmu u toku trijaske faze ekstenzije dinarske kontinentalne ploče (The character of magmatism and variations in its chemistry during the Triassic phase of the extension of the Dinaric continental plate). — Geološki anali Balkanskog poluostrva, Beograd, vol. 40, pp. 213–218.

KOCHER, R.N. 1981: Biochronostratigraphische Untersuchungen oberjurassischer radiolarienführender Gesteine, insbesondere der Südalpen. — Mitteilungen aus dem Geologischen Institut der Eidgenossischen Technischen Hochschule und der Universität Zürich, Neue Folge, no. 234, pp. 1–184.

KODRA, A., GJATA, K. and BAKALLI, F. 1993: Les principales étapes de l'évolution paléogéographique et géodynamique des Albanides internes au cours du Mésozoïque. — Bull. Soc. géol. France, vol. 164, no. 1, pp. 69–77.

KOJIMA, S. 1982: Some Jurassic, Triassic and Permian radiolarians from the eastern part of Takayama City, central Japan. — News of Osaka Micropaleontologists, Spec. vol. 5, pp. 81–91.

KOJIMA, S. 1989: Mesozoic terrane accretion in Northeast China, Sikhote-Alin and Japan regions. — Palaeogeography, Palaeoclimatology, Palaeoecology, vol. 69, pp. 213–232.

KOJIMA, S. and MIZUTANI, S. 1987: Triassic and Jurassic Radiolaria from the Nadanhada Range, Northeast China. — Transactions and Proceedings of the Palaeontological Society of Japan, New Series, no. 148, pp. 256–275.

KOSSMAT, F. 1924: Geologie des zentralen Balkan Halbinsel. (Mit einer Übersicht des dinarischen Gebirgsbaues). — In: Die Kriegschauplätze 1914–1918. geologisch dargestellt, H. 12, Berlin, pp. 1–198.

KOZUR, H. 1984: New radiolarian taxa from the Triassic and Jurassic. — Geologisch-Paläontologische Mitteilungen Innsbruck, vol. 13, no. 2, pp. 49–88.

KOZUR, H. 1985: The radiolarian genus Eoxitus n. gen. from the Unuma echinatus Zone (Bajocian) of northern Hungary. — Proceedings of the Koninklijke Nederlandse Akademie van Wetenschappen. Series B, vol. 88, no. 2, pp. 211–220.

KOZUR, H. 1991: The evolution of the Meliata-Hallstatt ocean and its significance for the early evolution of the Eastern Alps and Western Carpathians. — Palaeogeography, Palaeoclimatology, Palaeoecology, vol. 87, pp. 109–135.

KOZUR, H. and MOSTLER, H. 1983: The polyphyletic origin and classification of the Mesozoic saturnalids (Radiolaria). — Geol. Paläont. Mitt. Innsbruck, vol. 13, no. 1, pp. 1–47.

KOZUR, H. and MOSTLER, H. 1990: Saturnaliacea Deflandre and some other stratigraphically important radiolaria from

the Hettangian of Lenggries/Isar (Bavaria, Northern Calcareous Alps). — Geol. Paläont. Mitt. Innsbruck, vol. 17, pp. 179–248.

KRAUSE, F.F. and OLDERSHAW, A.E. 1979: Submarine carbonate breccia beds – A depositional model for two-layer, sediment gravity flows from the Sekwi Formation (Lower Cambrian), Mackenzie Mountains, Northwest Territories, Canada. — Can. J. Earth Sci., vol. 16, pp. 189–199.

LOZYNYAK, P. YU. 1969: Radiolyarii nizhnemelovykh otlozhenii Ukrainskikh Karpat (The radiolarians of the Lower Cretaceous deposits of the Ukranian Carpathians). — Vyalov, O. S., Izdatelstvo Lvovskogo Universiteta (Lvov University), pp. 29–41.

LYBERIS, N., CHOTIN, P. and DOUBINGER, J. 1980: Précisions stratigraphiques sur la série du Pinde (Grèce): la durée de sédimentation des "radiolarites". — C. R. Acad. Sc. Paris, vol. 290, no. 24, Ser. D, pp. 1513–1516.

MARCHANT, R. and STAMPFLI, G.M. (in press): Crustal and lithospharic structures and geodynamic evolution of the Tethyan margins of the Western Alps. — PNR/NFP–20 Final report: Deep Structures of Switzerland, Interpretation and synthesis.

MARCUCCI PASSERINI, M., BETTINI, P., DAINELLI, J. and SIRUGO, A. 1991: The "Bonarelli Horizon" in the central Apennines (Italy): radiolarian biostratigraphy. — Cretaceous Research, vol. 12, pp. 321–331.

MARCUCCI PASSERINI, M. and GARDIN, S. 1992: The Fosso Cupo Formation (northern Latium, Italy): redefinition and new age data from radiolarian and calcareous nannofossil biostratigraphy. — Cretaceous research, vol. 13, pp. 549–563.

MARKOVIĆ, B. 1966a: Osnovna geološka karta 1:100 000, list Dubrovnik. — Savezni geološki zavod, Beograd.

MARKOVIĆ, B. 1966b: Osnovna geološka karta 1:100 000, Tumač za list Dubrovnik (Explanatory text for Dubrovnik sheet). — Savezni geološki zavod, Beograd, pp. 1–39.

MAATÉ, A., MARTIN-ALGARRA, A., O'DOGHERTY, L., SANDOVAL, J. and BAUMGARTNER, P. 1993: Découverte du Dogger dans la Dorsale calcaire interne au Sud de Tétouan (Rif septentrional, Maroc). Conséquences paléogéographiques. — C. R. Acad. Sci. Paris, t. 317, sér. II, pp. 227–233.

MATSUOKA, A. 1982a: Jurassic two-segmented Nassellarians (Radiolaria) from Shikoku, Japan. — Journal of Geosciences, Osaka City University, vol. 25, pp. 71–86.

MATSUOKA, A. 1982b: Middle and Late Jurassic radiolarian biostratigraphy in the Sakawa and the Niyodo areas, Kochi Prefecture, southwest Japan. — News of Osaka Micropaleontologists, Spec. vol. 5, pp. 237–253.

MATSUOKA, A. 1983: Middle and Late Jurassic radiolarian biostratigraphy in the Sakawa and adjacent areas Shikoku, Southwest Japan. — Journal of Geosciences, Osaka City University, vol. 26, no. 1, pp. 1–48.

MATSUOKA, A. 1984: Late Jurassic four-segmented nassellarians (Radiolaria) from Shikoku, Japan. — Journal of Geosciences, Osaka City University, vol. 27, pp. 143–153.

MATSUOKA, A. 1985: Middle Jurassic Keta Formation of the southern part of the Middle Chichibu Terrane in the Sakawa area, Kochi Prefecture, Southwest Japan. — Jour. Geol. Soc. Japan, vol. 91, no. 6, pp. 411–420.

MATSUOKA, A. 1986a: Faunal change of radiolarians around the Jurassic-Cretaceous boundary – with special reference to some multi-segmented nassellarians. — Fossils, vol. 40, no. 6, pp. 1–15.

MATSUOKA, A. 1986b: Stratigraphic distribution of two species of Tricolocapsa in the Hisuikyo Section of the Kamiaso area, Mino Terrane. — News of Osaka Micropaleontologists, Spec. vol. 7, pp. 59–62.

MATSUOKA, A. 1986c: Tricolocapsa yaoi Assemblage (Late Jurassic radiolarians) from the Togano Group in Shikoku, Southwest Japan. — Journal of Geosciences, Osaka City University, vol. 29, pp. 101–115.

MATSUOKA, A. 1988: First appearance biohorizon of Tricolocapsa conexa within Jurassic siliceous mudstone sequences of the Kamiaso area in the Mino Terrane, central Japan; a correlation of radiolarian zones of the Middle Jurassic. — Journal of the Geological Society of Japan, vol. 94, no. 8, pp. 583–590.

MATSUOKA, A. 1990: Middle Jurassic Radiolarians from the Western Pacific. — Saito Ho-on Kai, Spec. Pub. No. 3 (Proceedings of Shallow Tethys 3), Sendai, pp. 163–173.

MATSUOKA, A. 1992: Jurassic and Early Cretaceous radiolarians from Leg. 129, Sites 800 and 801, Western Pacific Ocean. — In: LARSON, R.L., LANCELOT, Y. et al. (Eds.): Proceeding of the Ocean Drilling Program, Scientific Results, vol. 129, pp. 203–220.

MATSUOKA, A. and YAO, A. 1985: Latest Jurassic radiolarians from the Torinosu Group in Southeast Japan. — Journal of Geoscience, Osaka City University, vol. 28, pp. 125–145.

MATSUOKA, A. and YAO, A. 1986: A newly proposed radiolarian zonation for the Jurassic of Japan. — Marine Micropaleontology, vol. 11, no. 1–3, pp. 91–106.

MATSUYAMA, H., KUMON, F. and NAKAJO, K. 1982: Cretaceous radiolarian fossils from the Hidakagawa Group in the Shimanto Belt, Kii Peninsula, Southwest Japan. — News of Osaka Micropaleontologists, Spec. vol. 5, pp. 371–382.

MIRKOVIC, M. (in press): Litofacijalne i tektonske karakteristike terena Crne Gore (Lithofacies and tectonic characteristics of Montenegro). — Geološki glasnik, Titograd.

MIRKOVIĆ, M., KALEZIĆ, M. and PAJOVIĆ, M. 1968a: Osnovna geološka karta 1:100 000, list Bar. — Savezni geološki zavod, Beograd.

MIRKOVIČ, M., KALEZIĆ, M., PAJOVIĆ, M., ŽIVALJEVIĆ, M. and ŠKULETIĆ, D. 1968b: Tumač za listove Bar i Ulcinj

(Explanatory text for Bar and Ulcinj sheets). — Savezni geološki zavod, Beograd, pp. 1–61.

MIZUTANI, S. 1981: A Jurassic formation in the Hida-Kanayama Area, Central Japan. — Bulletin of the Mizunami Fossil Museum, vol. 8, pp. 147–190.

MIZUTANI, S. and KOIKE, T. 1982: Radiolarians in the Jurassic siliceous shale and the Triassic bedded chert of Unuma, Kagamigahara City, Gifu Prefecture, central Japan. — News of Osaka Micropaleontologists, Spec. vol. 5, pp. 117–134.

MIZUTANI, S., NISHIYAMA, H. and ITO, T. 1982: Radiolarian biostratigraphic study of the Shimanto Group in the Nanto-Nansei area, Mie Prefecture, Kii Peninsula, central Japan. — Journal of Earth Science, Nagoya University, vol. 30, pp. 31–107.

MIZUTANI, S. and KIDO, S. 1983: Radiolarians in Middle Jurassic siliceous shale from Kamiaso, Gifu Prefecture, Central Japan. — Transactions and Proceedings of the Palaeontological Society of Japan, New Series, vol. 132, pp. 253–262.

MIZUTANI, S., UEMURA, T. and YAMAMOTO, H. 1984: Jurassic radiolarians from the Tsugawa area, Niigata Prefecture, Japan. — Earth Sci., vol. 38, no. 5, pp. 352–358.

MIZUTANI, S. and KOJIMA, S. 1992: Mesozoic radiolarian biostratigraphy of Japan and collage tectonics along the eastern continental margin of Asia. — Palaeogeography, Palaeoclimatology, Palaeoecology, vol. 96, pp. 3–22.

MULLINS, H.T. and COOK, H.E. 1986: Carbonate apron models: alternatives to the submarine fan model for paleoenvironmental analysis and hydrocarbon exploration. — Sedimentary Geology, vol. 48, pp. 37–79.

MURATA, M., OHISHI, A., NISHIZONO, Y., SATO, T. and TAKEHARA, T. 1982: Late Mesozoic radiolarian fauna from the Sakaguchi Formation. — News of Osaka Micropaleontologists, Spec. vol. 5, pp. 327–337.

MUZAVOR, S.N. X. 1977: Die oberjurassische Radiolarienfauna von Oberaudorf am Inn. — Ludwig-Maximilians Universität, München, pp. 1–163, pl. 1–8.

NAGAI, H. 1985: Ray cross-section of middle Jurassic Hagiastridae and Patulibracchiidae (Radiolaria). — Bulletin of Nagoya University Museum, no. 1, pp. 1–13.

NAGAI, H. 1986: Jurassic Eucyrtidiellum (Radiolaria) from Central Japan. — Bulletin of the Nagoya University Museum, vol. 2, pp. 1–21.

NAGAI, H. 1987: Middle Jurassic Eucyrtidiellum (Radiolaria) from Kutsuwano, Gifu Prefecture, Central Japan. — Bulletin of the Nagoya University Museum, vol. 3, pp. 1–11.

NAGAI, H. 1988: Early Jurassic Eucyrtidiellum (Radiolaria) from Kamiaso, Gifu Prefecture, Central Japan. — Bulletin of the Nagoya University Museum, vol. 4, pp. 1–9.

NAGAI, H. 1989: Supersonic vibration effect on the surface texture of Jurassic Eucyrtidiellum (Radiolaria). — Bulletin of the Nagoya University, Furukawa Museum, vol. 5, pp. 1–19.

NAGAI, H. and MIZUTANI, S. 1990: Jurassic Eucyrtidiellum (Radiolaria) in the Mino Terrane. — Trans. Proc. Palaeont. Soc. Japan, N.S., vol. 159, pp. 587–602.

NAKASEKO, K., NISHIMURA, A. and SUGANO, K. 1979: Cretaceous Radiolaria in the Shimanto Belt, Japan. — News of Osaka Micropaleontologist, Spec. vol. 2, pp. 1–49.

NAKASEKO, K. and NISHIMURA, A. 1981: Upper Jurassic and Cretaceous Radiolaria from the Shimanto Group in Southwest Japan. — Science Reports, College of General Education, Osaka University, vol. 30, no. 2, pp. 133–203.

NEVIANI, A. 1900: Supplemento alla fauna a Radiolari delle rocce mesozoiche del Bolognese. — Bollettino della Societa geologica italiana, vol. 19, pp. 645–671.

NISHIZONO, Y., OHISHI, A., SATO, T. and MURATA, M. 1982: Radiolarian fauna from the Paleozoic and Mesozoic formations, distributed along the mid-stream of Kuma River, Kyushu, Japan. — News of Osaka Micropaleontologists, Spec. vol. 5, pp. 311–326.

NISHIZONO, Y. and MURATA, M. 1983: Preliminary studies on the sedimentary facies and radiolarian biostratigraphy of Paleozoic and Mesozoic sediments, exposed along the mid-stream of the Kuma River, Kyushu, Japan. — Kumanto Journal of Science, Geology, vol. 12, pp. 1–40.

O'DOGHERTY, L. 1994: Biochronology and paleontology of middle Cretaceous Radiolaria from Umbria Apennines (Italy) and Betic Cordillera (Spain). — Doct. Thesis, Faculty Sci., University Lausanne (unpubl.), pp. 1–332, pl. 1–73.

O'DOGHERTY, L., SANDOVAL, J., MARTIN-ALGARRA, A. and BAUMGARTNER, P.O. 1989: Las facies con radiolarios del Jurassico Subbetico (Cordillera Betica, sur de España). — Rev Soc. Mex. Paleontol., vol. 1, pp. 73–86.

OBRADOVIĆ, J. 1979: Srednjotriaski vulkanoklastiti Dinarida (Middle Triassic volcanoclastic rocks of the Dinarides). — Geološki anali Balkanskog poluostrva, Beograd, vol. 43–44, pp. 3–83.

OBRADOVIĆ, J., MIRKOVIĆ, B., MIRKOVIĆ, M., GORIČAN, Š. and VUJISIĆ, P. 1986: Silicijske stene iz mezozojskog karbonatnog kompleksa zone Budva, Crna Gora (Siliceous rocks from Mesozoic carbonate complex, Budva Zone, Montenegrin littoral). — Posebna izdanja Crnogorske akademije nauka i umjetnosti, posv. Zariji Bešiću, Titograd, vol. 2, pp. 317–343.

OBRADOVIĆ, J., MIRKOVIĆ, M. and ČADJENOVIĆ, D. 1988: Karbonatni turbiditi zone Budva (Carbonate turbidites from Budva Zone). — Geološki glasnik, Titograd, Posebno izdanje vol. 6 (Zbornik radova 6. skupa sedimentologa Jugoslavije), pp. 151–165.

OBRADOVIĆ, J., ČADJENOVIĆ, D. and MIRKOVIĆ, M. 1989: Chanellized Carbonate Debris Flows and Turbidites: an

Example from trough in Periadriatic Carbonate Platform, Yugoslavia. — 28th International Geological Congress, Abstracts, vol. 2 of 3., pp. 2–537.

OBRADOVIĆ, J. and GORIČAN, Š. 1989: Siliceous Deposits in Yugoslavia: Occurrences, Types and Ages. — In: HEIN, J. R. and OBRADOVIĆ, J. (Eds.): Siliceous Deposits of the Tethys and Pacific Regions. Springer-Verlag, New York, Berlin, Heidelberg, pp. 51–64.

ODIN, G.-S. and ODIN, C. 1990: Echelle numérique des temps géologiques. — Géochronique, vol. 35, pp. 12–21.

OKADA, H., HATAKENAKA, A. and NAKASEKO, K. 1982: Age of the Sorachi Group in its type area in Hokkaido. — News of Osaka Micropaleontologists, Spec. vol. 5, pp. 353–357.

OKAMURA, M. 1980: Radiolarian fossils from the northern Shimanto Belt (Cretaceous) in Kochi Prefecture, Shikoku. — Geology and Paleontology of the Shimanto Belt, pp. 153–178, pl. 19–23.

OKAMURA, M. and UTO, H. 1982: Notes on stratigraphic distributions of radiolarians from the Lower Cretaceous sequence of chert in the Yokonami Melange of Shimanto Belt, Kochi Prefecture, Shikoku. — Research Report of the Kochi University, Natural Sciences, vol. 31, pp. 87–94.

OKAMURA, M. and MATSUGI, H. 1986: Cretaceous radiolarians from the time equivalent formations of arc-trench system, Shikoku. — News of Osaka Micropaleontologists, Spec. vol. 7, pp. 117–129.

OWADA, K. and SAKA, Y. 1982: Preliminary note on the Paleozoic and the Mesozoic formations in the Chichibu Belt, Okutama District, Kwanto Mountains, Japan. — News of Osaka Micropaleontologists, Spec. vol. 5, pp. 67–80.

OŽVOLDOVA, L. 1975: Upper Jurassic radiolarians from the Kisuca Series in the Klippen Belt. — Zapadne Karpaty, seria paleontologia, Bratislava, vol. 1, pp. 73–86.

OŽVOLDOVA, L. 1979: Radiolarian assemblage of radiolarian cherts of Podbiel locality (Slovakia). — Časopis pro mineralogii a geologii, vol. 24, no. 3, pp. 249–261.

OŽVOLDOVA, L. 1988: Radiolarian associations from radiolarites of the Kysuca succession of the Klippen Belt in the vicinity of Myjava – Tura Luka (West Carpathians). — Geologica Carpathica, vol. 39, no. 3, pp. 369–392.

OŽVOLDOVA, L. 1990a: Occurrence of Albian Radiolaria in the underlier of the Vienna Basin. — Geologica Carpathica, vol. 41, no. 2, pp. 137–154.

OŽVOLDOVA, L. 1990b: Radiolarian microfauna from radiolarites of the Varin part of the west Carpathian Klippen Belt. — Geologica Carpathica, vol. 41, no. 3, pp. 295–310.

OŽVOLDOVA, L. 1992: The discovery of a Callovian radiolarian association in the upper Posidonia beds of the Pieniny succession of the Klippen Belt (Western Carpathians). — Geologica Carpathica, vol. 43, no. 2, pp. 111–122.

OŽVOLDOVA, L. and SYKORA, M. 1984: The radiolarian assemblage from Cachticke Karpaty Mts. limestones (the locality Sipkovsky Haj). — Geologicky Sbornik, Geologica Carpathica, vol. 35, no. 2, pp. 259–290.

OŽVOLDOVA, L. and PETERČAKOVA, M. 1987: Biostratigraphic research of upper Jurassic limestones of the Čachtice Carpathians (locality Bzince pod Javorinou). — Zapadne Karpaty, Ser. Paleont., vol. 12, pp. 115–124.

OŽVOLDOVA, L. and PETERČAKOVA, M. 1992: Hauterivian radiolarian association from the Lučkovska Formation, Manin Unit (Mt. Butkov, Western Carpathians). — Geologica Carpathica, vol. 43, no. 5, pp. 313–324.

PAMIĆ, J.J. 1982: Some Geological Problems of the Dinaric Ophiolites and Their Associations. — Earth Evolution Sciences, vol. 2, no. 1, pp. 30–35.

PAMIĆ, J.J. 1984a: Permo-Triassic rift faulting and magmatism of the Dinarides. — Ann. Soc. Géol. Nord., vol. 103, pp. 133–141.

PAMIĆ, J.J. 1984b: Triassic magmatism of the Dinarides in Yugoslavia. — Tectonophysics, vol. 109, pp. 273–307.

PAPA, A. 1970: Conceptions nouvelles sur la structure des Albanides (présentation de la Carte tectonique de l'Albanie au 500 000). — Bull. Soc. géol. France, sér. 7, vol. 12, no. 6, pp. 1096–1109.

PARONA, C.F. 1890: Radiolarie nei noduli selciosi del calcare giurese di Cittiglio presso Laverno. — Bollettino della Societa geologica italiana, vol. 9, no. 1, pp. 132–175.

PAVIĆ, A. 1970: Marinski paleogen Crne Gore. Stratigrafija, tektonika, paleogeografija (Paléogène marin du Monténégro, son importance stratigraphique, tectonique et paléogéographique). — Zavod za geološka istraživanja Crne Gore, Titograd, Posebna izdanja, pp. 1–192.

PAVŠIČ, J. and GORIČAN, Š. 1987: Lower Cretaceous Nannoplankton and Radiolaria from Vrsnik (western Slovenia). — Razprave IV. Razreda SAZU, Ljubljana, vol. 27, no. 2, pp. 15–36.

PESSAGNO, E.A. 1971: Jurassic and Cretaceous Hagiastridae from the Blake-Bahama Basin (Site 5A, JOIDES Leg 1) and the Great Valley Sequence, California Coast Ranges. — Bulletin of American Paleontology, vol. 60, no. 264, pp. 5–83.

PESSAGNO, E.A. 1973: Upper Cretaceous Spumellariina from the Great Valley Sequence, California Coast Ranges. — Bulletins of American Paleontology, vol. 63, no. 276, pp. 49–102.

PESSAGNO, E.A. 1976: Radiolarian zonation and stratigraphy of the Upper Cretaceous portion of the Great Valley Sequence, California Coast Ranges. — Micropaleontology, Special Publication No. 2, pp. 1–95.

PESSAGNO, E.A. 1977a: Upper Jurassic Radiolaria and radiolarian biostratigraphy of the California Coast Ranges. — Micropaleontology, vol. 23, no. 1, pp. 56–113.

PESSAGNO, E.A. 1977b: Lower Cretaceous radiolarian biostratigraphy of the Great Valley Sequence and Franciscan

Complex, California Coast Ranges. — Coush. Found. Foram. Res., Spec Publ. 15, pp. 1–87.

PESSAGNO, E.A. and NEWPORT, R. L. 1972: A technique for extracting Radiolaria from radiolarian cherts. — Micropaleontology, vol. 18, no. 2, pp. 231–234.

PESSAGNO, E.A., FINCH, W. and ABBOTT, P.L. 1979: Upper Triassic Radiolaria from the San Hipolito Formation, Baja California. — Micropaleontology, vol. 25, no. 2, 160–197.

PESSAGNO, E.A. and BLOME, C. 1980: Upper Triassic and Jurassic Pantanelliinae from California, Oregon and British Columbia. — Micropaleontology, vol. 26, no. 3, pp. 225–273.

PESSAGNO, E.A. and POISSON, A. 1981: Lower Jurassic Radiolaria from the Gümüslü Allochton of southwestern Turkey (Taurides Occidentales). — Bulletin of the Mineral Research and Exploration Institute of Turkey, no. 92, pp. 47–69.

PESSAGNO, E.A. and BLOME, C. 1982: Bizarre Nassellariina (Radiolaria) from the Middle and Upper Jurassic of North America. — Micropaleontology, vol. 28, no. 3, pp. 289–318.

PESSAGNO, E.A. and WHALEN, P. 1982: Lower and Middle Jurassic Radiolaria (multicyrtid Nassellariina) from California, east-central Oregon and the Queen Charlotte Islands, B.C. — Micropaleontology, vol. 28, no. 2, pp. 111–169.

PESSAGNO, E.A., BLOME, C. and LONGORIA, J. 1984: A revised radiolarian zonation from Upper Jurassic of western North America. — Bulletins of American Paleontology, vol. 87, no. 320, pp. 1–51.

PESSAGNO, E.A., WHALEN, P. and YEH, K.-Y. 1986: Jurassic Nassellariina (Radiolaria) from North American geologic terranes. — Bulletins of American Paleontology, vol. 9, no. 326, pp.1–75.

PESSAGNO, E.A., BLOME, C., CARTER, E., MACLEOD, N., WHALEN, P. and YEH, K.-Y. 1987: Studies of North American Jurassic Radiolaria; Part II. Preliminary radiolarian zonation for the Jurassic of North America. — Cushman Foundation, Special Publication 23 , pp. 1–18.

PESSAGNO, E.A., SIX, W.M. and YANG, Q. 1989: The Xiphostylidae Haeckel and Parvivaccidae, n. fam., (Radiolaria) from the North American Jurassic. — Micropaleontology, vol. 35, no. 3, pp. 193–255.

PESSAGNO, E.A., BLOME, C.D., MEYERHOFF HULL, D. and SIX, W.M. 1993: Jurassic Radiolaria from the Josephine ophiolite and overlying strata, Smith River subterrane (Klamath Mountains), northwestern California and southwestern Oregon. — Micropaleontology, vol. 39, no. 2, pp. 93–166.

PETKOVIĆ, K.V. 1956: Yougoslavie. — In: Lexique stratigraphique international. Centre National de la Recherche Scientifique, Paris, vol. 1 (Europe), no. 12a (Yougoslavie), pp. 1–54.

PRINCIPI, P. 1909: Contributo allo studio dei radiolari miocenici italiani. — Boll. Soc. geol. ital., vol. 28, no 1, pp. 1–22.

RADOIČIĆ, R. 1966: Microfacies du Jurassique des Dinarides Externes de la Yougoslavie. — Geologija, Ljubljana, vol. 9, pp. 5–170.

RADOIČIĆ, R. 1967: Bilješka o rasprostranjenju pelaških tintinina u spoljašnim Dinaridima Jugoslavije (Note sur la répartition des Tintinnines pélagiques dans les Dinarides Externes de Yougoslavie). — Geološki glasnik, Titograd, vol. 5, pp. 111–121.

RADOIČIĆ, R. 1982: Carbonate platforms of the Dinarides: the example of Montenegro – west Serbia sector. — Bull. T. 80 de l'Academie Serbe des Sciences et des Arts, Classe des Sciences naturelles et mathématiques, Beograd, vol. 22, pp. 35–46.

RADOIČIĆ, R. 1987a: The Dinaric Carbonate Platform: adjacent basins and depressions. — Mem. Soc. Geol. It., vol. 40, pp. 309–311.

RADOIČIĆ, R. 1987b: Preplatform and first carbonate platform development stages in the Dinarides (Montenegro – Serbia sector, Yugoslavia). — Mem. Soc. Geol. It., vol. 40, pp. 355–358.

RADOIČIĆ, R. 1987c: Spiraloconulus perconigi Allemann & Schroeder (Foraminifera) u nekim jurskim serijama Jugoslavije, Grčke i Iraka (Spiraloconulus perconigi Alleman & Schroeder (Foraminifera) in some Jurassic series of Yugoslavia, Greece and Iraq). — Geološki glasnik, Titograd, vol. 12, pp. 117–125.

RADOIČIĆ, R. and D'ARGENIO, B. 1988: Geology and Mesozoic -early Tertiary Facies of External Dinarids (Southern sector). — Guidebook, 74 Congresso Nazionale – Sorrento, Societa Geologica Italiana, pp. 1–79.

RAMPNOUX, J.-P. 1974: Contribution à l'étude géologique des Dinarides: un secteur de la Serbie méridionale et du Monténégro oriental (Yougoslavie). — Mém. Soc. géol. France, vol. 119, pp. 1–100.

REMANE, J. 1985: Calpionellids. — In: BOLLI, H.M., SAUNDERS, J.B. and PERCH-NIELSEN, K. (Eds.): Plankton Stratigraphy. Cambridge University Press , Cambridge, pp. 555–572.

RENZ, G.W. 1974: Radiolaria from Leg 27 of the Deep Sea Drilling Project. — In: VEEVERS, J.J., HEIRTZLER, J.R. et al. (Eds.): Initial Rep. Deep Sea Drill. Proj., vol. 27, pp. 769–841.

RIEDEL, W.R. and SANFILIPPO, A. 1974: Radiolaria from the southern Indian Ocean, DSDP Leg 26. — In: DAVIES, T.A., LUYENDYK, B.P. et al. (Eds.): Initial Rep. Deep Sea Drill. Proj., vol. 26, pp. 771–814.

RÜST, D. 1885: Beiträge zur Kenntniss der fossilen Radiolarien aus Gesteinen des Jura. — Palaeontographica, vol. 31, ser. 3, pp. 269–321.

RÜST, D. 1898: Neue Beiträge zur Kenntniss der Fossilen Radiolarien aus Gesteinen des Jura und der Kreide. — Palaeontographica, vol. 45, pp. 1–67.

SANFILIPPO, A. and RIEDEL, W.R. 1985: Cretaceous Radiolaria. — In: BOLLI, H. M., SAUNDERS, J.B. and PERCH-NIELSEN, K. (Eds.): Plankton Stratigraphy. Cambridge University Press, Cambridge, pp. 573–630.

SANO, H., YAMAGATA, T. and HORIBO, K. 1992: Tectonostratigraphy of Mino terrane: Jurassic accretionary complex of southwest Japan. — Palaeogeography, Palaeoclimatology, Palaeoecology, vol. 96, pp. 41–57.

SARTI, M., BOSELLINI, A. and WINTERER, E.L. 1992: Basin Geometry and Architecture of a Tethyan Passive Margin, Southern Alps, Italy. — In: WATKINS, J.S., ZHIQIANG, F. and MCMILLEN, K.J. (Eds.): Geology and Geophysics of Continental Margins. Memoir Amer. Assoc. Petrol. Geol., vol. 53, pp. 241–258.

SASHIDA, K. 1988: Lower Jurassic multisegmented Nassellaria from the Itsukaichi area, western part of Tokyo Prefecture, central Japan. — Science Reports of the Insitute of Geoscience, University of Tsukuba, Section B, vol. 9, pp. 1–27.

SASHIDA, K., IGO, H., IGO, H., TAKIZAWA, S., HISADA, K., SHIBATA, T., TSUKADA, K. and NISHIMURA, H. 1982: On the Jurassic radiolarian assemblages in the Kanto district. — News of Osaka Micropaleontologists, Spec. vol. 5, pp. 51–66.

SASHIDA, K., TONISHI, K. and IGO, H. 1986: Lower Jurassic radiolarians from the Takarazawa area of Itsukaichi Town, Tokyo Prefecture, central Japan. — News of Osaka Micropaleontologists, Spec. vol. 7, pp. 35–43.

SATO, T., NISHIZONO, Y. and MURATA, M. 1982: Paleozoic and Mesozoic radiolarian faunas from the Shakumasan Formation. — News of Osaka Micropaleontologists, Spec. vol. 5, pp. 301–310.

SATO, T., MURATA, M. and YOSHIDA, H. 1986: Triassic to Jurassic radiolarian biostratigraphy in the southern part of Chichibu terrain of Kyushu, Japan. — News of Osaka Micropaleontologists, Spec. vol. 7, pp. 9–23.

SATO, T. and NISHIZONO, Y. 1986: Triassic and Jurassic radiolarian assemblages from two continuous sections in the Kuma massif, Kyushu, Japan. — News of Osaka Micropaleontologists, vol. 11, pp. 33–47.

SAVARY, J. and GUEX, J. 1990: BioGraph, version 2.02. — Institute of Geology and Paleontology, University of Lausanne.

SAVARY, J. and GUEX, J. 1991: BioGraph: un nouveau programme de construction de corrélations biochronologiques basées sur les association unitaires. — Bull. Géol. Lausanne, no 313, pp. 317–340.

SCHAAF, A. 1981: Late Early Cretaceous Radiolaria from Deep Sea Drilling Project Leg 62. — In: THIEDE, J., VALLIER, T.L.et al. (Eds.): Initial Rep. Deep Sea Drill Proj., vol. 62, pp. 419–470.

SCHAAF, A. 1984: Les radiolaires du Crétacé inféreur et moyen: biologie et systématique. — Sciences Géologiques. Mém., vol. 75, pp. 1–189.

SCHLAGER, W. 1992: Sedimentology and sequence stratigraphy of reefs and carbonate platforms. — Continuing Education Course Note Series 34, Amer. Assoc. Petrol. Geol., Tulsa, pp. 1–71.

SCHMIDT-EFFING, R. 1980: Radiolarien der Mittel-Kreide aus dem Santa Elena-Massiv von Costa Rica. — Neues Jahrbuch für Geologie und Paläontologie. Abhandlungen, vol. 160, no. 2, pp. 241–257.

SEPTFONTAINE, M. 1980: Les foraminifères imperforés des milieux de plate-forme au Mésozoïque: détermination pratique, interprétation phylogénétique et utilisation biostratigraphique. — Revue de Micropaléontologie, vol. 23, no. 3–4, pp. 169–203.

SEPTFONTAINE, M. 1985: Milieux de dépôts et foraminifères (Lituolidés) de la plate-forme carbonatée du Lias moyen au Maroc. — Revue de Micropaleontologie, vol. 28, no. 4, pp. 265–289.

SEPTFONTAINE, M., ARNAUD-VANNEAU, A., BASSOULLET, J.-P., GUŠIĆ, I., RAMALHO, M. and VELIĆ, I. 1991: Les foraminifères imperforés des plates-formes carbonatées jurassiques: état des connaissances et perspectives d'avenir. — Bull. Géol. Lausanne, vol. 312, pp. 255–277.

SQUINABOL, S. 1903: Le Radiolarie dei noduli selciosi nella Scaglia degli Euganei (Contribuzione I). — Rivista italiana di paleontologia, vol. 9, no. 4, pp. 105–151.

SQUINABOL, S. 1904: Radiolarie cretacee degli Euganei. — Atti e memorie dell'Accademia di scienze, lettere ed arti. Padova, new series, vol. 20, pp. 171–244.

SQUINABOL, S. 1914: Contributo alla conoscenza dei Radiolarii fossili del Veneto. Appendice – Di un genera di Radiolari caratteristico del Secondario. — Memorie dell'Istituto geologico della Universita di Padova, vol. 2, pp. 249–306, pl. 20–24.

STAMPFLI, G. and PILLEVUIT, A. 1993: An alternative Permo-Triassic reconstruction of the kinematics of the Tethyan realm. — In: DERCOURT, J., RICOU, L.E. and VRIELYNCK, B. (Eds.): Atlas Tethys Palaeoenvironmental Maps. Explanatory notes., Gauthier-Villars, Paris, pp. 55–62.

STAMPFLI, G.M., MARCOUX, J. and BAUD, A. 1991: Tethyan margins in space and time. — Palaeogeography, Palaeoecology, Palaeoclimatology, spec. vol. 87, pp. 373–409.

STEIGER, T. 1981: Kalkturbidite im Oberjura der Nördlichen Kalkalpen (Barmsteinkalke, Salzburg, Österreich). — Facies, vol. 4, pp. 215–348.

STEIGER, T. 1992: Systematik, Stratigraphie und Palökologie der Radiolarien des Oberjura-Unterkreide-Grenzbereiches im Osterhorn-Tirolikum (Nördliche Kalkalpen, Salzburg und Bayern). — Zitteliana, vol. 19, pp. 1–132, pl. 1–27.

SUYARI, K. 1986: Radiolarian assemblages from the Torinosu Group and the cherts of the North Subbelt of the Shimanto Belt. — News of Osaka Micropaleontologists, Spec. vol. 7, pp. 245–254.

TAKEMURA, A. 1986: Classification of Jurassic Nassellarians (Radiolaria). — Palaeontographica, Abteilung A, vol. 195, no. 1–3, pp. 29–74.

TAKEMURA, A. and NAKASEKO, K. 1986: The cephalic skeletal structure of Jurassic "Eucyrtidium" (Radiolaria). — Journal of Paleontology, vol. 60, no. 5, pp. 1016–1024.

TAKETANI, Y. 1982a: Cretaceous radiolarian biostratigraphy of the Urakawa and Obira areas, Hokkaido. — Science Reports of the Tohoku University, Sendai, Series 2. Geology, vol. 52, no. 1–2, pp. 1–75.

TAKETANI, Y. 1982b: Cretaceous Radiolaria from Hokkaido. — News of Osaka Micropaleontologists, Spec. vol. 5, pp. 361–369.

TAKETANI, Y. and KANIE, Y. 1992: Radiolarian age of the Lower Yezo Group and the upper part of the Sorachi Group in Hokkaido. — In: ISHIZAKA, K. and SAITO, T. (Eds.): Centenary of Japanese Micropaleontology, Terra Scientific Publishing Company, Tokyo, pp. 365–373.

TAN, S.H. 1927: Over de samenstelling en het onstaan van krijt- en mergel-gesteenten van de Molukken . — In: BROUWER, H.A. (Ed.): Geologische onderzoekingen in den oostelijken Oost-Indischen Archipel, 5. Jaarb. Mijnwezen Nederl. (Oost-) Indië 55 (1926), pp. 5–165, pl. 1–16.

TANAKA, H., FUJITA, H., MIYAMOTO, T. and HASE, A. 1985: Discovery of late Jurassic radiolarian fossils from the Shinkai Formation developed to the south of Mt. Haidate, Oita Prefecture, Kyushu. — Jour. Geol. Soc. Japan, vol. 91, no. 8, pp. 569–571.

THIÉBAULT, F. 1982: Evolution géodinamique des Hellenides externes en Péloponnèse méridional (Grèce). — Soc. Géol. Nord, Lille, vol. 6, pp. 1–574.

THIÉBAULT, F. and CLÉMENT, B. 1992: Argiles et obduction. Le Jurassique supérieur et le Crétacé inférieur de la zone béotienne en Béotie (Grèce). — Bull. Soc. géol. France, vol. 163, no. 4, pp. 435–446.

THUROW, J. 1988: Cretaceous radiolarians of the North Atlantic Ocean: ODP Leg 103 (Sites 638, 640 and 641) and DSDP Legs 93 (Site 603) and 47B (Site 398). — In: BOILLOT, G., WINTERER, E.L. et al. (Eds.): Proceedings of the Ocean Drilling Program, Scientific Results, vol. 103, pp. 379–418.

TONIELLI, R. 1991: Associazioni a radiolari dei "Calcari e marne a Posidonia" del Monte Terminilletto (RI). — Paleopelagos, vol. 1, pp. 18–37.

TUMANDA, F. 1989: Cretaceous radiolarian biostratigraphy in the Eashi Mountain area, Northern Hokkaido, Japan. — Science Reports of the Institute of Geoscience University of Tsukuba, Section B, Geological Science, vol. 10, pp. 1–44.

TURNŠEK, D. 1969: Prispevek k paleoekologiji jurskih hidrozojev v Sloveniji (A contribution to the paleoecology of Jurassic Hydrozoa from Slovenia). — Razprave IV. Razr. SAZU, Ljubljana, vol. 9, pp. 335–428.

TURNŠEK, D., BUSER, S. and OGORELEC, B. 1981: An Upper Jurassic reef complex from Slovenia, Yugoslavia. — In: TOOMEY, D. F. (Ed.): European Fossil Reef Models. Soc. Econ. Paleontol. Mineral., Tulsa, Spec. Publ. no. 30, pp. 361–369.

VIDOVIĆ, M., MILIĆ, S. and DJERKOVIĆ, B. 1958: Globokovodna gornja kreda na terenu od Bara do Budve (Tiefseesedimente der Oberkreide in Gebiet zwischen Bar und Budva (Montenegro)). — Geološki glasnik, Titograd, vol. 2, pp. 311–332.

VINASSA DE REGNY, P.E. 1899: I radiolari delle ftaniti titoniane di Carpena (Spezia). — Palaeontographia italica, vol. 4, pp. 217–238, pl. 17–18.

VINASSA DE REGNY, P.E. 1900: Rocce e fossili dei dintorni di Grizzana e di Lagaro nel Bolognese. — Bollettino della Societa geologica italiana, vol. 19, no. 2, pp. 321–348.

VISHNEVSKAYA, V. S. 1984: Radiolyariti kak analogi sovremenih radiolyarievih ilov (Radiolarites as analogous of contemporary radiolarian silts). — Nauka, Moscow, pp. 1–120.

WAKITA, K. 1982: Jurassic radiolarians from Kuzuryo-ko – Gujo-hachiman area. — News of Osaka Micropaleontologists, Spec. vol. 5, pp. 153–171.

WAKITA, K. 1988: Early Cretaceous melange in the Hida-Kanayama area, central Japan. — Bulletin of the Geological Survey of Japan, vol. 39, no. 6, pp. 367–421.

WAKITA, K. and OKAMURA, Y. 1982: Mesozoic sedimentary rocks containing allochthonous blocks, Gujo-hachiman, Gifu Prefecture, central Japan. — Bulletin of the Geological Survey of Japan, vol. 33, no. 4, pp. 161–185.

WEISSERT, H.J. 1979: Die Paläozeanographie der südwestlichen Tethys in der Unterkreide. — Mitt. Geol. Inst. ETH Univ. Zürich, Neue Folge 226, pp. 1–174.

WEISSERT, H. and CHANNELL, J.E.T. 1989: Tethyan carbonate carbon isotope stratigraphy across the Jurassic-Cretaceous boundary: an indicator of decelerated global carbon cycling? — Paleoceanography, vol. 4, no. 4, pp. 483–494.

WEISSERT, H. and LINI, A. 1991: Ice Age Interludes During the Time of Cretaceous Greenhouse Climate? — In: MÜLLER, D.W. MCKENZIE, J.A. and WEISSERT, H. (Eds.): Controversies in Modern Geology: Evolution of Geological Theories in Sedimentology, Earth History and Tectonics., Academic Press, London, San Diego, New York, pp. 173–191.

WIDZ, D. 1991: Les radiolaires du Jurassique supérieur des radiolarites de la Zone des Klippes de Pieniny (Carpathes occidentales, Pologne). — Revue de Micropaléontologie, vol. 34, no. 3, pp. 231–260.

WIDZ, D. and DE WEVER, P. 1993: Nouveau Nassellaires (Radiolaria) des radiolarites jurassiques de la coupe de Szelogowy Potok (Zone de Klippes de Pieniny, Carpathes Occidentales, Pologne). — Revue de Micropaléontologie, vol. 36, no. 1., pp. 77–91.

WISNIOWSKI, T. 1889: Beitrag zur Kenntniss der Mikrofauna aus den oberjurassischen Feuersteinknollen der Umgegend von Krakau. — Jahrbuch der Kaiserlich-Königlichen geologischen Reichsanstalt, vol. 38, no. 4, pp. 657–702.

WU, H. 1986: Some new genera and species of Cenomanian Radiolaria from southern Xizang (Tibet). — Acta Micropalaeontologica Sinica , vol. 3, no. 4, pp. 347–360.

YAMAMOTO, H. 1983: Occurrence of late Jurassic radiolarians of the Mirifusus baileyi assemblage from Neo village, Gifu prefecture, central Japan. — Journal of the Geological Society of Japan, vol. 89, pp. 595–596.

YAMAMOTO, H. 1985: Geology of the late Paleozoic-Mesozoic sedimentary complex of the Mino Terrane in the southern Neo area, Gifu prefecture and the Mt. Ibuki area, Shiga prefecture, central Japan. — Journal of the Geological Society of Japan, vol. 91, pp. 353–369.

YAMAMOTO, H., MIZUTANI, S. and KAGAMI, H. 1985: Middle Jurassic radiolarians from Blake Bahama Basin, West Atlantic Ocean. — Bulletin Nagoya University Museum, no. 1, pp. 25–49.

YAMAUCHI, M. 1982: Upper Cretaceous radiolarians from the Northern Shimanto Belt along the course of Shimanto River, Kochi Prefecture, Japan. — News of Osaka Micropaleontologists, Spec. vol. 5, pp. 383–397.

YANG, Q. and WANG, Y. 1990: A taxonomic study of Upper Jurassic Radiolaria from Rutog county, Xizang (Tibet). — Acta Micropaleontologica Sinica, vol. 7, no. 3, pp. 195–218.

YAO, A. 1972: Radiolarian fauna from the Mino Belt in the northern part of the Inuyama Area, Central Japan, Part I: Spongosaturnalids. — Journal of Geosciences, Osaka City University, vol. 15, pp. 21–65.

YAO, A. 1979: Radiolarian fauna from the Mino Belt in the northern part of the Inuyama Area, Central Japan, Part II: Nassellaria I. — Journal of Geosciences, Osaka City University, vol. 22, pp. 21–72.

YAO, A. 1982: Middle Triassic to Early Jurassic radiolarians from the Inuyama area, central Japan. — Journal of Geosciences, Osaka City University, vol. 25, pp. 53–70.

YAO, A. 1984: Subdivision of the Mesozoic complex in Kii-Yura area, southwest Japan and its bearing on the Mesozoic basin development in the southern Chichibu terrane. — Journal of Geoscience, Osaka City University, vol. 27, pp. 41–103.

YAO, A. 1991: Triassic and Jurassic Radiolarians. — In: MIZUTANI, S. (Ed.):Radiolarian Biostratigraphy and its International Correlation. Report of Co-operative Research., Department of Earth Sci., Nagoya Univ., pp. 329–345.

YAO, A., MATSUDA, T. and ISOZAKI, Y. 1980: Triassic and Jurassic radiolarians from the Inuyama area, central Japan. — Journal of Geosciences, Osaka City University, vol. 23, pp. 135–154.

YAO, A., MATSUOKA, A. and NAKATANI, T. 1982: Triassic and Jurassic radiolarian assemblages in southwest Japan. — News of Osaka Micropaleontologists, Spec. vol. 5, pp. 27–43.

YOKOTA, S. and SANO, H. 1986: Radiolarian fossils from the Middle Jurassic Ammonites-bearing formation of Bisho, Yatsushiro district, Kumamoto Prefecture. — News of Osaka Micropaleontologists, Spec. vol. 7, pp. 53–58.

ŽIVALJEVIĆ, M.R. 1989: Geološka bibliografija Crne Gore (1838–1983) (Geological bibliography of Montenegro (1838–1983)). — Geološki glasnik, Titograd, Posebno izdanje vol. 7, pp. 1–309.

Appendix 1

Radiolarian inventory of the samples studied. Each radiolarian taxon is represented by a numerical code to enable computer treatment of data by the BioGraph program (Savary & Guex, 1991). Species within brackets were not treated in constructing the protoreferential. Sample numbers are given in parenthesis (see figs. 2.1 to 2.5 for the stratigraphic position of the samples in the different sections).

"BUDVA Jurassic–Cretaceous"

SECTION 2_VERIGE: bottom 1 – top 5

< 5{Ve 10}: 1114, 3170, 3171, 3216, 3241, 3292, 4015, 4073
< 4{Ve 9 }: 1040, 1054, 3017, 3145, 3161, 3170, 3171, 3182, 3224, 3241, 3263,{ 3267,} 3274, 3292, 4015
< 3{Ve 8}: 1040, 1114, 1116, 3017, 3065, 3069, 3145, 3161, 3170, 3171, 3241, 3263, 3274, 3292
< 2{Ve 7}: 3161, 3224, 3241,{ 3267,} 3274
< 1{Ve 6}: 3069, 3241, 3292, 4073

SECTION 3_BIJELA_I: bottom 1 – top 7

< 7{Bj 15}: 3065, 3069, 3090, 3122, 3181, 3193, 3199, 3224, 3241, 3263, 3292, 3305, 4055, 4079
< 6{Bj 14}: 2018, 3046, 3110, 3117, 3121, 3176, 3180, 3199, 3210, 3215, 3297, 3298
< 5{Bj 13}: 3237, 3273, 4044, 4054, 4060
< 4{Bj 12}: 1117, 2018, 3096, 3110, 3181, 3192,{ 3197,} 3210, 3237, 3271, 4010, 4034, 4044, 4063
< 3{Bj 11}: 1079, 3052, 3089, 3192,{ 3197,} 3231, 4010, 4044, 4058
< 2{Bj 10}: 1117,{ 1120,} 2018, 3039, 3041, 3073, 3074, 3089, 3096, 3194, 3195, 3253, { 4059,} 4059
< 1{Bj 9}: 3006, 3010, 3048, 3072, 3074, 3151, 3194, 3195

SECTION 3_1_BIJELA_II: bottom 1 – top 2

< 2{Bj 15/2}: 3161, 3171, 3177, 3241, 3274
< 1{Bj 15/1}: 1116,{ 1121,} 2018, 3017, 3065, 3069, 3100, 3137, 3181, 3193, 3210, 3224, 3243, 3305, 4055, 4079

SECTION 3_2_BIJELA_III/IV: bottom 1 – top 10

< 10{Bj 21}: 2002, 2004, 2008, 2010, 2013, 2014, 2016, 5582,{ 6107}
< 9{Bj 20+4.60}: 2001, 2002,{ 2005,} 2013, 2017, 2025, 3090,{ 6107}
< 8{Bj 20+3.10}: 2001, 2008, 2013, 2017, 2025, 3090
< 7{Bj 20}: { 1122,} 2001, 2002, 2007, 2008, 2013, 2020, 2025, 3065, 5073,{ 6107}
< 6{Bj 19}: 3065, 3090, 5073
< 5{Bj 18+1.50}: 2012, 2018, 2026, 3090,{ 3092,} 5012,{ 5049,} 5073,{ 5422,} 5462, 5595, 5712,{ 6107}
< 4{Bj 18}: 2018, 2026, 3065, 3185, 5012, 5462, 5595, 5712,{ 6107}
< 3{Bj 17}: 3087, 3185, 4026, 5073, 5229, 5426, 5462, 5481, 5636, 5712
< 2{BjIII 3.00}: 1114,{ 1115,} 1117, 2018, 3069, 3161, 3170, 3171, 3177, 3182, 3216, 3241, 3243,{ 3267,} 3274, 3292, 4015, 4055, 4073, 4079
< 1{BjIII 0.40}: 1054, 1114, 1116, 2018, 3017, 3066, 3122, 3161, 3170, 3171, 3182, 3216, 3224, 3241, 3274, 3292, 4073

SECTION 4_GORNJA_LASTVA: bottom 1 – top 23

< 23{GL 215}: 2002, 2004, 2010, 2011, 2014, 2016, 5582,{ 6107}
< 22{GL 9}: 2002, 2008, 2013, 2017, 3090, 5073, 5582,{ 6107}
< 21{GL 144}: 2012, 2025, 2026, 3065,{ 3092,} 3287, 4073, 5012, 5204, 5712
< 20{GL 214}: 3087, 3090, 3185, 4026, 5011, 5229
< 19:{GL 142}: 1050, 1104, 2018, 3019, 3065, 3087, 3090,{ 3092,} 3185, 3255, 3263, 3284, 4035, 6101
< 18{GL 139}: 1014, 1104, 2018, 3065, 3087, 3171, 3255, 3263, 3287,{ 6107}
< 17{GL 138}: 1014, 1050, 1054, 1104,{ 1124,} 2018, 3019, 3065, 3087, 3161,{ 3165,} 3170, 3171, 3185, 3241, 3263, 3286, 3287, 3292,{ 3294,} 3305, 4035, 6101
< 16{GL 137}: 3145, 3161, 3170, 3171, 4015
< 15{GL 210}: 1114, 1116, 2018, 3145, 3161, 3170, 3171, 3216, 3274, 3292, 4073
< 14{GL 209+6.60}: { 1028,} 1040,{ 1110,} 1114, 1116, 1117,{ 1123,} 2018, 3017, 3065, 3069, 3090, 3103, 3117, 3121, 3122,{ 3129,}{ 3133,} 3137, 3139,{ 3140,} 3145, 3161, 3162, 3170, 3181, 3193,{ 3197,} 3199, 3204, 3210, 3215, 3216, 3224, 3225, 3230, 3241, 3243, 3263,{ 3267,} 3274, 3292, 3305, 4015, 4055, 4073, 4079
< 13{GL 209}: 1032, 1037,{ 1110,} 1116, 2018, 3008,{ 3014,} 3017, 3052, 3100, 3103, 3117, 3121, 3137, 3139, 3193, 3205, 3210, 3215, 3223, 3224, 3243,{ 3279,} 3292, 4055, 4060
< 12{GL 208+1.00}: 1113, 1117, 3046, 3052, 3176, 3180, 3193, 3297, 3298, 4014, 4060
< 11{GL 208}: 3117, 3273, 3298
< 10{GL 207}: 1113, 2018, 3110, 3117, 3180, 3181,{ 3197,} 3210, 3215,{ 3221,} 3223, 3273,{ 3277,}{ 3279,} 3297, 4010, 4014, 4044
< 9{GL 135}: 1117, 3052, 3180, 3181,{ 3197,} 3237, 4014, 4034, 4044, 4054
< 8{GL 134}: 3052, 3096, 3181,{ 3197,} 3210, 3223, 3271, 3273, 4010, 4034, 4044, 4058
< 7{GL 6}: 1079,{ 1119,} 3089, 3096, 3181, 3192,{ 3197,} 3210, 3237, 3253, 4014, 4044, 4058, 4060
< 6{GL 132}: 1079, 3052, 3192,{ 3197,} 3231,{ 3558,}{ 4009,} 4010, 4034, 4044
< 5{ZB 28}: 1079,{ 1111,} 1117,{ 1120,}{ 1128,} 2018, 3006, 3052, 3074, 3089, 3096,{ 3123,}{ 3129,} 3192, 3195,{ 3197,} 3231, 3247, 3253, 3273, 3297,{ 3307,}{ 3558,}{ 4009,} 4010, 4044,{ 4049,} 4058,{ 4059,} 4059, 4063
< 4{GL 128}: 1117, 2018, 3039, 3041, 3052, 3192, 3194, 3223, 3231, 3253
< 3{GL 127}: 1117,{ 1125,}{ 1128,} 3010, 3039, 3041, 3048, 3052, 3072, 3074, 3089, 3096, 3192, 3194, 3195,{ 3197,} 3231, 3253, 4010, 4061
< 2{GL 125}: 1117, 3010, 3039, 3048, 3072, 3074, 3151, 3194, 3195, 3231, 4010
< 1{GL 123}: 1117, 2018, 3006, 3039, 3048, 3072, 3073, 3089, 3096, 3151, 3310, 4010, 4031

SECTION 5_GRBALJSKA_LASTVA: bottom 1 – top 3

< 3{Grb 12}: 2001, 2002, 2008, 2013, 2017, 3090,{ 6107}
< 2{Grb 11}: 2002, 2008, 2013, 2025
< 1{Grb 10}: 2001, 2002, 2007, 2008, 2013, 2020, 5073

SECTION 6_PETROVAC: bottom 1 – top 4

< 4{PK 1}: 2020, 3065
{PK 3: reworked - 1127, 2012, 2018, 3065, 3087, 3092, 3631, 4035, 5012, 5049, 5073, 5229, 5362, 5462, 5511, 5544, 5595, 5712, 5712, 6101}
{PK 104: reworked - 1014, 3019, 3066, 3087, 3165, 3170, 3171, 3263, 3286, 3292, 3305}

```
< 3{PK 7}: 1114, 1117, 2018, 3145, 3161, 3181, 3199, 3205, 3224, 3230, 3241,
    3263, 3292
< 2{PK 9}: 1037, 1116,{ 3014,} 3017, 3065, 3100, 3103, 3117, 3121,{ 3133,}
    3181, 3193, { 3197,} 3199, 3204, 3223, 3224, 3243, 3263, 3292
< 1{PK 12}: 1117, 2018, 3052, 3065, 3090, 3096, 3103, 3117, 3181, 3193, 3223,
    3292, 4060

SECTION 7_CANJ: bottom 1 — top 23
< 23{UPC 35}: 2002, 2010, 2011, 2021, 2022, 2023, 2024,{ 2027,}{ 6107}
< 22{UPC 34}: 2002, 2008, 2013, 2016, 2017, 2025, 3090, 5582,{ 6107}
< 21{UPC 33}: 2002, 2008, 2013, 2016, 2017, 2025, 5582,{ 6107}
< 20{UPC 32}: { 1122,}{ 1129,} 2012, 2013, 2018, 2025, 2026, 5073, 5595,{ 6107}
< 19{UPC 298.60}: 2012, 2018, 2026, 3065, 3287, 5012, 5073, 5204, 5462, 5595,
    5712, { 6107}
< 18{UPC 30}: 2018, 2025, 3065, 3087,{ 3092,} 3161, 3287,5073, 4026, 5462,
    5636,{ 6107}
< 17{UPC 29}: 1014, 3065, 3087, 3161,{ 3165,} 3170, 3263, 3286
< 16{UPC 28}: 1014, 1102, 3019, 3065, 3087, 3170, 3171, 3225, 3241, 3263, 3305,
    6101
< 15{UPC 27}: 1014, 1054, 1102, 3019, 3065, 3066, 3087, 3161, 3171,
    3185,{ 3189,} 3241, 3263, 3286, 3287, 3292, 3305,{ 3911}
< 14{UPC 26}: 1014, 3065, 3087, 3171, 3241, 3263
< 13{UPC 25}: 1014, 1054, 3019, 3065, 3161, 3170, 3171, 3241, 3292, 6101
< 12{UPC 262.70}: 1014, 1040, 1054, 1102, 1116, 3017, 3090, 3100, 3145, 3161,
    3170, 3171, 3179, 3182,{ 3189,} 3193, 3199, 3215, 3216, 3241, 3263, 3274,
    3292, 4015, 4073
< 11{UPC 257.10}: 1116, 1117, 3017, 3069, 3139, 3161, 3171, 3179, 3215, 3216,
    3224, 3230, 3241, 3263, 3274, 4055, 4079
< 10{UPC 251.50}: 1037, 1116, 1117, 2018, 3017, 3065, 3069, 3090, 3100, 3117,
    3121, { 3133,} 3137, 3145, 3180, 3181, 3193,{ 3197,} 3199, 3205, 3210,
    3223, 3224, 3243, 3259, 3263, 3292, 4055, 4073, 4079
< 9{UPC 23}: 1037, 1114, 2018, 3008, 3065, 3100, 3103,{ 3104,} 3117,
    3122,{ 3127,}{ 3129,}{ 3133,} 3137, 3139,{ 3140,} 3180, 3181, 3193, 3199,
    3205, 3223, 3224, 3243, 3259, 3263, 4055, 4060
< 8{UPC 22}: 1032,{ 1110,} 2018, 3017,{ 3133,} 3137, 3139,{ 3140,} 3180, 3181,
    3199, 3205, 3223, 3224, 3243, 4055
< 7{UPC 21}: 1116, 3096, 3100, 3117, 3121, 3139, 3180, 3181, 3193,{ 3197,}
    3199, 3205, 3215, 3223, 3224, 3225, 3243, 3273
< 6{UPC 20}: 1113, 1117,{ 3044,} 3046,{ 3197,} 3297, 3298
< 5{UPC 18}:{ 1111,} 1113, 1117,{ 1126,} 3008, 3017,{ 3044,}{ 3045,} 3046, 3121,
    3160, 3176, 3180, 3181, 3193, 3199, 3205, 3210, 3237, 3297, 3298, 4060
< 4{UPC 16}: 1117, 3041, 3096,{ 3197,} 3231
< 3{UPC 15}: 3006, 3039, 3041, 3073, 3074, 3096, 3194, 3195, 3253, 4061
< 2{UPC 14}: 1117, 3010, 3048, 3072, 3073, 3074, 3194, 3195, 3253
< 1{UPC 13}: 1117, 2018, 3006, 3010, 3048, 3072, 3195, 3247, 3253, 4061

SECTION 8_DIN_VRH: bottom 1 — top 8
< 8{DIN 31.50}: 2018, 2025, 3065, 3087, 3090, 3161, 3286, 4026, 4035, 5229,
    5462, 5481, 5636, 5712
< 7{DIN 29.30}: 1102, 1104,{ 1121,} 2018, 3019, 3182, 3185, 4035, 5636, 6101
< 6{DIN 24.30}: 1014, 1050, 2018, 3019, 3065, 3161, 3171, 3182, 3263, 3287,
    3292, 3305,{ 3911,} 4035, 4073
< 5{DIN 11.55}: 1054, 1102, 1114,{ 1115,} 2018, 3017, 3066, 3069,{ 3123,} 3161,
    3171, 3177, 3182, 3216, 3259, 3263, 3274, 3292,{ 3294,} 3305, 4055, 4079
< 4{DIN 7.00}: 1054, 2018, 3171, 4015, 4055
```

```
< 3{DIN 4.50}: 2018, 3017, 3069, 3224, 3230, 3241, 4055
< 2{DIN 2.35}: { 1028,} 1040, 1114, 1116, 1117, 2018, 3069, 3100, 3103, 3117,
    3121, 3122, 3139, 3145, 3161, 3170, 3179, 3181, 3199, 3210, 3215, 3216,
    3224, 3230, 3241, 3243, 3263, 3274, 4010
< 1{DIN 1.50}: 3017, 3117, 3122, 3161, 3181, 3193, 3241, 3274, 3292

SECTION 10_BAR: bottom 1 - top 10
< 10{BM 489.40}: { 2006,} 2012, 2013, 2020, 2025, 3065, 3090, 4073, 5073,
    5204,{ 5511,}{ 6107}
< 9{BM 478.60}: 2018, 2025, 3087, 3185, 3287, 4026, 4073, 5011, 5073, 5204,
    5229, 5426, 5462, 5481,{ 5532,} 5636, 5712,{ 6107}
< 8{BM 469.00}: 3087, 3287, 4026, 5073, 5229, 5462, 5636,{ 6107}
< 7{BM 466.40}: 2025, 3065, 3087, 4026, 4073, 5229, 5462, 5481
< 6{BM 8}: 1014, 1050, 3065, 3066, 3087, 3161, 3170, 3171, 3185, 3263, 3286,
    3287, 3292, 4073, 6101
< 5{BM 7}: 1014, 1102, 3019, 3065, 3087, 3161, 3170, 3171, 3241, 3263, 3274,
    3287, 3292
< 4{BM 6}: 3017, 3065, 3161, 3170, 3171, 3241, 3263, 3274, 3292, 4015
< 3{BM 5}: 1054, 1114, 3069, 3161, 3171, 3177,{ 3197,} 3241, 3274, 4015
< 2{BM 106}: 1040, 1054, 1102,{ 1115,} 1116, 1117, 2018, 3065, 3066, 3122,
    3145, 3161, 3170, 3171, 3177, 3182, 3193,{ 3197,} 3199, 3215, 3274, 3292,
    4015, 4079
< 1{BM 102}: 1032, 1037,{ 1110,} 1114, 1116, 1117, 2018, 3008,{ 3014,} 3017,
    3065, 3090, 3096, 3100,{ 3104,} 3117, 3121,{ 3123,}{ 3127,}{ 3129,} 3137,
    3139,{ 3147,} 3160, 3162, 3176, 3180, 3181, 3193,{ 3197,} 3199, 3204, 3205,
    3210, 3215, 3223, 3224, 3225, 3230, 3243, 3273, 3292, 4010, 4055
```

Appendix 2a:

Alphabetical index of genera and species with a corresponding code. Species marked with an * asterisk were not included in constructing the protoreferential.

3090 Acaeniotyle diaphorogona gr.
3092 Acaeniotyle umbilicata *
4063 Acaeniotyle variata s.l.
5012 Acanthocircus carinatus
3087 Acanthocircus dicranacanthos
3065 Acanthocircus trizonalis gr.
5011 Acanthocircus variabilis
2021 Afens liriodes
3145 Angulobracchia biordinalis
3147 Angulobracchia digitata
3911 Angulobracchia (?) sp. A *
2010 Archaeocenosphaera (?) sp. A
3263 Archaeodictyomitra apiarium
3287 Archaeodictyomitra excellens
5595 Archaeodictyomitra lacrimula
3305 Archaeodictyomitra minoensis
3237 Archaeodictyomitra (?) amabilis
2026 Archaeodictyomitra (?) sp. A
3271 Archaeohagiastrum munitum
4061 Ares spp.
3221 Bernoullius cristatus *
3223 Bernoullius dicera
4009 Bernoullius furcospinus *
4010 Bernoullius rectispinus s.l.
5229 Cecrops septemporatus
6101 Cinguloturris sp. A
3193 Cinguloturris carpatica
5532 Crolanium pythiae *
5204 Crucella cf. cachensis
2025 Cryptamphorella conara
1119 Cyrtocapsa aff. mastoidea *
3307 Cyrtocapsa mastoidea *
5422 Dibolachras tytthopora *
2024 Dictyomitra formosa
4014 Dictyomitrella (?) kamoensis
3631 Emiluvia spp.
3225 Emiluvia hopsoni
4015 Emiluvia ordinaria
3224 Emiluvia orea
3066 Emiluvia pessagnoi
3210 Emiluvia premyogii
3215 Emiluvia salensis

3253 Emiluvia splendida
3216 Emiluvia sedecimporata
3014 Eucyrtidiellum nodosum *
3017 Eucyrtidiellum ptyctum
3019 Eucyrtidiellum pyramis
3052 Eucyrtidiellum unumaense
3048 Eucyrtidiellum (?) quinatum
3279 Gongylothorax sp. aff. G. favosus *
1113 Guexella nudata
1032 Hagiastrid gen. indet. spp.
4026 Hemicryptocapsa capita
2022 Hemicryptocapsa polyhedra
2017 Hemicryptocapsa sp. A
2023 Hemicryptocapsa prepolyhedra
3656 Hexasaturnalis
3089 Hexasaturnalis tetraspinus
3110 Higumastra imbricata
6107 Holocryptocanium barbui *
3103 Homoeoparonaella argolidensis
3104 Homoeoparonaella elegans *
3195 Hsuum matsuokai
3182 Hsuum mclaughlini gr.
3151 Laxtorum (?) jurassicum
3074 Linaresia chrafatensis
3162 Mirifusus chenodes
3274 Mirifusus dianae dianae
3286 Mirifusus dianae minor
3161 Mirifusus dianae s.l.
3160 Mirifusus guadalupensis
5582 Mita gracilis
2004 Mita sp. B
2005 Mita sp. C *
1114 Napora bukryi gr.
4073 Noviforemanella diamphidia gr.
2014 Novixitus weyli
3204 Orbiculiforma sp. A
1037 Orbiculiforma sp. B
3205 Orbiculiforma sp. D
3008 Palinandromeda podbielensis
3006 Palinandromeda praepodbielensis
3010 Palinandromeda sp. A
1115 Pantanellium oligoporum *
2018 Pantanellium spp.
1120 Parahsuum officerense *
1117 Parahsuum spp.
4031 Parahsuum (?) grande
3072 Parahsuum (?) magnum
3073 Parahsuum (?) natorense
3310 Paronaella aff. corpulenta
3137 Paronaella broennimanni
1040 Paronaella cava
3140 Paronaella kotura *
3139 Paronaella mulleri
3133 Paronaella pygmaea *
3185 Parvicingula boesii gr.
3197 Parvicingula dhimenaensis *
5712 Parvicingula usotanensis
3255 Parvicingula cosmoconica
1028 Parvivacca blomei *
3100 Perispyridium ordinarium gr.
3230 Podobursa spinosa
3171 Podocapsa amphitreptera
3681 Praeconocaryomma
3292 Protunuma japonicus
4034 Protunuma turbo
3129 Pseudocrucella adriani *
3127 Pseudocrucella sp. B *
4035 Pseudodictyomitra carpatica
3284 Pseudodictyomitra depressa
2012 Pseudodictyomitra lanceloti
2008 Pseudodictyomitra lodogaensis
2007 Pseudodictyomitra pentacolaensis
3189 Pseudodictyomitra primitiva *
2011 Pseudodictyomitra pseudomacrocephala
5636 Pseudodictyomitra puga
1121 Pseudodictyomitra sp. C *
1122 Pseudodictyomitra sp. A *
1129 Pseudoeucyrtis hanni *
3177 Pseudoeucyrtis reticularis
1123 Pseudoeucyrtis sp. B *
3176 Pseudoeucyrtis sp. J
2016 Rhopalosyringium majuroense
2027 Rhopalosyringium sp. A
3241 Ristola altissima altissima
3165 Ristola cretacea *
1102 Saitoum dercourti
1124 Sethocapsa accincta *
1054 Sethocapsa horokanaiensis
5481 Sethocapsa kaminogoensis
5462 Sethocapsa uterculus
1050 Sethocapsa pseudouterculus
2001 Sethocapsa (?) perspicua
3199 Spongocapsula palmerae
3267 Spongocapsula perampla *
3243 Staurosphaera antiqua
3045 Stichocapsa naradaniensis *
3298 Stichocapsa robusta
2002 Stichomitra communis
3192 Stichomitra (?) sp. A
4044 Stichomitra (?) takanoensis gr.
3044 Stylocapsa catenarum *
3046 Stylocapsa (?) spiralis gr.
5049 Suna hybum *
5426 Syringocapsa limatum
3170 Syringocapsa sp. A
3273 Tetraditryma corralitosensis
3123 Tetraditryma pseudoplena *
3121 Tetratrabs zealis
3122 Tetratrabs bulbosa
5296 Thanarla elegantissima *

2013 Thanarla praeveneta
5073 Thanarla pulchra
3277 Theocapsomma cordis *
3181 Transhsuum brevicostatum gr.
3194 Transhsuum hisuikyoense
3179 Transhsuum okamurai
3180 Transhsuum maxwelli gr.
1110 Triactoma blakei *
1125 Triactoma cf. southforkensis *
3096 Triactoma jonesi
1111 Triactoma parablakei *
2020 Tricapsula costata
3297 Tricolocapsa conexa
1126 Tricolocapsa sp. A *
4054 Tricolocapsa tetragona
4049 Tricolocapsa (?) fusiformis *
3039 Trillus spp.
3117 Tritrabs casmaliaensis
1116 Tritrabs exotica gr.
3247 Turanta spp.
1079 Unuma darnoensis
3231 Unuma echinatus
4058 Unuma latusicostatus
4059 Unuma typicus
4055 Williriedellum carpathicum
3069 Williriedellum crystallinum
4060 Williriedellum sp. A
3294 Xitus gifuensis *
3259 Xitus sp. A
1104 Xitus (?) sp.
1128 Yamatoum spp. *
3558 Yamatoum (?) sp. A *
3041 Zartus spp.
4079 Zhamoidellum ovum
1014 Zhamoidellum sp. A

Appendix 2b:

Same as Appendix 2a, arranged by ascending order of numerical codes.

1014 Zhamoidellum sp. A
1028 Parvivacca blomei *
1032 Hagiastrid gen. indet. spp.
1037 Orbiculiforma sp. B
1040 Paronaella cava
1050 Sethocapsa pseudouterculus
1054 Sethocapsa horokanaiensis
1079 Unuma darnoensis
1102 Saitoum dercourti
1104 Xitus (?) sp.
1110 Triactoma blakei *
1111 Triactoma parablakei *
1113 Guexella nudata
1114 Napora bukryi gr.
1115 Pantanellium oligoporum *
1116 Tritrabs exotica gr.
1117 Parahsuum spp.
1119 Cyrtocapsa aff. mastoidea *
1120 Parahsuum officerense *
1121 Pseudodictyomitra sp. C *
1122 Pseudodictyomitra sp. A *
1123 Pseudoeucyrtis sp. B *
1124 Sethocapsa accincta *
1125 Triactoma cf. southforkensis *
1126 Tricolocapsa sp. A *
1128 Yamatoum spp. *
1129 Pseudoeucyrtis hanni *
2001 Sethocapsa (?) perspicua
2002 Stichomitra communis
2004 Mita sp. B
2005 Mita sp. C *
2007 Pseudodictyomitra pentacolaensis
2008 Pseudodictyomitra lodogaensis
2010 Archaeocenosphaera (?) sp. A
2011 Pseudodictyomitra pseudomacrocephala
2012 Pseudodictyomitra lanceloti
2013 Thanarla praeveneta
2014 Novixitus weyli
2016 Rhopalosyringium majuroense
2017 Hemicryptocapsa sp. A
2018 Pantanellium spp.
2020 Tricapsula costata
2021 Afens liriodes
2022 Hemicryptocapsa polyhedra
2023 Hemicryptocapsa prepolyhedra
2024 Dictyomitra formosa
2025 Cryptamphorella conara
2026 Archaeodictyomitra (?) sp. A
2027 Rhopalosyringium sp. A
3006 Palinandromeda praepodbielensis
3008 Palinandromeda podbielensis
3010 Palinandromeda sp. A
3014 Eucyrtidiellum nodosum *
3017 Eucyrtidiellum ptyctum
3019 Eucyrtidiellum pyramis
3039 Trillus spp.
3041 Zartus spp.
3044 Stylocapsa catenarum *
3045 Stichocapsa naradaniensis *
3046 Stylocapsa (?) spiralis gr.

3048 Eucyrtidiellum (?) quinatum
3052 Eucyrtidiellum unumaense
3065 Acanthocircus trizonalis gr.
3066 Emiluvia pessagnoi
3069 Williriedellum crystallinum
3072 Parahsuum (?) magnum
3073 Parahsuum (?) natorense
3074 Linaresia chrafatensis
3087 Acanthocircus dicranacanthos
3089 Hexasaturnalis tetraspinus
3090 Acaeniotyle diaphorogona gr.
3092 Acaeniotyle umbilicata *
3096 Triactoma jonesi
3100 Perispyridium ordinarium gr.
3103 Homoeoparonaella argolidensis
3104 Homoeoparonaella elegans *
3110 Higumastra imbricata
3117 Tritrabs casmaliaensis
3121 Tetratrabs zealis
3122 Tetratrabs bulbosa
3123 Tetraditryma pseudoplena *
3127 Pseudocrucella sp. B *
3129 Pseudocrucella adriani *
3133 Paronaella pygmaea *
3137 Paronaella broennimanni
3139 Paronaella mulleri
3140 Paronaella kotura *
3145 Angulobracchia biordinalis
3147 Angulobracchia digitata
3151 Laxtorum (?) jurassicum
3160 Mirifusus guadalupensis
3161 Mirifusus dianae s.l.
3162 Mirifusus chenodes
3165 Ristola cretacea *
3170 Syringocapsa sp. A
3171 Podocapsa amphitreptera
3176 Pseudoeucyrtis sp. J
3177 Pseudoeucyrtis reticularis
3179 Transhsuum okamurai
3180 Transhsuum maxwelli gr.
3181 Transhsuum brevicostatum gr.
3182 Hsuum mclaughlini gr.
3185 Parvicingula boesii gr.
3189 Pseudodictyomitra primitiva *
3192 Stichomitra (?) sp. A
3193 Cinguloturris carpatica
3194 Transhsuum hisuikyoense
3195 Hsuum matsuokai
3197 Parvicingula dhimenaensis *
3199 Spongocapsula palmerae
3204 Orbiculiforma sp. A
3205 Orbiculiforma sp. D
3210 Emiluvia premyogii
3215 Emiluvia salensis
3216 Emiluvia sedecimporata
3221 Bernoullius cristatus *
3223 Bernoullius dicera
3224 Emiluvia orea
3225 Emiluvia hopsoni
3230 Podobursa spinosa
3231 Unuma echinatus
3237 Archaeodictyomitra (?) amabilis
3241 Ristola altissima altissima
3243 Staurosphaera antiqua
3247 Turanta spp.
3253 Emiluvia splendida
3255 Parvicingula cosmoconica
3259 Xitus sp. A
3263 Archaeodictyomitra apiarium
3267 Spongocapsula perampla *
3271 Archaeohagiastrum munitum
3273 Tetraditryma corralitosensis
3274 Mirifusus dianae dianae
3277 Theocapsomma cordis *
3279 Gongylothorax sp. aff. G. favosus *
3284 Pseudodictyomitra depressa
3286 Mirifusus dianae minor
3287 Archaeodictyomitra excellens
3292 Protunuma japonicus
3294 Xitus gifuensis *
3297 Tricolocapsa conexa
3298 Stichocapsa robusta
3305 Archaeodictyomitra minoensis
3307 Cyrtocapsa mastoidea *
3310 Paronaella aff. corpulenta
3558 Yamatoum (?) sp. A *
3631 Emiluvia spp.
3656 Hexasaturnalis
3681 Praeconocaryomma
3911 Angulobracchia (?) sp. A*
4009 Bernoullius furcospinus *
4010 Bernoullius rectispinus s.l.
4014 Dictyomitrella (?) kamoensis
4015 Emiluvia ordinaria
4026 Hemicryptocapsa capita
4031 Parahsuum (?) grande
4034 Protunuma turbo
4035 Pseudodictyomitra carpatica
4044 Stichomitra (?) takanoensis gr.
4049 Tricolocapsa (?) fusiformis *
4054 Tricolocapsa tetragona
4055 Williriedellum carpathicum
4058 Unuma latusicostatus
4059 Unuma typicus
4060 Williriedellum sp. A
4061 Ares spp.
4063 Acaeniotyle variata s.l.
4073 Noviforemanella diamphidia gr.
4079 Zhamoidellum ovum
5011 Acanthocircus variabilis

5012 Acanthocircus carinatus
5049 Suna hybum *
5073 Thanarla pulchra
5204 Crucella cf. cachensis
5229 Cecrops septemporatus
5296 Thanarla elegantissima *
5422 Dibolachras tytthopora *
5426 Syringocapsa limatum
5462 Sethocapsa uterculus
5481 Sethocapsa kaminogoensis
5532 Crolanium pythiae *
5582 Mita gracilis
5595 Archaeodictyomitra lacrimula
5636 Pseudodictyomitra puga
5712 Parvicingula usotanensis
6101 Cinguloturris sp. A
6107 Holocryptocanium barbui *

PLATES

General remarks:

Related or similar forms are presented together to allow an easier comparison. The arrangement of illustrations therefore differs from the alphabetical order of genera and species followed in the text.

For each illustration the sample number, corresponding Unitary Association, age assignment of the given sample, SEM-negative number, and magnification are indicated.

Most scanning electron micrographs were taken on a CAMSCAN Series 4, at the Institute of Geology and Paleontology, University of Lausanne, others were taken on a JEOL JSM-330A at the Ivan Rakovec Paleontological Institute, Slovenian Academy of Sciences and Arts.

Rock samples, residues and SEM negatives are stored in the author's collection.

PLATE 1

1. *Trillus* sp.
GL/127 (U.A.3), Bajocian, 890237, 200x

2–4. *Zartus* spp.
2: BjI/10 (U.A.4), Bajocian, 910224, 200x
3: BjI/10 (U.A.4), Bajocian, 910223, 200x
4: GL/128 (U.A.5), Bajocian, 903412, 200x

5. *Cecrops septemporatus* (PARONA)
PK/3, 892636, 200x

6. *Gorgansium gongyloideum* KISHIDA & HISADA
BM/18, lower Liassic, 920806, 200x

7–9. *Pantanellium oligoporum* (VINASSA)
7: BM/106 (U.A.26), Kimmeridgian, 900530, 200x
8: BM/106 (U.A.26), Kimmeridgian, 900531, 200x
9: BM/106 (U.A.26), Kimmeridgian, 900528, 200x

10–13. *Pantanellium* spp.
10: DIN/29.30 (U.A.33), Berriassian-lower Valanginian, 910330, 200x
11: BM/102 (U.A.17), Oxfordian, 900403, 200x
12: BjIV/18 (U.A.38), lower Aptian, 915129, 150x
13: UPC/32 (U.A.40), lower Aptian, 921526, 200x

14–18. *Pantanellium tanuense* PESSAGNO & BLOME
14: GL/109, Hettangian, 921132, 200x
15: BM/11, Hettangian, 920706, 200x
16: BM/11, Hettangian, 920710, 200x
17: BM/11, Hettangian, 920707, 200x
18: BM/11, Hettangian, 920709, 200x

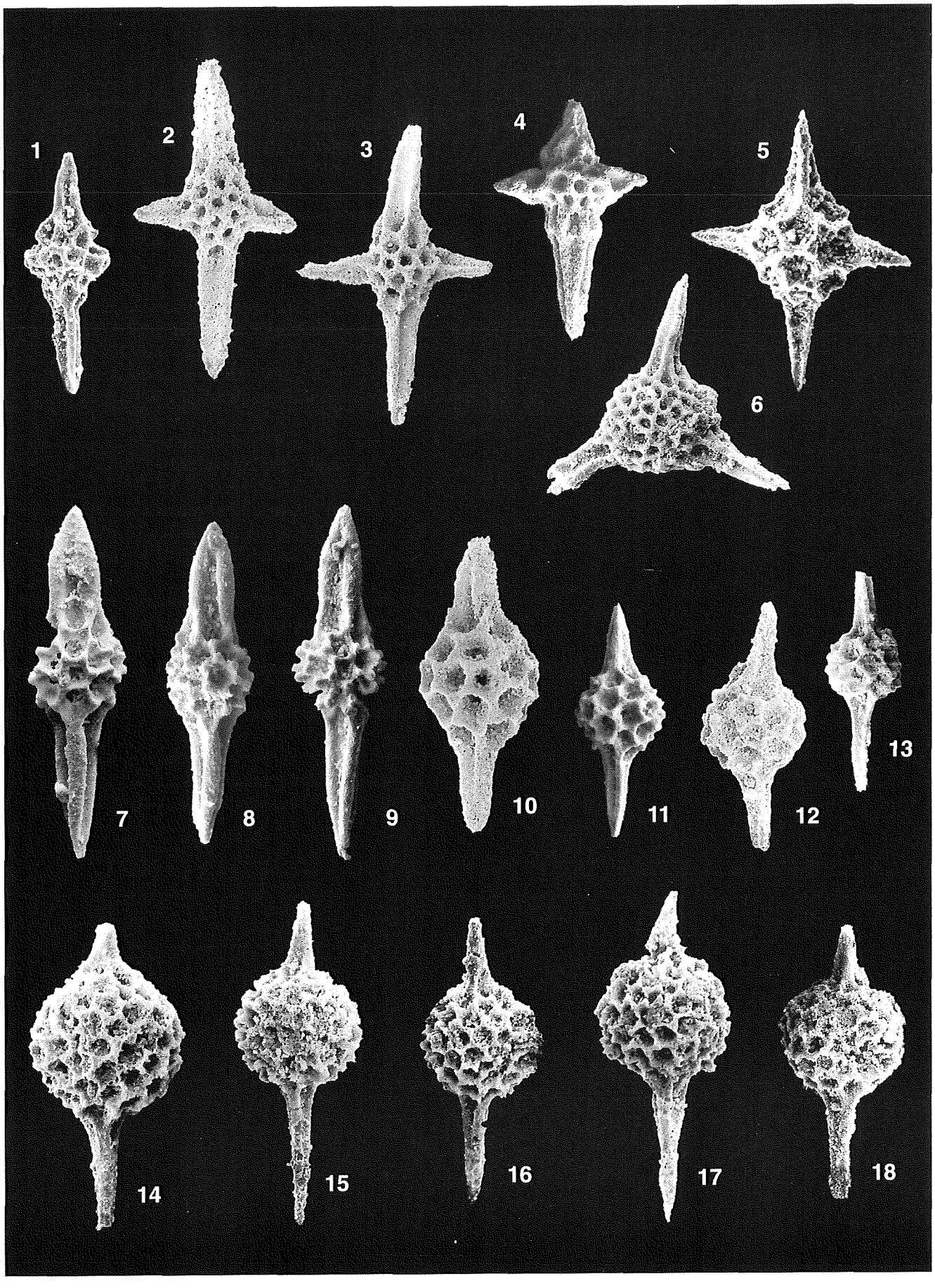
1
2
3
4
5
6
7
8
9
10
11
12
13
14
15
16
17
18

PLATE 2

1. *Suna hybum* (FOREMAN)
PK/3, 892633, 200x

2–3. *Parvivacca blomei* PESSAGNO & YANG
2: GL/209+6.60 (U.A.22), Oxfordian, 911002, 150x
3: DIN/2.35 (U.A.21), Oxfordian, 910123, 150x

4. *Triactoma parablakei* YANG & WANG
UPC/18 (U.A.15), Callovian, 922101, 150x

5–6. *Triactoma blakei* (PESSAGNO)
5: GL/209 (U.A.16), Oxfordian, 901701, 150x
6: GL/209+6.60 (U.A.22), Oxfordian, 911030, 150x

7. *Triactoma* cf. *southforkensis* (PESSAGNO & YANG)
GL/127 (U.A.3), Bajocian, 903103, 150x

8–9. *Triactoma jonesi* (PESSAGNO)
8: BM/102 (U.A.17), Oxfordian, 900214, 150x
9: GL/123 (U.A.1), Aalenian-lower Bajocian, 921013, 150x

10, 11, 15. *Acaeniotyle diaphorogona* FOREMAN gr.
10: UPC/34 (U.A.45), Albian, 920310, 150x
11: GL/209+6.60 (U.A.22), Oxfordian, 910936, 150x
15: BM/102 (U.A.17), Oxfordian, 900207, 150x

12. *Acaeniotyle umbilicata* (RÜST)
BjIV/18+1.55 (U.A.39), lower Aptian, 914812, 150x

13. *Praeconocaryomma* sp.
PK/20, lower Liassic, 920932, 200x

14. *Acaeniotyle variata* (OŽVOLDOVA) s.l.
ZB/28 (U.A.6), upper Bajocian, 890122, 150x

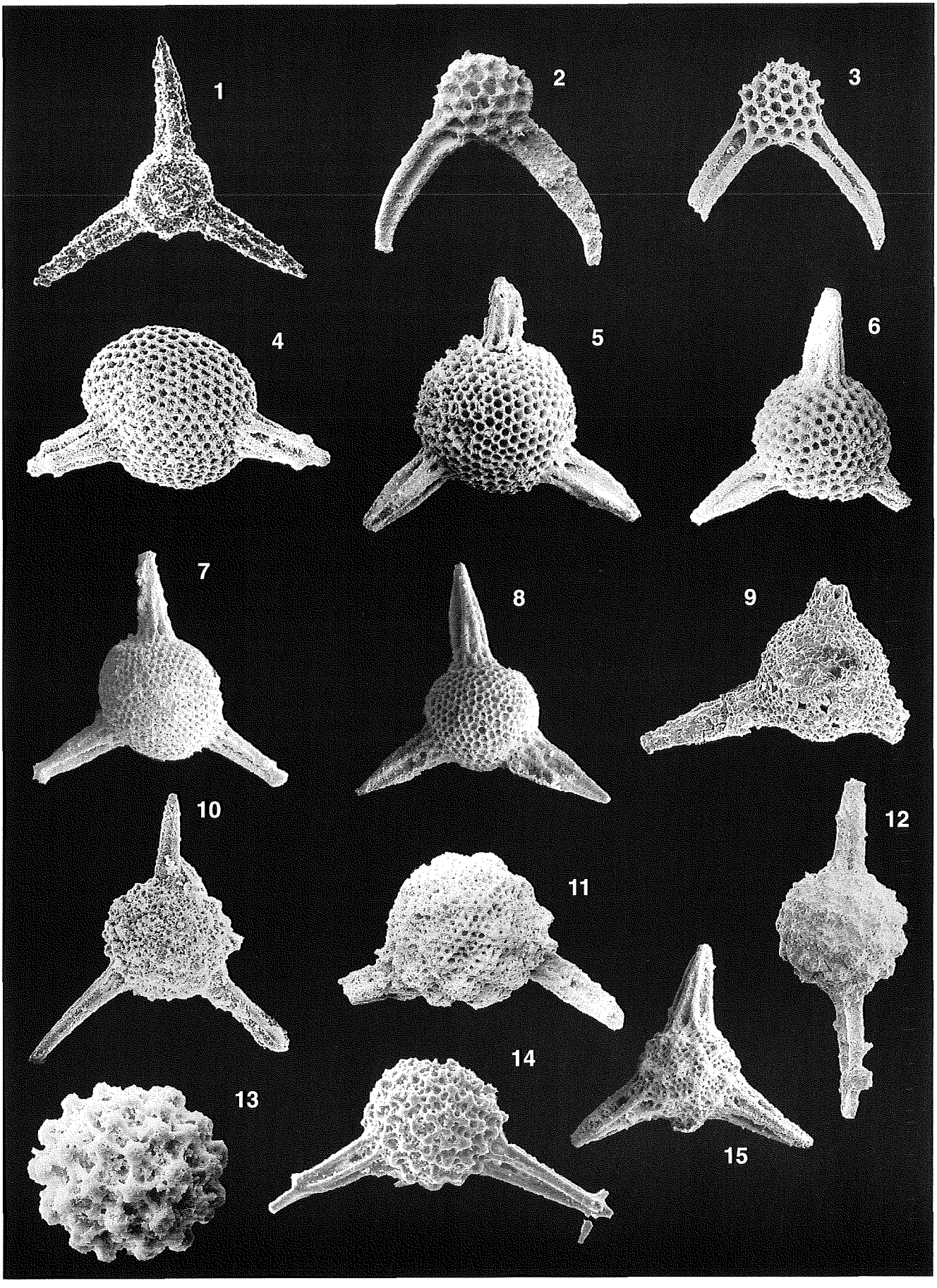
1
2
3
4
5
6
7
8
9
10
11
12
13
14
15

PLATE 3

1–2. *Acanthocircus trizonalis* (RÜST) gr.
1: BM/489.40 (U.A.41), upper Aptian-lower Albian, 913128, 100x
2: BM/102 (U.A.17), Oxfordian, 900210, 100x

3. *Acanthocircus variabilis* (SQUINABOL)
BM/478.60 (U.A.37), Hauterivian-Barremian, 914332, 200x

4. *Acanthocircus carinatus* FOREMAN
UPC/298.60 (U.A.39), lower Aptian, 915331, 200x

5–6. *Archaeocenosphaera* (?) sp.
5: UPC/35 (U.A.48), Turonian, 902416, 150x
6: UPC/35 (U.A.48), Turonian, 902415, 150x

7. *Orbiculiforma* sp.
GL/105, Hettangian, 921102, 200x

8–9. *Orbiculiforma* sp. B sensu WIDZ
8: UPC/23 (U.A.18), Oxfordian, 902826, 200x
9: BM/102 (U.A.17), Oxfordian, 900319, 200x

10–12. *Orbiculiforma* sp. D sensu WIDZ
10: UPC/18 (U.A.15), Callovian, 922120, 150x
11: UPC/21 (U.A.17), Oxfordian, 901301, 150x
12: UPC/23 (U.A.18), Oxfordian, 902825, 200x

13. *Orbiculiforma* sp.
GL/123 (U.A.1), Aalenian-lower Bajocian, 921917, 200x

14–15. *Orbiculiforma* sp. A sensu WIDZ
14: BM/102 (U.A.17), Oxfordian, 900102, 150x
15: BM/102 (U.A.17), Oxfordian, 900236, 150x

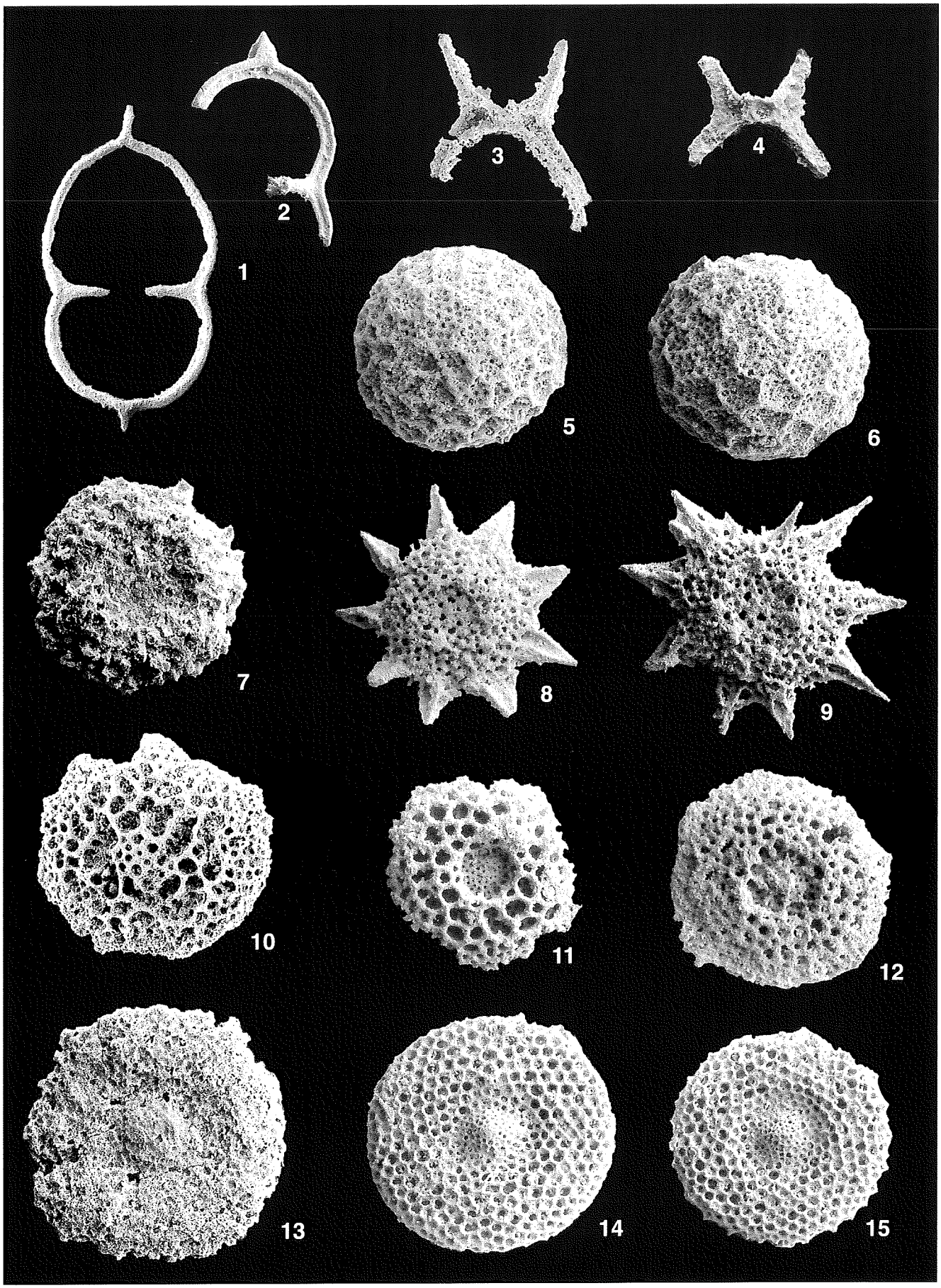
1
2
3
4
5
6
7
8
9
10
11
12
13
14
15

PLATE 4

1–2, 3a–b. *Emiluvia premyogii* BAUMGARTNER
1: GL/209+6.60 (U.A.22), Oxfordian, 910922, 150x
2: BM/102 (U.A.17), Oxfordian, 900312, 150x
3a–b: specimen with a pylome, BjII/15/1 (U.A.22), Oxfordian, 901807, 901808, 200x

4. *Emiluvia sedecimporata* (RÜST)
GL/209+6.60 (U.A.22), Oxfordian, 910915, 150x

5. *Emiluvia ordinaria* OŽVOLDOVA
GL/209+6.60 (U.A.22), Oxfordian, 911020, 150x

6. *Emiluvia pessagnoi* FOREMAN
BM/8 (U.A.30), Tithonian, 922702, 150x

7–8. *Emiluvia salensis* FOREMAN
7: BM/102 (U.A.17), Oxfordian, 900429, 100x
8: BM/102 (U.A.17), Oxfordian, 900118, 100x

9. *Emiluvia hopsoni* PESSAGNO
BM/102 (U.A.17), Oxfordian, 900209, 100x

10–11. *Emiluvia orea* BAUMGARTNER
10: UPC/23 (U.A.18), Oxfordian, 902906, 100x
11: DIN/2.35 (U.A.21), Oxfordian, 910119, 100x

12. *Emiluvia splendida* CARTER
ZB/28 (U.A.6), upper Bajocian, 890520, 150x

13–15. *Staurosphaera antiqua* (RÜST)
13: UPC/23 (U.A.18), Oxfordian, 902908, 100x
14: DIN/2.35 (U.A.21), Oxfordian, 910117, 100x
15: BM/102 (U.A.17), Oxfordian, 900230, 100x

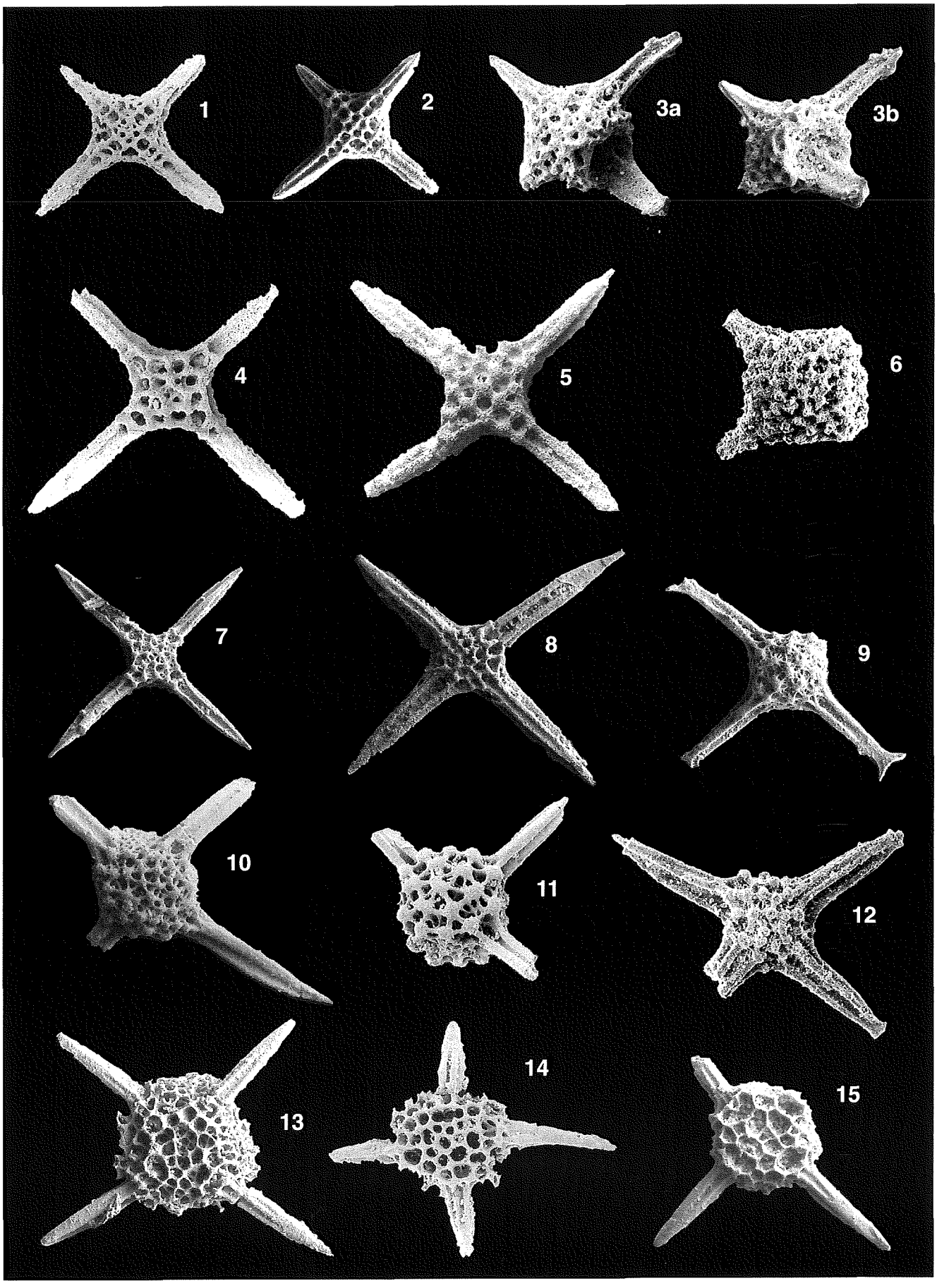
1
2
3a
3b
4
5
6
7
8
9
10
11
12
13
14
15

PLATE 5

1–2. Hagiastrid gen. indet. spp.
1: BM/102 (U.A.17), Oxfordian, 900106, 100x
2: BM/102 (U.A.17), Oxfordian, 900107, 100x

3–6. *Tritrabs exotica* (PESSAGNO) gr.
3: UPC/251.50 (U.A.19), Oxfordian, 912103, 100x
4: BM/102 (U.A.17), Oxfordian, 900432, 100x
5: UPC/21 (U.A.17), Oxfordian, 901316, 100x
6: UPC/251.50 (U.A.19), Oxfordian, 912104, 100x

7. *Tetratrabs bulbosa* BAUMGARTNER
GL/209+6.60 (U.A.22), Oxfordian, 910907, 100x

8–9. *Tritrabs casmaliaensis* (PESSAGNO)
8: GL 209+6.60, Oxfordian, 910905, 150x
9: UPC/21 (U.A.17), Oxfordian, 901321, 150x

10–11. *Tetratrabs zealis* (OŽVOLDOVA)
10: BM/102 (U.A.17), Oxfordian, 900414, 100x
11: BM/102 (U.A.17), Oxfordian, 900101, 100x

12. *Tetraditryma pseudoplena* BAUMGARTNER
BM/102 (U.A.17), Oxfordian, 900408, 100x

13. *Higumastra imbricata* (OŽVOLDOVA)
BjI/12 (U.A.10), Bathonian, 901516, 150x

14. *Archaeohagiastrum munitum* BAUMGARTNER
BjI/12 (U.A.10), Bathonian, 901501, 200x

15–16. *Tetraditryma corralitosensis* (PESSAGNO)
15: GL/134 (U.A.9), Bathonian, 922431, 200x
16: BM/102 (U.A.17), Oxfordian, 903137, 150x

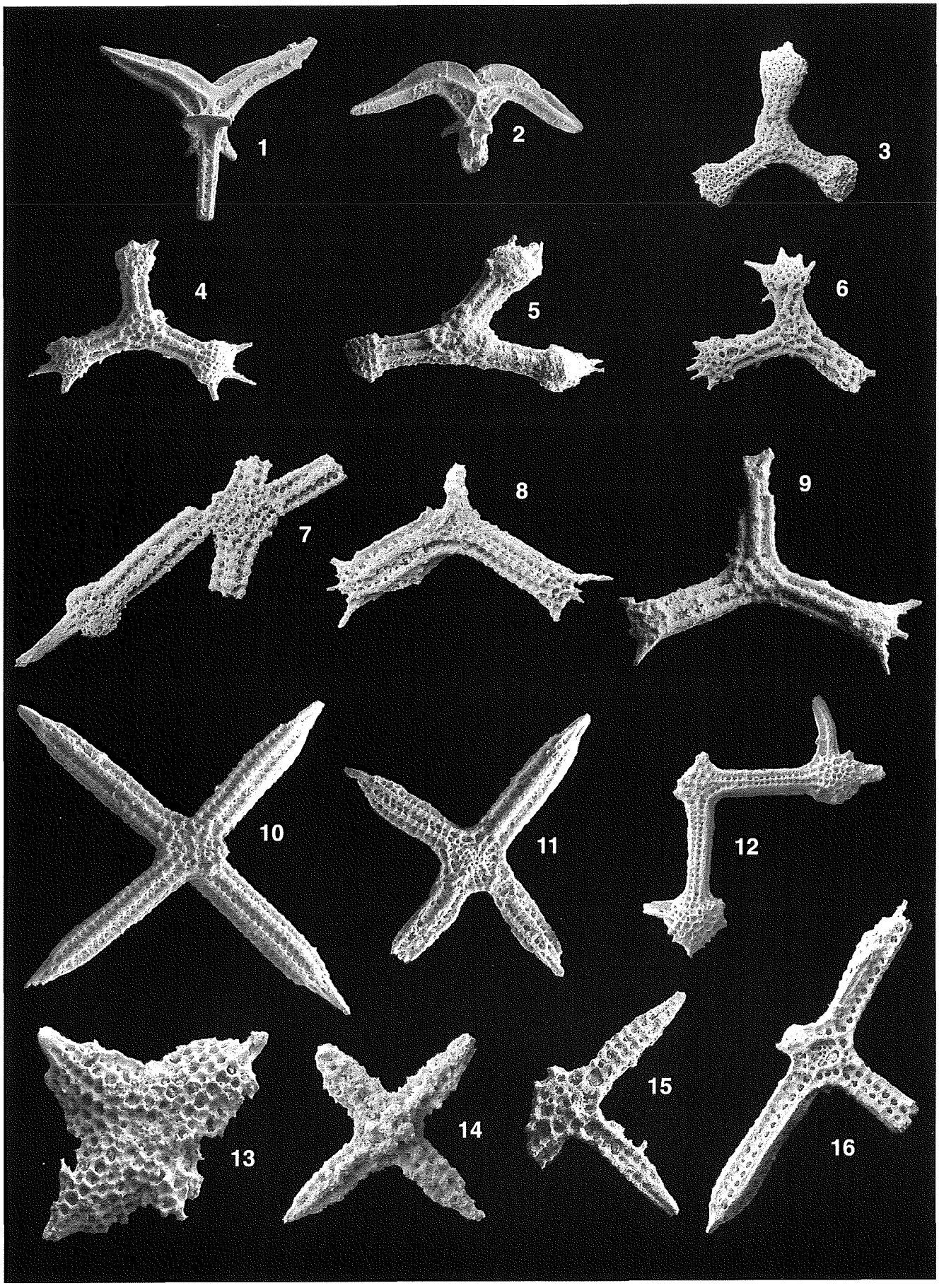
1
2
3
4
5
6
7
8
9
10
11
12
13
14
15
16

PLATE 6

1. *Angulobracchia digitata* BAUMGARTNER
BM/102 (U.A.17), Oxfordian, 900121, 100x

2–3. *Angulobracchia biordinalis* OŽVOLDOVA
2: UPC/251.50 (U.A.19), Oxfordian, 912028, 100x
3: GL/209+6.60 (U.A.22), Oxfordian, 910908, 100x

4–5. *Homoeoparonaella argolidensis* BAUMGARTNER
4: GL/209 (U.A.16), Oxfordian, 901605, 100x
5: GL/209+6.60 (U.A.22), Oxfordian, 910920, 100x

6–7, 9–10. *Paronaella broennimanni* PESSAGNO
6: UPC/23 (U.A.18), Oxfordian, 902909, 150x
7: UPC/251.50 (U.A.19), Oxfordian, 912105, 150x
9: BM/102 (U.A.17), Oxfordian, 900218, 100x
10: BM/102 (U.A.17), Oxfordian, 900412, 100x

8. *Homoeoparonaella elegans* (PESSAGNO)
BM/102 (U.A.17), Oxfordian, 900418, 100x

11. *Crucella* cf. *cachensis* PESSAGNO
BM/489.40 (U.A.41), upper Aptian-lower Albian, 913016, 150x

12. *Pseudocrucella* sp. B sensu BAUMGARTNER
BM/102 (U.A.17), Oxfordian, 900407, 150x

13–14. *Pseudocrucella adriani* BAUMGARTNER
13: BM/102 (U.A.17), Oxfordian, 900413, 150x
14: GL/209+6.60 (U.A.22), Oxfordian, 900407, 150x

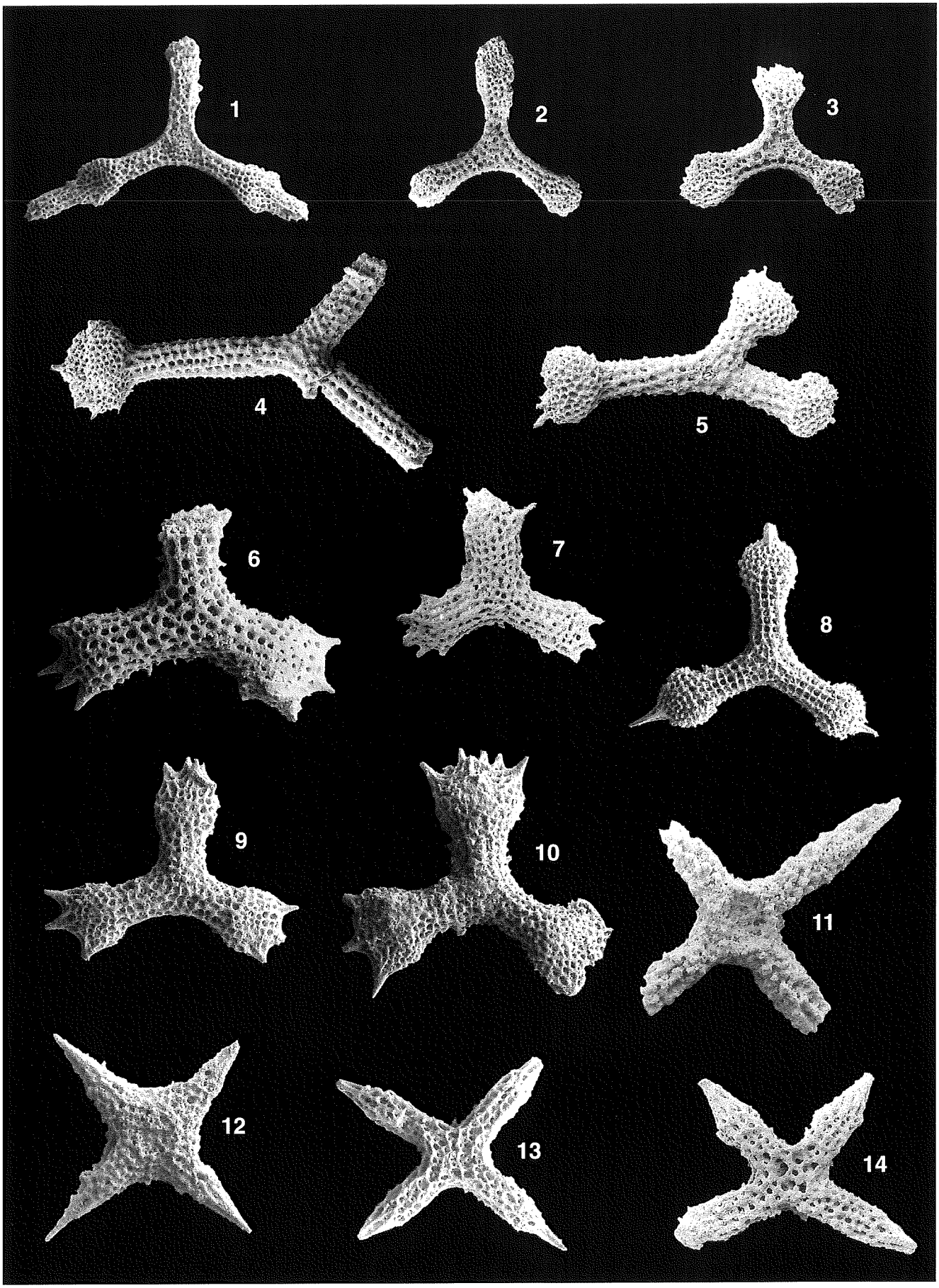
1
2
3
4
5
6
7
8
9
10
11
12
13
14

PLATE 7

1–3. *Noviforemanella diamphidia* (FOREMAN) gr.
1: GL/209+6.60 (U.A.22), Oxfordian, 910901, 150x
2: BM/489.40 (U.A.41), upper Aptian-lower Albian, 913124, 150x
3: GL/144 (U.A.39), lower Aptian, 915610, 150x

4–6. *Paronaella cava* (OŽVOLDOVA)
4: GL/209+6.60 (U.A.22), Oxfordian, 910903, 100x
5: GL/209+6.60 (U.A.22), Oxfordian, 910902, 100x
6: BM/106 (U.A.26), Kimmeridgian, 900601, 100x

7. *Angulobracchia* (?) sp. A
UPC/27 (U.A.29), Tithonian, 901928, 150x

8–10. *Paronaella mulleri* PESSAGNO
8: BM/102 (U.A.17), Oxfordian, 900307, 150x
9: UPC/22 (U.A.17), Oxfordian, 903009, 150x
10: UPC/257.10 (U.A.23), upper Oxfordian-Kimmeridgian, 911913, 150x

11. *Paronaella* sp.
UPC/41.50, lower Liassic, 921018, 100x

12. *Paronaella kotura* BAUMGARTNER
UPC/23 (U.A.18), Oxfordian, 902904, 100x

13. *Paronaella pygmaea* BAUMGARTNER
UPC/22 (U.A.17), Oxfordian, 902934, 200x

14–16. *Paronaella* aff. *corpulenta* DE WEVER
14: GL/123 (U.A.1), Aalenian-lower Bajocian, 921909, 100x
15: GL/123 (U.A.1), Aalenian-lower Bajocian, 921904, 100x
16: GL/123 (U.A.1), Aalenian-lower Bajocian, 893602, 150x

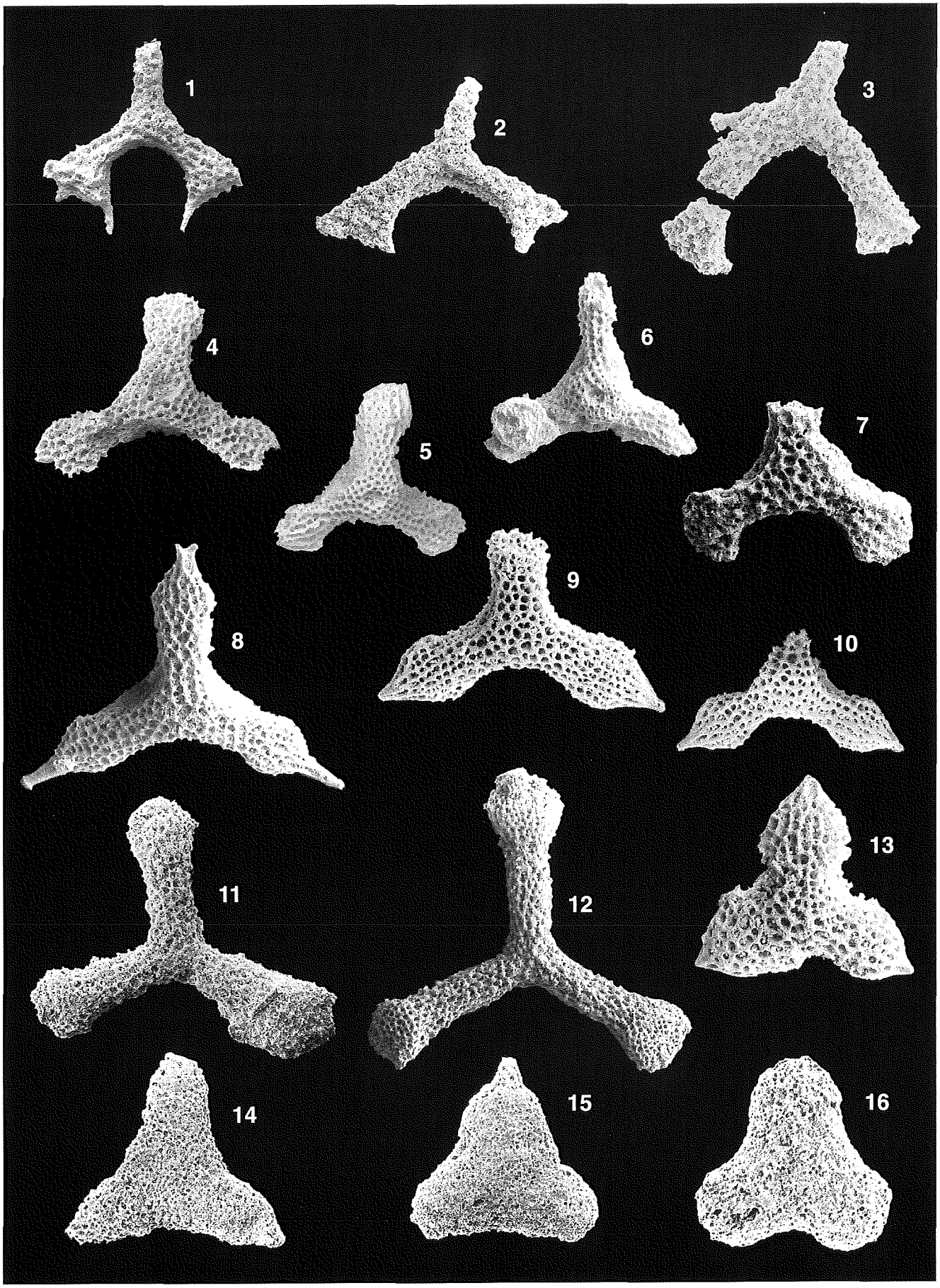
1
2
3
4
5
6
7
8
9
10
11
12
13
14
15
16

PLATE 8

1–4. *Bernoullius dicera* (BAUMGARTNER)
1: BM/102 (U.A.17), Oxfordian, 900223, 150x
2: UPC/23 (U.A.18), Oxfordian, 902834, 200x
3: BM/102 (U.A.17), Oxfordian, 900223, 150x
4: GL/128 (U.A.5), Bajocian, 903413, 150x

5. *Bernoullius cristatus* BAUMGARTNER
GL/207 (U.A.12), Bathonian, 901012, 150x

6. *Bernoullius* cf. *cristatus* BAUMGARTNER
BM/102 (U.A.17), Oxfordian, 900428, 150x

7–9, 11–18. *Bernoullius rectispinus* KITO, DE WEVER, DANELIAN & CORDEY s.l.
7: GL/134 (U.A.9), Bathonian, 890813, 200x
8: GL/134 (U.A.9), Bathonian, 922508, 200x
9: BM/102 (U.A.17), Oxfordian, 900431, 150x
11: ZB/28 (U.A.6), upper Bajocian, 890509, 200x
12: BM/102 (U.A.17), Oxfordian, 900213, 150x
13: DIN/2.35 (U.A.21), Oxfordian, 910114, 150x
14: GL/127 (U.A.3), Bajocian, 903106, 200x
15: BM/102 (U.A.17), Oxfordian, 900425, 150x
16: BM/102 (U.A.17), Oxfordian, 900423, 150x
17: GL/128 (U.A.5), Bajocian, 903414, 150x
18: ZB/28 (U.A.6), upper Bajocian, 890407, 150x

10. *Bernoullius* (?) sp.
BM/102 (U.A.17), Oxfordian, 900117, 150x

19. *Bernoullius furcospinus* KITO, DE WEVER, DANELIAN & CORDEY
ZB/28 (U.A.6), upper Bajocian, 890134, 150x

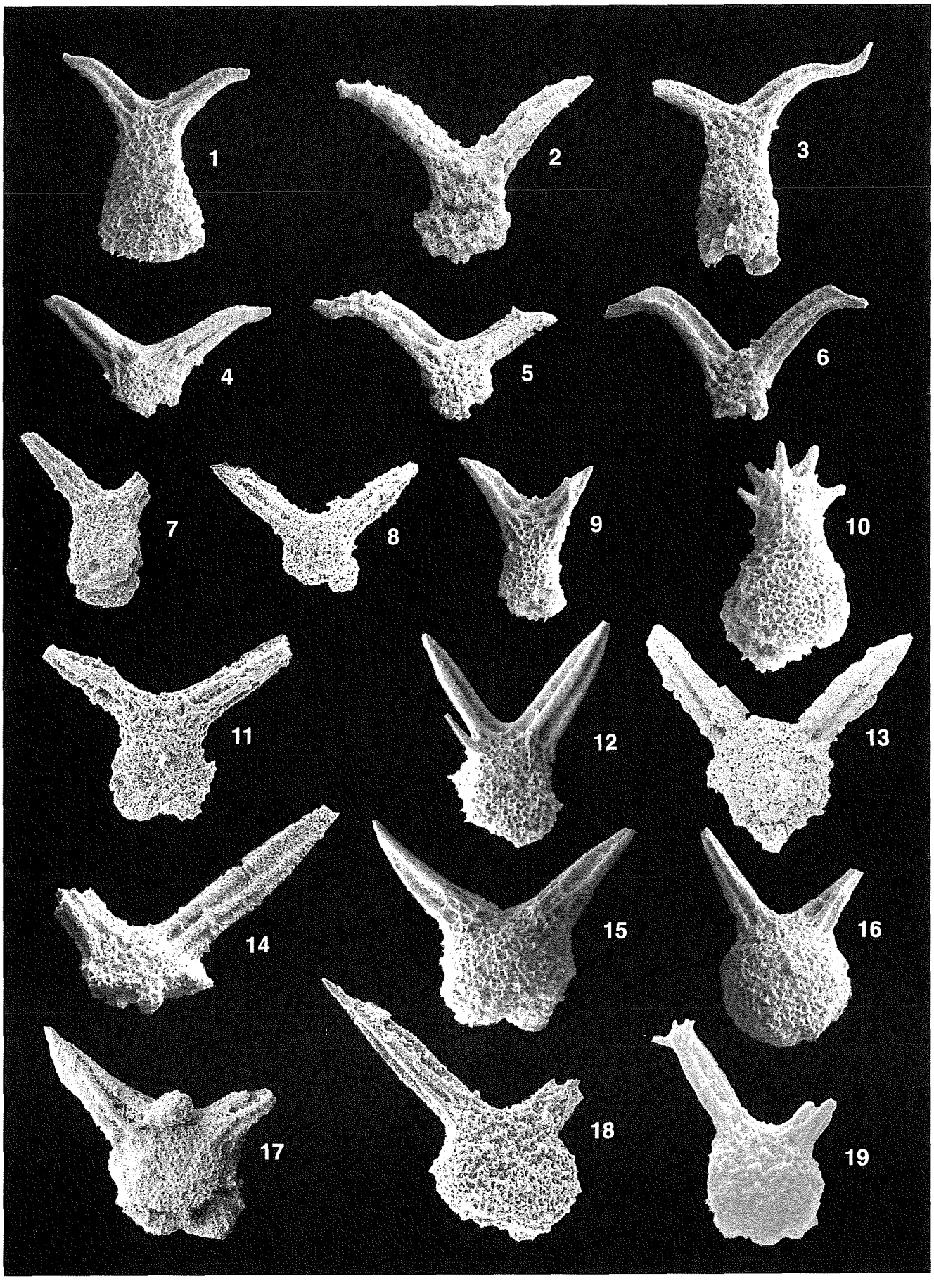
1
2
3
4
5
6
7
8
9
10
11
12
13
14
15
16
17
18
19

PLATE 9

1–2. *Eucyrtidiellum ptyctum* (RIEDEL & SANFILIPPO)
1: UPC/18 (U.A.15), Callovian, 900516, 300x
2: BjII/15/1 (U.A.22), Oxfordian, 901831, 300x

3–4. *Eucyrtidiellum pyramis* (AITA)
3: GL/142 (U.A.34), Berriasian-lower Valanginian, 892021, 300x
4: DIN/29.30 (U.A.33), Berriasian-lower Valanginian, 910406, 300x

5–6. *Eucyrtidiellum unumaense* (YAO)
5: GL/209 (U.A.16), Oxfordian, 900712, 300x
6: GL/209 (U.A.16), Oxfordian, 900805, 300x

7. *Eucyrtidiellum nodosum* WAKITA
GL/209 (U.A.16), Oxfordian, 900706, 300x

8–12. *Eucyrtidiellum* (?) *quinatum* TAKEMURA
8: GL/127 (U.A.3), Bajocian, 890429, 300x
9: GL/127 (U.A.3), Bajocian, 890428, 300x
10: GL/125 (U.A.2), Aalenian-lower Bajocian, 892503, 300x
11: GL/125 (U.A.2), Aalenian-lower Bajocian, 892437, 300x
12: GL/125 (U.A.2), Aalenian-lower Bajocian, 892425, 300x

13. *Theocapsomma cordis* KOCHER
GL/207 (U.A.12), Bathonian, 901037, 400x

14. *Tricolocapsa* (?) *fusiformis* YAO
ZB/28 (U.A.6), upper Bajocian, 903337, 300x

15. *Cyrtocapsa mastoidea* YAO
ZB/28 (U.A.6), upper Bajocian, 890131, 300x

16. *Guexella* sp.
ZB/28 (U.A.6), upper Bajocian, 852700, 200x

17–19. *Guexella nudata* (KOCHER) s.l.
17: GL/207 (U.A.12), Bathonian, 901035, 300x
18: UPC/20 (U.A.15), Callovian, 901331, 300x
19: UPC/18 (U.A.15), Callovian, 900507, 200x

20. *Cyrtocapsa* aff. *mastoidea* YAO
GL/6 (U.A.8), Bathonian, 890622, 400x

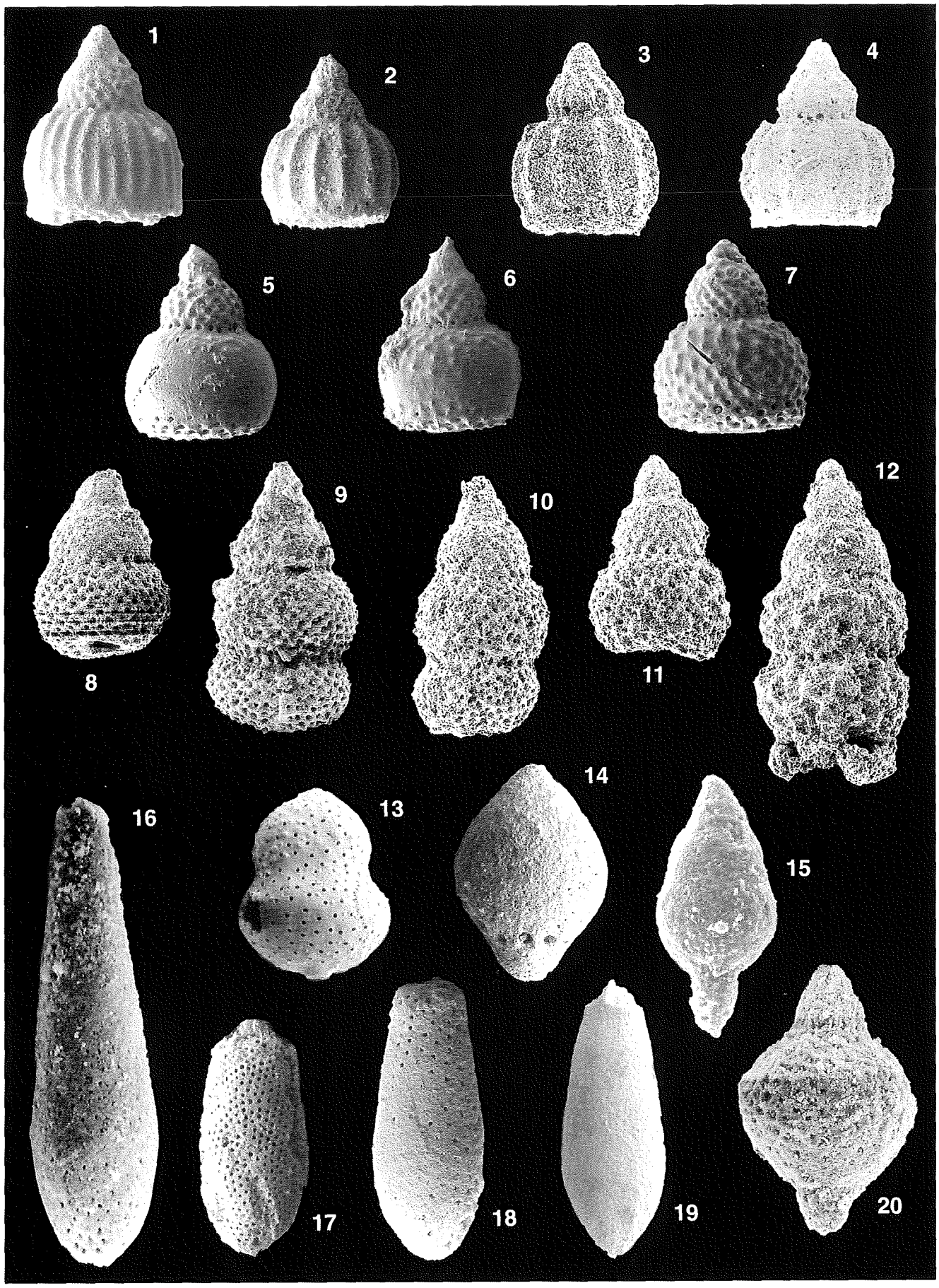
1
2
3
4
5
6
7
8
9
10
11
12
13
14
15
16
17
18
19
20

PLATE 10

1–2. *Protunuma japonicus* MATSUOKA & YAO
1: BM/102 (U.A.17), Oxfordian, 900217, 300x
2: UPC/27 (U.A.29), Tithonian, 901921, 200x

3–4. *Tricapsula costata* WU
3: BjIV/20 (U.A.42), upper Aptian-lower Albian, 921536, 300x
4: BjIV/20 (U.A.42), upper Aptian-lower Albian, 921604, 300x

5a–b, 6. *Protunuma turbo* MATSUOKA
5a–b: BjI/12 (U.A.10), Bathonian, a: 901502, 300x; b: antapical view, 901504, 300x
6: GL/134 (U.A.9), Bathonian, 922428, 300x

7, 8, 9a–b. *Unuma darnoensis* KOZUR
7: ZB/28 (U.A.6), upper Bajocian, 890416, 300x
8: ZB/28 (U.A.6), upper Bajocian, 890515, 300x
9a–b: ZB/28 (U.A.6), upper Bajocian, 890418, 890419, 300x

10–11. *Unuma echinatus* ICHIKAWA & YAO
10: GL/127 (U.A.3), Bajocian, 890241, 300x
11: GL/132 (U.A.7), upper Bajocian, 892135, 300x

12. *Unuma latusicostatus* (AITA)
ZB/28 (U.A.6), upper Bajocian, 890339, 300x

13. *Unuma typicus* ICHIKAWA & YAO
BjI/10 (U.A.4), Bajocian, 910231, 300x

14–15. *Yamatoum* spp.
14: GL/127 (U.A.3), Bajocian, 903116, 300x
15: ZB/28 (U.A.6), upper Bajocian, 861338, 300x

16. *Yamatoum* (?) sp. A
ZB/28 (U.A.6), upper Bajocian, 903336, 300x

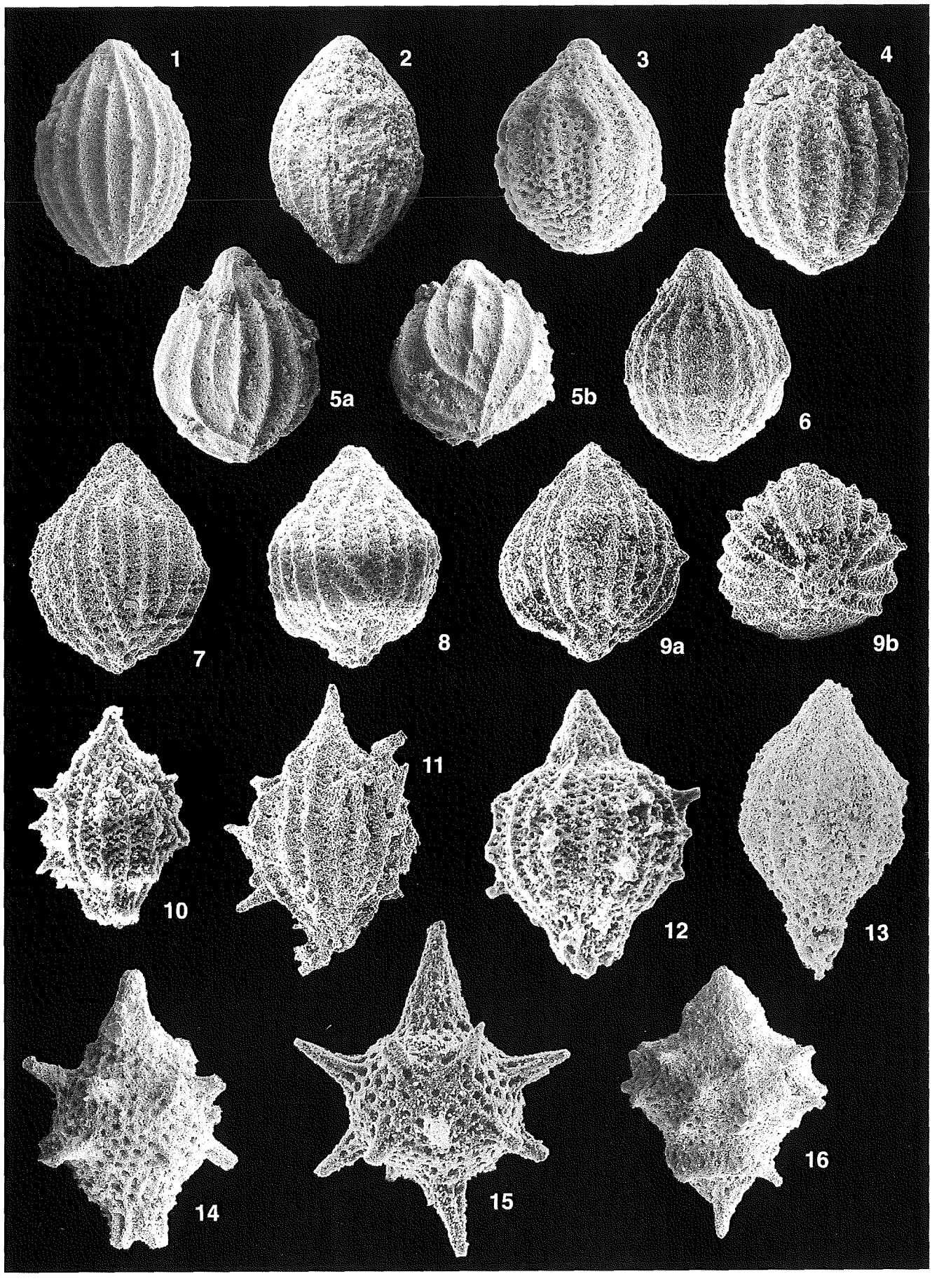
1
2
3
4
5a
5b
6
7
8
9a
9b
10
11
12
13
14
15
16

PLATE 11

1a–c, 2. *Stylocapsa* (?) *spiralis* MATSUOKA gr.
1a–c: UPC/18 (U.A.15), Callovian; 1a: 922209, 1b: apical view, 922210 1c: antapical view, 922211, 300x
2: UPC/18 (U.A.15), Callovian, 922137, 300x

3–5. *Stylocapsa catenarum* MATSUOKA
3: UPC/18 (U.A.15), Callovian, 922109, 400x
4: UPC/18 (U.A.15), Callovian, 922110, 400x
5: UPC/18 (U.A.15), Callovian, 922130, 400x

6. *Stichocapsa naradaniensis* MATSUOKA
UPC/18 (U.A.15), Callovian, 922324, 300x

7–10. *Tricolocapsa conexa* MATSUOKA
7a–b: UPC/18 (U.A.15), Callovian, 7a: 922204, 7b: antapical view, 922205, 300x
8: UPC/18 (U.A.15), Callovian, 900510, 300x
9: ZB/28 (U.A.6), upper Bajocian, 903328, 300x
10a–b: UPC/18 (U.A.15), Callovian, 10a: 922108, 10b: antapical view, 922107, 300x

11–13. *Tricolocapsa* sp. A
11a–b: UPC/18 (U.A.15), Callovian, 11a: 922214, 11b: antapical view, 922215, 300x
12a–b: UPC/18 (U.A.15), Callovian, 12a: 922323, 12b: antapical view, 922322, 300x
13a–b: UPC/18 (U.A.15), Callovian, 13a: 922321, 13b: antapical view, 922320, 300x

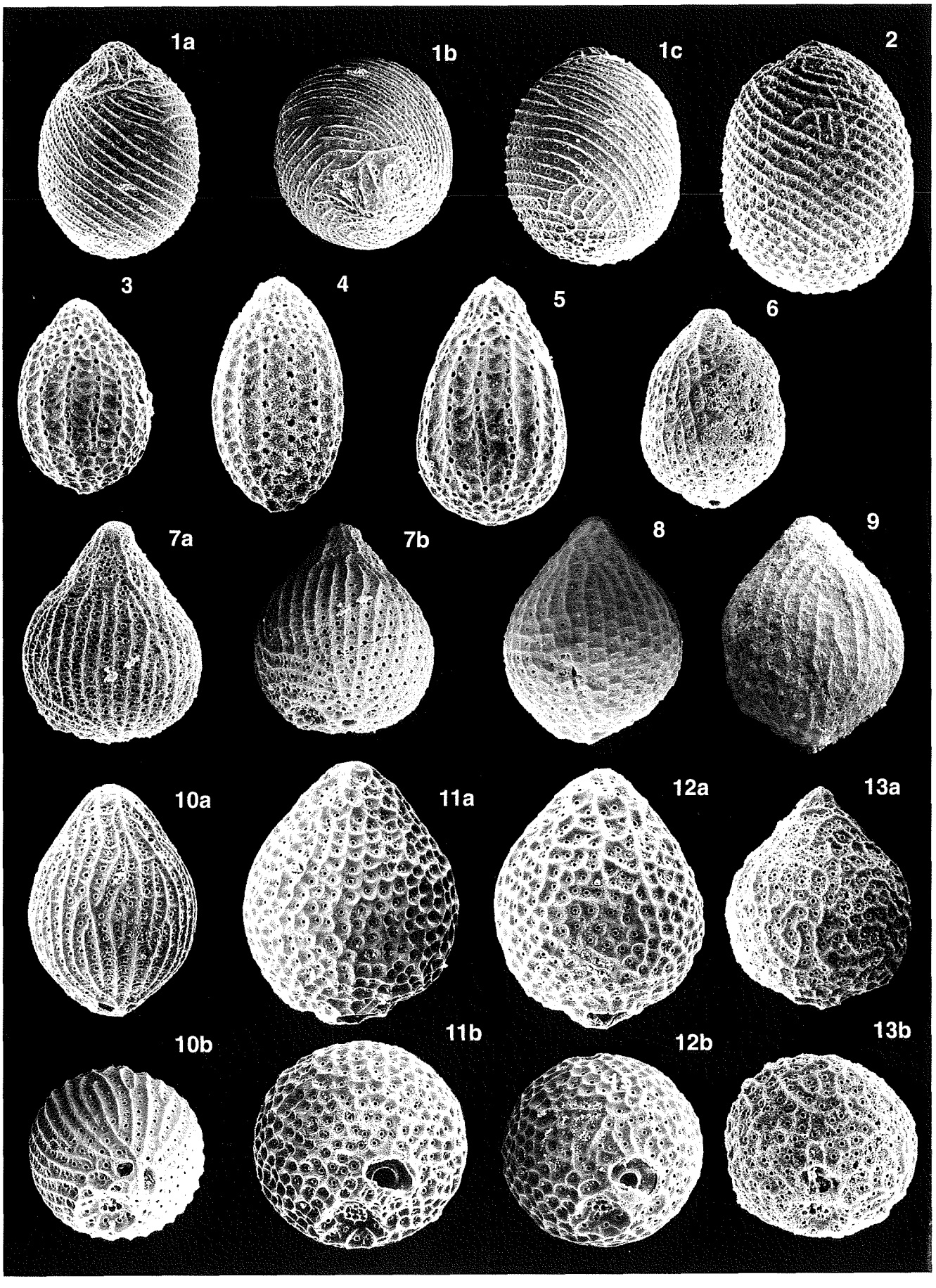
1a
1b
1c
2
3
4
5
6
7a
7b
8
9
10a
11a
12a
13a
10b
11b
12b
13b

PLATE 12

1, 2a–c. *Williriedellum crystallinum* DUMITRICA
1: BjII/15/1 (U.A.22), Oxfordian, 901820, 300x
2a–c: BjII/15/1 (U.A.22), Oxfordian, 2a: 901825, 2b: apical view, 901824, 2c: antapical view, 901823, 300x

3–5. *Hemicryptocapsa capita* TAN
3: DIN/31.50 (U.A.35), upper Valanginian-Hauterivian, 920108, 300x
4: DIN/31.50 (U.A.35), upper Valanginian-Hauterivian, 920111, 300x
5: GL/214 (U.A.37), Hauterivian-Barremian, 915619, 200x

6a–b, 7, 8: *Williriedellum carpathicum* DUMITRICA
6a–b: GL/209 (U.A.16), Oxfordian, 6a: antapical view, 900809, 6b: 900808, 300x
7: UPC/251.50 (U.A.19), Oxfordian, 912131, 300x
8: DIN/11.55 (U.A.26), Kimmeridgian, 911528, 300x

9–11: *Williriedellum* sp. A sensu MATSUOKA
9a–c: GL/209 (U.A.16), Oxfordian, 9a: apical view, 900902, 9b: 900903, 9c: antapical view, 900839, 300x
10a–c: UPC/18 (U.A.15), Callovian, 10a: 922232, 10b: apical view, 922234, 10c: antapical view, 922233, 300x
11a–b: UPC/23 (U.A.18), Oxfordian, 11a: 902804, 11b: 902803, 300x

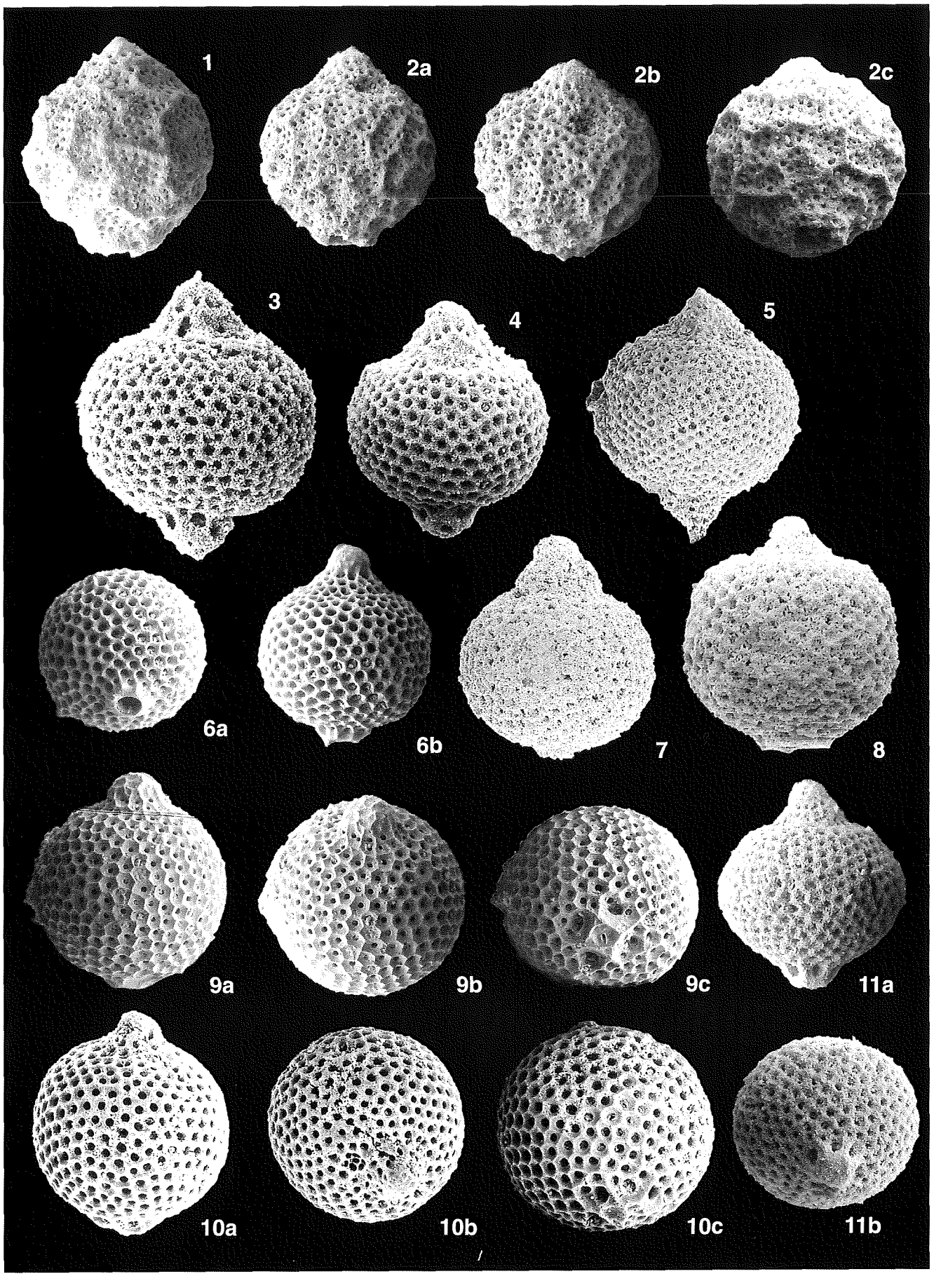
1
2a
2b
2c
3
4
5
6a
6b
7
8
9a
9b
9c
11a
10a
10b
10c
11b

PLATE 13

1–2. *Zhamoidellum* sp. A
1: UPC/27 (U.A.29), Tithonian, 902005, 300x
2: GL/138 (U.A.31), Tithonian, 921821, 300x

3–7. *Zhamoidellum ovum* DUMITRICA
3: DIN/11.55 (U.A.26), Kimmeridgian, 911531, 300x
4: BM/106 (U.A.26), Kimmeridgian, 900613, 300x
5: BjII/15/1 (U.A.22); Oxfordian, 5a: 901907, 5b: antapical view, 901908, 300x
6: UPC/257.10 (U.A.23), upper Oxfordian-Kimmeridgian, 911932, 300x
7: UPC/257.10 (U.A.23), upper Oxfordian-Kimmeridgian, 911936, 300x

8, 10. *Tricolocapsa tetragona* MATSUOKA
8: GL 135, Bathonian, 922414, 300x
10: BjI/13 (U.A.11), Bathonian, 902401, 300x

9a–c, 11a–c. *Gongylothorax* aff. *favosus* DUMITRICA
9a–c: GL/207 (U.A.12), Bathonian, 9a: antapical view, 903130, 9b: apical view, 903131, 9c: 903129, 400x
11a–c: GL/209 (U.A.16), Oxfordian, 11a: antapical view, 900826, 11b: apical view, 900825, 11c: 900824, 400x

12, 13a–b. *Stichocapsa robusta* MATSUOKA
12: UPC/18 (U.A.15), Callovian, 922135, 300x
13a–b: UPC/18 (U.A.15), Callovian, 13a: 922218, 13b: antapical view, 922219, 300x

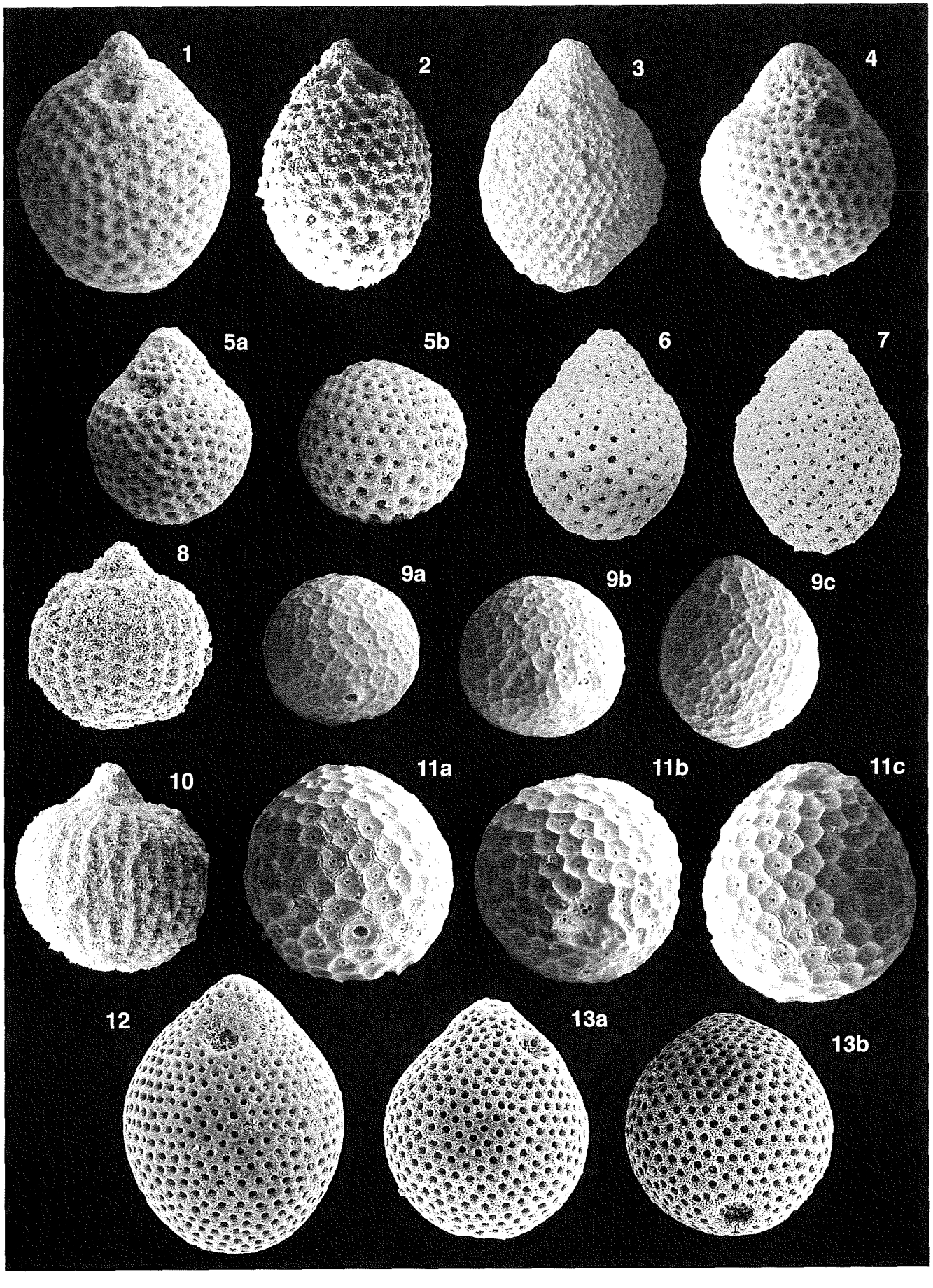
1
2
3
4
5a
5b
6
7
8
9a
9b
9c
10
11a
11b
11c
12
13a
13b

PLATE 14

1, 2a–b, 3. *Hemicryptocapsa* sp. A
1: UPC/33 (U.A.45), Albian, apical view, 920322, 300x
2a–b: UPC/34 (U.A.45), Albian, 2a: apical view, 920308, 2b: antapical view, 920307, 300x
3: UPC/34 (U.A.45), Albian, lateral view with sutural pore, 920208, 300x

4, 9. *Hemicryptocapsa prepolyhedra* DUMITRICA
4: UPC/35 (U.A.48), Turonian, 921404, 300x
9: UPC/35 (U.A.48), Turonian, 921406, 300x

5–6. Transitional forms between *Hemicryptocapsa prepolyhedra* DUMITRICA and *H. polyhedra* DUMITRICA
5: UPC 35 (U.A.48), sutural pore, 921407, 300x
6: UPC 35 (U.A.48), aperture, 921402, 300x

7–8. *Hemicryptocapsa polyhedra* DUMITRICA
7: UPC/35 (U.A.48), Turonian, 921405, 300x
8: UPC/35 (U.A.48), Turonian, 921401, 300x

10, 13–14. *Holocryptocanium barbui* DUMITRICA
10a–b: BjIV/20 (U.A.42), upper Aptian-lower Albian; 10a: apical view, 902720, 10b: aperture, 902721, 200x
13a–b: BjIV/21 (U.A.46), Albian-lower Cenomanian; 13a: apical view, 914534, 13b: aperture, 914533, 200x
14a–b: BjIV/21 (U.A.46), Albian-lower Cenomanian; 14a: apical view, 914535, 14b: aperture, 914536, 200x

11, 12a–b. *Cryptamphorella conara* (FOREMAN)
11: DIN/31.50 (U.A.35), upper Valanginian-Hauterivian, 920116, 200x
12a–b: BjIV/20 (U.A.42), upper Aptian-lower Albian, 12a: 902702, 12b: sutural pore, 902701, 200x

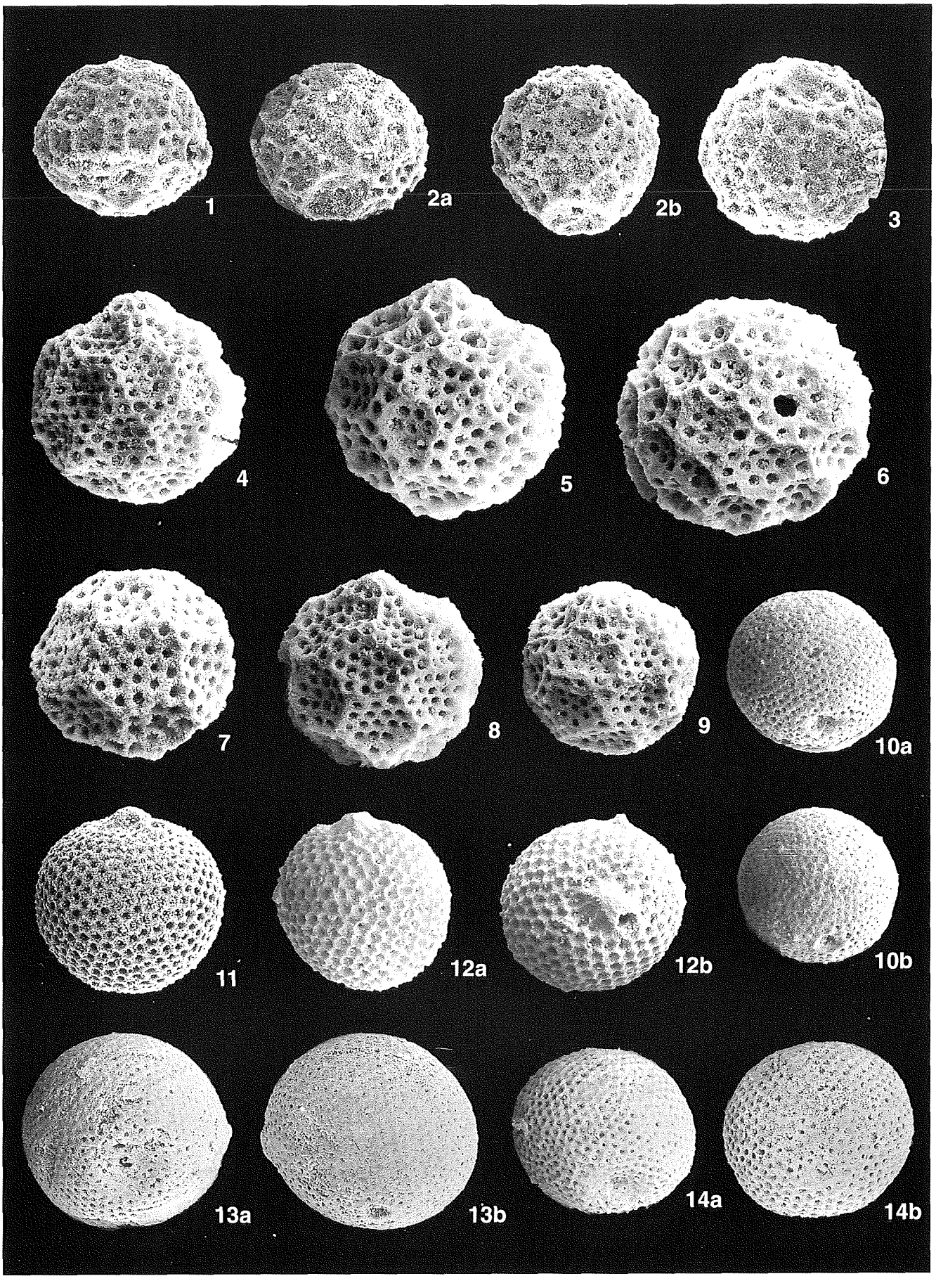
1
2a
2b
3
4
5
6
7
8
9
10a
11
12a
12b
10b
13a
13b
14a
14b

PLATE 15

1–3. *Palinandromeda* sp. A
1: BjI/9 (U.A.2), Aalenian-lower Bajocian, 893625, 150x
2: UPC/13 (U.A.3), Bajocian, 892125, 150x
3: GL/127 (U.A.3), Bajocian, 903114, 150x

4–5. *Palinandromeda praepodbielensis* (BAUMGARTNER)
4: GL/123 (U.A.1), Aalenian-lower Bajocian, 893629, 150x
5: UPC/13 (U.A.3), Bajocian, 892102, 150x

6. *Palinandromeda podbielensis* (OŽVOLDOVA)
BM/102 (U.A.17), Oxfordian, 900226, 150x

7. *Sethocapsa kaminogoensis* AITA
DIN/31.50 (U.A.35), upper Valanginian-Hauterivian, 920106, 300x

8. *Sethocapsa accincta* STEIGER
GL/138 (U.A.31), Tithonian, 921817, 300x

9–10. *Sethocapsa horokanaiensis* KAWABATA
9: BM/5 (U.A.26), Kimmeridgian, 891612, 300x
10: BM/106 (U.A.26), Kimmeridgian, 900536, 300x

11–15. *Sethocapsa uterculus* (PARONA)
11: UPC/298.60 (U.A.39), lower Aptian, 915410, 300x
12: BM/478.60 (U.A.37), Hauterivian-Barremian, 914221, 300x
13: DIN/31.50 (U.A.35), upper Valanginian-Hauterivian, 920202, 300x
14: UPC/298.60 (U.A.39), lower Aptian, 915414, 300x
15: BjIV/18+1.55 (U.A.39), lower Aptian, 914834, 300x

16–17. *Sethocapsa pseudouterculus* AITA
16: DIN/24.30 (U.A.31), Tithonian, 911833, 300x
17: DIN/24.30 (U.A.31), Tithonian, 911829, 300x

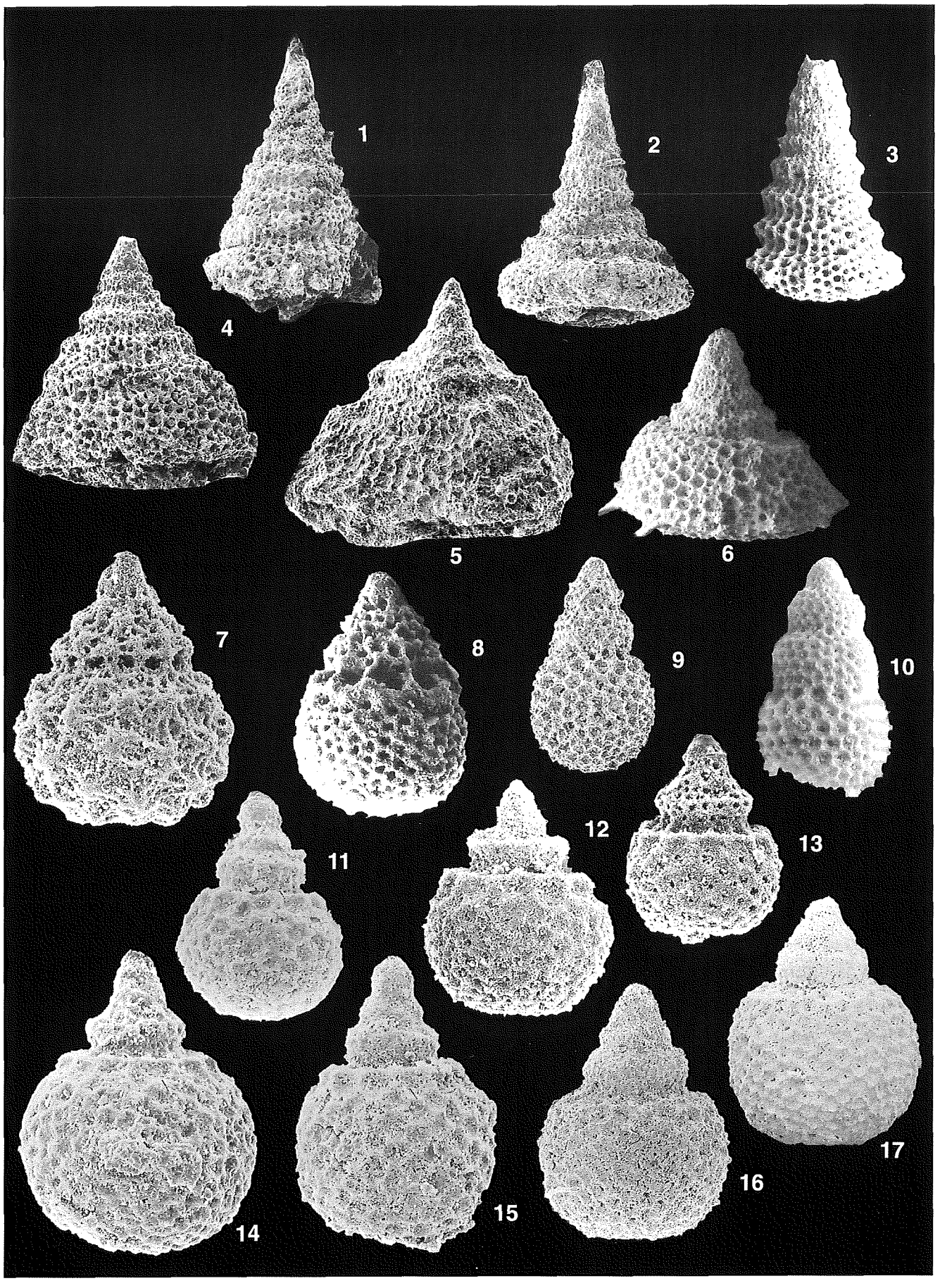
1
2
3
4
5
6
7
8
9
10
11
12
13
14
15
16
17

PLATE 16

1–3. *Podocapsa amphitreptera* FOREMAN
1: BM/6 (U.A.26–27), Kimmeridgian, 891410, 150x
2: BM/5 (U.A.26), Kimmeridgian, 891525, 150x
3: BM/6 (U.A.26–27), Kimmeridgian, 891329, 150x

4. *Dibolachras tytthopora* FOREMAN
BjIV/18+1.55 (U.A.39), lower Aptian, 914737, 150x

5. *Podobursa spinosa* (OŽVOLDOVA)
GL/209+6.60 (U.A.22), Oxfordian, 911011, 100x

6–7. *Syringocapsa* sp. A
6: Bj/III/3.00 (U.A.25), Kimmeridgian, 911312, 150x
7: BM/6 (U.A.26–27), Kimmeridgian, 891408, 150x

8. *Syringocapsa limatum* FOREMAN
Bj/IV/17 (U.A.37), Hauterivian-Barremian, 915203, 150x

9, 10. *Katroma* spp.
9: PK/20, lower Liassic, 920934, 150x
10: PK/20, lower Liassic, 921003, 200x

11–13. *Gigi fustis* DE WEVER
11: PK/20, lower Liassic, 920913, 150x
12: PK/20, lower Liassic, 920930, 200x
13: PK/20, lower Liassic, 920910, 150x

14–15. *Gigi* sp. A
14: GL/4, lower Liassic, 853560, 200x
15: BM/21, lower Liassic, 920901, 150x

16. *Pseudoeucyrtis hanni* TAN
UPC/32 (U.A.40), lower Aptian, 921531, 200x

17–18. *Pseudoeucyrtis* sp. J sensu CONTI & MARCUCCI
17: BM/102 (U.A.17), Oxfordian, 900317, 150x
18: BM/102 (U.A.17), Oxfordian, 900314, 150x

19–20. *Pseudoeucyrtis* sp. B sensu WIDZ
19: GL/209+6.60 (U.A.22), Oxfordian, 911017, 150x
20: GL/209+6.60 (U.A.22), Oxfordian, 911016, 150x

21–22. *Pseudoeucyrtis reticularis* MATSUOKA & YAO
21: BM/106 (U.A.26), Kimmeridgian, 900534, 150x
22: BM/106 (U.A.26), Kimmeridgian, 900533, 150x

23. *Pseudoeucyrtis* sp.
BM/21, lower Liassic, 920818, 150x

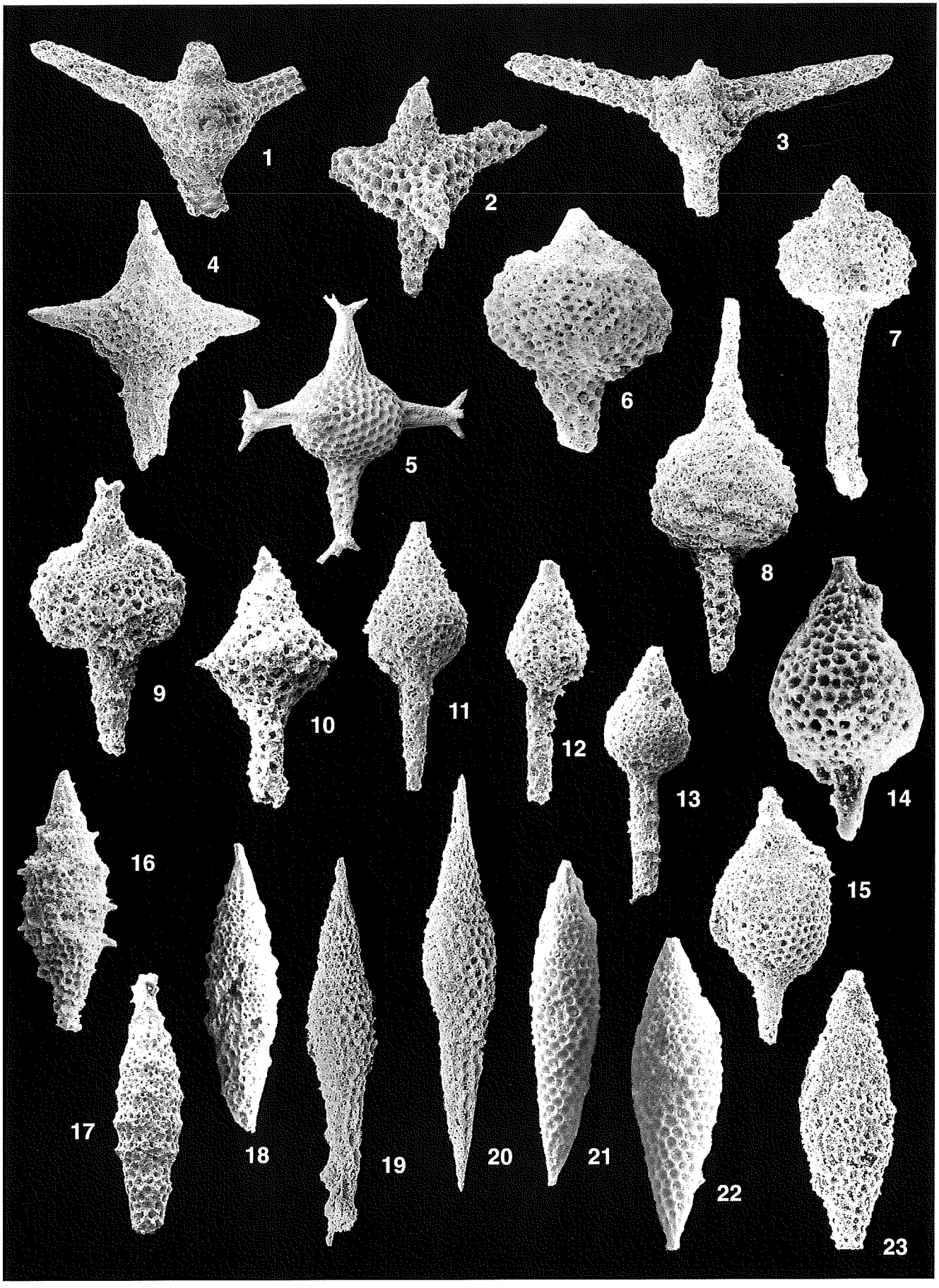
1
2
3
4
5
6
7
8
9
10
11
12
13
14
15
16
17
18
19
20
21
22
23

PLATE 17

1–7. *Parahsuum* spp.
1: Bj/III/3.00 (U.A.25), Kimmeridgian, 922722, 200x
2: UPC/257.10 (U.A.23), upper Oxfordian-Kimmeridgian, 912006, 200x
3: GL/209+6.60 (U.A.22), Oxfordian, 911204, 200x
4: UPC/18 (U.A.15), Callovian, 922327, 200x
5: GL/127 (U.A.3), Bajocian, 890422, 300x
6: GL/128 (U.A.5), Bajocian, 903432, 200x
7: UPC/20 (U.A.15), Callovian, 901332, 200x

8. *Parahsuum officerense* (PESSAGNO & WHALEN)
BjI/10 (U.A.4), Bajocian, 910230, 200x

9–10, 12. *Parahsuum simplum* YAO
9: UPC/41.50, lower Liassic, 921029, 200x
10: PK/20, lower Liassic, 920936, 200x
12: UPC/41.50, lower Liassic, 921026, 200x

11. *Bagotum* sp.
PK/20, lower Liassic, 920915, 200x

13. *Parahsuum ovale* HORI & YAO
PK/20, lower Liassic, 920919, 200x

14, 20. *Droltus* sp.
14: BM/18, lower Liassic, 920736, 200x
20: BM/11, Hettangian, 920711, 200x

15. *Droltus* (?) sp.
BM/18, lower Liassic, 920735, 300x

16. *Wrangellium* sp.
BM/21, lower Liassic, 920904, 200x

17–19. *Canoptum* spp.
17: PK/20, lower Liassic, 920929, 200x
18: BM/18, lower Liassic, 920737, 200x
19: BM/11, Hettangian, 920712, 200x

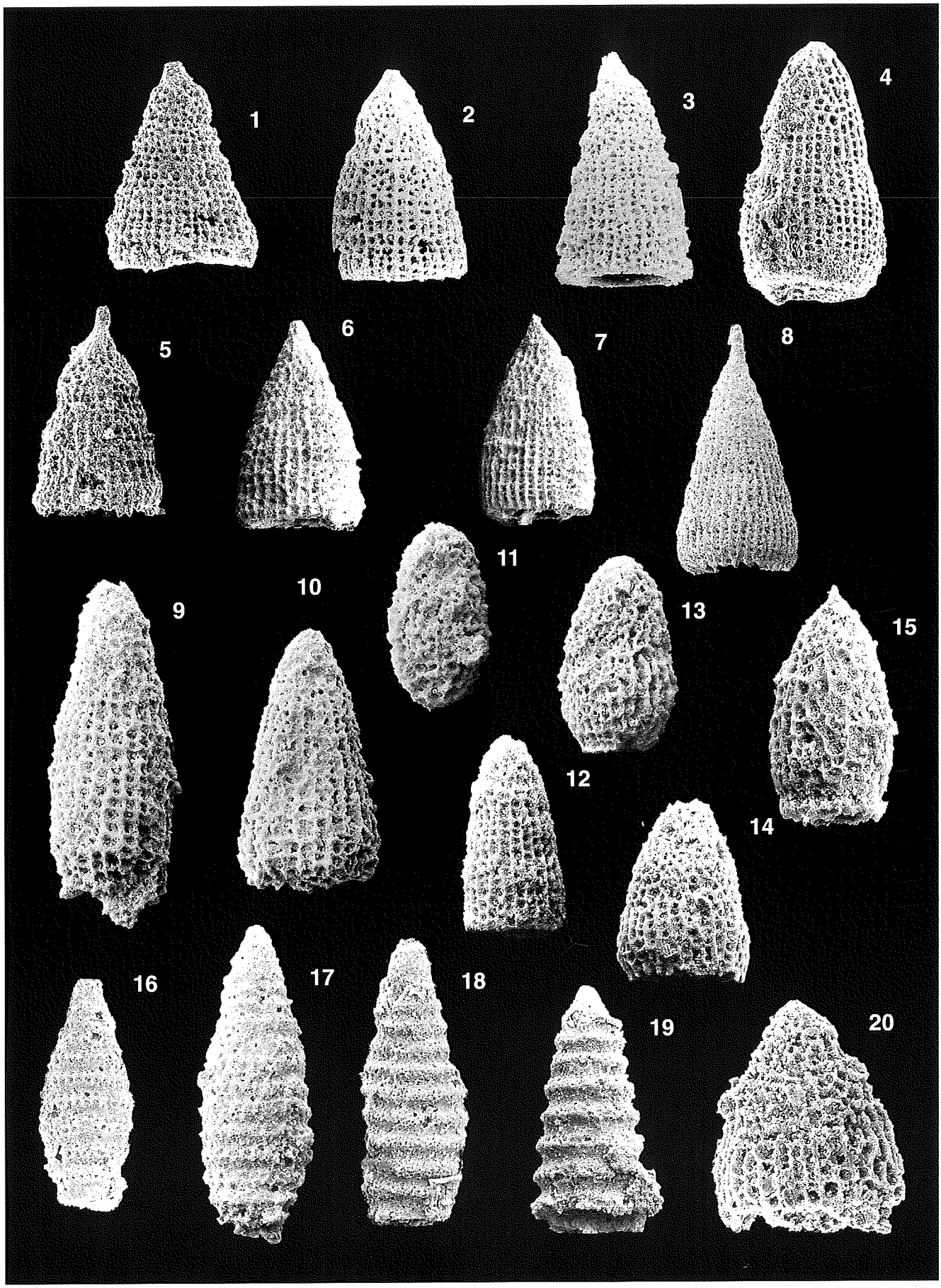
1
2
3
4
5
6
7
8
9
10
11
12
13
14
15
16
17
18
19
20

PLATE 18

1–4. *Transhsuum maxwelli* (PESSAGNO) gr.
1: UPC/23 (U.A.18), Oxfordian, 902832, 200x
2: BM/102 (U.A.17), Oxfordian, 900203, 200x
3: UPC/18 (U.A.15), Callovian, 922114, 200x
4: GL/207 (U.A.12), Bathonian, 901029, 200x

5. *Transhsuum okamurai* (MIZUTANI)
DIN/2.35 (U.A.21), Oxfordian, 922626, 200x

6–8. *Transhsuum brevicostatum* (OŽVOLDOVA) gr.
6: BjII/15/1 (U.A.22), Oxfordian, 901812, 200x
7: BM/102 (U.A.17), Oxfordian, 900219, 200x
8: GL/207 (U.A.12), Bathonian, 901018, 200x

9–11. *Parahsuum* (?) *grande* HORI & YAO
9: GL/123 (U.A.1), Aalenian-lower Bajocian, 921920, 150x
10: GL/123 (U.A.1), Aalenian-lower Bajocian, 921926, 150x
11: GL/123 (U.A.1), Aalenian-lower Bajocian, 921929, 150x

12–14. *Transhsuum hisiukyoense* (ISOZAKI & MATSUDA)
12: GL/128 (U.A.5), Bajocian, 903420, 200x
13: GL/125 (U.A.2), Aalenian-lower Bajocian, 892307, 200x
14: GL/127 (U.A.3), Bajocian, 903110, 150x

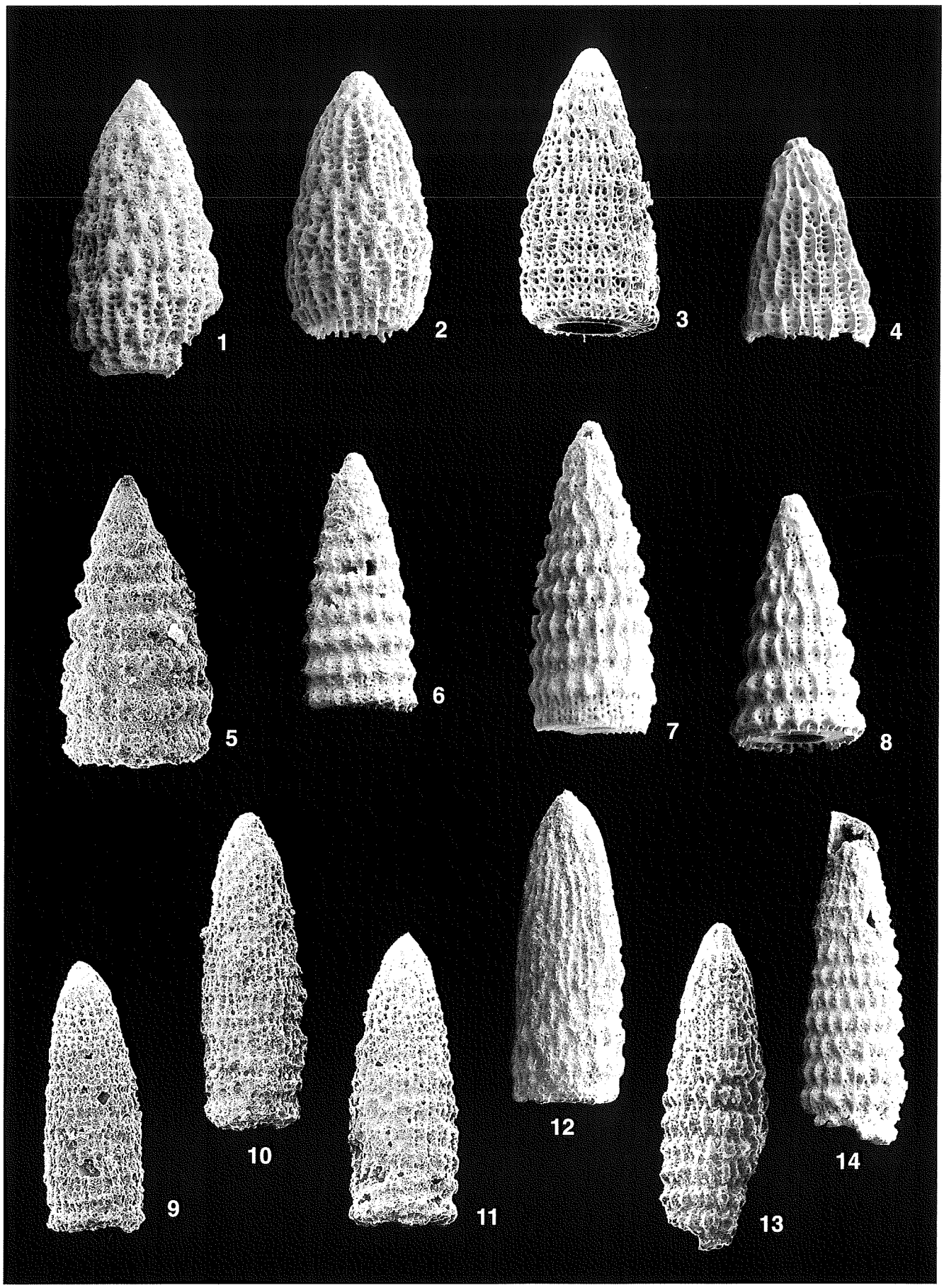
1
2
3
4
5
6
7
8
9
10
11
12
13
14

PLATE 19

1–5. *Hsuum mclaughlini* PESSAGNO & BLOME gr.
1: DIN/29.30 (U.A.33), Berriasian-lower Valanginian, 910327, 200x
2: Bj/III/3.00 (U.A.25), Kimmeridgian, 922716, 200x
3: Bj/III/3.00 (U.A.25), Kimmeridgian, 922708, 200x
4: Bj/III/3.00 (U.A.25), Kimmeridgian, 922731, 200x
5: Bj/III/3.00 (U.A.25), Kimmeridgian, 922706, 200x

6–8. *Hsuum* sp.
6: Bj/III/3.00 (U.A.25), Kimmeridgian, 922718, 200x
7: Bj/III/3.00 (U.A.25), Kimmeridgian, 922734, 200x
8: UPC/262.70 (U.A.27), Kimmeridgian, 922609, 200x

9, 11–13. *Hsuum matsuokai* ISOZAKI & MATSUDA
9: UPC/13 (U.A.3), Bajocian, 892121, 200x
11: BjI/9 (U.A.2), Aalenian-lower Bajocian, 893626, 200x
12: GL/125 (U.A.2), Aalenian-lower Bajocian, 892306, 200x
13: GL/127 (U.A.3), Bajocian, 890431, 200x

10. *Linaresia chrafatensis* EL KADIRI
BjI/9 (U.A.2), Aalenian-lower Bajocian, 893614, 200x

14, 18. *Parahsuum* (?) *natorense* (EL KADIRI)
14: UPC/14 (U.A.3), Bajocian, 892104, 150x
18: GL/123 (U.A.1), Aalenian-lower Bajocian, 921931, 150x

15–17. *Parahsuum* (?) *magnum* TAKEMURA
15: BjI/9 (U.A.2): Aalenian-lower Bajocian, 893621, 200x
16: GL/123 (U.A.1), Aalenian-lower Bajocian, 922009, 150x
17: GL/123 (U.A.1), Aalenian-lower Bajocian, 922008, 150x

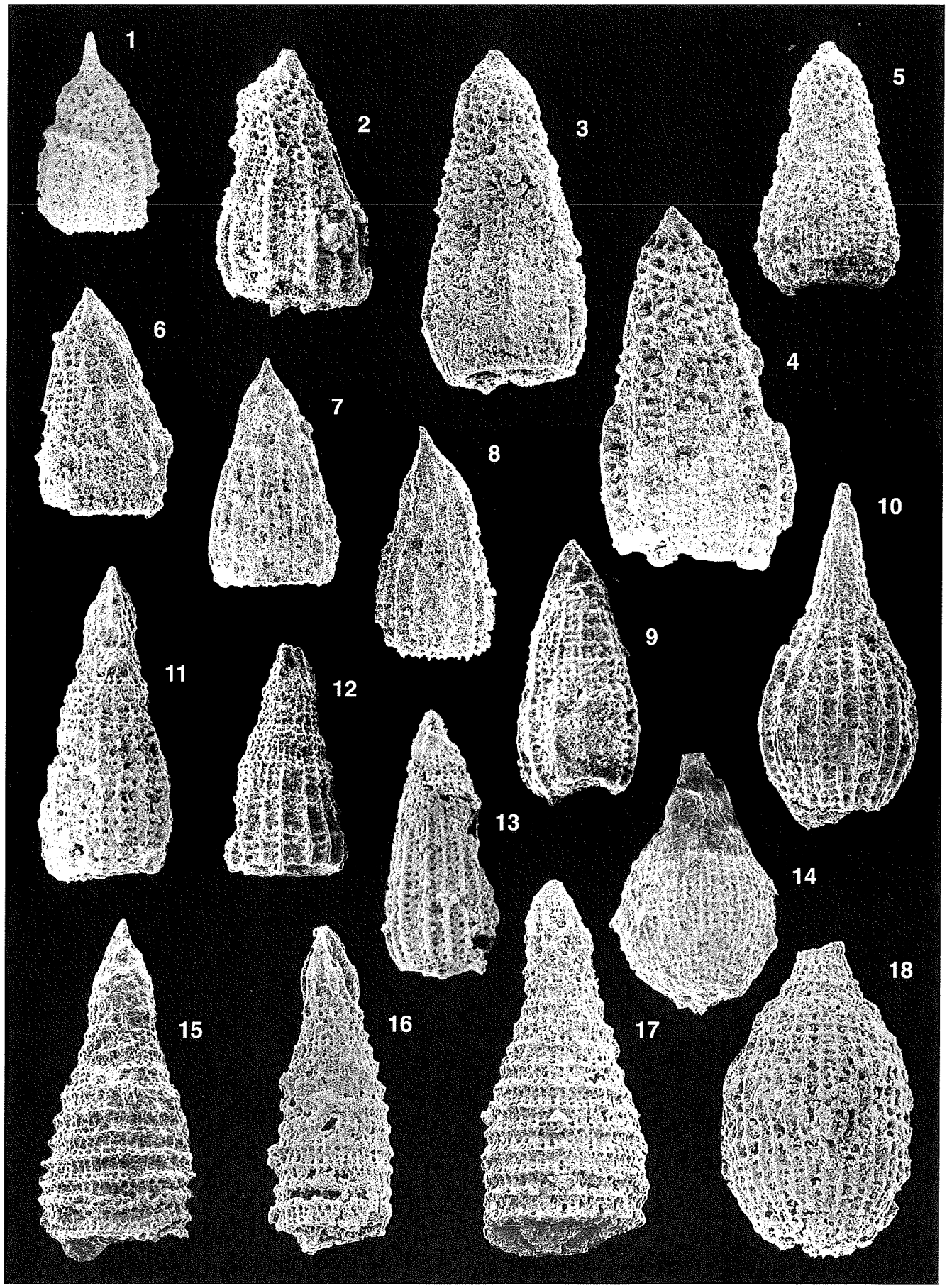
1
2
3
5
6
4
7
8
10
11
12
9
13
14
18
15
16
17

PLATE 20

1. *Archaeodictyomitra* (?) *amabilis* AITA
UPC/18 (U.A.15), Callovian, 922138, 200x

2–4. *Archaeodictyomitra excellens* (TAN)
2: UPC/27 (U.A.29), Tithonian, 901927, 200x
3: GL/144 (U.A.39), lower Aptian, 915505, 200x
4: UPC/298.60 (U.A.39), lower Aptian, 915420, 200x

5–6, 12, 17–18. *Archaeodictyomitra apiarium* (RÜST)
5: GL/142 (U.A.34), Berriasian-lower Valanginian, 910624, 200x
6: UPC/27 (U.A.29), Tithonian, 901922, 200x
12: BjI/15 (U.A.22), Oxfordian, 901129, 200x
17: UPC/23 (U.A.18), Oxfordian, 902815, 200x
18: GL/209+6.60 (U.A.22), Oxfordian, 911133, 200x

7–8, 13. Transitional forms between *Archaeodictyomitra apiarium* (RÜST) and *Archaeodictyomitra minoensis* (MIZUTANI)
7: UPC/28 (U.A.29), Tithonian, 921831, 200x
8: BM/8 (U.A.30), Tithonian, 922705, 200x
13: BjI/15 (U.A.22), Oxfordian, 901128, 200x

9, 14–15, 19–20. *Archaeodictyomitra minoensis* (MIZUTANI)
9: PK/104, Tithonian, 910715, 200x
14: BjI/15 (U.A.22), Oxfordian, 901127, 200x
15: BjII/15/1 (U.A.22), Oxfordian, 901815, 200x
19: GL/209+6.60 (U.A.22), Oxfordian, 911135, 200x
20: BjII/15/1 (U.A.22), Oxfordian, 901818, 200x

10. *Pseudodictyomitra depressa* BAUMGARTNER
GL/142 (U.A.34), Berriasian-lower Valanginian, 910620, 200x

11, 16. *Archaeodictyomitra* spp.
11: BjI/15 (U.A.22) Oxfordian, 901124, 200x
16: GL/209 (U.A.16), Oxfordian, 900913, 300x

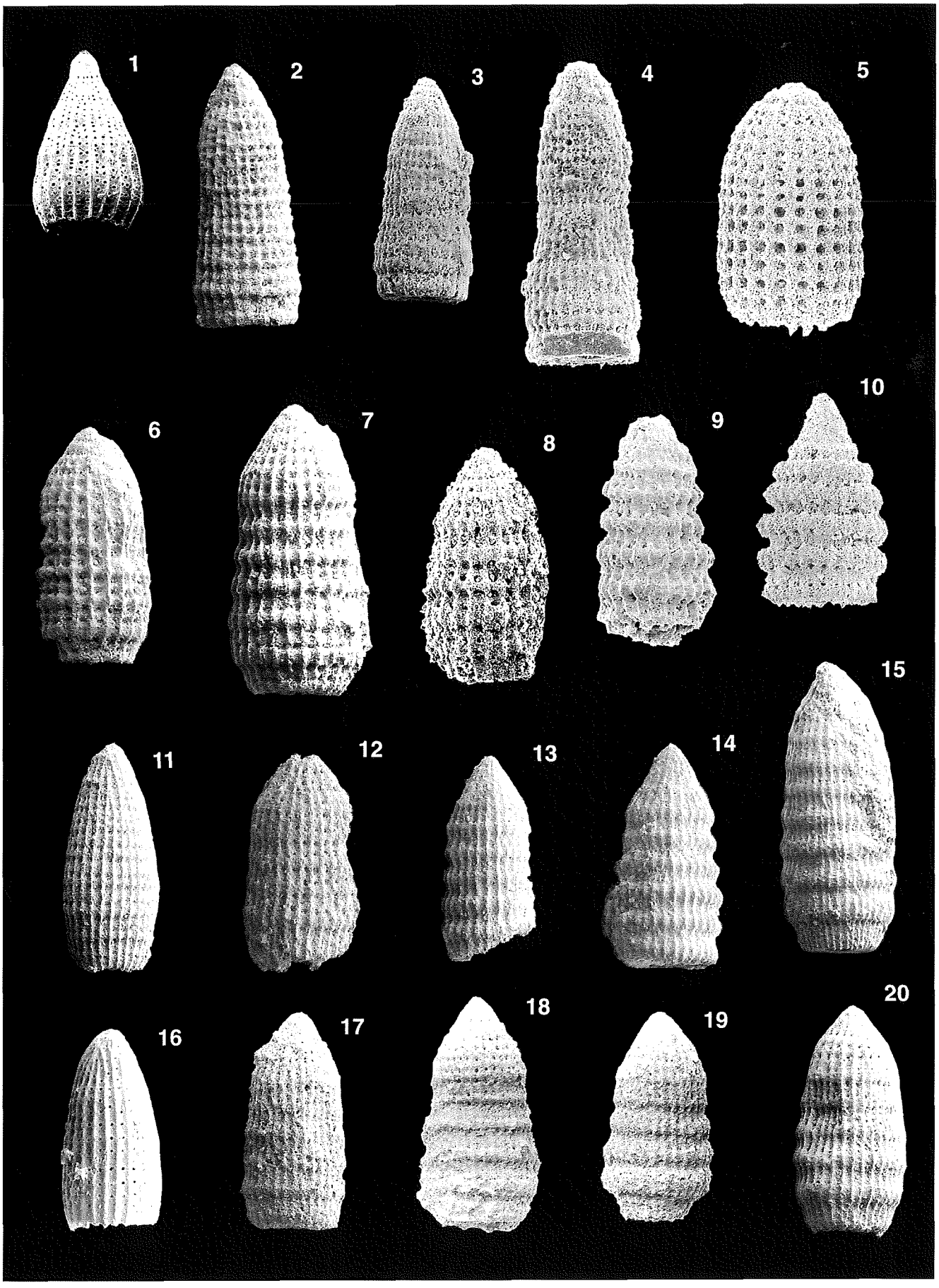
1
2
3
4
5
6
7
8
9
10
11
12
13
14
15
16
17
18
19
20

PLATE 21

1–2. *Archaeodictyomitra* (?) sp. A
1: UPC/32 (U.A.40), lower Aptian, 921506, 200x
2: UPC/32 (U.A.40), lower Aptian, 921509, 200x

3–4. *Thanarla praeveneta* PESSAGNO
3: UPC/32 (U.A.40), lower Aptian, 921501, 200x
4: BjIV/20 (U.A.42), upper Aptian-lower Albian, 902727, 200x

5–6. *Archaeodictyomitra lacrimula* (FOREMAN)
5: UPC/32 (U.A.40), lower Aptian, 902512, 200x
6: BjIV/18+1.55 (U.A.39), lower Aptian, 914819, 200x

7. *Thanarla pulchra* (SQUINABOL)
UPC/298.60 (U.A.39), lower Aptian, 915417, 200x

8. *Thanarla elegantissima* (CITA)
GL/215 (U.A.47), Albian-lower Cenomanian, 914729, 200x

9. *Mita* sp.
BM/489.40 (U.A.41), upper Aptian-lower Albian, 913028, 100x

10. *Mita* sp. C sensu THUROW
BjIV/20+4.60 (U.A.43), Albian, 915033, 100x

11–12. *Mita* sp. B sensu THUROW
11: BjIV/21 (U.A.46), Albian-lower Cenomanian, 914532, 150x
12: BjIV/21 (U.A.46), Albian-lower Cenomanian, 914531, 150x

13. *Sethocapsa* (?) *perspicua* (SQUINABOL)
BjIV/20+4.60 (U.A.43), Albian, 914932, 100x

14–17. *Mita gracilis* (SQUINABOL)
14: BjIV/21 (U.A.46), Albian-lower Cenomanian, 914615, 150x
15: UPC/34 (U.A.45), Albian, 920302, 150x
16: GL/215 (U.A.47), Albian-lower Cenomanian, 914719, 150x
17: UPC/33 (U.A.45), Albian, 20335, 150x

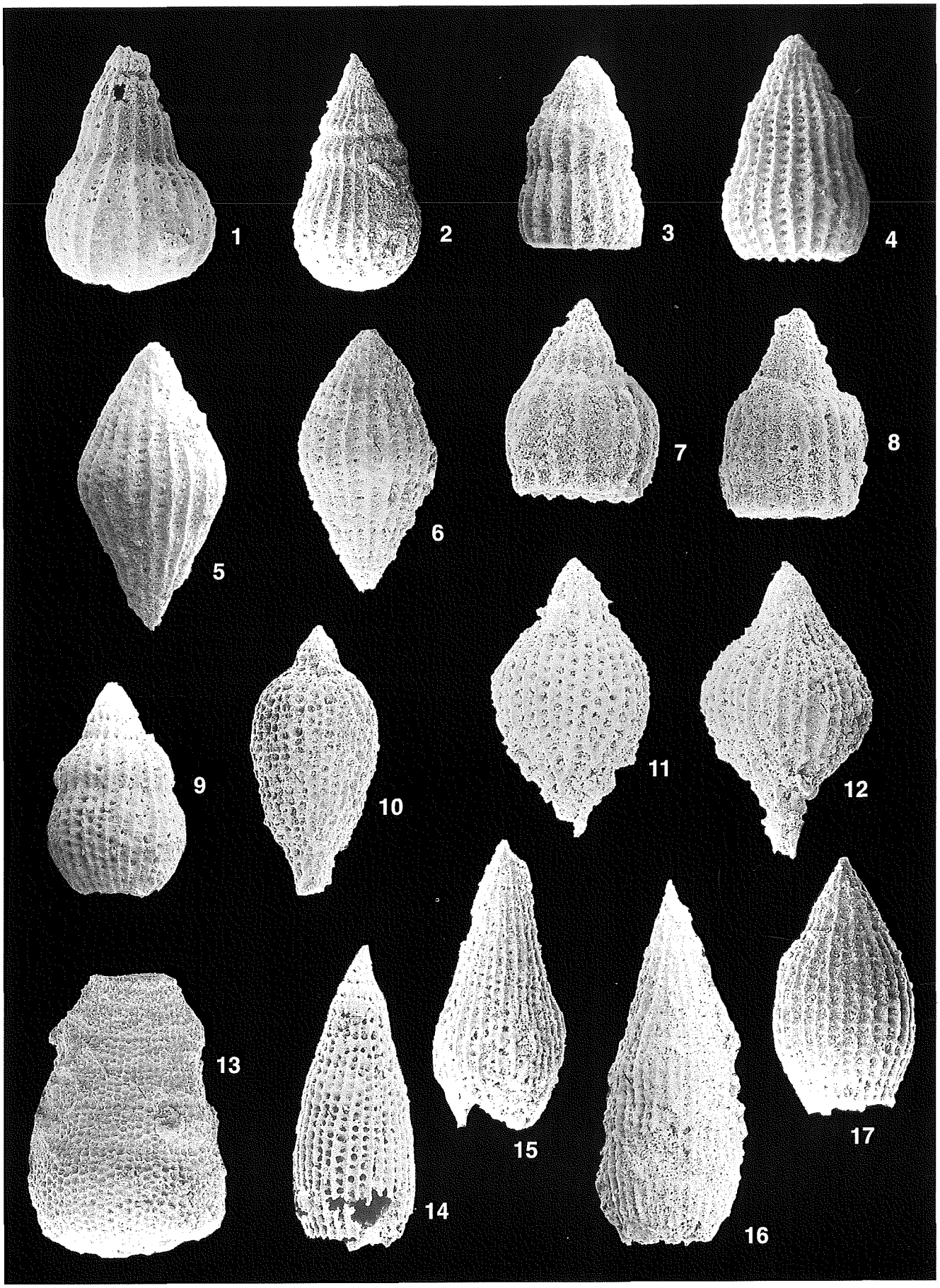
1
2
3
4
5
6
7
8
9
10
11
12
13
14
15
16
17

PLATE 22

1–3. *Dictyomitra formosa* SQUINABOL
1: UPC/35 (U.A.48), Turonian, 921320, 200x
2: UPC/35 (U.A.48), Turonian, 902413, 200x
3: UPC/35 (U.A.48), Turonian, 921315, 200x

4. *Pseudodictyomitra pseudomacrocephala* (SQUINABOL)
UPC/35 (U.A.48), Turonian, 902407, 150x

5–7. *Pseudodictyomitra lodogaensis* PESSAGNO
5: UPC/34 (U.A.45), Albian, 920305, 200x
6: BjIV/20 (U.A.42), upper Aptian-lower Albian, 921623, 200x
7: UPC/34 (U.A.45), Albian, 920227, 200x

8–9. *Pseudodictyomitra* sp. A
8: UPC/32 (U.A.40), lower Aptian, 902523, 200x
9: BjIV/20 (U.A.42), upper Aptian-lower Albian, 921622, 200x

10–11. *Pseudodictyomitra lanceloti* SCHAAF
10: UPC/298.60 (U.A.39), lower Aptian, 915428, 200x
11: GL/144 (U.A.39), lower Aptian, 915517, 200x

12–13. *Pseudodictyomitra pentacolaensis* PESSAGNO
12: BjIV/20 (U.A.42), upper Aptian-lower Albian, 902730, 200x
13: BjIV/20 (U.A.42), upper Aptian-lower Albian, 902731, 200x

14–15. *Pseudodictyomitra* sp. C sensu YAO
14: BjII/15/1 (U.A.22), Oxfordian, 901912, 200x
15: DIN/29.30 (U.A.33), Berriasian-lower Valanginian, 910326, 200x

16. *Pseudodictyomitra primitiva* MATSUOKA & YAO
UPC/27 (U.A.29), Tithonian, 901923, 200x

17. *Pseudodictyomitra carpatica* (LOZYNYAK)
GL/142 (U.A.34), Berriasian-lower Valanginian, 910618, 150x

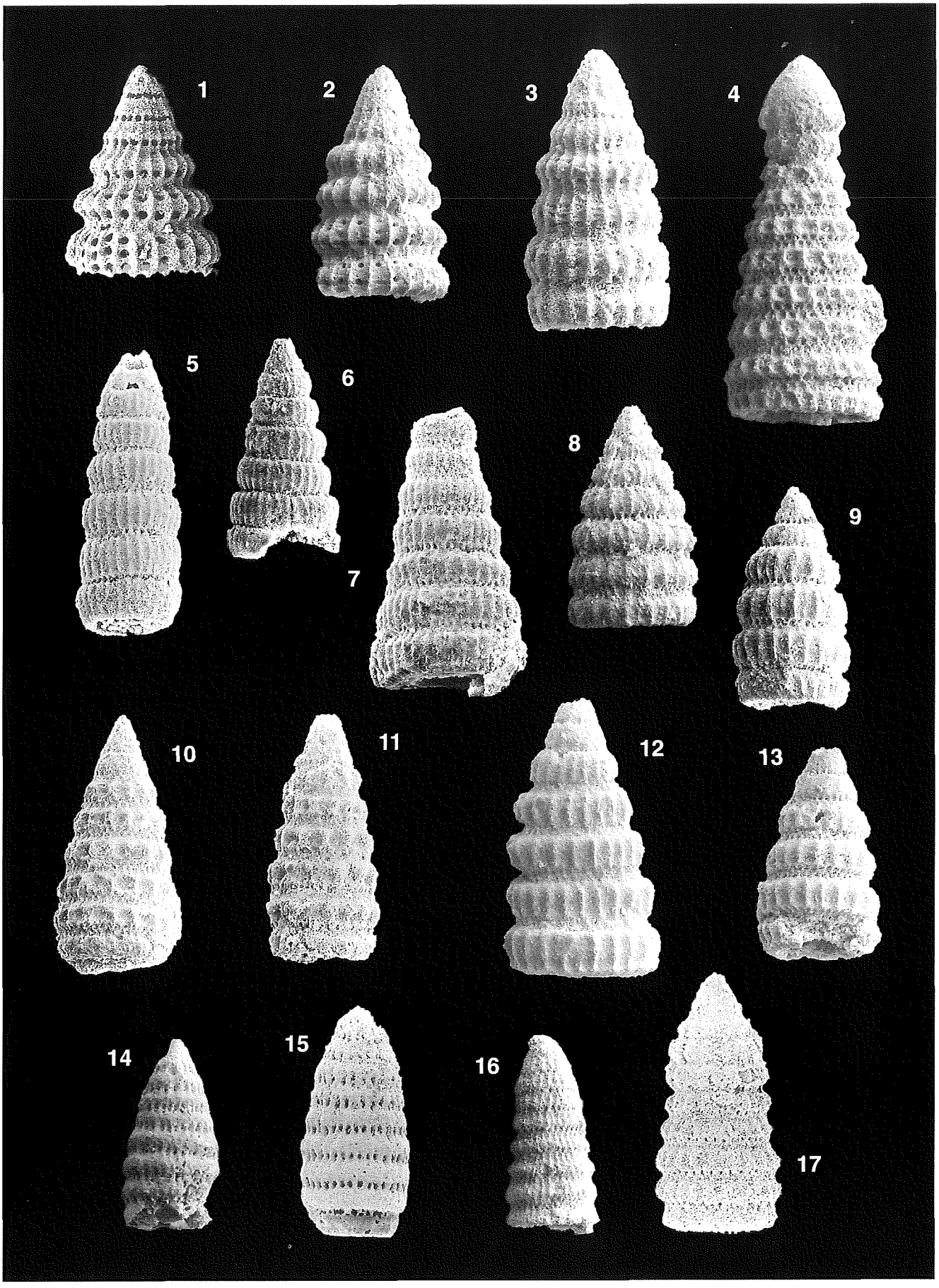
1
2
3
4
5
6
7
8
9
10
11
12
13
14
15
16
17

PLATE 23

1, 6–11. *Cinguloturris carpatica* DUMITRICA
1: GL/209+6.60 (U.A.22), Oxfordian, 911120, 200x
6: UPC/21 (U.A.17), Oxfordian, 901309, 200x
7: UPC/21 (U.A.17), Oxfordian, 901310, 200x
8: BM/102 (U.A.17), Oxfordian, 900120, 200x
9: UPC/18 (U.A.15), Callovian, 922111, 200x
10: GL/209 (U.A.16), Oxfordian, 900815, 200x
11: BM/106 (U.A.26), Kimmeridgian, 900611, 200x

2. Transitional form between *Cinguloturris carpatica* DUMITRICA and *Cinguloturris* sp. A
GL/209+6.60 (U.A.22), Oxfordian, 911205, 200x

3–5. *Cinguloturris* sp. A
3: UPC/25 (U.A.29), Tithonian, 922620, 200x
4: GL/138 (U.A.31), Tithonian, 921804, 200x
5: GL/138 (U.A.31), Tithonian, 921807, 200x

12–13. *Laxtorum jurassicum* ISOZAKI & MATSUDA
12: BjI/9 (U.A.2), Aalenian-lower Bajocian, 893620, 200x
13: GL/125 (U.A.2), Aalenian-lower Bajocian, 903409, 200x

14–15. *Stichomitra* (?) sp. A
14: GL/127 (U.A.3), Bajocian, 903111, 200x
15: ZB/28 (U.A.6), upper Bajocian, 890525, 200x

16. *Stichomitra* (?) *takanoensis* AITA
ZB/28 (U.A.6), upper Bajocian, 890414, 200x

17–19. *Spongocapsula palmerae* PESSAGNO
17: UPC/18 (U.A.15), Callovian, 922123, 150x
18: BM/102 (U.A.17), Oxfordian, 900421, 150x
19: GL/209+6.60 (U.A.22), Oxfordian, 911134, 150x

20. *Spongocapsula perampla* (RÜST)
Bj/III/3.00 (U.A.25), Kimmeridgian, 922726, 150x

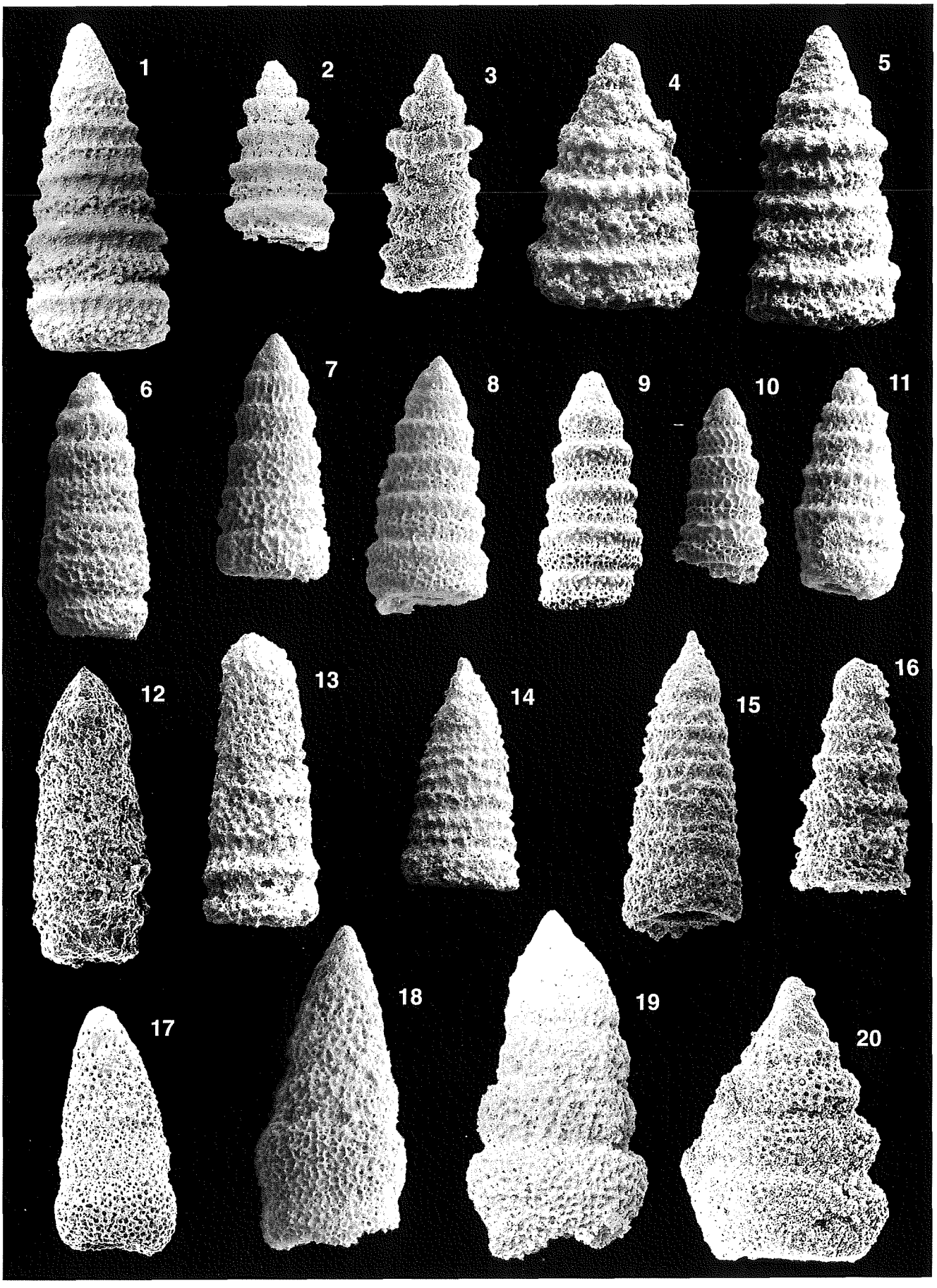
1
2
3
4
5
6
7
8
9
10
11
12
13
14
15
16
17
18
19
20

PLATE 24

1. *Dictyomitrella* (?) *kamoensis* MIZUTANI & KIDO
GL/207 (U.A.12), Bathonian, 903128, 300x

2–3. *Parvicingula cosmoconica* (FOREMAN)
2: GL/142 (U.A.34), Berriasian-lower Valanginian, 910621, 200x
3: GL/142 (U.A.34), Berriasian-lower Valanginian, 910604, 200x

4–5. *Pseudodictyomitra puga* (SCHAAF)
4: DIN/31.50 (U.A.35), upper Valanginian-Hauterivian, 920201, 200x
5: DIN/31.50 (U.A.35), upper Valanginian-Hauterivian, 920103, 200x

6–7. *Ristola altissima altissima* (RÜST)
6: DIN/2.35 (U.A.21), Oxfordian, 922628, 150x
7: GL/138 (U.A.31), Tithonian, 890913, 150x

8. *Ristola cretacea* (BAUMGARTNER)
GL/138 (U.A.31), Tithonian, 890912, 150x

9–10. *Mirifusus chenodes* (RENZ)
9: BM/102 (U.A.17), Oxfordian, 900302, 150x
10: GL/209+6.60 (U.A.22), Oxfordian, 911012, 150x

11, 14–15. *Parvicingula boesii* (PARONA) gr.
11: BjIV/18 (U.A.38), lower Aptian, 915107, 200x
14: UPC/27 (U.A.29), Tithonian, 901931, 200x
15: GL/142 (U.A.34), Berriasian-Valanginian, 910606, 200x

12–13. *Parvicingula dhimenaensis* BAUMGARTNER
12: ZB/28 (U.A.6), upper Bajocian, 890138, 200x
13: GL/209+6.60 (U.A.22), Oxfordian, 911213, 200x

16. *Parvicingula usotanensis* TUMANDA
BjIV/18+1.55 (U.A.39), lower Aptian, 914836, 200x

17. *Mirifusus guadalupensis* PESSAGNO
BM/102 (U.A.17), Oxfordian, 900237, 100x

18–19. *Mirifusus dianae dianae* (KARRER)
18: GL/209+6.60 (U.A.22), Oxfordian, 911007, 100x
19: DIN/2.35 (U.A.21), Oxfordian, 910111, 100x

20. *Mirifusus dianae minor* BAUMGARTNER
BM/8 (U.A.30), Tithonian, 891511, 100x

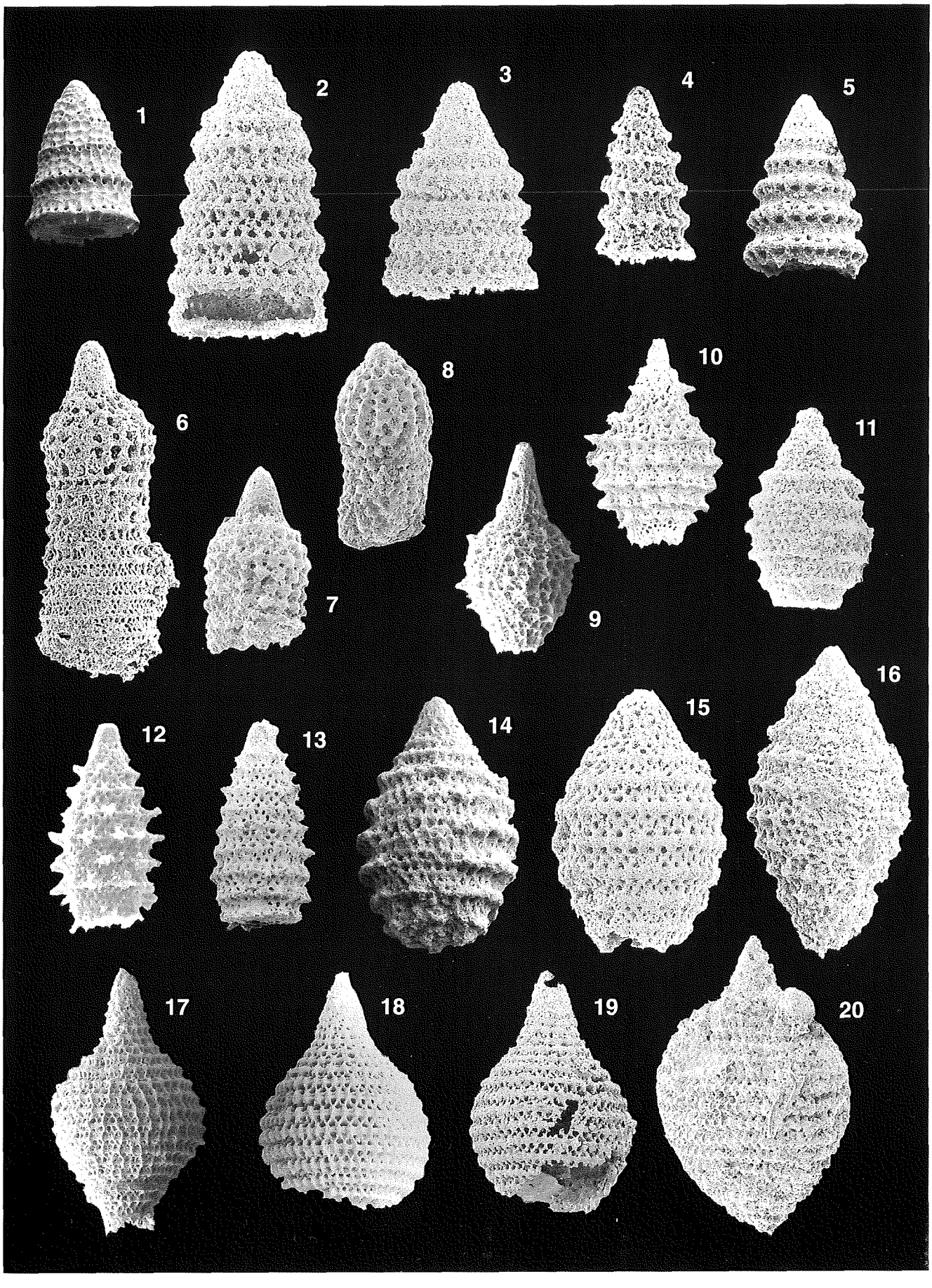
1
2
3
4
5
6
7
8
9
10
11
12
13
14
15
16
17
18
19
20

PLATE 25

1–5. *Stichomitra communis* SQUINABOL
1: BjIV/20+4.60 (U.A.43), Albian, 915019, 150x
2: Grb/12 (U.A.43), Albian, 920426, 150x
3: UPC/34 (U.A.45), Albian, 920219, 150x
4: UPC/35 (U.A.48), Turonian, 921310, 150x
5: UPC/35 (U.A.48), Turonian, 902420, 150x

6–7. *Crolanium pythiae* SCHAAF
6: BM/478.60 U.A.37), Hauterivian-Barremian, 914423, 200x
7: BM/478.60 U.A.37), Hauterivian-Barremian, 914422, 200x

8–9. *Novixitus weyli* SCHMIDT-EFFING
8: GL/215 (U.A.47), Albian-lower Cenomanian, 914708, 150x
9: BjIV/21 (U.A.46), Albian-lower Cenomanian, 914602, 150x

10. *Xitus* (?) sp. sensu STEIGER
GL/142 (U.A.34), Berriasian-lower Valanginian, 892022, 200x

11–12. *Xitus gifuensis* MIZUTANI
11: GL/138 (U.A.31), Tithonian, 921827, 200x
12: DIN/11.55 (U.A.26), Kimmeridgian, 911509, 200x

13–15. *Xitus* sp. A sensu WIDZ
13: UPC/23 (U.A.18), Oxfordian, 902809, 200x
14: UPC/251.50 (U.A.19), Oxfordian, 912133, 150x
15: DIN/11.55 (U.A.26), Kimmeridgian, 911515, 150x

16. *Xitus* cf. *gifuensis* MIZUTANI
GL/209+6.60 (U.A.22), Oxfordian, 911123, 200x

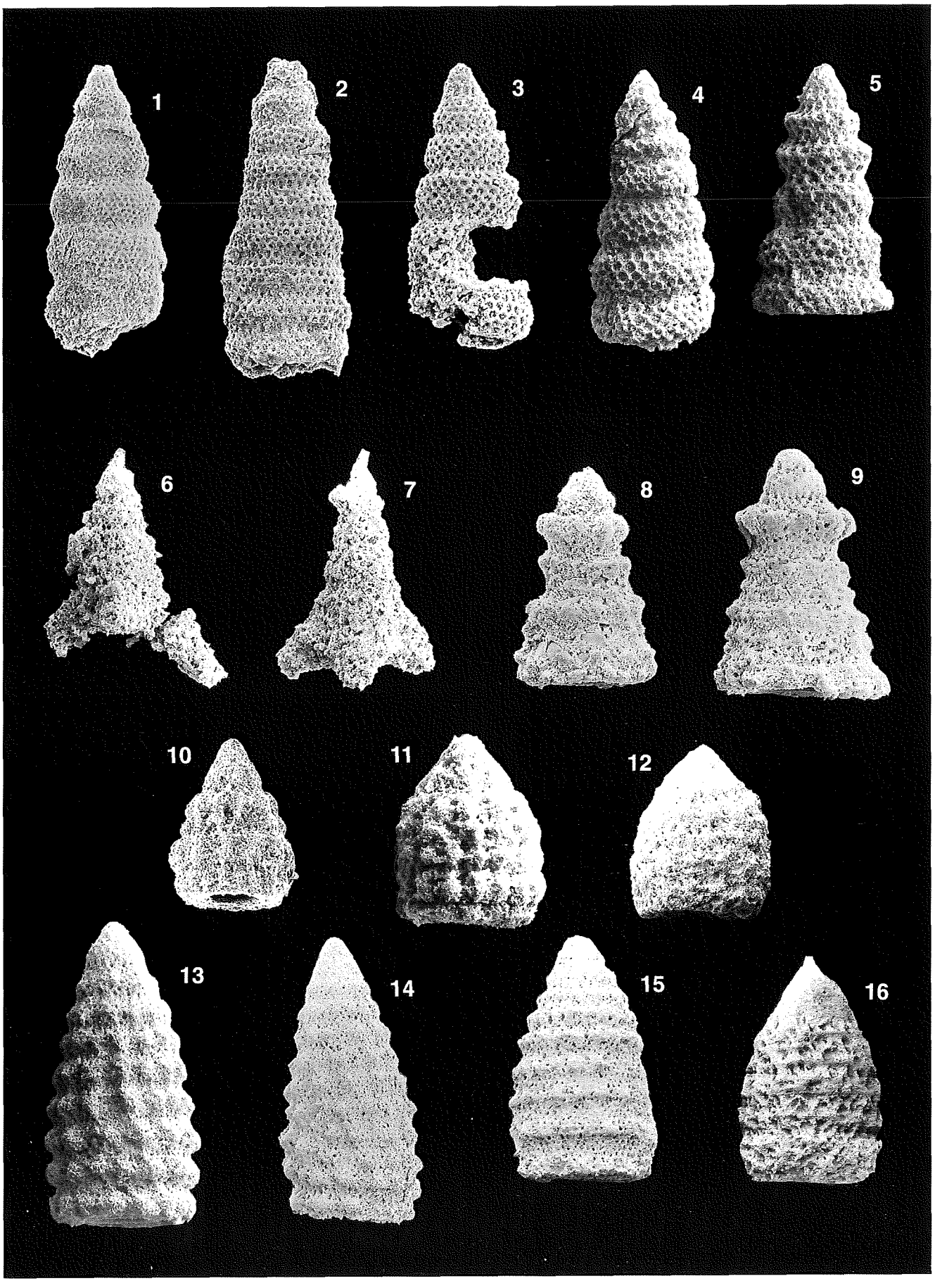
1
2
3
4
5
6
7
8
9
10
11
12
13
14
15
16

PLATE 26

1–2. *Afens liriodes* RIEDEL & SANFILIPPO
1: UPC/35 (U.A.48), Turonian, 921417, 200x
2: UPC/35 (U.A.48), Turonian, 921306, 300x

3–5. *Saitoum dercourti* WIDZ & DE WEVER
3: DIN/29.30 (U.A.33), Berriasian-lower Valanginian, 910403, 300x
4: BM/7 (U.A.28), Tithonian, 891423, 300x
5: BM/106 (U.A.26), Kimmeridgian, 900537, 300x

6. *Rhopalosyringium* sp. A
UPC/35 (U.A.48), Turonian, 921412, 300x

7–10. *Rhopalosyringium majuroense* SCHAAF
7: BjIV/21 (U.A.46), Albian-lower Cenomanian, 914707, 300x
8: BjIV/21 (U.A.46), Albian-lower Cenomanian, 914537, 300x
9: GL/215 (U.A.47), Albian-lower Cenomanian, 914721, 300x
10: GL/215 (U.A.47), Albian-lower Cenomanian, 914720, 300x

11–12. *Napora bukryi* PESSAGNO gr.
11: BM/102 (U.A.17), Oxfordian, 900109, 150x
12: GL/209+6.60 (U.A.22), Oxfordian, 911008, 150x

13–14. *Ares* spp.
13: GL/127 (U.A.3), Bajocian, 903109, 150x
14: GL/127 (U.A.3), Bajocian, 903108, 150x

15. *Turanta* sp.
UPC/13 (U.A.3), Bajocian, 892119, 150x

16. *Perispyridium ordinarium* (PESSAGNO) gr.
BjII/15/1 (U.A.22), Oxfordian, 901801, 200x

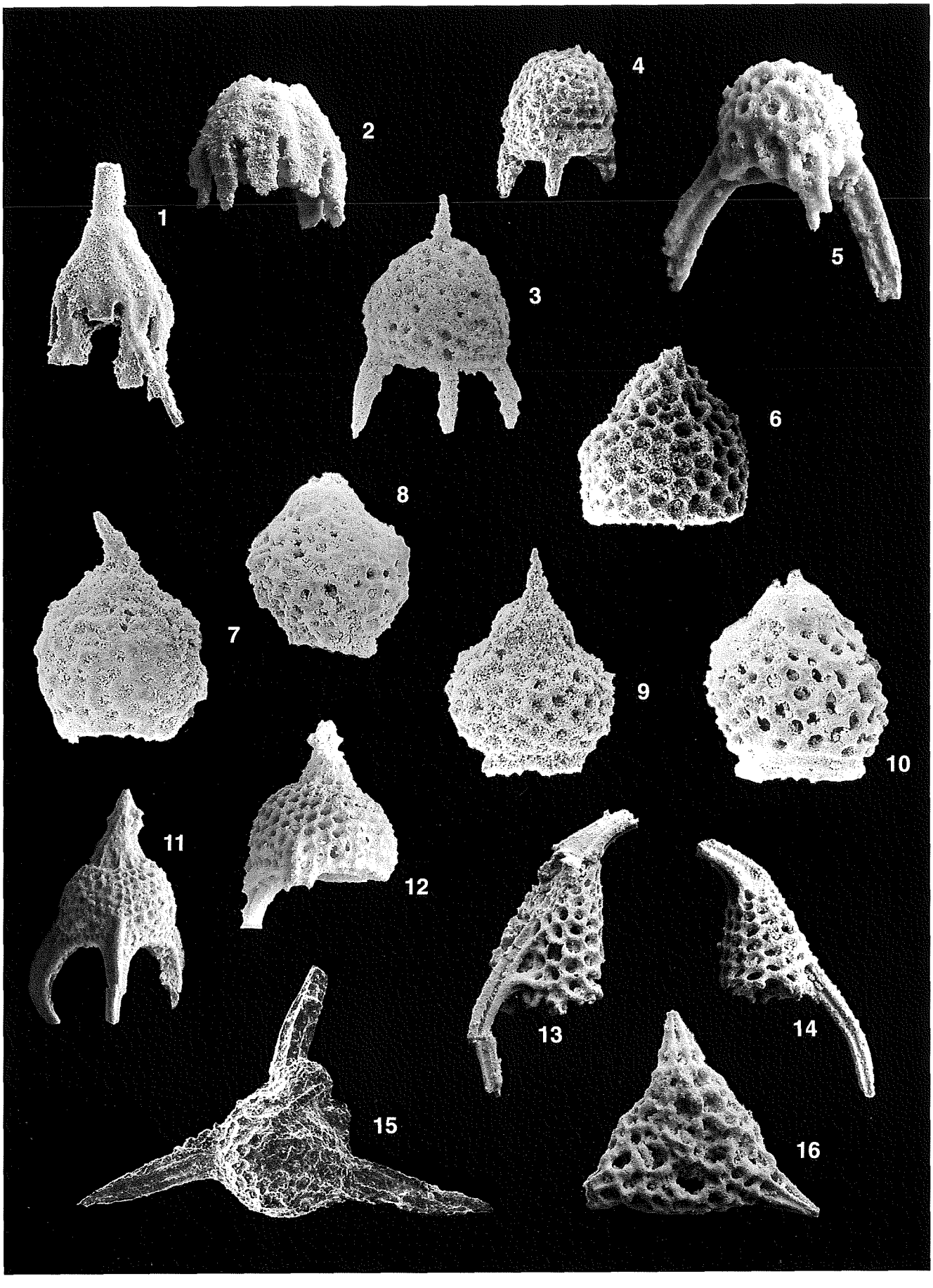
1
2
3
4
5
6
7
8
9
10
11
12
13
14
15
16

PLATE 27

Microfacies of the Bar Limestone Formation

1. Oolitic packstone.
   Upper Member, Sutomore section (106 m), magnification 20x.

2. Micrograded cross-laminated silt-size interval. Mostly pellets with some larger peloids in the lower part. Numerous radiolarians and sponge spicules occur on the top.
   Lower Member, Gornja Lastva section (60.40 m), magnification 5x.

3. Densely packed ooids in a partly dolomitized matrix. *Gutnicella cayeuxi* (LUCAS) as nucleus in the lower right corner.
   Calcarenite interbedded in shale sequence of the Lastva Radiolarite Formation, Gornja Lastva section (225.70 m), magnification 23x.

4. Fine-grained conglomerate microfacies: bimodal, radiolarian-mudstone intraclasts and shallow-water derived debris.
   Lower Member, Gornja Lastva section (135 m), magnification, 10x.

5. Calcarenite microfacies: echinoderm plates, algae (*Boueina* sp. near the center), ooids, intraclasts of radiolarian mudstone.
   Lower Member, Bijela section (103 m), magnification 23x.

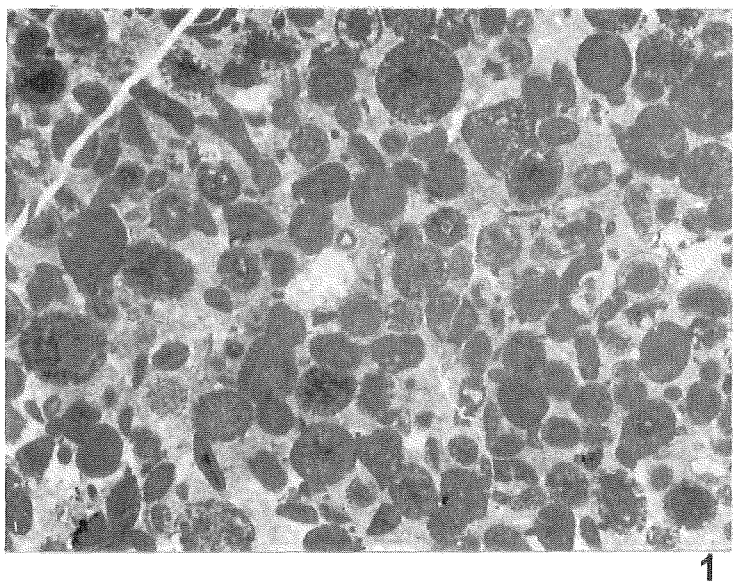

1

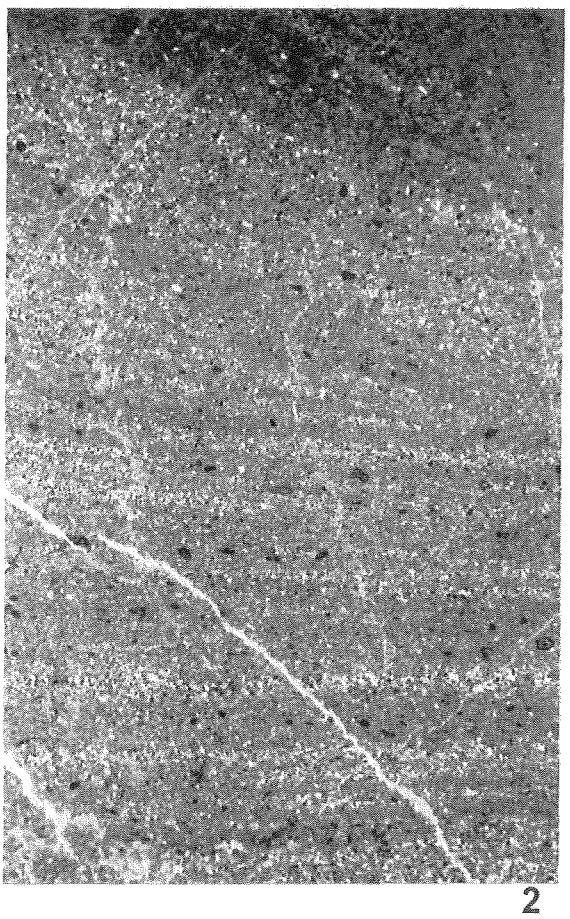

2

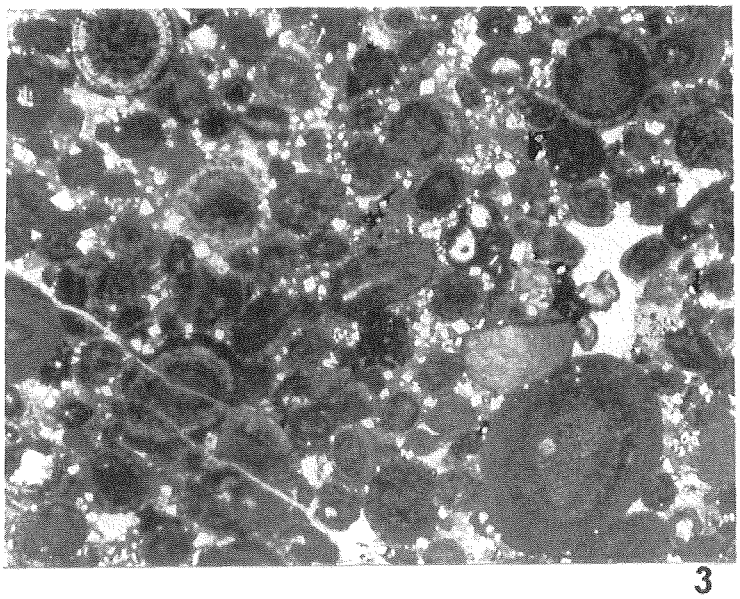

3

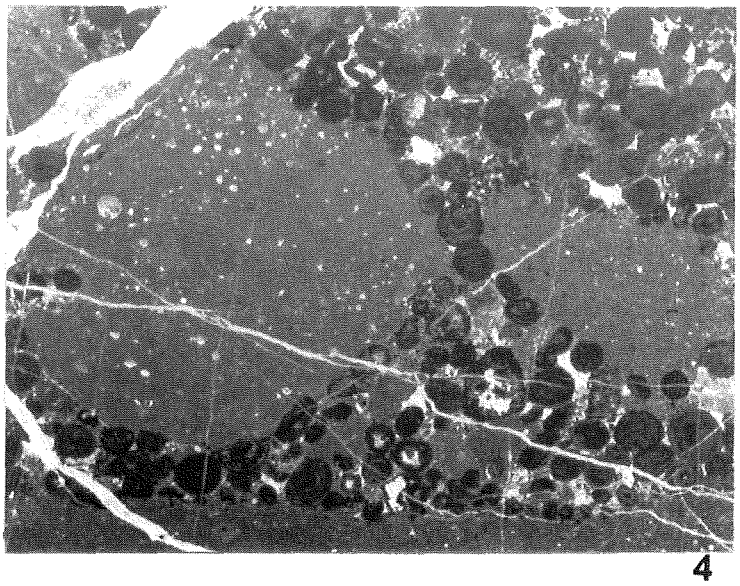

4

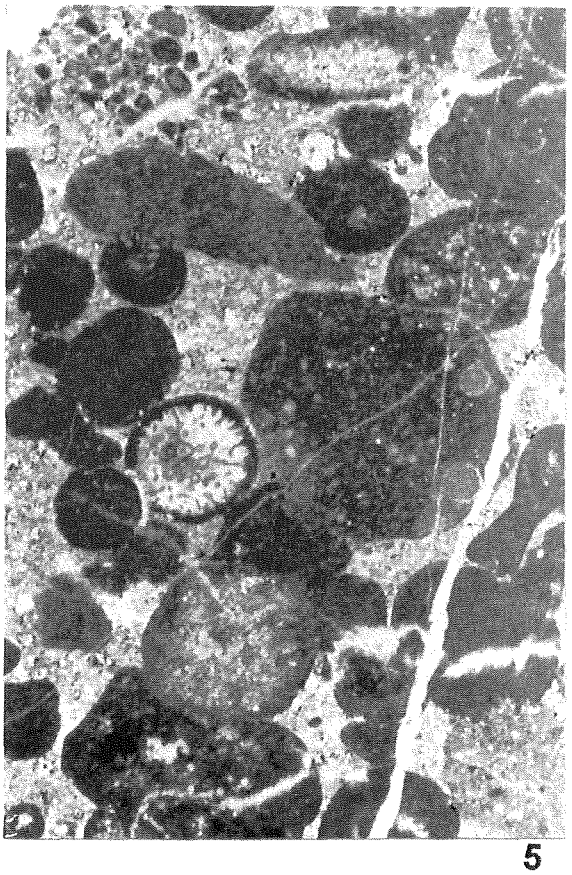

5

PLATE 28

1. Bar section, general view of the Bar Limestone Formation. The arrow points to the contact between the Lower and the Upper Member. A part of the Praevalis Limestone is visible in the background. The topmost massive light limestone belongs to the overlying High Karst Zone.

2. Bar section, closer view of the Upper Member of the Bar Limestone Formation. (220 m to 370 m in the lithological column, Fig. 2.2)

3. Bar Limestone Formation, Lower Member. Conglomerate with subrounded and tabular pelagic-limestone clasts, showing subparallel orientation.
Canj section. Detail of a plurimetric fallen block on the beach, broken off the thickest conglomerate unit (for lithological column see Fig. 2.2).

4. Lastva Radiolarite Formation, lower variegated (V1) radiolarite. Light beds are spicule/radiolarian sandstones.
Bijela I section (at 140 m in the lithological column, Fig. 2.3).

5. Lastva Radiolarite Formation, upper variegated (V2) radiolarite. The two thicker beds above the hammer are silicified calcarenites.
Gornja Lastva section (at 277 m in the lithological column, Fig. 2.3).

6. Praevalis Limestone Formation. Detail of a deformed chert bed.
Petrovac section (at 167 m in the lithological column, Fig. 2.5).

7. Praevalis Limestone Formation. Irregular chert nodules in chaotic slump deposits.
Petrovac section (at 160 m in the lithological column, Fig. 2.5).

8. Praevalis Limestone Formation. Clasts of the Tithonian red ribbon radiolarite incorporated in pelagic limestone.
Petrovac section (at 152 m in the lithological column, Fig. 2.5).


1

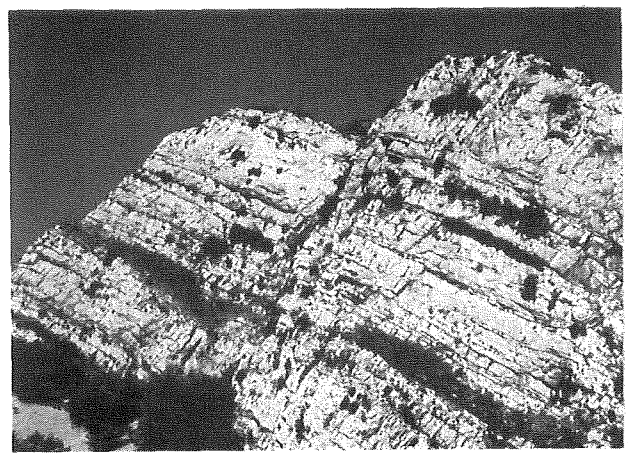
2

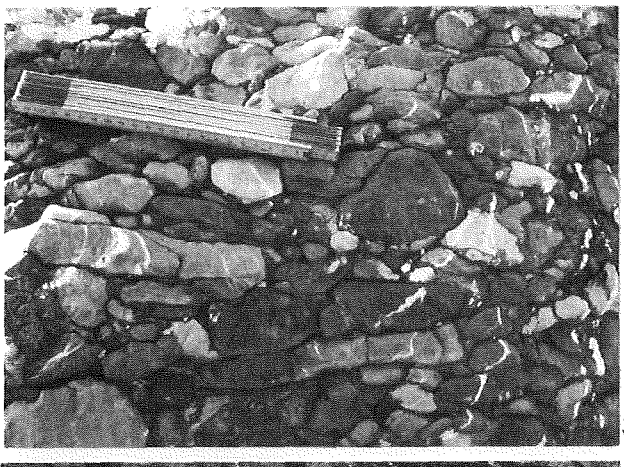
3


4


5


6

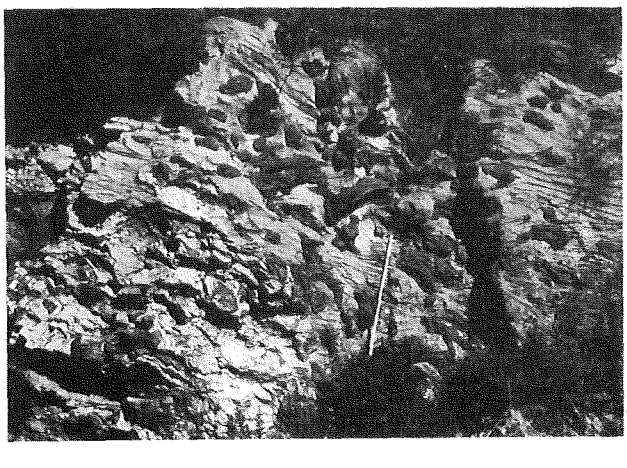
7

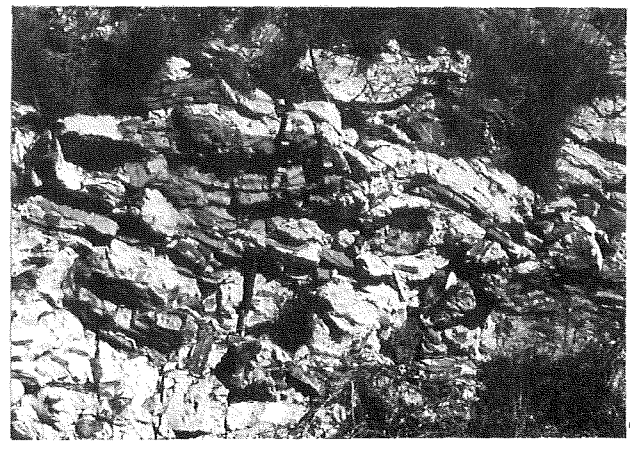
8

Mémoires de Géologie (Lausanne)

No. 1 BAUD A. 1987. Stratigraphie et sédimentologie des calcaires de Saint-Triphon (Trias, Préalpes, Suisse et France). 202 pp., 53 text-figs., 29 pls.

No. 2 ESCHER A, MASSON H. and STECK A. 1988. Coupes géologiques des Alpes occidentales suisses. 11 pp., 1 text-figs., 1 map

No. 3 STUTZ E. 1988. Géologie de la chaîne Nyimaling aux confins du Ladakh et du Rupshu (NW-Himalaya, Inde). Evolution paléogéographique et tectonique d'un segment de la marge nord-indienne. 149 pp., 42 text-figs., 11 pls. 1 map.

No. 4 COLOMBI A. 1989. Métamorphisme et géochimie des roches mafiques des Alpes ouest-centrales (géoprofil Viège-Domodossola-Locarno). 216 pp., 147 text-figs., 2 pls.

No. 5 STECK A., EPARD J.-L., ESCHER A., MARCHANT R., MASSON H. and SPRING L. 1989 Coupe tectonique horizontale des Alpes centrales. 8 pp., 1 map.

No. 6 SARTORI M. 1990. L'unité du Barrhorn (Zone pennique, Valais, Suisse). 140 pp., 56 text-figs., 3 pls.

No. 7 BUSSY F. 1990. Pétrogenèse des enclaves microgrenues associées aux granitoïdes calco-alcalins: exemple des massifs varisque du Mont-Blanc (Alpes occidentales) et miocène du Monte Capanne (Ile d'Elbe, Italie). 309 pp., 177 text-figs.

No. 8 EPARD J.-L. 1990. La nappe de Morcles au sud-ouest du Mont-Blanc. 165 pp., 59 text-figs.

No. 9 PILLOUD C. 1991 Structures de déformation alpines dans le synclinal de Permo-Carbonifère de Salvan-Dorénaz (massif des Aiguilles Rouges, Valais). 98 pp., 59 text-figs.

No. 10 BAUD A., THELIN P. and STAMPFLI G. 1991. (Eds.) Paleozoic geodynamic domains and their alpidic evolution in the Tethys. IGCP Project No. 276. Newsletter No. 2. 155 pp.

No. 11 CARTER E.S. 1993 Biochronology and Paleontology of uppermost Triassic (Rhaetian) radiolarians, Queen Charlotte Islands, British Columbia, Canada. 132 pp., 15 text-figs., 21 pls.

No. 12 GOUFFON Y. 1993. Géologie de la "nappe" du Grand St-Bernard entre la Doire Baltée et la frontière suisse (Vallée d'Aoste -Italie). 147 pp., 71 text-figs., 2 pls.

No. 13 HUNZIKER J.C., DESMONS J., and HURFORD AJ. 1992. Thirty-two years of geochronological work in the Central and Western Alps: a review on seven maps. 59 pp., 18 text-figs., 7 maps.

No. 14 SPRING L. 1993. Structures gondwaniennes et himalayennes dans la zone tibétaine du Haut Lahul-Zanskar oriental (Himalaya indien). 148 pp., 66 text-figs, 1 map.

No. 15 MARCHANT R. 1993. The Underground of the Western Alps. 137 pp., 104 text-figs.

No. 16 VANNAY J.-C. 1993. Géologie des chaînes du Haut-Himalaya et du Pir Panjal au Haut-Lahul (NW-Himalaya, Inde). Paléogéographie et tectonique. 148 pp., 44 text-figs., 6 pls.

No. 17 PILLEVUIT A. 1993. Les blocs exotiques du Sultanat d'Oman. Evolution paleogeographique d'une marge passive flexurale. 249 pp., 138 text-figs., 7 pls.

No. 18 GORICAN S. 1994. Jurassic and Cretaceous radiolarian biostratigraphy and sedimentary evolution of the Budva Zone (Dinarides, Montenegro). 120 pp., 20 text-figs., 28 pls.

No. 19 JUD R. 1994. Biochronology and systematics of Early Cretaceous Radiolaria of the Western Tethys. 147 pp., 29 text-figs., 24 pls.

No. 20 DI MARCO, G. 1994. Les terrains accrétés du sud du Costa Rica. Evolution tectonostratigraphique de la marge occidentale de la plaque Caraïbe. 166 pp., 89 text-figs., 6 pls.

No. 21 O'DOGHERTY L. 1994. Biochronology and paleontology of Mid-Cretaceous radiolarians from Northern Apennines (Italy) and Betic Cordillera (Spain). 415 pp., 35 text-figs., 73 pls.

No. 22 GUEX J. and BAUD A. (Eds.) 1994. Recent Development on Triassic Stratigraphy. 184 pp.

No. 23 INTERRAD Jurassic -Cretaceous Working Group. BAUMGARTNER, P.O. et al. (Eds.) 1994. Middle Jurassic to Lower Cretaceous Radiolaria of Tethys: Occurrences, Systematics, Biochronolgy. env. 900 pp., 400 pls.

Order from **Institut de Géologie et Paléontologie,**
Université de Lausanne. BFSH-2. CH-1015, SWITZERLAND.
Bank Transfer: Banque Cantonale Vaudoise 1002 Lausanne
Account Number: **C. 323.52.56** Institut de Géologie, rubrique: Mémoires

Price $ 20 or CHF 30 per volume (volume 23 price on request) includes postage and handling.
Payment in U.S. Dollars or Swiss Francs

- Please do not send check -